Technical Report

Lithium & Potassium Resource Estimate Maricunga Joint Venture, III Region, Chile

Prepared for:

Lithium Power International,

Minera Salar Blanco S.A., and

Bearing Lithium Corp

Prepared by:

Frits Reidel, BSc, CPG

Murray Brooker, MSc, RPG, MAIG

Peter Ehren, MSc, MAusIMM

Effective Date: August 25, 2017

flo solutions
fluid thinking • solid decisions

DATE AND SIGNATURE PAGE

This report titled "Technical Report: Lithium and Potassium Resource Estimate, Maricunga Joint Venture, III Region Chile - dated June 30, 2017 was prepared and signed by the following authors:

(Signed & Sealed) "*Frederik Reidel*"

Dated at Santiago, Chile
Effective and sighed August 25th, 2017

Frederik Reidel, CPG
Consulting Hydrogeologist

(Signed & Sealed) "Murray Brooker"

Dated at Santiago, Chile
Effective and sighed August 25th, 2017

Murray Brooker
Consulting Hydrogeologist

Signed & Sealed) "*Peter Ehren*"

Dated at Santiago, Chile
Effective and sighed August 25th

Peter Ehren, MAusIMM
Mineral Processing Consultant

TABLE OF CONTENTS

1 SUMMARY 1
1.1 Property Description and Ownership 1
1.2 Physiography, Climate, and Access 1
1.3 Exploration and Drilling 2
1.4 Geology and Mineralization 4
1.4.1 Geology 4
1.4.2 Mineralization 4
1.5 Status of Exploration, Development and Operations 4
1.6 Brine Resource Estimates 5
1.7 Exploration Target 6
1.8 Conclusions and Recommendations 7
2 INTRODUCTION 8
2.1 Terms of Reference 8
2.2 Sources of Information 8
2.3 Units 9
3 RELIANCE ON OTHER EXPERTS 10
4 PROPERTY DESCRIPTION AND LOCATION 11
4.1 Property Description and Location 11
4.2 Tenure 11
4.3 History of ownership 13
4.4 Permits 16
4.5 Royalties 16
4.6 Environmental Liabilities 16
4.7 Other Significant Factors and Risks 16
5 ACCESSIBILITY, CLIMATE, LOCAL RESOURCES, INFRASTRUCTURE AND PHYSIOGRAPHY 17
5.1 Physiography 17
5.2 Accessibility 17
5.3 Climate 17
5.3.1 Temperature 17
5.3.2 Precipitation 18
5.3.3 Solar Radiation 24
5.3.4 Evaporation 26
5.4 Local Resources 29
5.5 Infrastructure 29
6 HISTORY 30
6.1 CORFO (1980's) 30
6.2 Prior Ownership and Ownership Changes 30
6.3 Brine Exploration Work by Previous Owners 31
6.3.1 SLM Litio (2007) 31
6.3.2 MLE / Li3 - Resource Evaluation Program (2011/2) 31
6.3.3 BBL - AMT Geophysics and Pumping tests (2015) 32
6.3.4 MSB - Resource Evaluation Program (2016/7) 32

6.3.5 Previous Water Exploration in Salar de Maricunga 32
7 GEOLOGICAL SETTING AND MINERALIZATION 37
7.1 Regional Geology 37
7.2 Local Geology 41
7.3 Mineralization 56
8 DEPOSIT TYPE 60
8.1 General 60
8.2 Hydrogeology 61
8.3 Water Balance (DGA 2009) 64
8.4 Drainable Porosity 65
8.5 Permeability 65
9 EXPLORATION 67
9.1 Overview 67
9.2 Geophysical Surveys 67
9.2.1 Seismic refraction tomography (2011) 67
9.2.2 AMT / TEM (2015) 70
9.2.3 Gravimetry 71
9.3 Test Trenching (2011) 71
10 DRILLING 75
10.1 Overview 75
10.2 Exploration drilling 75
10.2.1 Sonic Drilling 75
10.2.2 Rotary tricone/HWT drilling 79
10.3 Monitoring - and Production Well Drilling 79
10.3.1 Reverse circulation (RC) drilling and piezometer installations (2011) 79
10.3.2 Production well drilling (2011 and 2016) 79
10.3.3 Piezometer installations - 2016 79
10.4 Pumping Tests (2015 and 2017) 81
11 SAMPLE PREPARATION, ANALYSIS, AND SECURITY 95
11.1 Sampling Methods 95
11.1.1 Sonic drilling sampling procedures 95
11.1.2 RC drilling sampling procedures 97
11.1.3 Rotary /HWT brine sampling procedures 2017 97
11.2 Brine Analysis and Quality Control Results 98
11.2.1 Analytical methods 98
11.2.2 Analytical Quality Assurance and Quality Control (“QA/QC”) 2011 Program 101
11.2.3 Analytical accuracy 2011 Program 101
11.2.4 Analytical Quality Assurance and Quality Control (“QA/QC”) 2017 Program 106
11.2.5 Analytical accuracy 2017 Program 106
11.2.6 Additional QA/QC analysis 2017 Program 110
11.3 Drainable Porosity Analysis and Quality Control Results 112
11.3.1 DBSA 2011 112

11.3.2 GSA 2017 116
12 DATA VERIFICATION **130**
13 MINERAL PROCESSING AND METALLURGICAL TESTING **131**
13.1 Background - Li3 / LME 2011 Exploration Program 131
13.2 Experimental Procedure 131
13.3 Results of the Evaporation Tests 132
13.4 POSCO Process Tests – 2012/13 138
13.5 2016 and 2017 Evaporation Pond Tests 138
14 BRINE RESOURCE ESTIMATES **140**
14.1 Overview 140
14.2 Resource Model Domain and Aquifer Geometry 140
14.3 Specific Yield 140
14.4 Brine Concentrations 141
14.5 Resource Category 141
14.6 Resource Model Methodology and Construction 143
14.6.1 Variography 143
14.6.2 Model validation 146
14.7 Resource Estimate 148
15 MINERAL RESERVE ESTIMATES **153**
16 MINING METHODS **154**
17 RECOVERY METHODS **155**
18 PROJECT INFRASTRUCTURE **156**
19 MARKET STUDIES AND CONTRACTS **157**
19.1 Lithium Supply 157
19.2 Lithium Demand 159
19.3 Prices 167
19.4 Contracts 168
19.5 Chilean Regulations Respecting Lithium Production 168
20 ENVIRONMENTAL STUDIES, PERMITTING AND SOCIAL OR COMMUNITY IMPACT **169**
20.1 Environmental Studies 169
20.2 Project Permitting 169
20.3 Social or Community Requirements 169
21 CAPITAL AND OPERATING COSTS **170**
22 ECONOMIC ANALYSIS **171**
23 ADJACENT PROPERTIES **172**
24 EXPLORATION POTENTIAL **173**
25 INTERPRETATION AND CONCLUSIONS **176**
26 RECOMMENDATIONS **178**
27 REFERENCES **179**

LIST OF TABLES

Table 1.1 Maximum, average and minimum elemental concentrations of the MJV brine 4
Table 1.2 Drainable porosity values applied in the resource model 5
Table 1.3 Measured, Indicated and Inferred Lithium and Potassium Resources for the MJV - dated July 12, 2017 6
Table 1.4 MJV resources expressed LCE and potash 6
Table 4.1 MJV mining concessions 11
Table 5.1 Average monthly temperature at the Marte Lobo Project (0C) 18
Table 5.2 DGA Meteorological stations with long-term precipitation records 18
Table 5.3 Selected PUC-DGA weather stations with partial precipitation records 18
Table 5.4 Monthly solar radiation data (W/M2) for the Marte and Lobo Stations 24
Table 5.5 Evaporation rates used for the Maricunga Basin water balance 28
Table 5.6 Climate data collected at the MSB weather station in Salar de Mariacunga (Nov 2016 – Jun 2017) 28
Table 6.1 Estimated mineral resources for the Litio 1-6 claims – April 9, 2012 32
Table 7.1 Maximum, average and minimum elemental concentrations of the MJV brine 57
Table 7.2 Average values (g/L) of key components and ratios for the Maricunga brine 57
Table 7.3 Comparative chemical composition of various salars (weight %) 59
Table 8.1 Water Balance for the Salar de Maricunga Basin 64
Table 8.2 Results of drainable porosity analyses (2011-2017) 65
Table 8.3 Summary of Permeability values 66
Table 9.1 Results of Trench pumping tests 72
Table 10.1 Summary of 2011 and 2016 boreholes 78
Table 10.2 Wells P1, P2 and P4 pumping test layout 81
Table 10.3 P-1 pumping test results 86
Table 10.4 P-2 pumping test results 89
Table 10.5 P-2 pumping test results (2017) 91
Table 10.6 P-4 pumping test results (2017) 94
Table 11.1 List of analyses requested from the University of Antofagasta and Alex Stewart Argentina SA Laboratories 100
Table 11.2 Standards analysis results from U. Antofagasta (2011) 103
Table 11.3 Check assays (U. Antofagasta vs. Alex Stewart): RMA regression statistics 104
Table 11.4 Check assays between the University of Antofagasta and Alex Stewart 104
Table 11.5 Duplicate analyses from the University of Antofagasta 105
Table 11.6: Standards analysis results from U. Antofagasta (2017) 108
Table 11.7: Check assays between the University of Antofagasta and Alex Stewart 109
Table 11.8 Duplicate analyses from the University of Antofagasta 110
Table 11.9 Comparison of lithium concentrations in centrifuge and bailed brine samples 111
Table 11.10: Results of laboratory specific yield (S_y) analyses 114

Table 11.11 GSA laboratory tests performed 117
Table 11.12 Sample lithology and GSA clasification 118
Table 11.13 Summary of total porosity and specific yield by lithological group and laboratory 125
Table 11.14 Comparison of S_y values between GSA and Corelabs 127
Table 11.15 Comparison of Total Porosity between GSA and Corelabs 128
Table 13.1 Chemical composition (% weight) of brines used in the test work 131
Table 13.2 Brine compositions during evaporation of the untreated brine 133
Table 13.3 Salts compositions during evaporation of the untreated brine 134
Table 13.4 Crystalized Salts in the harvest 135
Table 13.5 Brine composition during evaporation of the treated brine 137
Table 13.6 Wet salt compositions during evaporation of the treated brine 138
Table 14.1 Drainable porosity values applied in the resource model 141
Table 14.2 Summary of brine chemistry composition 141
Table 14.3: Parameter for the calculation of the experimental variograms 143
Table 14.4: Comparison between the Ordinary Kriging results and the Nearest-Neighbor 146
Table 14.5: Measured, Indicated and Inferred Lithium and Potassium Resources of the MJV Project – Dated July 12, 2017 151
Table 14.6: MJV resources expressed LCE and potash 151
Table 19.1: Key attributes of brine and hard rock lithium deposits 158
Table 19.2: New vehicle build by engine type 162
Table 19.3: Lithium carbonate price impact on electric vehicle selling price 166
Table 19.4: Global mine production of lithium by company - 2015 167
Table 25.1 Summary of the avarage MJV brine composition (g/L) 176
Table 25.2 Measured, Indicated and Inferred Lithium and Potassium Resources of the MJV Project – Dated July 12, 2017 177
Table 25.3 MJV resources expressed LCE and potash 177
Table 26.1 Estimated costs for the deep exploration program 178

LIST OF FIGURES

Figure 4.1 Location map of the MJV 14
Figure 4.2 Location map of the MJV mining concessions 15
Figure 5.1 Isotherm map for Salar de MaricungaSource: DGA 2009 19
Figure 5.2a Precipitation data for the Maricunga weather station (PUC-DGA) 2007/2008 20
Figure 5.3 Precipitation data from the Marte and Lobo stations 2009/2010 21
Figure 5.4 Isohyet map for Salar de Maricunga Source: DGA 2009 22
Figure 5.5 MSB weather station in the plant site area 23
Figure 5.6 Solar radiation distribution in Chile 25
Figure 5.7 Average hourly solar radiation intensity at the Marte and Lobo stations 2009/2010 26

Figure 5.8 Elevation versus average annual pan evaporation....26
Figure 5.9 Monthly distribution of average annual Pan Evaporation....27
Figure 6.1 Location map of wells installed by Compania Mantos de Oro and Chevron 1988/1990....34
Figure 6.2 Lithological logs of Compania Mantos de Oro wells SP-2, SR-3 and SR-6....35
Figure 6.3 Lithological logs of Compania Mantos de Oro wells SR-1, SR-2, SR-4, SP-4 and Chevron well CAN-6....36
Figure 7.1 Morphotectonic units of the Andean Cordillera in northern Chile....37
Figure 7.2 Regional Geology of the Maricunga Basin....38
Figure 7.3 W-E Section showing the Maricunga geological model, looking north....42
Figure 7.4 Photo of the Upper Halite....43
Figure 7.5 N-S Section showing the distribution of the Upper Halite unit....43
Figure 7.6 Isopach map on the Upper Halite....44
Figure 7.7 N-S section showing the Clay Core, looking west....45
Figure 7.8 Isopach map on the Clay Core....46
Figure 7.9 Photo of the Clay Core unit....47
Figure 7.10 Section between boreholes S-18 and C-2 showing the distribution of the Deep Halite....48
Figure 7.11 Distribution of the East Alluvium....49
Figure 7.12 Distribution of the NW Alluvium....50
Figure 7.13 The NW Alluvium....51
Figure 7.14 E-W section with the spatial distribution of the Lower Alluvium....51
Figure 7.15 Drill core and cuttings of the Lower Alluvium....52
Figure 7.16 Drill core of the Volcaniclastic material....52
Figure 7.17 W-E section showing the spatial distribution of the Volcaniclastics....53
Figure 7.18 Isopach map on the Volcaniclastics Unit....54
Figure 7.19 Isopach map of the Lower Sand....55
Figure 7.20 Drill cuttings of the Lower Sand (Borehole S-5)....56
Figure 7.21 Comparison of brines from various salars in Janecke Projection....58
Figure 8.1 Conceptual model for mature and immature salars showing the distribution of the facies and the main hydrogeological components. (Houston, *et al*., 2011.)....60
Figure 8.2 W-E Hydrogeological cross section....62
Figure 8.3 Salar de Maricunga hydrographic basin....62
Figure 9.1 Location map of seismic refraction tomography, AMT and gravity profiles....69
Figure 9.2 Seismic Tomography Line 1....70
Figure 9.3 Test Trench T6 in the Upper Halite....72
Figure 9.4a – 9.4e Pumping test analyses for Trench pumping tests T1, T2, T3, T5 and T6....73
Figure 10.1 Location map of the boreholes (2011 and 2016 programs)....76
Figure 10.2 Collecting RC Airlift Flow Measurements (2011)....80
Figure 10.3 Installation of surface casing in well P-1 (2011)....80
Figure 10.4 Layout of pumping test P-1 and P-2....83
Figure 10.5 Pumping test P-1 layout....84

Figure 10.6 V-notch tank during P-1 constant rate test....84
Figure 10.7 Water level responses P-1 constant rate test....85
Figure 10.8 P-1 pumping test interpretation....86
Figure 10.9 Pumping test P-2 layout....87
Figure 10.10 Water level responses P-2 constant rate test....88
Figure 10.11 P-2 pumping test interpretation....89
Figure 10.12 Li and K concentrations during the P-1 and P-2 pumping tests....90
Figure 10.13 Water level responses P-2 constant rate test (2017)....91
Figure 10.14 Pumping test P-4 layout....93
Figure 10.15 Water level responses P-4 constant rate test (2017)....94
Figure 10.16 P-4 pumping test interpretation....94
Figure 11.1 Collection of field parameters of the brine samples at the wellhead....96
Figure 11.2 Porosity and brine samples....96
Figure 11.3 RC drill chip samples....97
Figure 11.4 Fluorescein tracer dye in the rotary drilling fluid....98
Figure 11.5 Comparison of lithium concentrations in centrifuge and bailed brine samples....111
Figure 11.6 Relative Solution Release Capacity (RSRC) HQ core sample testing....120
Figure 11.7 GSA specific yield vs GSA total porosity....122
Figure 11.8 Lithologically classified *Pt* and *Sy* distributions and statistics....123
Figure 11.9 Comparison of total porosity estimated by GSA using RSRC method and Core laboratory using the Centrifuge method....125
Figure 11.10 Comparison of specific yield estimated by GSA using RSRC method and Core laboratory using the Centrifuge method....126
Figure 11.11 Comparison of S_y values between GSA and Corelabs....127
Figure 11.12 Comparison of Total Porosity between GSA and Corelabs....129
Figure 13.1 General view of evaporation chambers....132
Figure 13.2 Evaporation curves plotted versus % Li in the brine....136
Figure 13.3 MSB evaporation ponds....139
Figure 14.1: Experimental variogram and variogram model for lithium....144
Figure 14.2: Experimental variogram and variogram model for potassium....145
Figure 14.3: Lithium concentration distribution....147
Figure 14.4: Potassium concentration distribution....147
Figure 14.5: N-S section through the resource model showing the lithium grade distribution....148
Figure 14.6: W-E section through the resource model showing the lithium grade distribution....149
Figure 14.7: NW-SE section through the resource model showing the lithium grade distribution....149
Figure 14.8: Distribution of resource classification areas....150
Figure 14.9: Lithium grade tonnage curve....152
Figure 19.1: Lithium supply by country and forecast supply to 2025....159
Figure 19.2: Global lithium demand – 2013 – 2025....160
Figure 19.3: Electric vehicle demand to 2025....161

Figure 19.4: Vehicle demand to 2030 162
Figure 19.5: Electric vehicle demand to 2030 163
Figure 19.6: Lithium demand forecast to 2026 164
Figure 19.7: Battery pack production costs 165
Figure 24.1 Schematic of the deep lithium exploration target (200-400 m) below the MJV 173

1 SUMMARY

The Maricunga Joint Venture (herein "MJV", Proyecto Blanco, or the "Project") (previously known as the Maricunga Lithium Project) is owned and operated by Minera Salar Blanco S.A. (MSB). MSB is in turn owned by Lithium Power International (ASX:LPI) 50%; Minera Salar Blanco SpA (previously BBL) 32.3%; and Bearing Lithium Corp.(TSXV: BRZ) 17.7%. MSB retained FloSolutions to prepare this Technical Report for the MJV in the III Region of Chile. The objective of this report is to prepare an updated estimate of brine resources based on exploration work carried out between 2011 and 2017 on the MJV mineral claims in Salar de Maricunga. Resource estimates are for lithium and potassium contained in brine.

1.1 Property Description and Ownership

The MJV is located 170 km northeast of Copiapo in the III Region of northern Chile at an elevation of 3,750 masl. The property is more particularly described as being centered at approximately 492,000 mE, 7,025,000 mN (WGS 84 datum UTM Zone 19). The Project covers some 2,563 ha of mineralized ground in Salar de Maricunga; 100 ha just to the northeast of the Salar for camp and evaporation test facilities, and an additional 1,800 ha some eight km north of the Salar for the future construction of evaporation ponds, process and plant facilities.

The mineralized area of the MJV is comprised of the following mining concessions: *Litio 1-6* (1,438 ha), *Cocina 19-27* (450 ha), *Salamina, Despreciada, and San Francisco* (675 ha). The *Cocina 19-27, San Francisco, Despreciada and Salamina* concessions were constituted under the 1932 Chilean mining law and have "grand-fathered" rights for the production and sale of lithium products; unlike the *Litio 1-6* concessions which were constituted under the 1982 Chilean mining law and require additional government permits for the production and sale of lithium.

1.2 Physiography, Climate, and Access

The hydrographic basin of Salar de Maricunga covers 2,195 km^2 in the Altiplano of the III Region. The average elevation of the basin is 4,295 masl while the maximum and minimum elevations are 6,749 masl and 3,738 masl respectively. The Salar itself is located in the northern extent of the hydrographic basin and covers 142.2 km2 (DGA 2009).The salar nucleus sits at an elevation of approximately 3,750 masl.

The principal surface water inflow into the lower part of basin occurs from Rio Lamas which originates in Macizo de Tres Cruces. Average flow in Rio Lamas (at El Salto) is measured at 240 l/s. All flows from the Rio Lamas infiltrate into the Llano de Cienaga Redonda (DGA 2009). The second largest surface water inflow to the lower part of the basin occurs from Quebrada Cienaga Redonda. Average flow (at La Barrera) is measured at 20 l/s; all flow infiltrates also in to the Llano de Cienaga Redonda (DGA 2009).

Laguna Santa Rosa is located at the southwest extent of the basin valley floor and is fed mainly locally by discharge of groundwater. Laguna Santa Rosa drains north via a narrow natural channel into the Salar itself. Additional groundwater discharge occurs along the path of this channel and surface water flow north towards the Salar has been recorded at a range of 200-300 l/s (DGA 2009). Tres Cruces National Park is located in the southern part of the Maricunga watershed and includes Laguna Santa Rosa.

The Maricunga property is accessed from the city of Copiapo via National Highway 31. Highway 31 is paved for approximately one-half of the distance and is a well maintained gravel surface road thereafter.

National Highway 31 extends through to Argentina via the Paso San Francisco. Access to Maricunga from the city of El Salvador is via a well maintained gravel surface highway. Occasional high snowfalls in the mountains may close the highways for brief periods during the winter.

The climate at the property is that of a dry, cold, high altitude desert, which receives irregular rainfall from storms between December and March and snowfall during the winter months of late May to September. The average annual temperature in Salar de Maricunga is estimated at 5 to 6°C. Average annual precipitation is estimated at 150 mm and average annual potential evaporation is estimated between 2,100 mm and 2,400 mm.

1.3 Exploration and Drilling

Bearing Lithium (previously as Li3 Energy) carried out an initial brine resource investigation program on the *Litio 1-6* claims during 2011/2 that consisted of the following components:

- Six sonic boreholes (C-1 through C-6) were completed to a depth of 150 m. Undisturbed samples were collected from the sonic core at three meter intervals for porosity analyses (318 samples). Brine samples were collected during the sonic drilling at three meter intervals for chemistry analyses (431 primary samples and 192 QA/QC samples). All sonic boreholes were completed as observation wells on completion of drilling.
- A total of 915 m of exploration RC drilling was carried out for the collection of chip samples for geologic logging, brine samples for chemistry analyses and airlift data to assess relative aquifer permeability. The RC boreholes were completed as observation wells for use during future pumping tests. Two test production wells (P-1 and P-2) were installed to a total depth of 150 m each for future pumping trials.
- A seismic tomography survey was carried out by GEC along six profiles (S1 though S6) for a total of 23 line km to help define basin lithology and geometry.
- Six test trenches adjacent to the sonic boreholes were completed to a depth of 3 m and 24-hour pumping tests were carried out in each trench.
- Evaporation test work was initiated on the Maricunga brine at the University of Antofagasta to evaluate the suitability of conventional brine processing techniques. Test work was also initiated by Li3's then strategic partner (POSCO) to evaluate the application of proprietary technology on the recovery of lithium.

BBL carried out a field program during 2015 that consisted of the following components:

- An AMT / TEM geophysical survey was completed by Wellfield Services along 6 profiles across the Salar covering a total of 75 line km. 383 AMT sounding were collected at 200 m to 250 m station spacing; 15 TDEM soundings were carried out at the end and center of each AMT profile. The purpose of the AMT survey was to help map the basin geometry and the fresh water / brine interface.
- Two long-term pumping tests were carried out on production wells P-1 (14 days) and P-2 (30 days) at 37 L/s and 38 L/s, respectively.

MSB initiated a phased work program in August 2016 to complete a Feasibility Study and Environmental Impact Assessment for the MJV. The first phase of this work program consisted of exploration drilling

and well testing focused on the *Cocina,Litio, San Francisco, Salamina and Despreciada* mining claims as follows:

- Four exploration holes (S-1A, S-2, S-18, and S-20) for a total of 627 m were drilled using the sonic method (4"x6" system). Core recovery took place in 1.5 m runs in alternating plastic sleeves and lexan liners. The overall achieved sonic core recovery was 92.5%. Undisturbed samples were cut from the lexan core at 3 m depth intervals. Brine sampling during the sonic drilling took place at 6 m depth intervals. Each sonic borehole was completed as a piezometer through the installation of 2-inch diameter blank and screened PVC casing.
- Eight exploration boreholes (S-3, S-3A, S-5, S-6, S-10, S-11 (or M2), S-13, and S-19) for a total of 1,709 m were drilled using the tricone rotary method at 3-7/8 and 5-1/2 inch diameter; HWT casing was installed in each borehole to selected depths as required to provide adequate borehole stability. Drill cuttings were collected at 2 m intervals. Brine samples were collected a 6 m interval. Six of the nine exploration holes were completed as piezometers through the installation of 2-inch diameter blank and screened PVC casing.
- Six boreholes (S-8, S-12, S-15, S-16, S-17, and S-21) for a total of 205 m were drilled as monitoring wells using the rotary method at 5-1/2 inch diameter. Drill cutting were collected at 2 m intervals; brine sampling took place at selected depth intervals. All six holes were completed with 2-inch diameter blank and screened PVC casing.
- One production well (P-4) was drilled at 17-1/2 inch diameter to a depth of 180 m using the flooded reverse method (rotary drilling). The well was completed with 12-inch diameter PVC blank and screened production casing. The screened interval of the well was completed in the lower semi-confined to confined aquifer, below and isolated from the upper halite mix zone.
- One 30-day pumping test was carried on production well P-4 at a pumping rate of 25 l/s. Water level measurements were made in adjacent monitoring wells P4-1 (lower aquifer completion), P4-2 (upper halite), P4-3 (upper halite) and P4-4 (upper halite).
- One 7-day pumping test was carried out on the previously drilled production well P-2 at a flow rate of 45 l/s. A packer was installed in the well at 40 m depth so that brine inflow during the pumping test was limited to the upper halite aquifer. Water level measurements were made in four adjacent monitoring wells during the 7-day pumping test.
- A regional gravity survey was carried out along six profiles (parallel to the AMT survey) for a total of 75 line km across the Salar. The station spacing along the profiles varied between 250 m and 500 m. The objective of the gravity survey was to help define the geometry of the bedrock contact in the Salar.
- 635 brine samples were sent to the University of Antofagasta and Alex Steward Assayers in Argentina for laboratory chemistry analysis. 343 brine samples were from the exploration drilling; 133 samples were collected from monitoring wells and pumping tests, and 159 samples were QA/QC samples (incl. Round Robin , duplicates, blank and standards)
- 192 undisturbed samples from the sonic core were analyzed by Geo Systems Analysis (GSA) and Corelabs (for QA/QC) for drainable porosity and physical parameters .

1.4 Geology and Mineralization

1.4.1 Geology

Based on the drilling campaigns carried out in the Salar between 2011 and 2017, ten major geological units were identified (8 of 10 of these were included in the concession area) and correlated from the logging of drill cuttings and undisturbed core to a general depth of up to 200 m. One deep borehole (S-19) was drilled to a depth of 360 m. No borehole reached bedrock. Salar de Maricunga is a mixed style salar, with a halite nucleus of up to 34 m in thickness in the central northern part. The halite unit is underlain by a clay core on the eastern and central part of the Salar. The clay is locally interbedded with silt and silty sands. The Salar is surrounded by relative coarse grained alluvial and fluvial sediments. These fans demark the perimeter of the actual salar and at depth grade towards the center of the Salar where they form the distal facies with an increase in sand and silt. At depth two unconsolidated volcaniclastics units have been identified that appear quite similar. These two volcaniclastic are separated by a relatively thin and continuous sand unit which may be reworked material of the lower volcaniclastic unit.

1.4.2 Mineralization

The brines from Maricunga are solutions saturated in sodium chloride with an average concentration of total dissolved solids (TDS) of 311 g/L. The average density is 1.20 g/cm3. Other components present in the Maricunga brine are: K, Li, Mg, Ca, SO_4, HCO_3 and B. Elevated values of strontium (mean of 359 mg/L) also have been detected.

Table 1.1 shows a breakdown of the principal chemical constituents in the Maricunga brine including maximum, average, and minimum values, based on the brine samples that were collected from the exploration boreholes during the 2011 and 2016 drilling programs.

Table 1.1 Maximum, average and minimum elemental concentrations of the MJV brine

Analyte	HCO_3	B	Ca	Cl	Li	Mg	K	Na	SO4	Density
Units	mg/L as $CaCO_3$	mg/L	mg/L	mg/L	mg/L	mg/L	mg/L	mg/L	mg/L	g/cm³
Maximum	2,730	1,193	36,950	230,902	3,375	21,800	20,640	104,800	2,960	1.31
Average	471	596	13,490	190,930	1,123	7,337	8,237	85,190	709	1.20
Minimum	76	234	4,000	89,441	460	2,763	2,940	37,750	259	1.10

1.5 Status of Exploration, Development and Operations

MSB has contracted Worley Parson to complete a Preliminary Feasibility Study (PFS) for the project in Q4 2017 (with the potash part of the study to be completed to a lower level of certainty as a Preliminary Economic Assessment, as potash production would not commence until several years after lithium production). Brine chemistry and evaporation tests are on-going in the Salar. Lithium processing methodology and optimization is being evaluated with several international firms. The feasibility study (FS) is planned to commence during 2018, following completion of the PFS. MWH-Stantec have been contracted to oversee the preparation of an Environmental Impact Statement (EIA) for the Project by Q1 2018.

1.6 Brine Resource Estimates

The brine resource estimate was determined by defining the aquifer geometry, the drainable porosity or specific yield (Sy) of the hydrogeological units in the Salar, and the concentration of the elements of economic interest, mainly lithium and potassium. Brine resources were defined as the product of the first three parameters.

The model resource estimate is limited to the MSB mining concessions in Salar de Maricunga that cover an area of 2,563 ha.

The resource model domain is constrained by the following factors:

- The top of the model coincides with the brine level in the Salar that was measured in the monitoring wells installed in the Salar.
- The lateral boundaries of the model domain are limited to the area of the MSB mining concessions.
- The bottom of the model domain coincides with a total depth of 200 m.

The specific yield values used to develop the resources are based on results of the logging and hydrogeological interpretation of chip samples and recovered core of 8 rotary boreholes and 10 sonic boreholes, results of drainable porosity analyses carried out on 501 undisturbed samples from sonic core by GeoSystems Analysis, Daniel B Stephens and Associated, Corelabs, and four pumping tests. The boreholes within the measured and indicated resource areas are appropriately spaced at a borehole density of one bore per 1.5 km2. Table 1.2 shows the drainable porosity values assigned to the different geological units for the resource model.

Table 1.2 Drainable porosity values applied in the resource model

Unit	Sy
Upper Halite	0.07
Clay Core	0.02
Deep Halite	0.05
NW Alluvium	0.15
Lower Alluvium	0.06
Volcaniclastic	0.10
Lower Sand	0.06
Lower Volcaniclastic	0.10

The distributions of lithium and potassium concentrations in the model domain are based on a total of 487 brine analyses (not including QA/QC analyses) mentioned in Section 1.4.2 above.

The resource estimation for the Project was developed using the Stanford Geostatistical Modeling Software (SGeMS) and the geological model as a reliable representation of the local lithology. The resource estimate was developed using SgeMS software. The authors were closely involved with the block model development; all results have been reviewed and checked at various stages and are believed to valid and appropriate for these resource estimates. Table 1.3 shows the Measured, Indicated and Inferred lithium and potassium resources for the MJV.

Table 1.3 Measured, Indicated and Inferred Lithium and Potassium Resources for the MJV - dated July 12, 2017

	Measured		Indicated		Inferred		M+I	
	Li	K	Li	K	Li	K	Li	K
Area (Km2)	18.88		6.76		14.38		25.64	
Aquifer volume (km3)	3.06		1.35		0.72		4.41	
Mean specific yield (Sy)	0.05		0.11		0.09		0.07	
Brine volume (km3)	0.15		0.14		0.06		0.30	
Mean grade (g/m3)	56	409	114	801	114	869	74	529
Concentration (mg/L)	1,174	8,646	1,071	7,491	1,289	9,859	1,143	8,292
Resource (tonnes)	170,000	1,250,000	155,000	1,100,000	80,000	630,000	325,000	2,350,000

Notes to the resource estimate:

1. CIM definitions (2014) were followed for Mineral Resources.
2. The Qualified Persons for this Mineral Resource estimate are Frits Reidel, CPG and Murray Brooker, PGeo.
3. No cut-off values have been applied to the resource estimate.
4. Numbers may not add due to rounding.
5. The effective date is July 12, 2017.

Table 1.4 shows the total resources of the MJV expressed as lithium carbonate equivalent (LCE) and potash (KCl).

Table 1.4 MJV resources expressed LCE and potash

	Measured and Indicated		Inferred	
	LCE	KCL	LCE	KCL
Tonnes	1,725,000	4,500,000	425,000	1,200,000

1. Lithium is converted to lithium carbonate (Li2CO3) with a conversion factor of 5.32.
2. Potassium is converted to potash with a conversion factor of 1.9
3. Numbers may not add due to rounding

1.7 Exploration Target

Based on the results of borehole S-19, an exploration target of 1.0 to 2.5 Mt of lithium carbonate equivalent (LCE) and 2.9 to 6.6 Mt of potassium chloride (KCl) has been identified (below the current resource) between a depth of 200 m and 400 m. The exploration target provides significant potential for resource expansion.

1.8 Conclusions and Recommendations

Based on the analyses and interpretation of the results of the exploration work carried out on the MJV in Salar de Maricunga between 2011 and 2017, the following concluding statements are prepared:

- The entire MJV project area has been covered by exploratory drilling between 2011 and 2017 at an approximate borehole density of one exploration borehole per 1.5 km^2; it is the opinion of the authors that such borehole density is appropriate for the mineral resource estimate described herein.
- The results of the drilling (10 sonic boreholes and 8 rotary/HWT boreholes) and the analysis of 487 primary brine samples identify distinct brine composition and grade at specific depth intervals, showing a relatively uniform distribution of lithium bearing brines throughout the MJV project area to a depth of 200 m.
- The lithium bearing brine contains sufficient levels of lithium and potassium to be potentially economic for development.
- The results of pumping tests and drainable porosity analyses suggest that the MJV exhibits favorable hydrogeological conditions for future brine abstraction with a conventional brine production wellfield.
- It is the opinion of the authors that the Salar geometry, brine chemistry composition and the specific yield of the Salar sediments have been adequately defined to a depth of 200 m to support the Measured, Indicated and Inferred Resource estimate described in Section 14 and shown in Table 1.3.
- Based on results of exploration borehole S-19 to a depth of 360 m, it is the opinion of the authors that a significant exploration target exists below the current resource defined to 200 m depth.
- The Salar de Maricunga brine is suitable for conventional processing, which principally consists in solar evaporation of the brine to a suitable concentration where the brine can be treated in a lithium carbonate production plant. The concentrated Maricunga brine will require a boron, calcium and magnesium removal stages. The ongoing test work is optimizing these stages in order to have the lowest operational costs and most environmentally friendly process.
- It is recommended by the authors that the PFS and FS for the MJV are completed as currently planned during 2017 and 2018. Studies in support of the EIA should be completed as is currently planned by early 2018.
- A work program should be initiated to continue expanding the MJV resource estimate by exploring the deeper portions of the Salar. It is recommended that the proposed work program includes the following components:
    - Deep drilling (7-10 holes) using a suitable drilling method to a depth of 400 m across the MJV properties. The drilling target will be the coarser grained sediments on the Lower Alluvium and Volcaniclastics.
    - Sampling protocols need to be developed to properly characterize the hydraulic parameters and the brine chemistry of these deeper units.

The estimated cost for the above exploration program is approximately USD 6 million.

2 INTRODUCTION

2.1 Terms of Reference

The Maricunga Joint Venture (herein "MJV", Blanco Project or the "Project") (previously known as the Maricunga Lithium Project) is owned and operated by Minera Salar Blanco S.A. (MSB). MSB is in turn owned by Lithium Power International (ASX:LPI) 50%; Minera Salar Blanco SpA. 32.3%; and Bearing Lithium Corp.(TSXV: BRZ) 17.7%. MSB retained FloSolutions to prepare this Technical Report for the MJV in the III Region of Chile. The objective of this report is to prepare an updated estimate of brine resources based on exploration work carried out between 2011 and 2017 on the MJV mineral claims in Salar de Maricunga. Resource estimates are for lithium and potassium contained in brine.

This report has been prepared in conformance with the requirements of National Instrument 43-101 – *Standards of Disclosure for Mineral Projects* and the associated Companion Policy 43-101CP and Form 43-101F1 of the Canadian Securities Administrators and the associated Best Practice Guidelines for Industrial Minerals and Mineral Processing as issued by the Canadian Institute of Mining and Metallurgy. The Report also includes technical judgment of appropriate additional technical parameters to accommodate certain specific characteristics of minerals hosted in liquid brine as outlined in CIM Best Practice Guidelines for Resource and Reserve Estimation for Lithium Brines and as discussed by Houston (Houston et al, 2011).

2.2 Sources of Information

Previous technical reports prepared for the Project include:

- Maricunga Lithium Brine Project; 3.7 Fold Increase in Mineral Resource Estimate; Lithium Power International JORC report dated 12 July 2017.
- Technical Report on the Maricunga Lithium Project, Region III, Chile. NI 43-101 Technical Report for Bearing Resources prepared by Don Hains March 20, 2017.
- Technical Report on the Maricunga Lithium Project, Region III, Chile. NI 43-101 Technical Report for Li3 Energy Inc prepared by Don Hains and Frits Reidel April 17, 2012.
- Technical Report on the Salar de Maricunga Lithum Project, Northern Chile prepared for Li3. NI 43-101 Technical report prepared by Donald H Hains, Amended May 26, 2011.

The authors were provided full access to the MJV database including drill core and cuttings, drilling and testing results, brine chemistry and porosity laboratory analyses, aquifer testing results, geophysical surveys and all other information available from the work carried out on the Project area between 2011 and 2017. The documentation reviewed, and other sources of information, are listed at the end of this report in Section 27 References.

Numerous site visits were carried out to the Project area between 2011 and 2017. The authors were closely involved with the work carried out during the 2011, 2015 and 2016 field campaigns.

The report was prepared by Frits Reidel, CPG, "qualified person" (QP) who is independent of MSB as such terms are defined by NI 43-101,Murray Brooker RPGeo, MAIG and Peter Ehren, MAusIMM, also QP's and independent of MSB as such terms are defined by NI 43-101. The authors have relevant experience in the evaluation of brine deposits in South America.

2.3 Units

The metric (si system) units of measure is used in this report unless otherwise noted.

List of abbreviations

All currency in this report is US dollars (US$) unless otherwise noted.

µ	micron
°C	degree Celsius
°F	degree Fahrenheit
µg	microgram
A	ampere
a	annum
bbl	barrels
Btu	British thermal units
C$	Canadian dollars
cal	calorie
cfm	cubic feet per minute
cm	centimetre
cm^2	square centimetre
d	day
dia.	diameter
dmt	dry metric tonne
dwt	dead-weight ton
ft	foot
ft/s	foot per second
ft^2	square foot
ft^3	cubic foot
g	gram
G	giga (billion)
Gal	Imperial gallon
g/L	gram per litre
g/t	gram per tonne
gpm	Imperial gallons per minute
gr/ft^3	grain per cubic foot
gr/m^3	grain per cubic metre
hr	hour
ha	hectare
hp	horsepower
in	inch
in^2	square inch
J	joule
k	kilo (thousand)
kcal	kilocalorie
kg	kilogram
km	kilometre
km/h	kilometre per hour
km^2	square kilometer
kPa	kilopascal
kVA	kilovolt-amperes
kW	kilowatt
kWh	kilowatt-hour
L	litre
L/s	litres per second
M	metre
M	mega (million)
m^2	square metre
m^3	cubic metre
Min	minute
MASL	metres above sea level
Mm	millimetre
Mph	miles per hour
MVA	megavolt-amperes
MW	megawatt
MWh	megawatt-hour
m^3/h	cubic metres per hour
opt, oz/st	ounce per short ton
Oz	Troy ounce (31.1035g)
Ppm	part per million
Psia	pound per square inch absolute
Psig	pound per square inch gauge
PWL	Pumping water level
RL	relative elevation
S	Second
Sy	Specific Yield
St	short ton
Stpa	short ton per year
Stpd	short ton per day
SWL	Static water level
T	metric tonne
Tpa	metric tonne per year
Tpd	metric tonne per day
US$	United States dollar
USg	United States gallon
USgpm	US gallon per minute
V	volt
W	watt
Wmt	wet metric tonne
yd^3	cubic yard
Yr	year

3 RELIANCE ON OTHER EXPERTS

The authors have relied on the following expert:

Mr. J.P. Bambach of the legal firm Philippi, Prietocarrizosa, Ferrero DU & Uria in Santiago, Chile for the legal opinion on the status of the Project's mining claims. For the purpose of this report, the authors have relied on ownership information provided by MSB. MSB has relied on a legal opinion by Philippi y Prietocarrizosa, Ferrero DU & Uria dated August 18, 2017 respecting legal title to the properties.

The authors also rely on the topographic information regarding property locations provided by MSB and Philippi y Prietocarrizosa, Ferrero DU & Uria.

4 PROPERTY DESCRIPTION AND LOCATION

4.1 Property Description and Location

The MJV is located approximately 170 km northeast of Copiapo in the III Region of northern Chile at an elevation of approximately 3,750 masl. Figure 4.1 shows the location of the Project. The property is more particularly described as being centered at approximately 492,000 mE, 7,025,000 mN (WGS 84 datum, UTM Zone 19). The Project covers 2,563 ha of mineralized ground in Salar de Maricunga, 100 ha just to the northeast of the Salar for camp and evaporation test facilities, and an additional 1,800 ha some eight km north of the Salar for the future construction of evaporation ponds, process and plant facilities.

4.2 Tenure

The mineralized area of the MJV is comprised of the following mining concessions: *Litio 1-6* (1,438 ha), *Cocina 19-27* (450 ha), *Salamina, Despreciada, and San Francisco* (675 ha). Figure 4.2 shows the MJV land tenure and concession boundaries in the northern part of Salar de Maricunga. Table 4.1 provides a detailed listing of the MJV concessions.

The *Cocina 19-27, San Francisco, Despreciada and Salamina* concessions were constituted under the 1932 Chilean mining law and have "grand-fathered" rights for the production and sale of lithium products; unlike the *Litio 1-6* concessions which were constituted under the 1983 Chilean mining law and require additional government permits for the production and sale of lithium.

Table 4.1 MJV mining concessions

Property	Role Number	Area (ha)	Registered Owner	Mining Code
Litio 1, 1 al 29	03201-6516-4	131	SML Litio 1	1983
Litio 2, 1 al 30	0321-6517-2	143	SML Litio 2	1983
Litio 3, 1 al 58	03201-6518-0	286	SML Litio 3	1983
Litio 4, 1 al 60	03201-6519-9	300	SML Litio 4	1983
Litio 5, 1 al 60	03201-6520-2	297	SML Litio 5	1983
Litio 6, 1 al 60	03201-6521-0	282	SML Litio 6	1983
Cocina 19-27	03201-2110-19	450	MSB	1932
San Francisco 1 al 10	03201-0006-2	425	MSB	1932
Despreciada 6 al 7	03201-0007-0	100	MSB	1932
Salamina 1 al 3	03201-0005-4	150	MSB	1932
Blanco*	N/A	1,800	MSB	1983
Camp*	N/A	100	MSB	1983

* Note: concessions were not included in legal opinion of Mr Bambach.

Verification of the land titles and mining rights owned by MSB, was conducted by Juan Paulo Bambach Salvatore of the legal firm *Philippi Prietocarrizosa Ferrero DU & Uria* in Santiago. Mr. Bambach documented his legal opinion in a letter dated August 18, 2017 and concluded the following:

- Minera Salar Banco SpA has been duly incorporated and is a validly existing company under the laws of Chile and is in good standing.
- MSB owns 96% of the shares over six mining legal companies (*sociedades legales mineras*) Litio 1 up to Litio 6, which in turn are respectively the exclusive owners of six Mining Exploitation Concessions, as shown in Table 4.1.
- Minera Salar Blanco S.A. (MSB) has all necessary corporate faculties and authority to carry on its business as now conducted by it and to own its properties and assets.
- Minera Salar Blanco S.A. is duly licensed to carry on its business in Chile.
- The Company currently has a portfolio of 10 Mining Concessions, as follows:
    - 4 Old Legislation Concessions (*pertenencias*)
    - 6 1983 Exploitation Concessions (*pertenencias*)
- All titles of the Mining Concessions set out in Table 4.1 are in good standing and there are no encumbrances on such Mining Concessions.
- Minera Salar Blanco S.A. is empowered to conduct exploration activities on the Exploration Concessions, and exploration and development activities on the Mining Claims.
- By means of the Old Mining Chilean Legislation, MSB is entitled to explore and exploit lithium, fulfilling all legal requirements provided by the Chilean legislation.
- The 1983 Exploitation Concessions do not allow to explore nor exploit lithium, unless a Special Operation Contract for Lithium, CEOL is obtained, but do permit the exploration and exploitation of any other mining substances, whether metallic or non-metallic, for example potassium, where lithium may be a sub product. In other words, the 1983 Exploitation Concessions, do not entitle to appropriate the extracted lithium, but only other concessionable substances.
- According to the legal documentation reviewed, the Mining Concessions are valid and in force.
- To date, the granting processes of the applications under proceeding (the “Applications”) have been carried out according to the law, and they would not present defects that could lead to the expiration of the application.
- The Mining Concessions have no marginal records evidencing mortgages, encumbrances, prohibitions, interdictions or litigations.
- The Mining Concessions have all their last four periods of mining licenses duly paid.
- All the Mining Concessions have preferential rights over the relevant area. There are no mining concession nor mining rights held or filed by third parties challenging the rights and preference of the Mining Concessions.

- From a technical point of view and after having requested the review of the complete area by the expert in mining property Mr. Juan Bedmar, we can confirm that the location of the Mining Concessions is correct.

4.3 History of ownership

- LI3 Energy Corp. (Li3 – now Bearing Lithium) through its 100% owned Chilean subsidiary Minera Li Energy (MLE) acquired its original interest in the Salar de Maricunga through the purchase of a 60% interest in SLM Litio 1 through 6 (which are the legal entities holding the *Litio 1-6* concessions) on May 20, 2011. MLE acquired 100% of the *Cocina 19-27* concessions on April 16, 2013.
- On November 5, 2013 Li3 announced an agreement with BBL SpA (BBL) for BBL to acquire 51% of MLE in return for specified funding of Li3's exploration program. BBL purchased another 36% interest in SML Litio 1-6 held by another third party. The remaining 4% interest in the *Litio 1-6* claims remains held by third-party individuals.
- In 2016 BBL, Lithium Power International Ltd and Li3 agreed to form a new company, Minera Salar Blanco S.A, (MSB) in which LPI acquired 50%, BBL (now Minera Salar Blanco SpA) 32.3% and Li3 17.7%. Through this agreement MSB holds 96% interest in the *Litio 1-6* concessions and 100% in the *Cocina, San Francisco, Despreciada and Salamina, Camp* and *Blanco* concessions (the MJV concessions).
- Bearing Lithium Corp. is acquiring 100% of the common shares of Li3 and as a result will assume Li3's 17.7% interest in the MJV.

Figure 4.1 Location map of the MJV

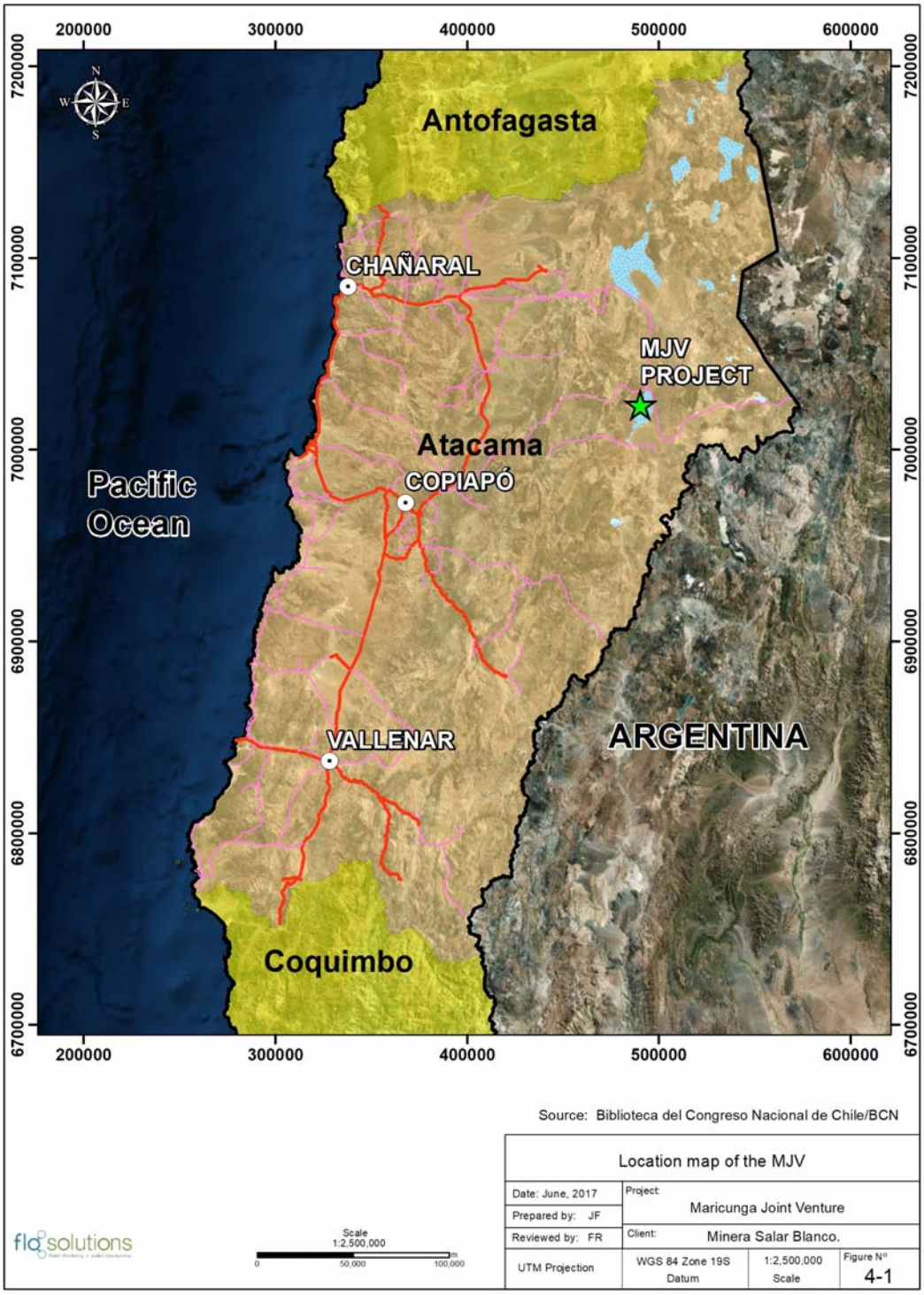

Figure 4.2 Location map of the MJV mining concessions

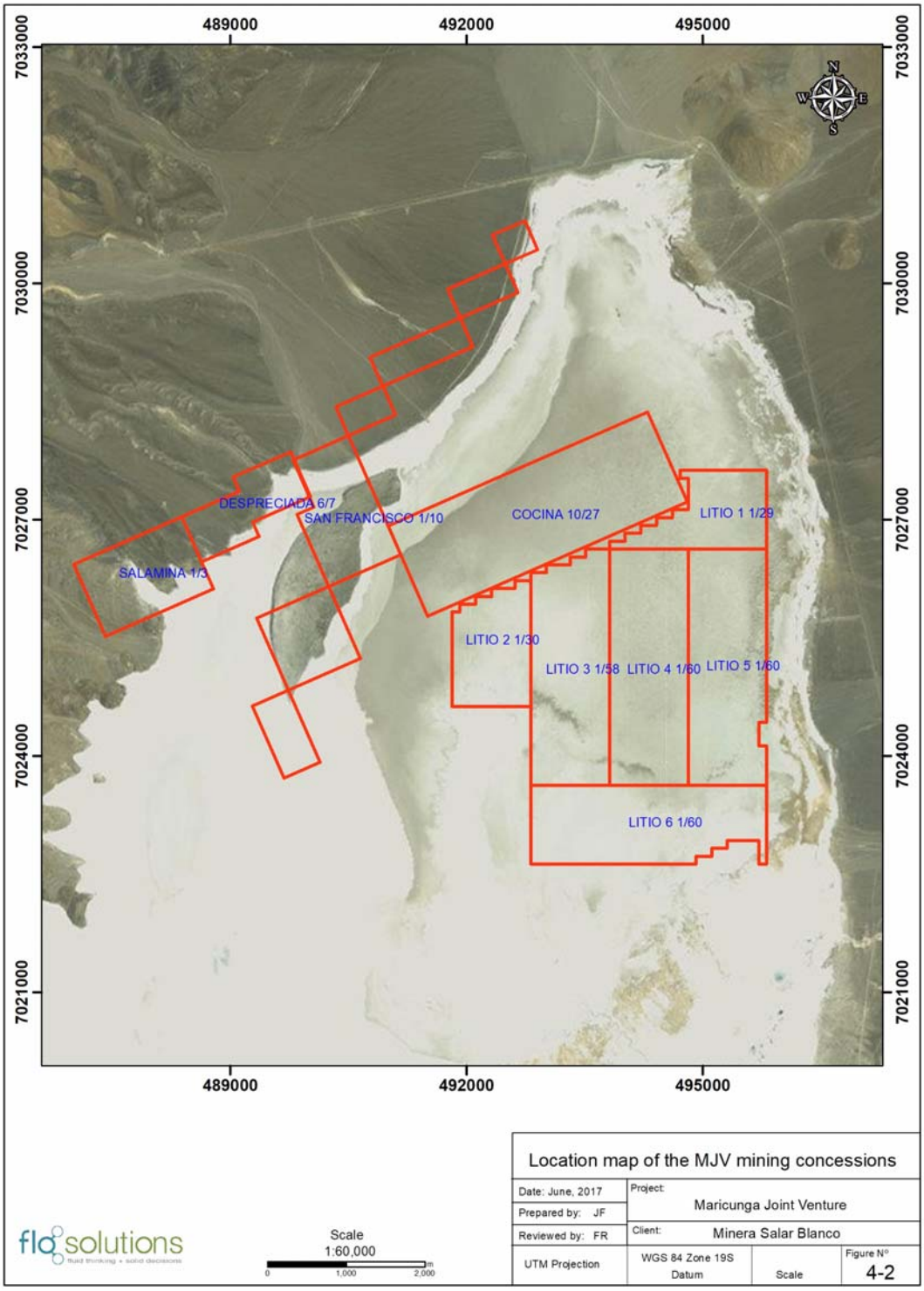

4.4 Permits

MSB obtained all necessary environmental approvals through the Sistema Evaluacion Ambiental (SEA) to carry out drilling, aquifer testing, road building and operate the evaporation test and camp facilities. The MJV concessions are located in a Zona de Interes Turistico (ZOIT) and, therefore, SEA approvals are required to carry out exploration work. The approvals were obtained in 2013 through the filing and successful permitting of a Declaracion Impacto Ambiental (DIA).

4.5 Royalties

The Chilean government is currently reviewing a future royalty and permitting regime for lithium production. The MJV fully owns its mineral concessions and will not be exposed to additional royalty payments to CORFO, who collects royalties from holders of properties which it owns in the Salar de Atacama.

4.6 Environmental Liabilities

The authors are not aware that the MJV is subject to any material environmental liabilities.

4.7 Other Significant Factors and Risks

A number of normal risk factors are associated with the Maricunga properties These risks include, but are not limited to the following. It is not anticipated they will affect access, title or the ability to perform work on the Salar de Maricunga:

- The risk of obtaining final environmental approvals from the necessary authorities in a timely manner.
- The risk of obtaining all the necessary licenses and permits on acceptable terms, in a timely manner or at all.
- Regulatory risks associated with the government revisions to regulations for exploitation of lithium.
- The risk of changes in laws and their implementation, impacting activities on the properties.
- The risk of activities on adjacent properties having an impact on the Maricunga project.

5 ACCESSIBILITY, CLIMATE, LOCAL RESOURCES, INFRASTRUCTURE AND PHYSIOGRAPHY

5.1 Physiography

The hydrographic basin of Salar de Maricunga covers 2,195 km2 in the Altiplano of the III Region. The average elevation of the basin is 4,295 masl while the maximum and minimum elevations are 6,749 masl and 3,738 masl respectively. The Salar itself is located in the northern extent of the hydrographic basin and covers 142.2 km2 (DGA 2009).The salar nucleus sit evation of approximately 3,750 masl.

The principal surface water inflow into the lower part of basin occurs from Rio Lamas which originates in Macizo de Tres Cruces. Average flow in Rio Lamas (at El Salto) is measured at 240 l/s. All flows from the Rio Lamas infiltrate into the Llano de Cienaga Redonda (DGA 2009). The second largest inflow to the lower part of the basin occurs from Quebrada Cienaga Redonda. Average flow (at La Barrera) is measured at 20 l/s; all flow infiltrates in to the Llano de Cienaga Redonda (DGA 2009).

Laguna Santa Rosa is located at the southwest extent of the basin valley floor and is fed mainly locally by discharge of groundwater. Laguna Santa Rosa drains north via a narrow natural channel into the Salar itself. Additional groundwater discharge occurs along the path of this channel and surface water flow has been recorded at 200-300 l/s (DGA 2009). Tres Cruces National Park is located in the southern part of the Maricunga watershed and includes Laguna Santa Rosa.

5.2 Accessibility

The Maricunga property is accessed from the city of Copiapo via National Highway 31. Highway 31 is paved for approximately one-half of the distance and is a well maintained gravel surface road thereafter. National Highway 31 extends through to Argentina via the Paso San Francisco. Access to Maricunga from the city of El Salvador is via a well maintained gravel surface highway. Occasional high snowfalls in the mountains may close the highways for brief periods during the winter.

5.3 Climate

5.3.1 Temperature

The climate at the property is a dry, cold, high altitude desert with cold, dry winters and dry summers. Summer temperatures range from 10^0C – 20^0C, with the winter daytime temperatures averaging approximately 4^0C – 0^0C. The average annual temperature at Salar de Maricunga is estimated at 5-6 ^{0}C as shown in Figure 5.1 (DGA 2009).

Long-term historical temperature data are not available for the immediate Project area. The DGA maintained Lautaro Embalso meteorological station (1,110 masl) located 160 km southwest of the Project area has average monthly temperature records available for the period of 1966 through to date.

A weather station at the Marte Lobo Project site located in the southern extension of the Maricunga basin at an elevation of 4,090 masl, (30 km to the south of the Project) has average monthly temperature records available for the period of January 1997 to December 1998. Table 5.1 shows average monthly temperature data for the Marte Lobo Project (Golder Associates 2011) while Figure 5.1 provides an isotherm map for the Salar de Maricunga region.

Table 5.1 Average monthly temperature at the Marte Lobo Project (0C)

Jan	Feb	Mar	Apr	May	Jun	Jul	Aug	Sep	Oct	Nov	Dec
8.5	6.6	6.5	2.5	-0.5	-5.0	-3.5	-2.5	-0.5	1.0	3.7	5.8

(re-elaborated after Golder Associates 2011)

5.3.2 Precipitation

Precipitation in Salar de Maricunga may occur during the months of January and February as a result of "Bolivian winter" effects and during the months of June through September. The intensity of these annual rainfall patterns are significantly influenced by the El Nino-Southern Oscillation.

The nearest long-term historical precipitation records for the Project are available from DGA maintained meteorological stations at Las Vegas (70 km northwest) at an elevation of 2,250 masl and Pastos Grande (60 km WSW) at an elevation of 2,260 masl. No long-term historical precipitation records are available for the III Region above 2,500 masl elevation. Table 5.2 provides summary information of the Las Vegas and Pastos Grande stations.

Table 5.2 DGA Meteorological stations with long-term precipitation records

Station	BNA code	Basin	Elevation (masl)	Distance from Project	Record
Las Vegas	03210001-5	Rio Salado	2,250	70 km NW	1984 – to date
Pastos Grande	03441001-1	Rio Copiapo	2,260	60 km WSW	1966 – to date

Source: DGA, 2009

Additional rainfall records are available from selected weather stations that are part of the "Pilot System for the III Region" operated by the Catholic University of Chile (PUC) in conjunction with the DGA. Table 5.3 provides summary information for the Maricunga and Pedernales Sur weather stations.

Table 5.3 Selected PUC-DGA weather stations with partial precipitation records

Station	Basin	UTM (WGS 84)		Elevation (masl)	Record
Maricunga	Maricunga	7,000,372 mN	486,326 mE	3,852	2007 – 2008
Pedernales Sur	Pedernales	7,049,016 mN	493,056 mE	3,774	2007 – 2008

Source: DGA, 2009

Figures 5.2a and 5.2b show monthly precipitation records for the Marigunca and Pedernales Sur weather stations for the 2007/8 period. It is believed that these data are representative of a relative dry year (DGA 2009).

Precipitation records collected at the Marte Lobo Project weather station during the 1997/1998 period show an annual cumulative precipitation (rainfall and snowfall water equivalent) of 451 mm (Golder Associates 2011). Further analyses of rainfall records of the III Region indicate that the 1997/8 cumulative precipitation coincides with a 100 year precipitation event. Additional precipitation data collected at the Marte and Lobo stations between 2009 and 2010 are shown in Figure 5.3.

Figure 5.1 Isotherm map for Salar de Maricunga

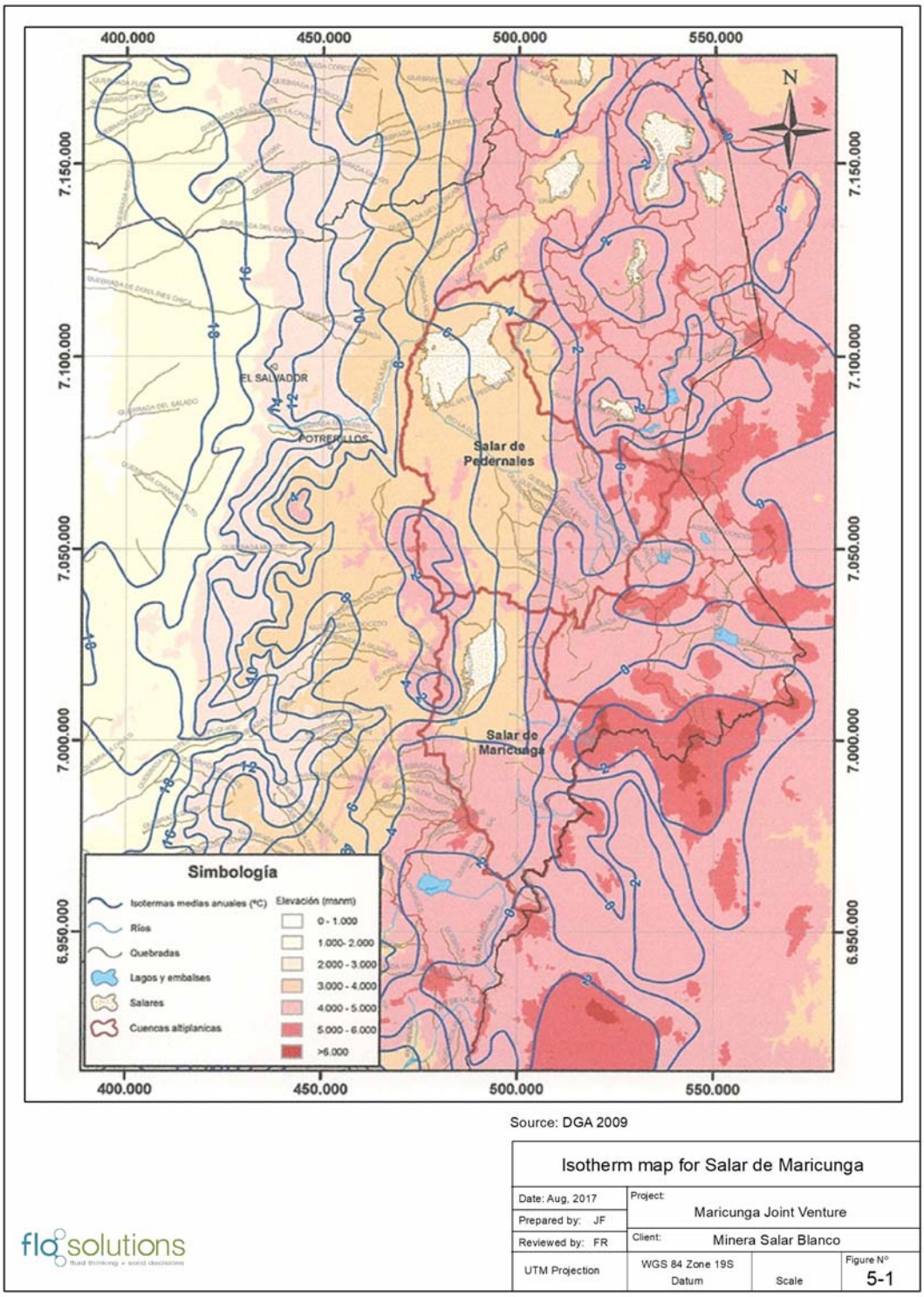

Source: DGA 2009

Average annual precipitation estimates were prepared as part the "Balance Hidrico de Chile" (DGA 1987). Figure 5.4 shows an isohyet map for the Salars de Maricunga and Pedernales. The map suggests that the average annual precipitation in Salar de Maricunga is 100 mm - 150 mm.

Figure 5.2a Precipitation data for the Maricunga weather station (PUC-DGA) 2007/2008

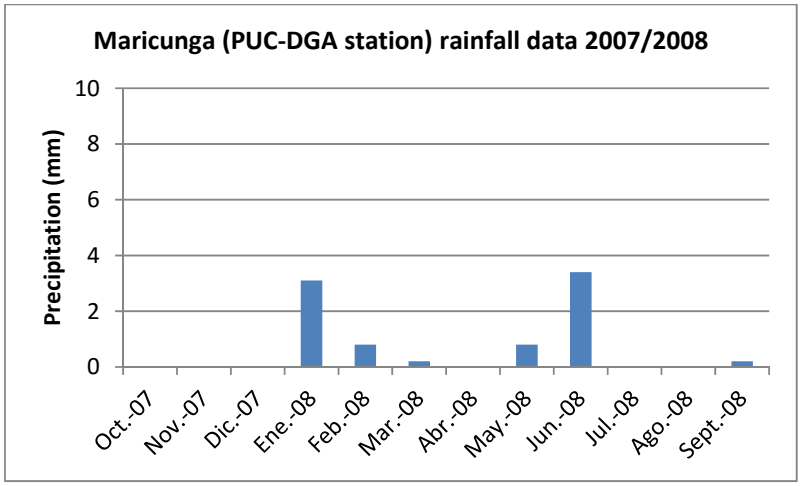

Source: DGA 2009

Figure 5.2b Precipitation data for the Pedernales Sur weather station (PUC-DGA) 2007/2008

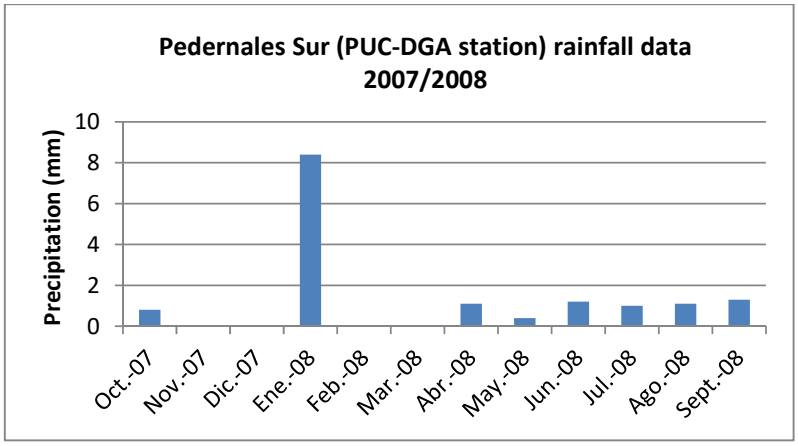

Source: DGA 2009

Figure 5.3 Precipitation data from the Marte and Lobo stations 2009/2010

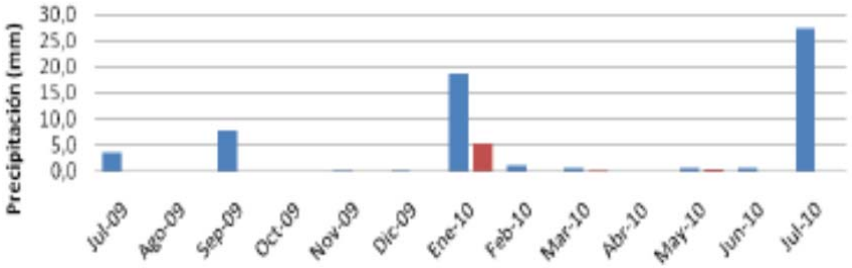

Source: AMEC 2011

Figure 5.4 Isohyet map for Salar de Maricunga

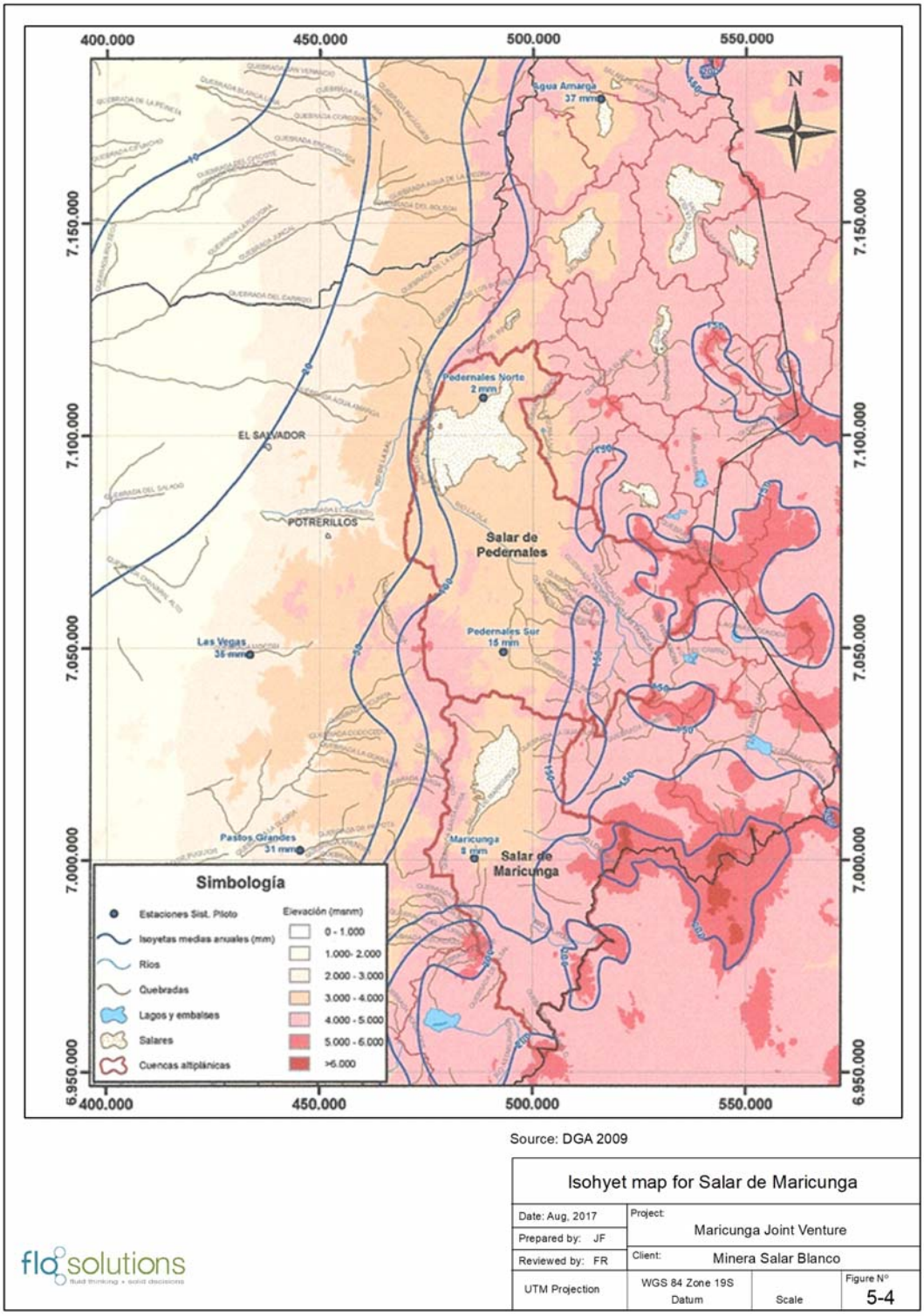

Source: DGA 2009

EDRA (1998) carried out a hydrogeological investigation for the Salar de Maricunga and Piedra Pomez areas and described the following precipitation – elevation relationship:

P = 0.038H – 53

Where:

P is average annual precipitation (mm); and H is elevation (masl)

Using this correlation the average annual precipitation for Salar de Maricunga is estimated at 90 mm.

The DGA (2006) carried out a hydrogeological investigation for Salar de Maricunga in which the following precipitation – elevation relationship was developed:

P = 0.1H – 300

Where:

P is average annual precipitation (mm); and H is elevation (masl)

Using this correlation the average annual precipitation for Salar de Maricunga is estimated at 75 mm.

MSB installed a weather station in Salar de Maricunga in 2016 to validate the results of previous precipitation studies and third party data sets (Figure 5.5). Table 5.6 shows a summary of the data collected between November 2016 and June 2017.

Figure 5.5 MSB weather station in the plant site area

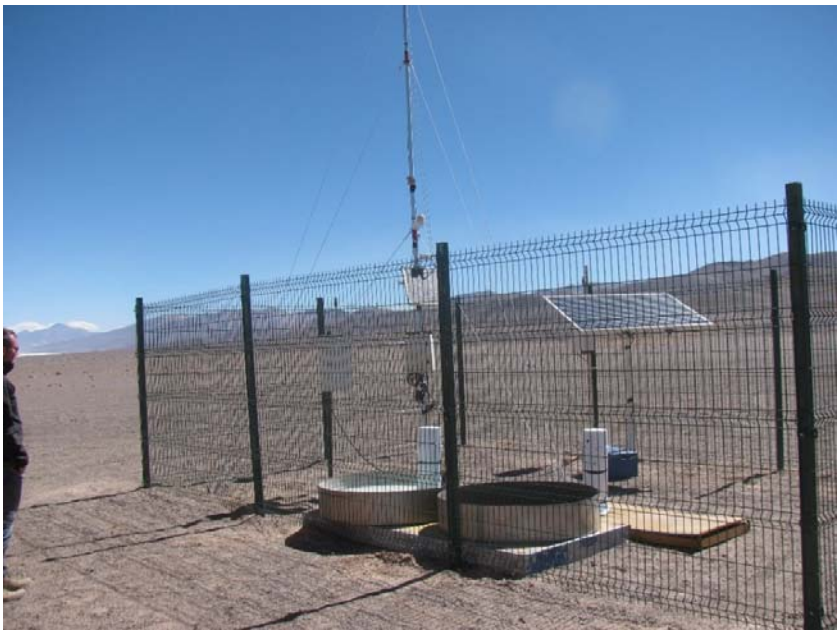

5.3.3 Solar Radiation

Solar radiation is the most important energy input for evaporation. Long-term solar radiation data are not available for Salar de Maricunga directly. Regional solar radiation estimates are shown in Figure 5.6 and suggest that solar radiation in Salar de Maricunga falls in the range of 1,700 – 1,900 KWh/m^2 per year. Partial solar radiation data are available from the Marte Lobo Project site and are reported in Amec 2011. Table 5.4 shows monthly records solar radiation records in Watts/m^2 for the Marte and Lobo stations.

Table 5.4 Monthly solar radiation data (W/M2) for the Marte and Lobo Stations

Mes	Lobo			Marte		
	Mínimo	Promedio	Máximo	Mínimo	Promedio	Máximo
Jul-09	0.0	194.2	974.0	s/d	s/d	s/d
Ago-09	0.0	244.7	1078.7	s/d	s/d	s/d
Sep-09	0.0	324.0	1164.1	0.0	299.9	1019.2
Oct-09	0.0	374.3	1246.8	0.0	331.7	1157.6
Nov-09	0.0	394.7	1217.0	0.0	387.8	1171.0
Dic-09	0.0	417.6	1221.0	0.0	408.1	4981.0
Ene-10	0.0	397.4	1229.0	0.0	386.8	1154.0
Feb-10	0.0	375.8	1349.0	0.0	356.7	1156.0
Mar-10	0.0	328.0	1132.0	0.0	312.0	1019.0
Abr-10	0.0	259.6	1009.0	0.0	247.3	918.0
May-10	0.0	193.6	866.0	0.0	187.1	825.0
Jun-10	0.0	171.6	914.0	0.0	163.9	746.1
Jul-10	0.0	198.6	785.1	0.0	196.8	796.8

Source: AMEC 2011

Figure 5.6 Solar radiation distribution in Chile

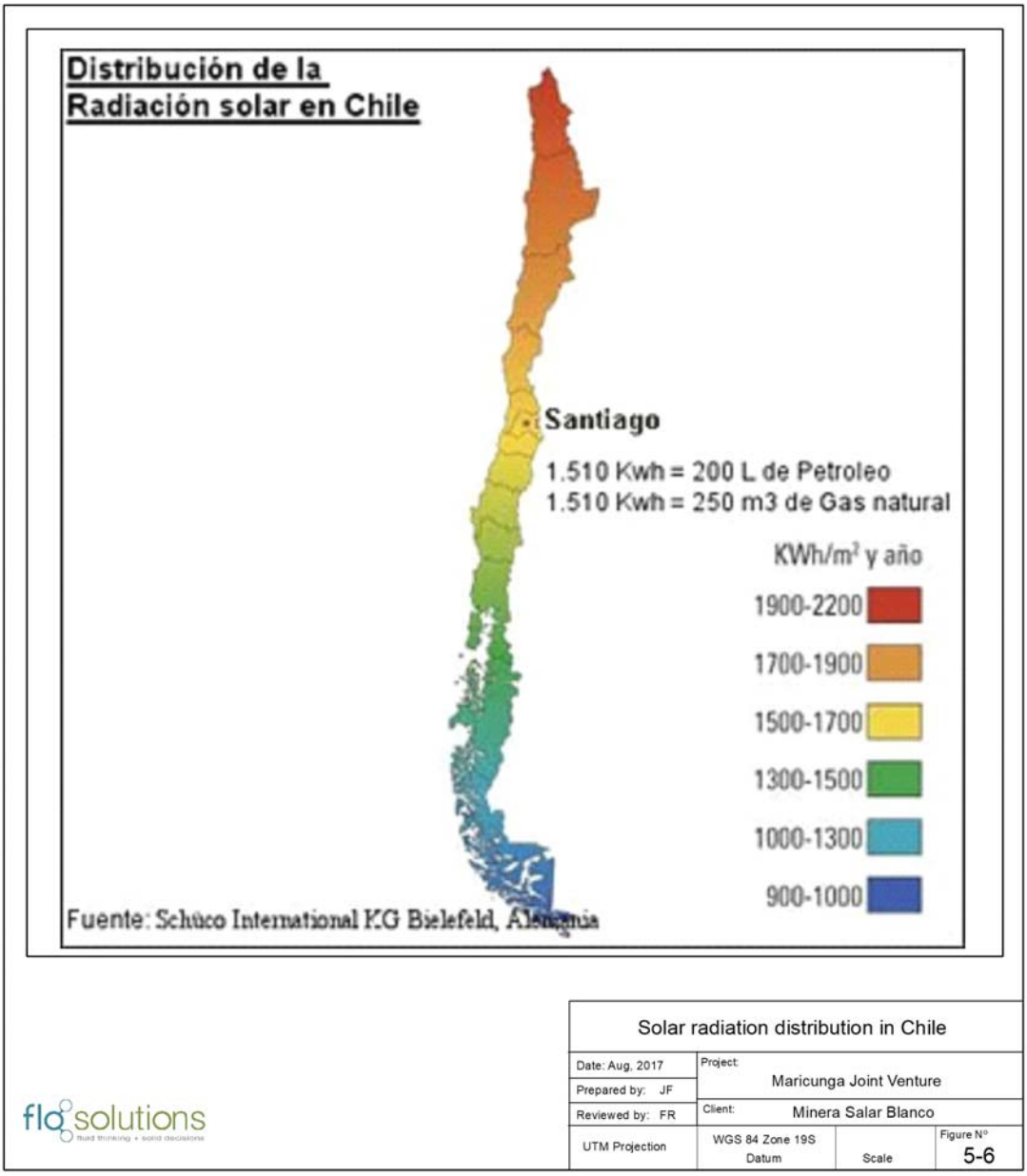

Figure 5.7 Average hourly solar radiation intensity at the Marte and Lobo stations 2009/2010

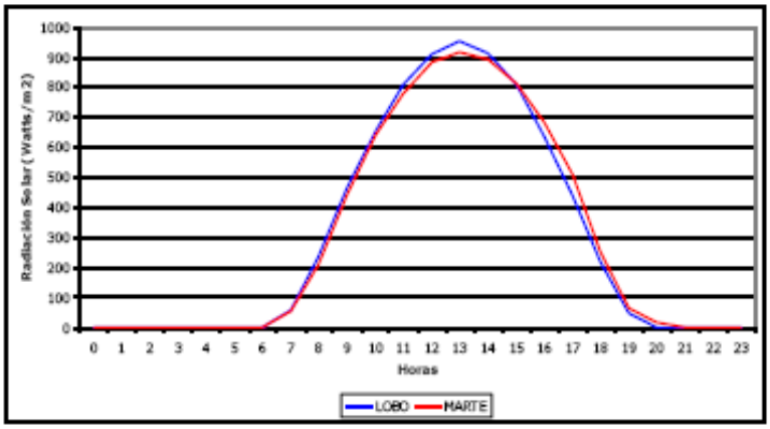

Source: AMEC 2011

The MSB weather station installed on site is collecting local solar radiation data in support of the evaporation tests that are currently in progress.

5.3.4 Evaporation

The DGA (2009) has developed a relationship between elevation and average annual pan evaporation based on pan evaporation records from some 40 stations across the I, II, and III Regions of northern Chile as shown in Figure 5.8. Based on this correlation the annual average pan evaporation rate for Salar de Maricunga is estimated at 2,400 mm.

Figure 5.8 Elevation versus average annual pan evaporation

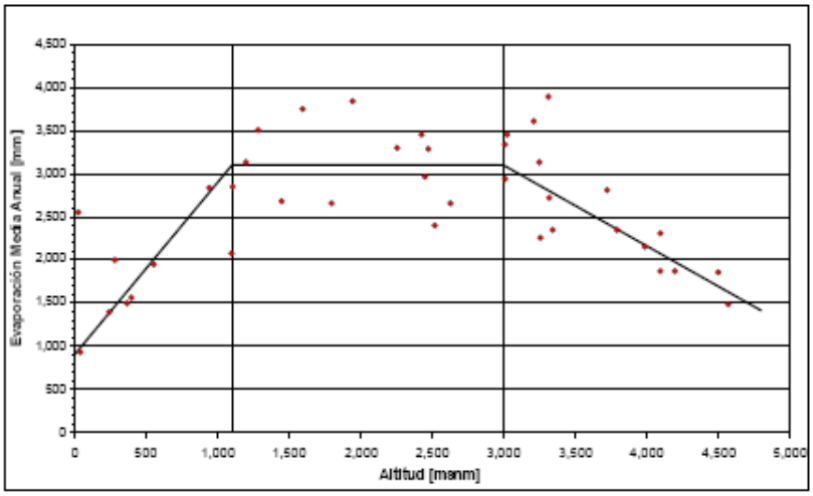

Source: DGA 2009

A similar relationship between elevation and average annual pan evaporation has been described by Houston (2006) as follows:

$$MAE_{pan} = 4364 – (0.59*A)$$

Where: MAE_{pan} is mean annual pan evaporation (mm) and A is elevation (m) for stations above 1,000 masl.

Using this correlation the mean annual pan evaporation rate for Salar de Maricunga is estimated at 2,150 mm.

Houston (2006) further describes the effects of brine density on mean annual pan evaporation rates as:

MAE_{pan} = 10026 – 6993D; where D is fluid density

Applying this to Maricunga brine (D = 1.2 g/ml), the annual average brine pan evaporation rate is estimated at 1,600 mm.

The DGA (2008) described the monthly distribution of average annual pan evaporation based on observations made from records (1977-2008) of the Linzor (4,096 masl) and Inacaliri (4,000 masl) stations in the II Region of northern Chile. Figure 5.9 summarizes this monthly distribution of the annual average pan evaporation (Golder Associates 2011).

Figure 5.9 Monthly distribution of average annual Pan Evaporation

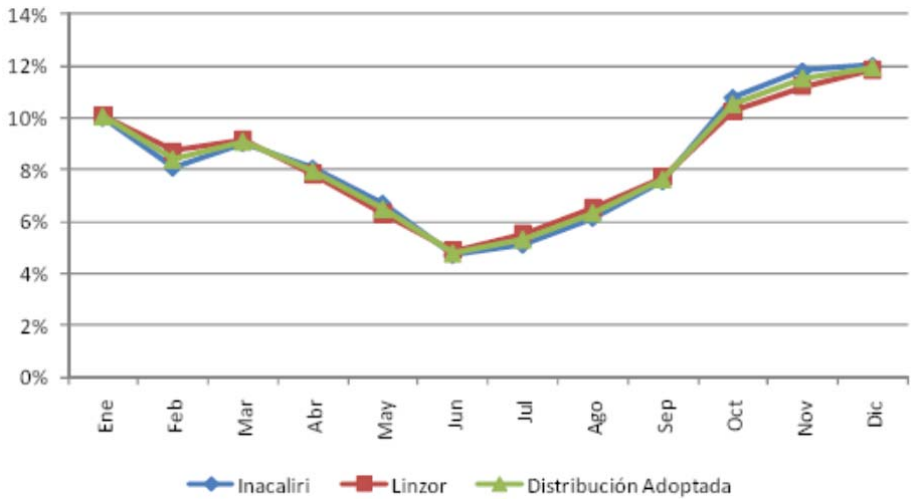

Source: Golder Associates 2011

The DGA (2009) carried out a detailed field investigation program in Salar de Maricunga to establish evaporation rates as a function of soil type and depth to groundwater. Table 5.5 summarizes the findings of this investigation.

Table 5.5 Evaporation rates used for the Maricunga Basin water balance

Type	Mean annual evaporation rate (mm)
Open water	6.1
Humid soil	4.1
Vegas	2.1
Salar crust	1.8

Source: Modified from DHA 2009 and Golder 2011

The MJV has installed several Class A evaporation pans (fresh water and brine) at the weather station and a series of test evaporation ponds adjacent to the camp site. These pans and test ponds are designed to validate previous evaporation studies and confirm evaporation pathways for lithium brine concentration.

Table 5.6 Climate data collected at the MSB weather station in Salar de Mariacunga (Nov 2016 – Jun 2017)

Month	Precipitation (mm)	Average Temperature (°C)	Freshwater Pan Evaporation (mm)	Brine Pan Evaporation (mm)
January	7,40	9,68	350,58	253,23
February	8,20	6,68	243,00	185,00
March	1,30	5,72	251,90	199,90
April	11,10	1,86	137,30	191,30
May	284.2 **	-3,56	40,40	35,40
June	240.4 **	-8,92	0,00	0,00
July				
August				
September				
October				
November	3,50	4,30	274,80	181,80
December	17,00	6,60	323,61	236,60
Annual Total:				

** data to be corrected by Algoritmos

5.4 Local Resources

Local resources are absent at the Salar. Copiapo is a major regional mining center. Drilling contractors, drilling equipment, exploration tools and heavy mining equipment and machinery are all available.

5.5 Infrastructure

Local infrastructure at the Salar includes National Highway 31 and an electrical power line running parallel to the highway. There is a customs post at the north end of the Salar that is staffed on a 24 hour basis.

Copiapo is a major city and provides a full range of services. Copiapo is serviced by daily flights with connections to Santiago and other major cities in Chile, as well as service to Argentina and Bolivia. The port of Caldera is located approximately 80 km west of Copiapo. The port has excellent dock facilities for general cargo, liquid fuel and bulk cargo. The port of Chañaral is located approximately 250 km from the Salar.

6 HISTORY

6.1 CORFO (1980's)

CORFO, under the aegis of the Comite de Sales Mixtas, (CORFO, 1982) conducted a major study of the northern Chilean salars in the 1980s with the objective of determining the economic potential of the salars for production of potassium, lithium, and boron. CORFO undertook systematic hydrogeological and geological studies and sampling of the various salars. Exploration work at Salar de Maricunga consisting of sampling shallow pits (50 cm deep) covered the northern half of the Salar. It was determined that the phreatic level of the brine was at 15 cm below the Salar surface. Estimates of contained mineral resources were developed based on the assay results and assuming a constant porosity of 10% down to a 30 m depth. CORFO estimated lithium metal resources in Salar de Maricunga at 224,300 tonnes. This estimate does not comply with NI 43-101 standards.

CORFO currently does not control any mineral rights in Salar de Maricunga

6.2 Prior Ownership and Ownership Changes

- SLM Litio, a Chilean corporation, acquired the *Litio 1-6* mining claims in 2004.
- Li3 through its 100% owned Chilean subsidiary MLE acquired a 60% interest in the *Litio 1-6* concessions on May 20, 2011.
- MLE acquired 100% of the *Cocina 19-27* concessions on April 16, 2013.
- Li3 announced an agreement with BBL SpA (BBL) for BBL to acquire 51% of MLE in return for specified funding of exploration activities and mining concession acquisition expenses on November 5, 2013.
- BBL purchased the 36% interest (of the 40% interest not held by MLE) in the *Litio 1-6* claims from third parties on August 25, 2014. The remaining 4% interest in the *Litio 1-6* claims remains held by third-party individuals as of to date.
- BBL entered into an option agreement to purchase a 100% stake in the Salamina, San Francisco and Despreciada concessions on December 30, 2014.
- BBL changed its name to Minera Salar Blanco SpA on September 2, 2015.
- BBL acquired the *Blanco* and *Camp* concessions on December 31, 2015
- Minera Salar Blanco SpA, Lithium Power International Ltd and Li3 agreed to form a new company, Minera Salar Blanco S.A (MSB) (and which has 100 % ownership of the MJV), in which LPI owns 50%, Minera Salar Blanco SpA 32.3% and Li3 17.7%.
- MSB (or the MJV) on completion of the merger agreement holds a 96% interest in the *Litio 1-6* concessions and a 100% interest in the *Cocina, San Francisco, Despreciada and Salamina, Camp* and *Blanco* concessions (the MJV concessions).
- Bearing Lithium Corp. on December 11, 2016 announced a binding agreement to acquire 100% of the common shares of Li3 and as a result will assume Li3's 17.7% interest in the MJV.

6.3 Brine Exploration Work by Previous Owners

6.3.1 SLM Litio (2007)

SLM Litio carried out an initial exploration program on the *Litio 1-6* concessions during February 2007 that consisted of the following components:

- 58 reverse circulation holes were drilled on a 500 m x 500 m grid to 20 m depth. Holes were 3.5" diameter and cased with either 40 mm PVC or 70 mm HDPE pipe inserted by hand to resistance. 232 brine samples were collected from these holes (using an airlift methodology) at 2 m to 10 m depth and 10 m to 20 m depth. The brine samples were analysed by Cesmec in Antofagasta.
- No NI 43-101 compliant resource estimate was prepared by SML Litio.

6.3.2 MLE / Li3 - Resource Evaluation Program (2011/2)

Li3 carried out an initial brine resource investigation program on the *Litio 1-6* claims during 2011/2 that consisted of the following components:

- Six sonic boreholes (C-1 through C-6) were completed to a depth of 150 m. Undisturbed samples were collected from the sonic core at three meter intervals for porosity analyses (318 samples). Brine samples were collected during the sonic drilling at three meter intervals for chemistry analyses (431 primary samples and 192 QA/QC samples). All sonic boreholes were completed as observation wells on completion of drilling. Figure 10.1 shows the location of the six sonic boreholes
- A total of 915 m of exploration RC drilling was carried out for the collection of chip samples for geologic logging, brine samples for chemistry analyses and airlift data to assess relative aquifer permeability. The RC boreholes were completed as observation wells for use during future pumping tests. Two test production wells (P-1 and P-2) were installed to a total depth of 150 m each for future pumping trials.
- A seismic tomography survey was carried out by GEC along six profiles (S1 through S6) for a total of 23 line km to help define basin lithology and geometry.
- Six test trenches adjacent to the sonic boreholes were completed to a depth of 3 m and 24-hour pumping tests were carried out in each trench.
- Evaporation test work was initiated on the Maricunga brine at the University of Antofagasta to evaluate the suitability of conventional brine processing techniques. Test work was also initiated by Li3's strategic partner to evaluate the application of proprietary technology on the recovery of lithium.
- Environmental baseline monitoring of flora, fauna, surface water and groundwater were initiated by consultants GHD.
- A NI 43-101 Technical report (*Technical Report on the Maricunga Lithium Project, III Region, Chile*, prepared for Li3 Energy by D. Hains and F. Reidel, dated April 17, 2012) was prepared on the lithium and potassium resources of the *Litio 1-6* mining claims based on the results of the 2011 work program. Table 6.1 summarizes the resource estimate therein.

Table 6.1 Estimated mineral resources for the Litio 1-6 claims – April 9, 2012

	Lithium		Potassium	
	Measured	Inferred	Measured	Inferred
Area (km^2)	14.38	7.06	14.38	7.06
Depth interval (m)	0-150	150-180	0-150	150-180
Aquifer volume (km^3)	2.157	0.212	2.157	0.212
Avg grade (g/m^3)	50	50	360	360
Lithium metal (t)	107,850	10,590		
Potassium (t)			776,250	76,320

6.3.3 BBL - AMT Geophysics and Pumping tests (2015)

BBL carried out a field program during 2015 that consisted of the following components:

- An AMT / TEM geophysical survey was completed by Wellfield Services along 6 profiles across the Salar covering a total of 75 line km. 383 AMT sounding were collected at 200 m to 250 m station spacing; 15 TDEM soundings were carried out at the end and center of each AMT profile. The purpose of the AMT survey was to help map the basin geometry and the fresh water / brine interface.
- Two long-term pumping tests were carried out on production wells P-1 (14 days) and P-2 (30 days) at 37 L/s and 38 L/s, respectively.
- The results of the 2015 program were reported in "*Proyecto Blanco, Informe Tecnico, Programa de Pruebas de Bombeo 2015, Analisis y Resultados*", prepared for BBL SpA by FloSolutions in October 2015.

The results of the field program are discussed in further detail in Sections 7 and 9 herein.

6.3.4 MSB - Resource Evaluation Program (2016/7)

MSB initiated a phased work program in August 2016 to complete a FS and EIA for the MJV. The first phase of this work program consisted of exploration drilling and well testing focused on the *Cocina, San Francisco, Salamina and Despreciada* mining claims. Sections 9 and 10 herein provide a detailed description of the MSB program.

6.3.5 Previous Water Exploration in Salar de Maricunga

A significant amount of hydrogeological and water resources studies have been carried in the Maricunga basin in the past. Below is a list of work and references relevant to this investigation.

- Balance Hídrico de Chile, Dirección General de Aguas, 1987.
- Mapa hidrogeológico de la cuenca Salar de Maricunga: sector Salar de Maricunga, Escala 1:100.000, Región de Atacama. Nº Mapa: M62.- Autor: Iriarte D., Sergio. SERNAGEOMIN, 1999.

- Mapa hidrogeológico de la Cuenca Salar de Maricunga: sector Ciénaga Redonda, escala 1:100.000, Región de Atacama. N° Mapa: M65. Venegas, M.; Iriarte, S. y Aguirre, I. SERNAGEOMIN, 2000.
- Geología del Salar de Maricunga, Región de Atacama, Escala 1:50.000. Nº Mapa: M54.- Autor: Tassara O., Andrés. SERNAGEOMIN, 1997.
- Ref. 14 Mapa Hidrogeológico de la Cuenca Campo de Piedra Pómez-Laguna Verde.
- Región de Atacama, Escala 1:100.000. N° Mapa: M66.- Autor: Santibáñez I., Venegas M. Formato JPG. SERNAGEOMIN, 2005.
- Geoquímica de Aguas en Cuencas Cerradas: I, II y III Regiones de Chile, Volumen I, Síntesis. S.I.T Nº 51, de los autores Risacher, Alonso y Salazar, Convenio de Cooperación DGA – UCN – IRD, 1999.
- Análisis de la Situación Hidrológica e Hidrogeológica de la Cuenca del Salar de Maricunga, III Región. DGA, Departamento de Estudios y Planificación (2006). S.D.T. Nº 255.
- Hidrogeología Sector Quebrada Piedra Pómez. EDRA, 1999.
- Evaluation of the Hydrogeological Interconnection between the Salar de Maricunga and the Piedra Pomez Basins, Atacama Region, Chile; An Isotope and Geochemical Approach. Iriarte, Santibáñez y Aravena, 2001.
- Levantamiento Hidrogeologico para el Desarrollo de Nuevas Fuentas de Agua en Areas Prioritarias de la Zone Norte de Chile, Regiones XV, I, II, y III. Etapa 2 Sistema Piloto III Region Salares de Maricunga y Pedernales. Realizado por Departamento de Ingeniera Hidraulica y Ambiental Pontifica Universidad Catolica de Chile (PUC). SIT No. 195, Noviembre 2009.
- Hidrogeologia Campo de Pozos Piedra Pomez- Compania Minera Casale; prepared by SRK Consulting; May 2011.
- Linea Base Hidrogeologica y Hidrologica Marte Lobo y Modelo Hidrogeologico Cienaga Redonda – Kinross Gold Corporation; prepared by Golder Associates, June 2011.

Compania Mantos de Oro and Chevron Minera Corporation of Chile carried out several water well drilling campaigns between 1988 and 1990 during which a total of 10 wells were installed around the perimeter of Salar de Maricunga as shown in Figure 6.1. Figures 6.2 and 6.3 show the available lithological logs for these wells.

Figure 6.1 Location map of wells installed by Compania Mantos de Oro and Chevron 1988/1990

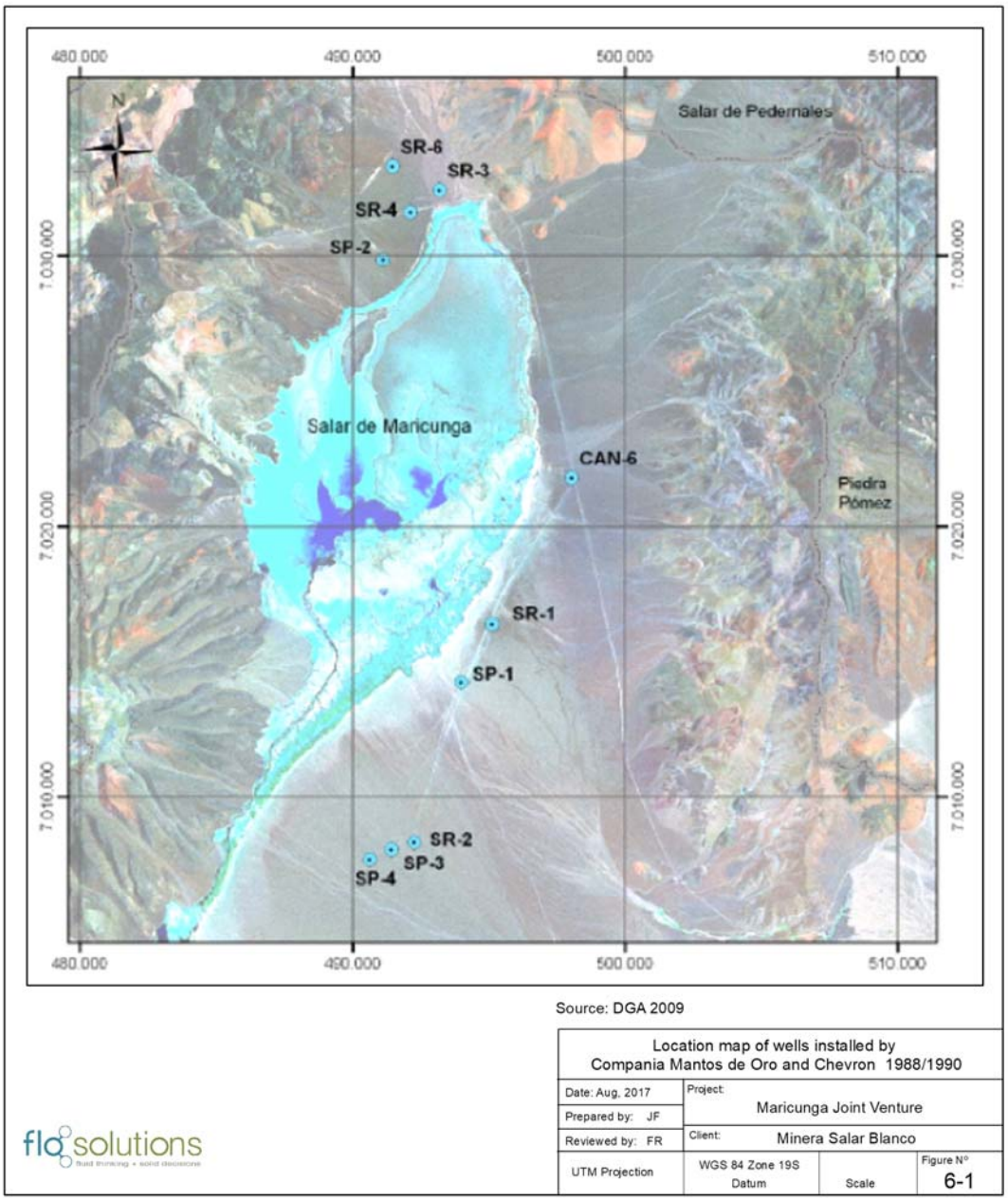

Source: DGA 2009

Figure 6.2 Lithological logs of Compania Mantos de Oro wells SP-2, SR-3 and SR-6

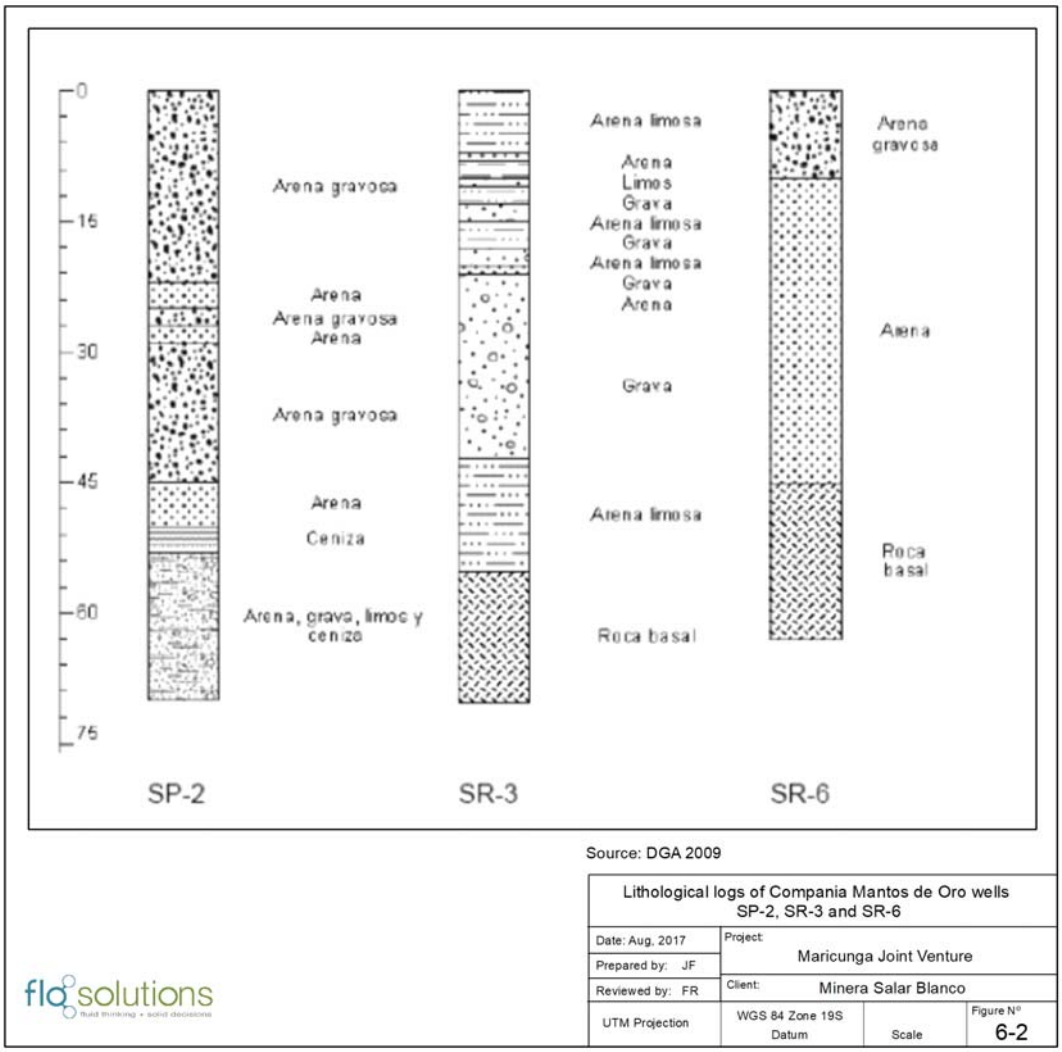

Source: DGA 2009

Figure 6.3 Lithological logs of Compania Mantos de Oro wells SR-1, SR-2, SR-4, SP-4 and Chevron well CAN-6

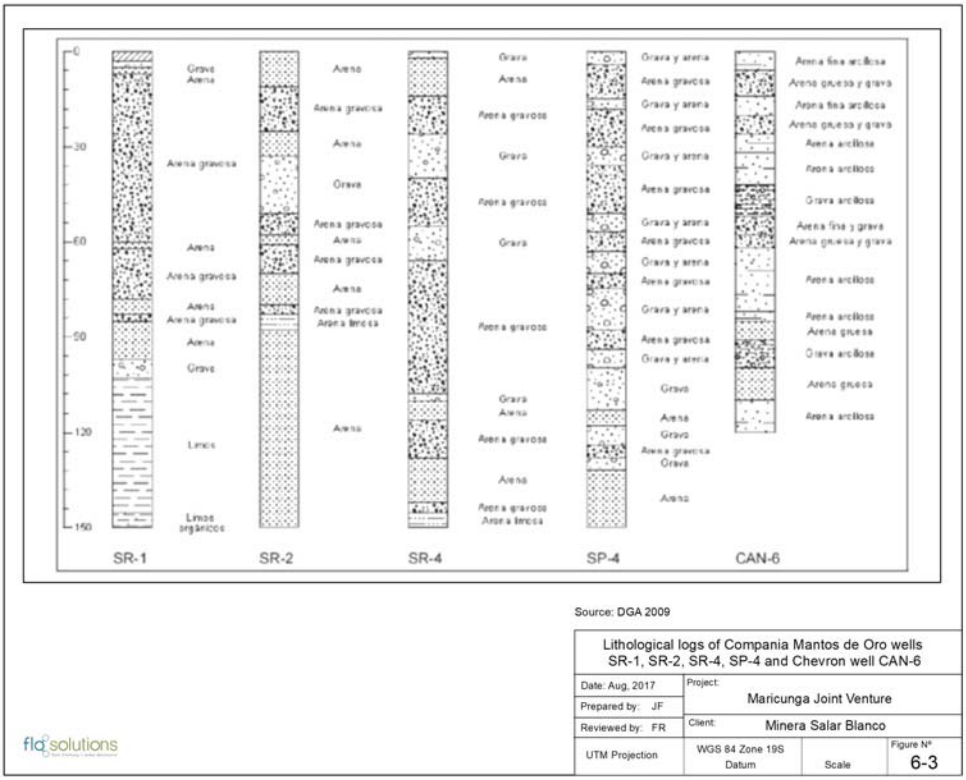

Source: DGA 2009

7 GEOLOGICAL SETTING AND MINERALIZATION

7.1 Regional Geology

The Andean Cordillera in northern Chile is divided in five (Figure 7.1) well-defined morphotectonic units: The Coastal Cordillera and Central Depression, Precordillera (or Cordillera de Domeyko), Preandean depressions (Pedernales and Maricunga basins) and the Western Cordillera (where the Cordillera Claudio Gay separates the Western Cordillera from the Maricunga Basin). The Coastal Cordillera comprise the eroded remnants of Jurassic-early Cretaceous magmatic arc represented by large plutonic complexes, a Jurassic andesitic to basaltic volcanic sequence (La Negra Formation, Garcia, 1967), and Upper Jurassic-Early Cretaceous andesitic to dacitic lavas (Punta del Cobre Group Lara and Godoy, 1998). The main tectonic feature in the Coastal Cordillera is the Atacama Fault System, which originated in the Jurassic as a "trench-linked" structural system along the axis of the early Andean magmatic arc. Backarc Jurassic-early Cretaceous marine and continental sedimentary units appear further east in the Precordillera overlying Late Paleozoic igneous basement units (Cornejo et al., 1993). To the east, in the Precordillera, the Mesozoic back-arc sediments are intruded by Eocene sub volcanic stocks and porphyries and deformed by the Eocene Sierra del Castillo-Agua Amarga fault and Potrerillos Fault and Thrust Belt (Tomlinson et al., 1994; Mpodozis et al., 1995; Tomlinson et al., 1999) which form part of the regionally important Domeyko Fault system. Finally, The Cordillera Claudio Gay is an uplifted basement block, covered by Eocene-Miocene sedimentary and volcanic sequences (Mpodozis and Clavero, 2002).

Figure 7.1 Morphotectonic units of the Andean Cordillera in northern Chile

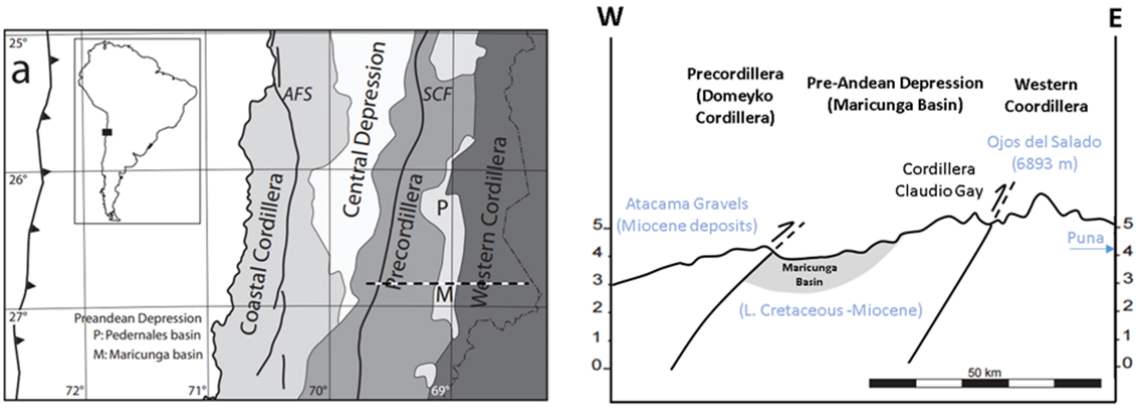

Modified from Nalpas (2008)

The Project is located in the Maricunga Basin within the pre-andean depression. Uplift and denudation should have produced a large amount of sediments during the Cenozoic era. Nevertheless, only the Maricunga and Pedernales Basins preserve a large amount of sediments while in the Precordillera and Central Depression only a thin blanket of Miocene sediments (Atacama Gravels) forms the infill of a Tertiary paleovalley network (Sillitoe et al., 1968 ; Mortimer 1980 ; Riquelme, 2003; Gabalda et al., 2005). The geodynamic framework and geological evolution that makes possible the formation, thickening and preservation of the Maricunga basin is presented and summarized in five stages inside the project area as shown in Figure 7.2.

Figure 7.2 Regional Geology of the Maricunga Basin

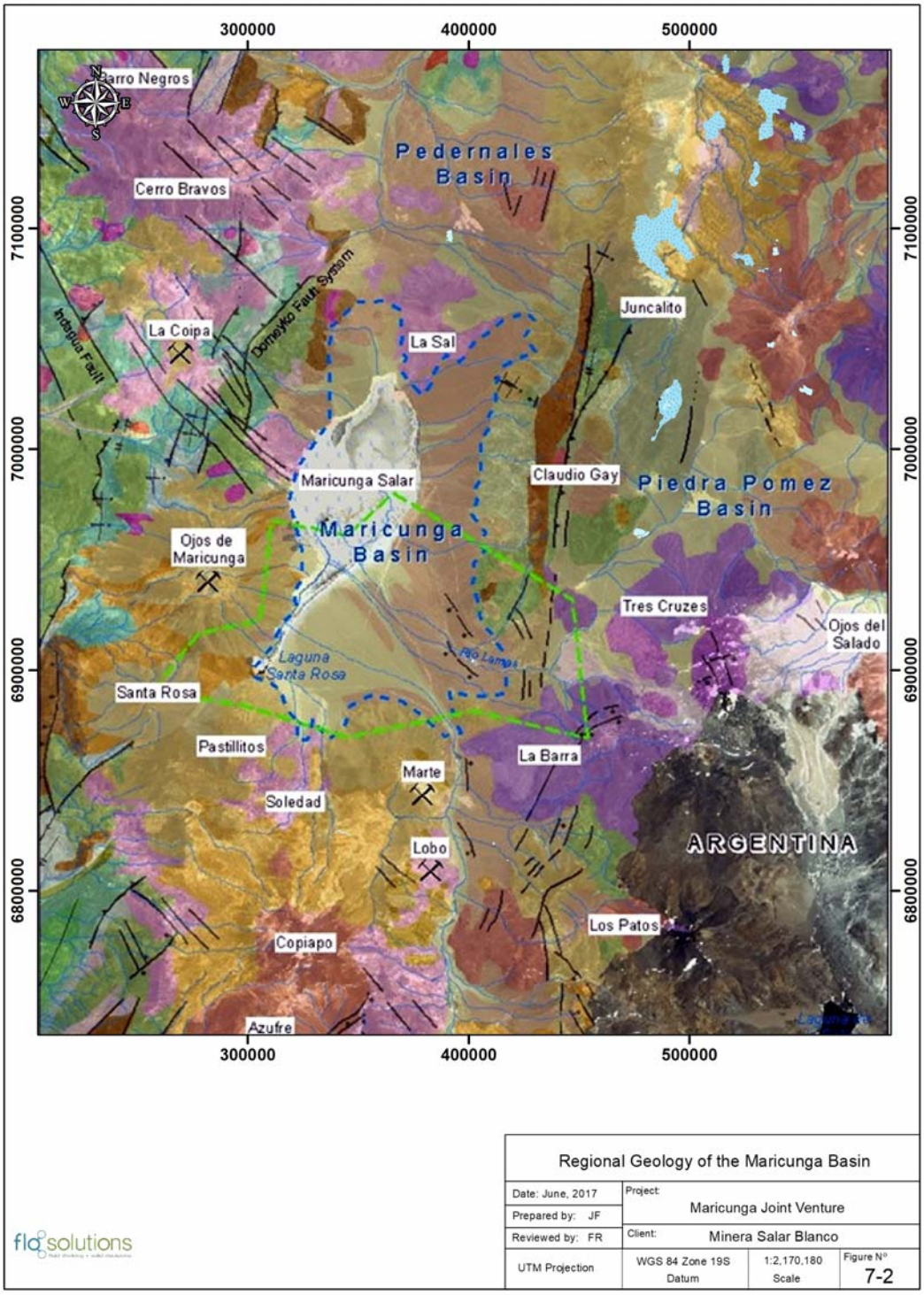

First stage: Pre-Basin evolution (299 to 66 Ma)

The oldest outcrops near the Maricunga basin are related to a Late Paleozoic granitoids and rhyolites in the precordillera and the Claudio Gay cordillera (Mpodozis and Clavero, 2002), they are uplifted basement blocks that are overlain by Devonian to Carboniferous sandstones, shales and mudstones of the Chinches Formation, abruptly covered by Triassic deposits corresponding to the continental El Mono Beds (Mercado 1982; Corneto et al. 1998), consisting of a thick succession of breccias and conglomerates with rhyolitic and andesitic clasts, and intercalations with huge boulders (1m in diameter), laminated black carbonaceous lacustrine shale and sandstones containing Triassic fauna, and matrix-supported conglomerated and sandstones. This succession is continuous with Early Jurassic marine deposits of the Montandón Formation.

Other Mesozoic formations are described near as the Pantanoso Formation or El Leoncito sequence. The Mesozoic cover is formed by sedimentary rocks, mainly arkosic sandstones and carbonaceous black shales of the late Triassic La Ternera Formation (Brüggen, 1950), Jurassic marine limestone and volcanic rocks of the Lautaro Formation, sandstone of the late Jurassic to early Cretaceous Quebrada Monardes Formation, and volcaniclastic rocks of the late Cretaceous Quebrada Seca Formation. The Mesozoic cover is capped by andesitic breccias and agglomerates of late Cretaceous to early Tertiary age.

Second stage: Early volcanic episode (66 to 21 Ma)

During this stage occurred the earliest volcanic episode of the Maricunga arc. This volcanic event erupted over a moderately dipping subduction zone through a crust that was likely near 40 km thick. These centers mark the frontal arc west of the backarc basalt. This is seen in the Cerros Bravos–Barros Negros centers that are located along a NW-trending sinistral strike-slip faults that are part of the Domeyko Fault System (Cornejo et al., 1993; Mpodozis et al., 1995; Tomlinson et al., 1999). K/Ar ages from these centers range from 25 to 21.7 Ma (Mpodozis et al., 1995; Tomlinson et al., 1999). Many of the dome complexes and associated tuff and pyroclastic breccia rings are hydrothermally altered. Epithermal, high-sulfidation, gold-silver and porphyry-style gold mineralization occurred during this stage at La Coipa, Esperanza, and La Pepa (Vila and Sillitoe, 1991; Mpodozis et al., 1995; Muntean and Einaudi, 2001).

Activity at the Cerros Bravos–Barros Negros centers began with the eruption of small-volume rhyodacitic ignimbrites that were subsequently covered by main stage pyroxene and hornblende-andesitic lava and block and ash deposits. Crystal-rich hornblende and dacitic domes were then emplaced in the cores of the stratovolcanoes. A series of subcircular domes that host the Esperanza epithermal gold and silver deposit (Vila and Sillitoe, 1991; Moscoso et al., 1993) were emplaced in an 8-km long belt along a reactivated NW-trending fault zone (Cornejo et al. 1993) on the northeastern flank of Cerros Bravos. The domes at Esperanza are surrounded by a rhyolitic lapilli tuffs with K/Ar ages ranging from 24 to 20 Ma. Alteration ages range from 23 to 19 Ma (Sillitoe et al. 1991; Moscoso et al. 1993). The northeastern most domes are intruded by unaltered dacitic porphyry dikes with biotite K/Ar ages of 22.5 and 22.4 Ma (Cornejo et al., 1993; Kay et al., 1994).

A few kilometers at the south of Cerro Bravos, a multistage dome complex was emplaced at La Coipa. This complex is located where west-verging, north-trending thrusts (Domeyko Fault System) intersect the sinistral northwest-trending (Quebrada Indagua fault). The La Coipa dome cluster K/Ar ages range from 24.6 to 22.9 Ma (Zentilli 1974; Moscoso et al., 1993). The domes are surrounded by an extensive coeval blanket of intensely altered, coarse pyroclastic breccias, and poorly welded lapilli tuffs with biotite

K/Ar ages of 24.7 and 24.0 Ma. Volcanism in the La Coipa region ended with the emplacement of middle Miocene domes (Mpodozis et al., 1995).

Third stage: Compressional and crustal thickening (21 to 17 Ma)

This stage begins with a virtual volcanic lull during a period of compressional deformation and crustal thickening. Evidence for compressional deformation is seen in the Cordillera Claudio Gay (Mpodozis and Clavero, 2002). The depositional regime changed dramatically as east-verging, high-angle reverse faults uplifted the Late Paleozoic basement of the Cordillera Claudia Gay. Intense volcanism followed as large 20–19 Ma dome complexes with extensive block and ash-flow aprons erupted along the northern Cordillera Claudio Gay. These domes are covered by the widespread 18–19 Ma dacitic ignimbrite that has been correlated with the huge Rio Frio ignimbrite (Cornejo and Mpodozis, 1996). All these volcanic deposits are the base of the Maricunga basin.

In the middle Miocene, the Claudia Gay Cordillera was affected by the last compressional deformation in the region of the modern pre-Andean depression. Evidence for this deformation comes from the alluvial gravels interbedded with distal ignimbrites (K/Ar age of 15–16 Ma) in the Rio Lamas sequence. These gravels show progressive unconformities and intraformational folds indicative of synsedimentary deformation (Gardeweg et al., 1997; Mpodozis and Clavero, 2002).

Fourth stage: Stratovolcanic complexes (17 to 11 Ma)

The fourth stage was marked by the construction of voluminous, andesitic to dacitic stratovolcanic complexes along the length of the Maricunga arc. From north to south, these centers include the Ojos de Maricunga, Santa Rosa, Pastillitos volcanoes were emplaced during the inital stages at some centers. Most centers are little eroded and preserve much of their original form. The third stage ended with the emplacement of structurally controlled, shallow-level, quartz-dioritic stocks hosting gold and copper mineralization (Marte, and Lobo, gold porphyries; Vila and Sillitoe, 1991).

The largest group of middle Miocene volcanic centers in the Maricunga Belt is the cluster of stratovolcanoes to the west and south of the Salar de Maricunga. The northernmost of these centers is the well-preserved Ojos de Maricunga volcano (4985 m) with a basal diameter of 15 km and a central crater filled by a dacite dome dated at 15.8 ± 0.9 Ma (whole-rock K/Ar; Mpodozis et al., 1995). The slopes of the volcano are covered by unconsolidated hornblende andesite block and ash deposits that have yielded K/Ar ages from 16.2 ± 0.6 to 15.1 ± 0.7 Ma (Zentilli, 1974; Mpodozis et al., 1995) and a 40Ar/39Ar age of 14.5 ± 0.1 Ma (McKee et al., 1994). The block and ash deposits overlie two ignimbrites of uncertain origin. The older is a welded red tuff (60%–62% SiO2) that is up to 100 m thick and has a wholerock K/Ar age of 15.8 ± 0.8 Ma. The younger, which is exposed on the southwestern slope, is a slightly welded, pumice-rich biotite-bearing ignimbrite with biotite K/Ar ages of 14.3 ± 1.6 Ma and 13.7 ± 2.6 Ma (Zentilli, 1974).

Other middle Miocene volcanic centers to the south are principally made of hornblende- and pyroxene-bearing andesite. They include the Santa Rosa, Cerro Lagunillas, and Pastillitos, volcanoes. Blocks from a coarse blanket of reworked pyroclastic block and ash deposits on the slopes of the Santa Rosa cone have K/Ar ages of 15.4 ± 0.55 Ma (hornblende, McKee et al., 1994) and 13.8 ± 0.6 Ma (whole rock, González-Ferrán et al., 1985). Whole-rock K/Ar ages from a Cerro Lagunillas lava, a block from the Pastillitos center, and a Cerro Las Cluecas lava range from 16.2 ± 0.6 to 15.9 ± 1.4 Ma (Mpodozis et al., 1995).

Fifth stage: Volcanic arc migration (11 to 4 Ma)

A radical change in the distribution of volcanic centers occurred during this stage as most of the volcanic activity at the north of Laguna Negro Francisco became concentrated in the silicic andesitic to dacitic Copiapó volcanic complex. Volcanic activity in the Maricunga Belt from 11 to 7 Ma was largely restricted to the Copiapó volcanic complex at the intersection of the northwest-trending Valle Ancho– Potrerillos fault system with the Maricunga Belt. The silicic andesitic to dacitic pyroclastic flows, domes, and lavas that make up the Copiapó complex cover an area of more than 200 km2.

The Ojos del Salado volcanic region is located near the southern termination of the modern Central Volcanic Zone near 27°S latitude. This region is home to the Central Volcanic Zone arc and the late Oligocene to Miocene volcanic centers that erupted in the backarc of the Maricunga arc, which is over 40 km to the west. Between 9 and 6 Ma, the Maricunga arc volcanic activity dramatically decreased and then ceased as volcanism increased significantly in the backarc. By 4 Ma, the main frontal volcanic arc was essentially in the Ojos del Salado region. The distribution, age, and geochemistry of the Ojos del Salado region volcanic rocks reflect complex magmatic-tectonic interactions associated with arc migration, crustal thickening, and uplift (Mpodozis et al., 1996; Kay et al., 2006). Considering the modern subduction geometry and assuming that the magmatic front of the Maricunga arc was located around 100 km above the subducting Nazca slab, a significant portion of the forearc crust and frontal arc lithosphere should have been removed from below this region after 8 Ma (Kay and Mpodozis, 2002; Kay et al., 2006).

The late Miocene to Pliocene is marked by the eruption of small-volume bimodal centers at the southern end of the Maricunga arc. These eruptions include ignimbrites associated with the fault-controlled Jotabeche rhyodacitic caldera and glassy mafic andesitic to andesitic Pircas Negras lavas emplaced along faults (Mpodozis et al., 1995; Kay et al., 1994). The chemistry (very high La/Yb ratios and Na2O and Sr contents) of these magmas are uncommon in the central Andes and have been associated with a very thick crust and contamination of the mantle wedge by crustal material removed from the forearc by subduction erosion. Climatic conditions change from 9 to 10 Ma to a hyper-arid climate (Hartley and May, 1998), both sedimentation and erosion came to a halt. This is also attributed to an important change on the mass transfer regime that occurred between the Oligocene when all the sediments are exported out of the drainage system towards the ocean, and the Miocene, when the sediments started to accumulate along the drainage network (Nalpas et al., 2008).

7.2 Local Geology

Based on the drilling campaigns carried out in the Salar between 2011 and 2016, ten major geological units were identified and correlated from the detailed geological logging of drill cuttings and undisturbed core to a general depth of up to 200 m. One deep borehole (S-19) was drilled to a depth of 360 m. No boreholes reached bedrock. Salar de Maricunga is a mixed style salar, with a halite nucleus of up to 34 m in thickness in the central northern part. The halite unit is underlain by a clay core on the eastern and central part of the Salar. The clay is locally interbedded with silt and silty sands. The Salar is surrounded by relative coarse grained alluvial and fluvial sediments These sedimentary fans demark the perimeter of the actual salar and at depth grade towards the center of the Salar where they form the distal facies with an increase in sand and silt. At depth two un-consolidated volcaniclastic units have been identified that appear quite similar. These two volcaniclastics are separated by a relatively thin and continuous sand unit which may be reworked material of the lower volcaniclastic unit. Figure 7.3 is a W-E Section through the Salar schematically showing the geological model.

Figure 7.3 W-E Section showing the Maricunga geological model, looking north

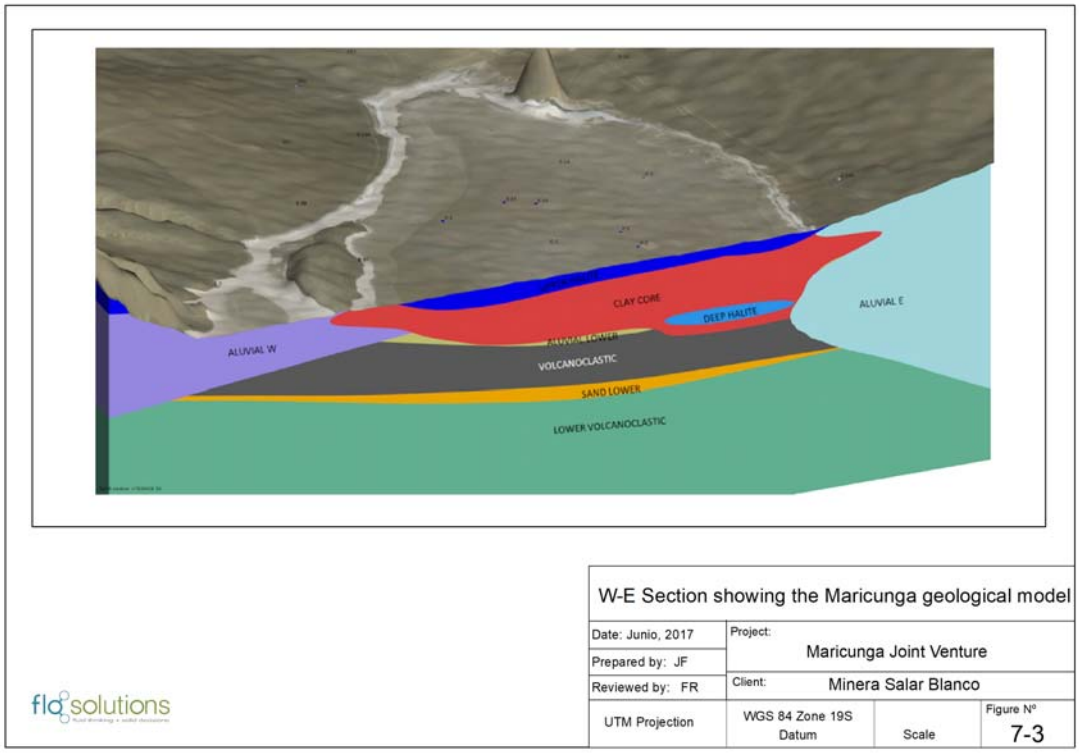

Upper Halite

The nucleus of the Salar is comprised of a halite crust. This unit is characterized by coarse translucent crystals of (1 to 10 mm) of euhedral halite Figure 7.4. Locally it has traces of interstitial clay and /or ulexite and minor thin strings of clay with halite.

The halite crust thickens towards the center and north. The halite has a thickness of 30 m in borehole C-2 and 34 m in P-2. Halite pinnacles of up to 60 cm height have developed in the central part of the Salar (Rugosa crust) showing an absence of flooding in this area. In the south (holes S-8 and C-5) the halite unit has a thickness of approximately 1 m; and in the north (holes S-1A, C-1, S-10 and S-19 a thickness of approximately 6 m. Towards the edges of the Salar the crust thins, until it is a saline efflorescence surface that includes areas of re-solution and precipitation from rainwater or recent flooding. Figure 7.5 is a North-South section through the Salar showing the distribution of the Upper Halite. Figure 7.6 is an isopach map on the Upper Halite showing the thickness of this unit.

Figure 7.4 Photo of the Upper Halite

Figure 7.5 N-S Section showing the distribution of the Upper Halite unit

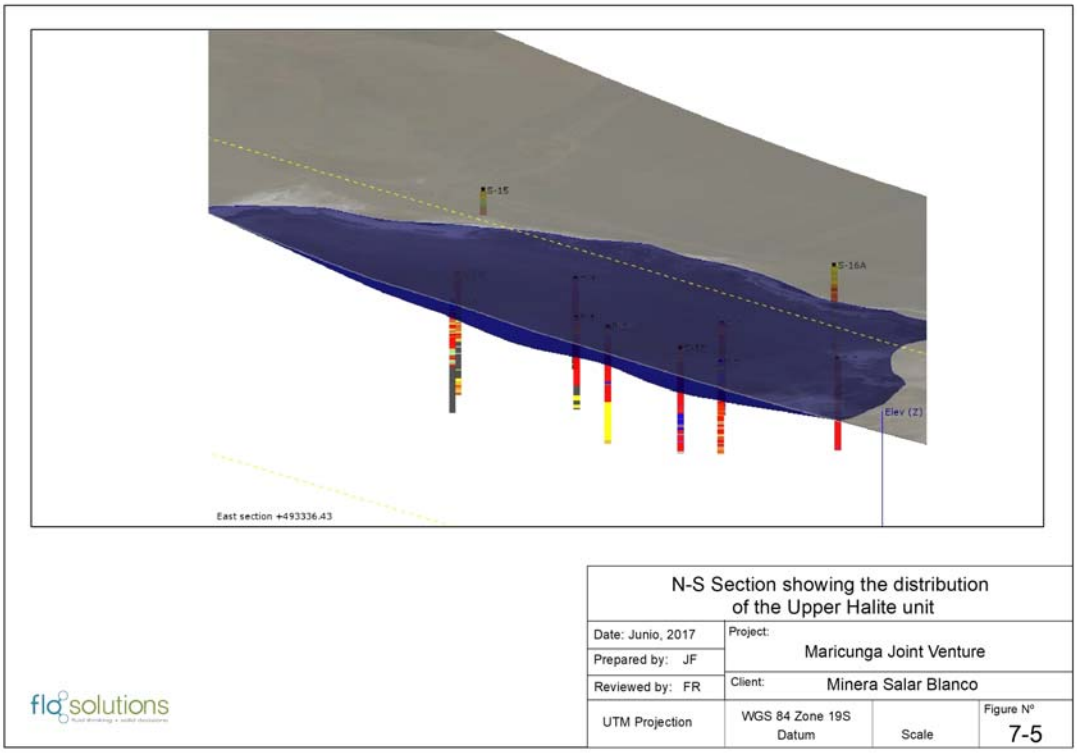

Figure 7.6 Isopach map on the Upper Halite

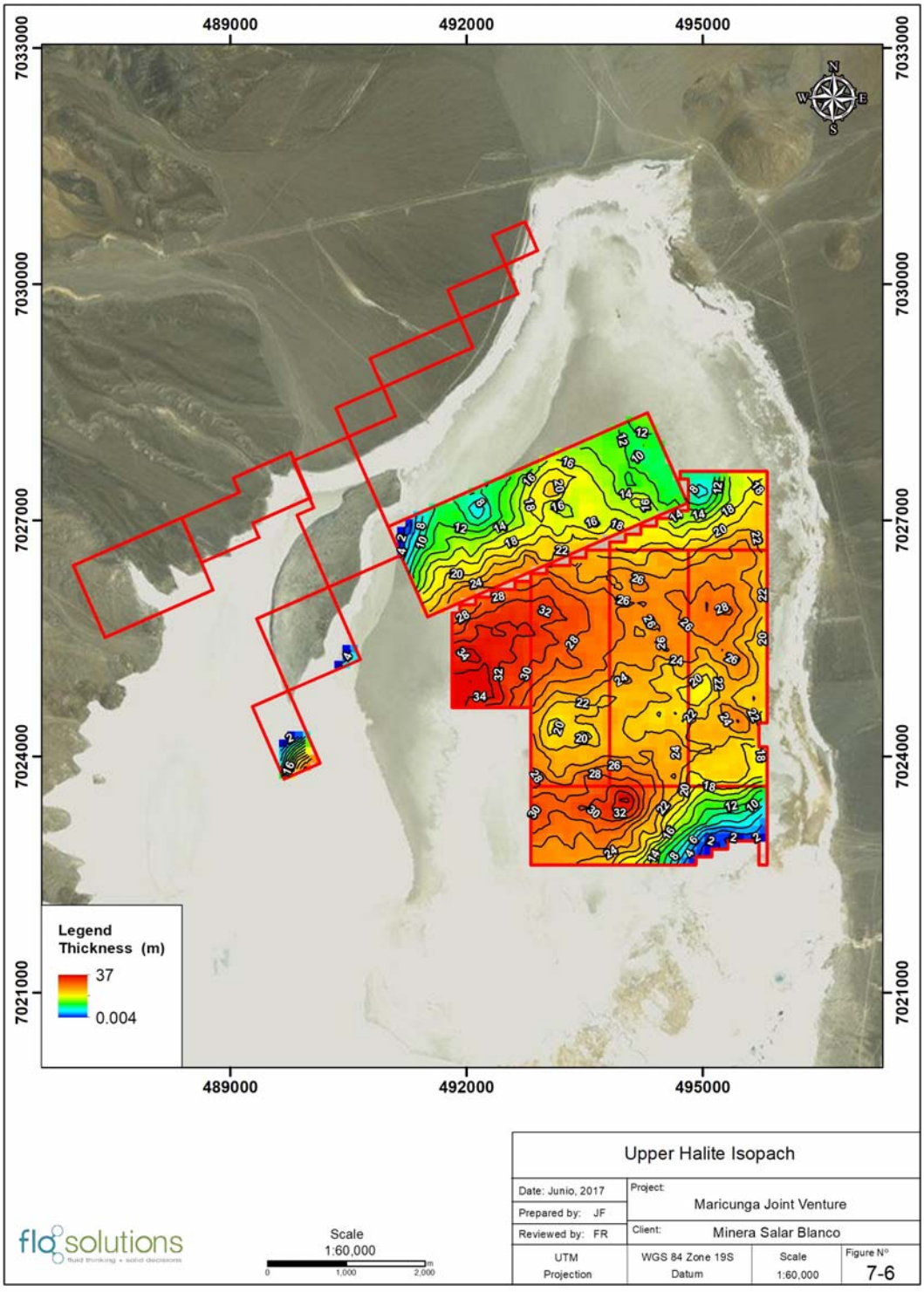

Clay Core

Immediately beneath the Upper Halite unit, a thick clay unit was identified with a thickness of up to 140 m (Hole S-18) and which thins towards the edges of the Salar (Figure 7.7). This Clay Core unit extends below the alluvial sediments on the east side of the basin (the East Alluvium unit as further described below) as identified in hole S-16. Geological logs of previously drilled boreholes (by Minera Mantos de Oro) MDO-08, MDO-10, MDO-24 and CAN-6 suggest that the Clay Core continues as far south as under the Rio Llamas fluvial fan. Figure 7.8 shows an isopach map on the Clay Core.

The clay core is well defined by the sonic boreholes C1-C6 in the *Litio 1-6* concessions, although not all holes penetrated the full thickness of the Clay Core. The unit is characterized by reddish, green, brown and in small amounts black clays in horizontal parallel layers with occasional 1 m interbedded layers of ulexite (Figure 7.9).. Locally and near the edges of the Salar the Clay Core is intercalated locally with fine layers of sand and towards the center of the Salar with thin layers of halite. At the contact with the overlying Upper Halite the Clay Core contains abundant disseminated halite crystals (up to 50%).

Figure 7.7 N-S section showing the Clay Core, looking west

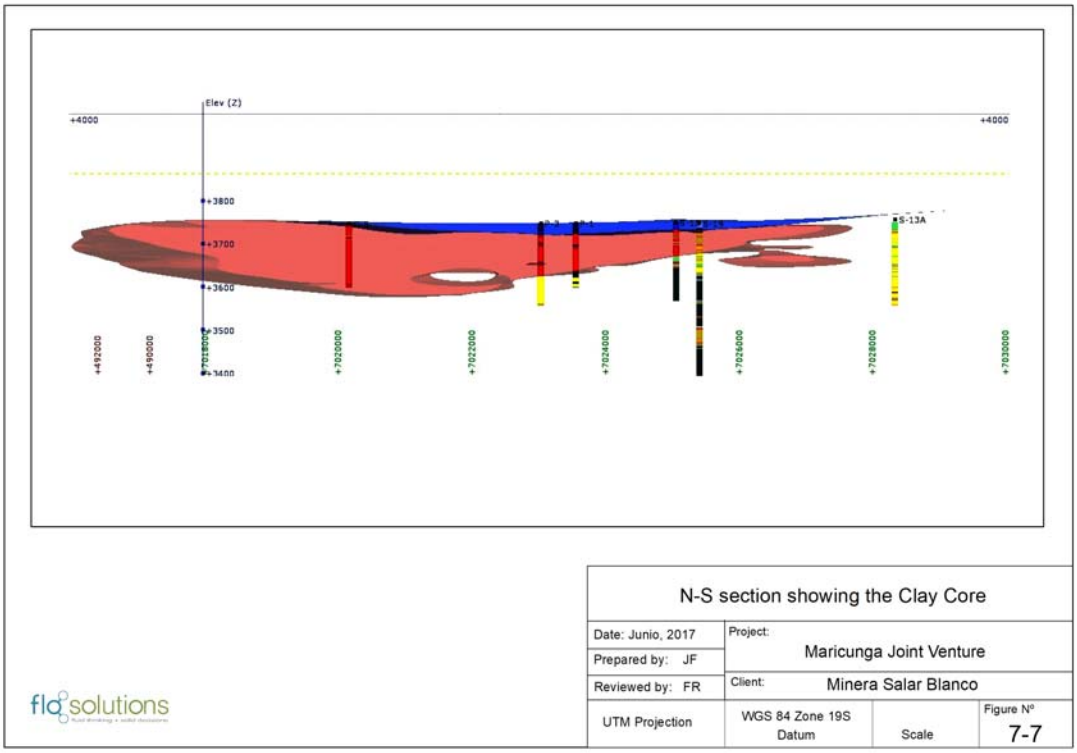

Figure 7.8 Isopach map on the Clay Core

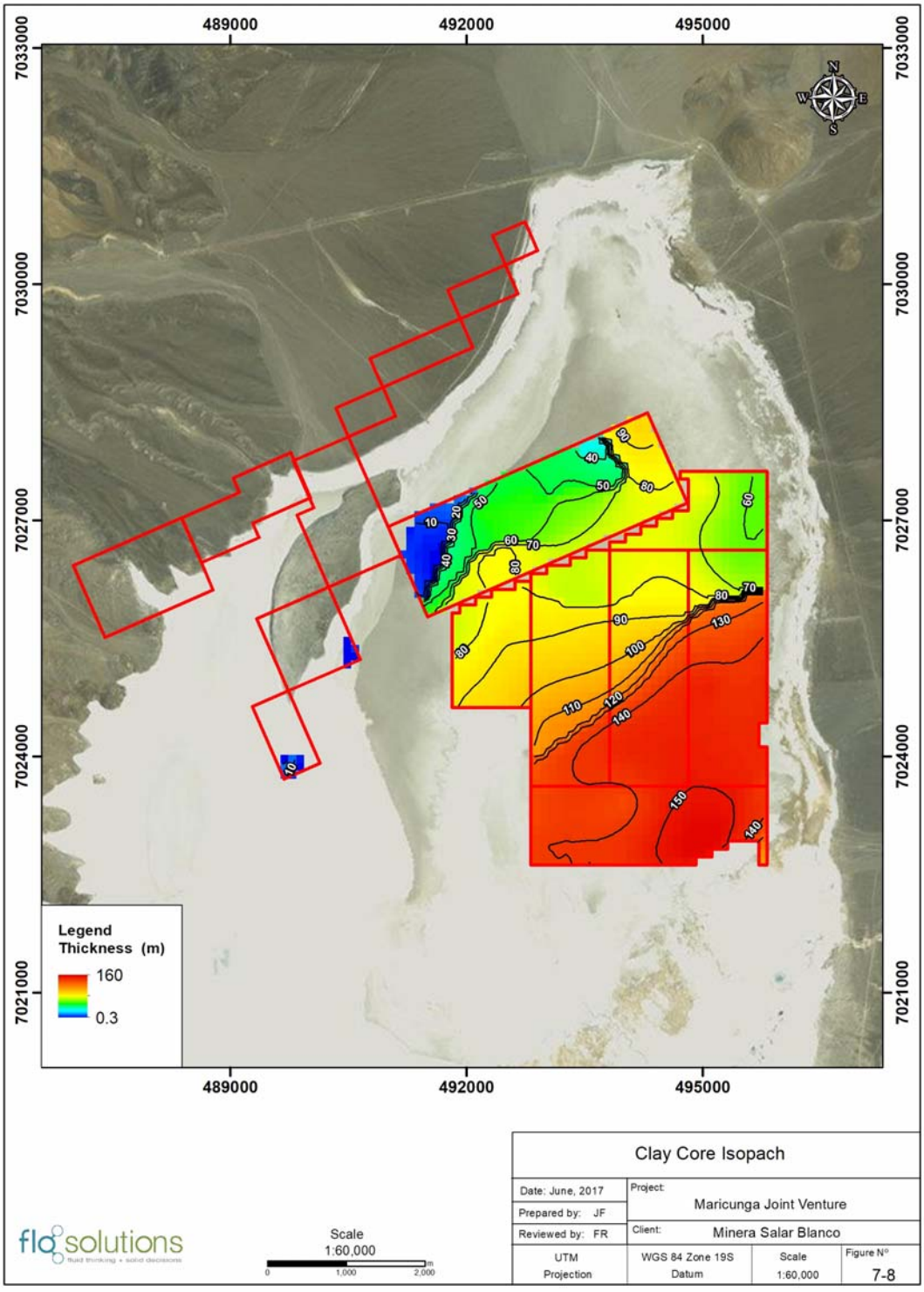

Figure 7.9 Photo of the Clay Core unit

Deep Halite

A Deep Halite unit was identified between boreholes S-18 and C-3. This Deep Halite unit has a thickness of up to 20 m and was interested at a depth of around 110 m; it is entirely contained within the Clay Core unit (Figure 7.10). This unit is characterized by whitish, massive compacted halite with crystals of between 1 to 5 mm with interstitial clay and ulexite. A fine layer of black clay and some ulexite with a thickness of approximately 1 m was also identified in these two boreholes.

Figure 7.10 Section between boreholes S-18 and C-2 showing the distribution of the Deep Halite

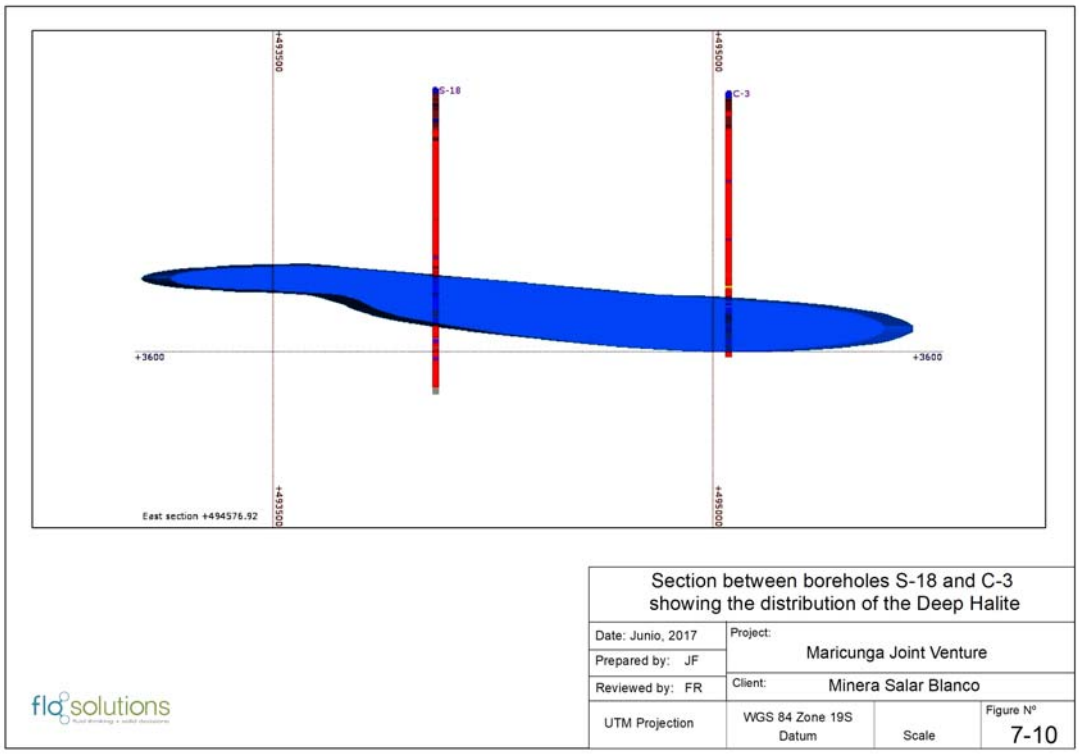

East Alluvium

The unit was identified in the boreholes S-15, S16, S-17 drilled on the east side of the Salar. The East Alluvium is present along the entire eastern side of the Salar and is interbedded with layers of sand. It forms the foothills of the Claudio Gay Range (the eastern limit of the basin). Figure 7.11 shows the lateral distribution of the East Alluvium. In the area of borehole S-16 it is inter-fingered with clays and sands of the Salar's nucleus.

The unit is characterized by a heterogeneous sequence of clayey gravels made up of many sub-rounded clasts of up to 5 cm in a matrix of brown clayey-silty sand and grading at depth into finer-grained layers of brown silty- and clayey sands. At the surface one can find sands (S-16A) and gravels (S-15),

Figure 7.11 Distribution of the East Alluvium

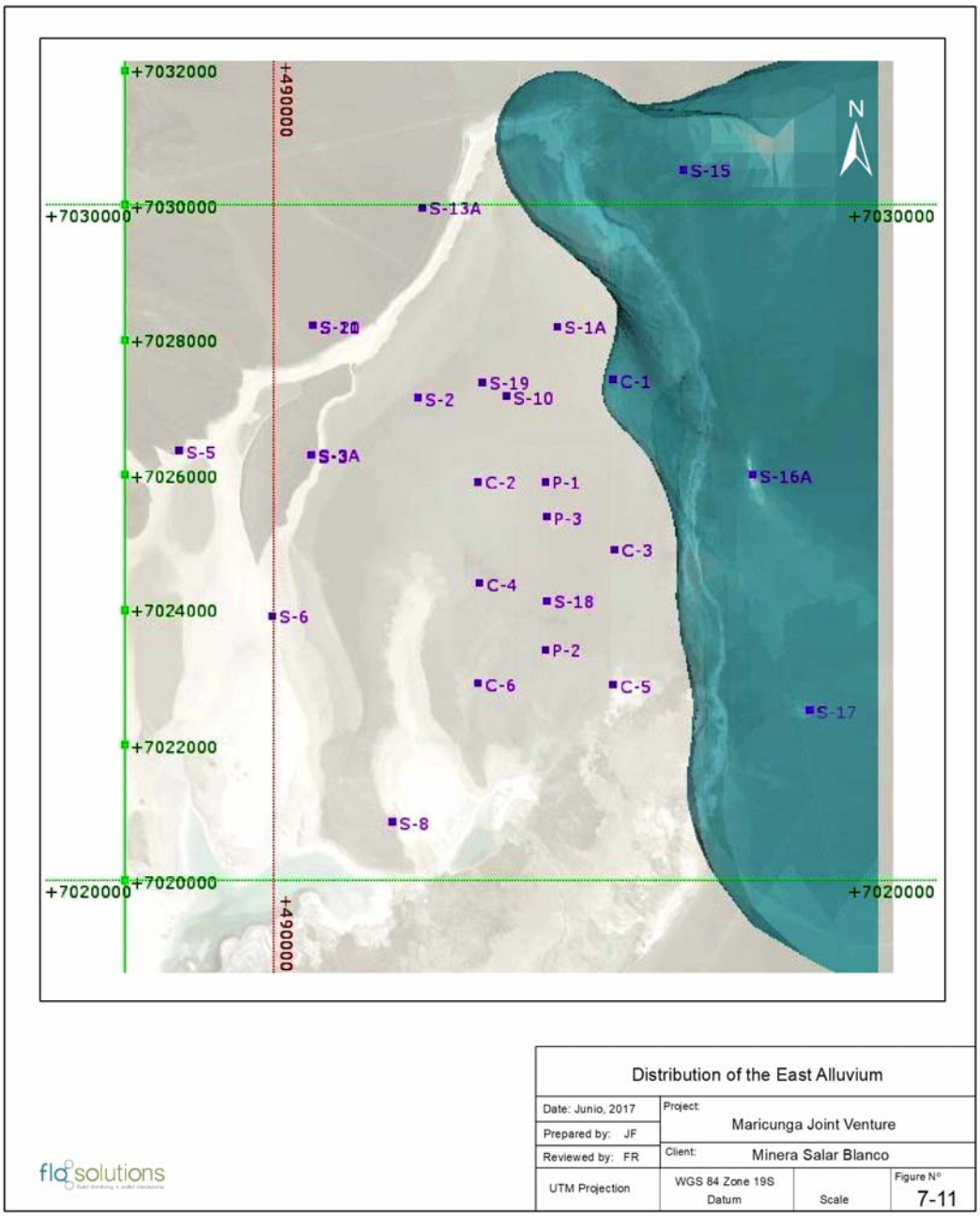

NW Alluvium

The northwestern part of the Salar is characterized by a series of W-E fluvial/alluvial fans, associated with recent intermittent drainages and older drainage systems that form the limit of the basin in the area around Quebrada Caballo Muerto. Figure 7.12 shows the lateral extent of the NW Alluvium.

The unit was encountered and correlated between boreholes S-11 [M2], S-13A, S-3A and S-10. The Lower Alluvium (described below) is interpreted as the distal and deep facies of the NW Alluvium. The NW Alluvium is characterized by a sequence of gravels and sandy gravels with rounded and sub-rounded clasts. Locally it can contain layers of coarse- to very coarse sands. Figure 7.13 shows the texture of the NW alluvium.

Figure 7.12 Distribution of the NW Alluvium

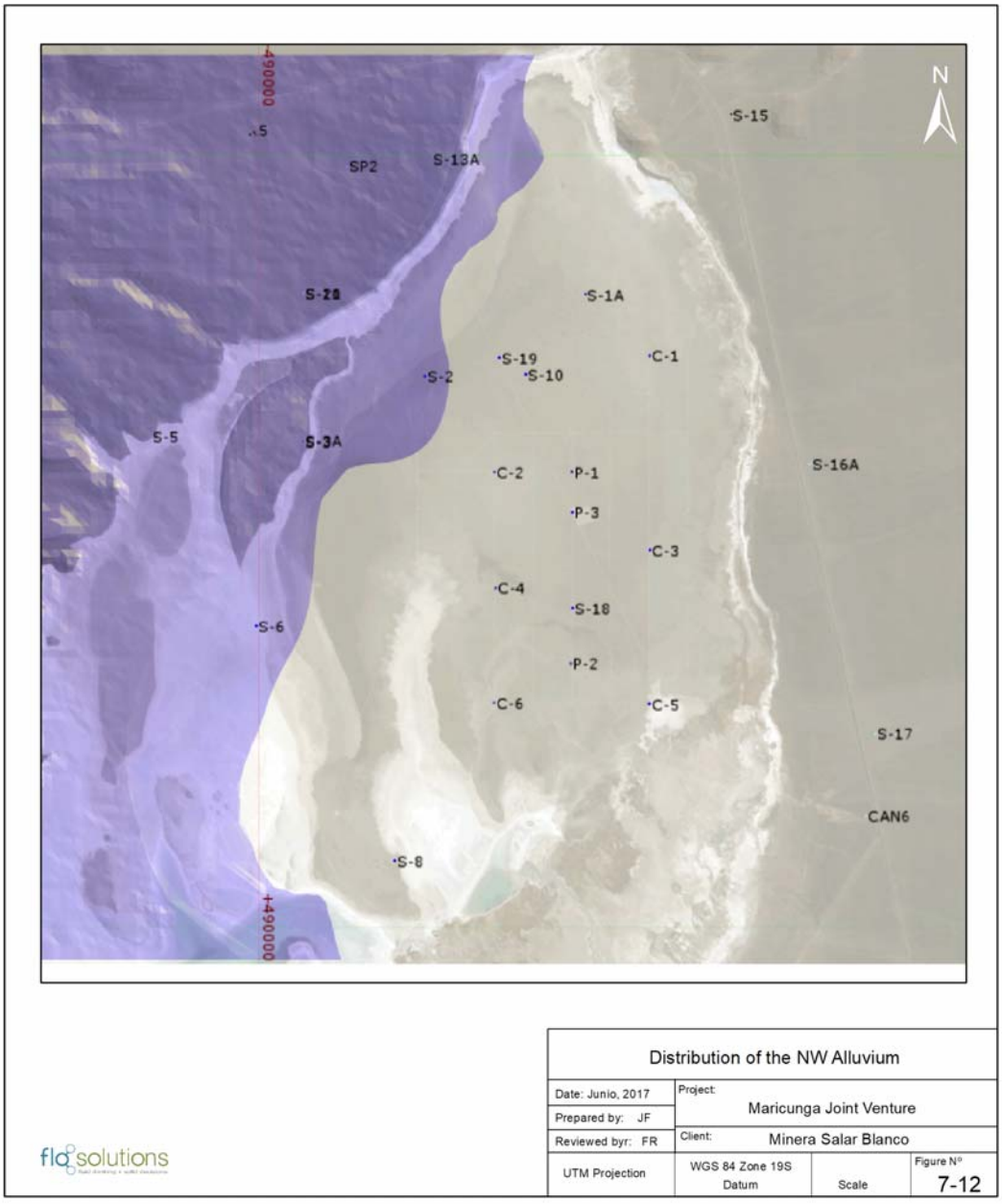

Figure 7.13 The NW Alluvium

Lower Alluvium

The Lower Alluvium consists of gravels, sands and silty sands and is spatially interpreted as the distal part of NW Alluvium system that enters the salar from the northwest. This unit is inter-fingered with the Clay Core further east in the salar. The Lower Alluvium is interpreted in part as reworked material of the underlying volcaniclastic sequences. The Lower Alluvium was encountered in boreholes S-1A [M1A], S-2, S-10, S-19, C-1, C-2 y C-4. Figure 7.14 shows the spatial distribution of the Lower Alluvium and Figure 7.15 shows drill cuttings of the Lower alluvium.

Figure 7.14 E-W section with the spatial distribution of the Lower Alluvium

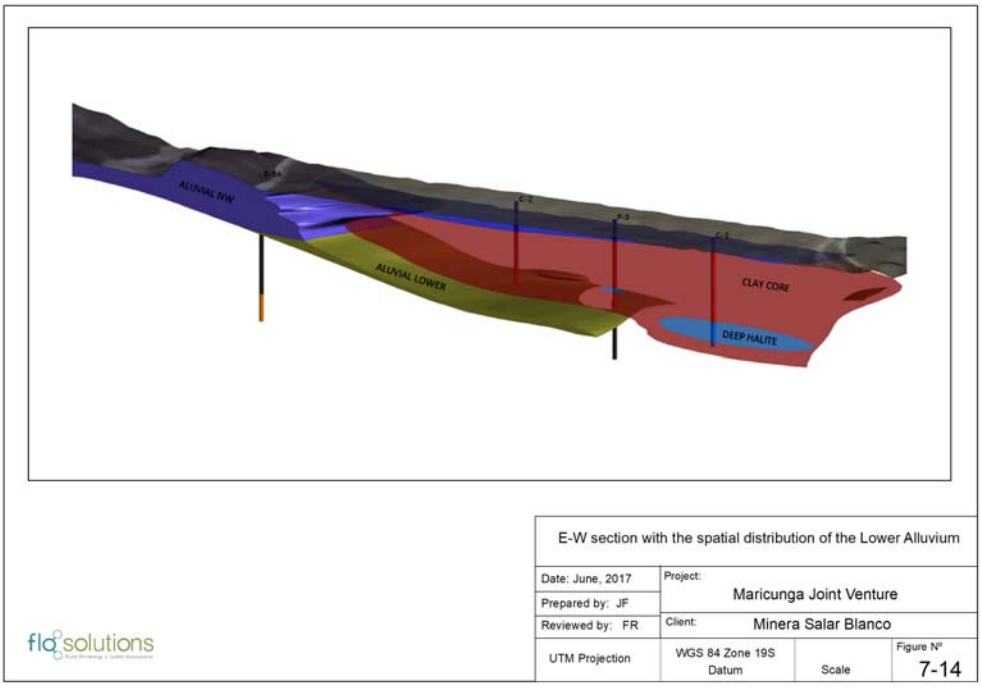

Figure 7.15 Drill core and cuttings of the Lower Alluvium

Volcaniclastic

This Volcaniclasticsunit is found in numerous wells (C-1, C-2, P-1, S-1A, S-2, S-3A, S-5, S-6, S-10, S-11, S-13A and S-19). It is comprised of an array of friable volcaniclastic material, matrix supported, with some 1 to 15 mm isolated grey, brown and reddish sub-angular aphanitic clasts (3-5%) and abundant whitish pumice fragments in a light brown silty matrix (volcanic ash) as shown in Figure 7.16. The unit is unconsolidated and it interpreted as a volcanics air-fall deposit.

The unit has a tilted wedge shape distribution with the greatest thickness to the west (borehole S-11: 139 m) and deepening to the east. The spatial distribution of the unit is shown in Figure 7.17 and Figure 7.18 shows an isopach map for the unit.

Figure 7.16 Drill core of the Volcaniclastic material

Figure 7.17 W-E section showing the spatial distribution of the Volcaniclastics

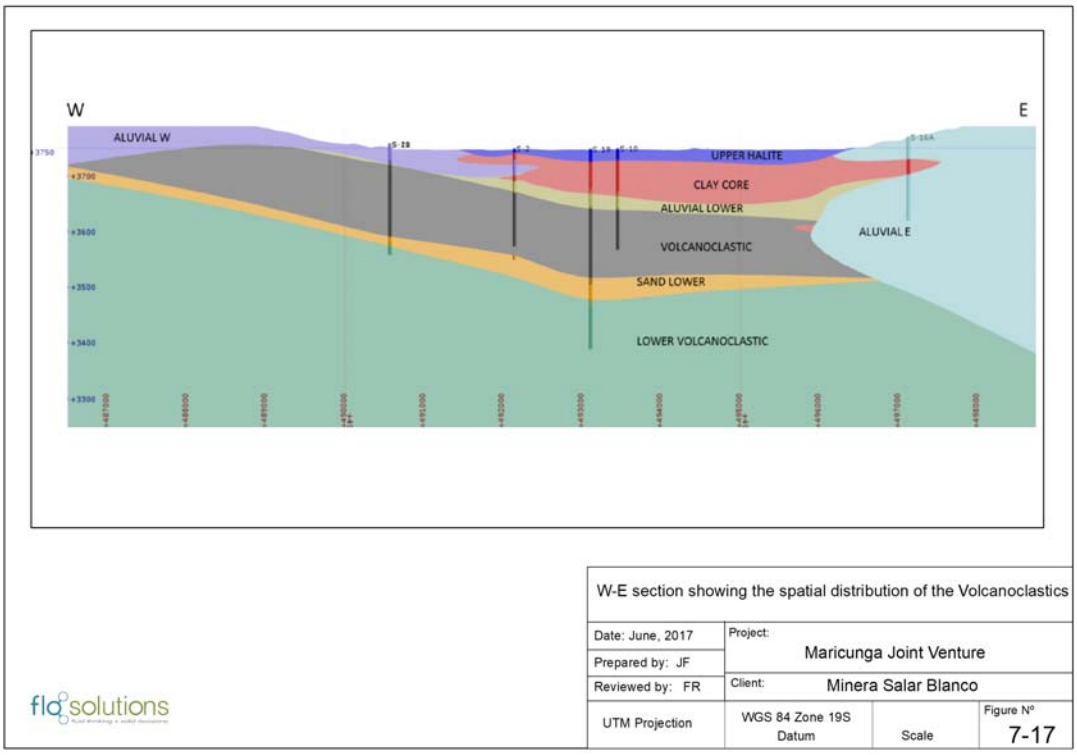

W-E section showing the spatial distribution of the Volcanoclastics			
Date: June, 2017	Project: Maricunga Joint Venture		
Prepared by: JF			
Reviewed by: FR	Client: Minera Salar Blanco		
UTM Projection	WGS 84 Zone 19S Datum	Scale	Figure Nº 7-17

Figure 7.18 Isopach map on the Volcaniclastics Unit

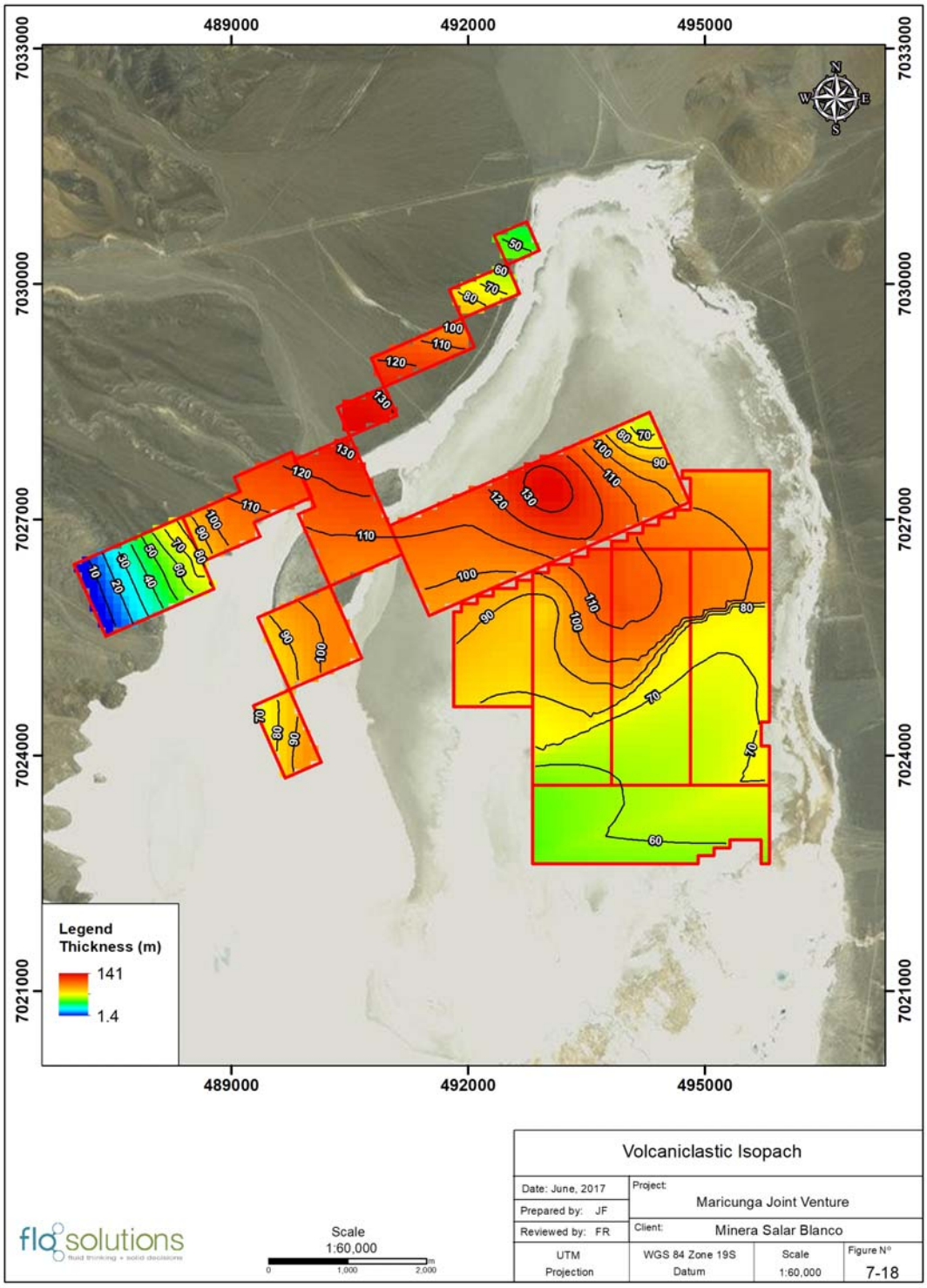

Lower Sand

The Lower Sand is a well-defined unit that separates the overlying Volcaniclastic from the Lower Volcaniclastic (describe below). The Lower Sand was identified in boreholes S-1A [M1A], S-3A, S-5, S-6, S-11, S-13A and S-19 and can be interpreted as reworked material of the underlying Volcaniclasticssequence, indicating a gap in the eruption. Figure 7.19 shows the spatial distribution and isopach contours on the Lower Sand. The unit consists of fine to medium grained sand and locally it can include fine to coarse sand with traces of silt. Figure 7.20 shows drill cutting of the Lower Sand.

Figure 7.19 Isopach map of the Lower Sand

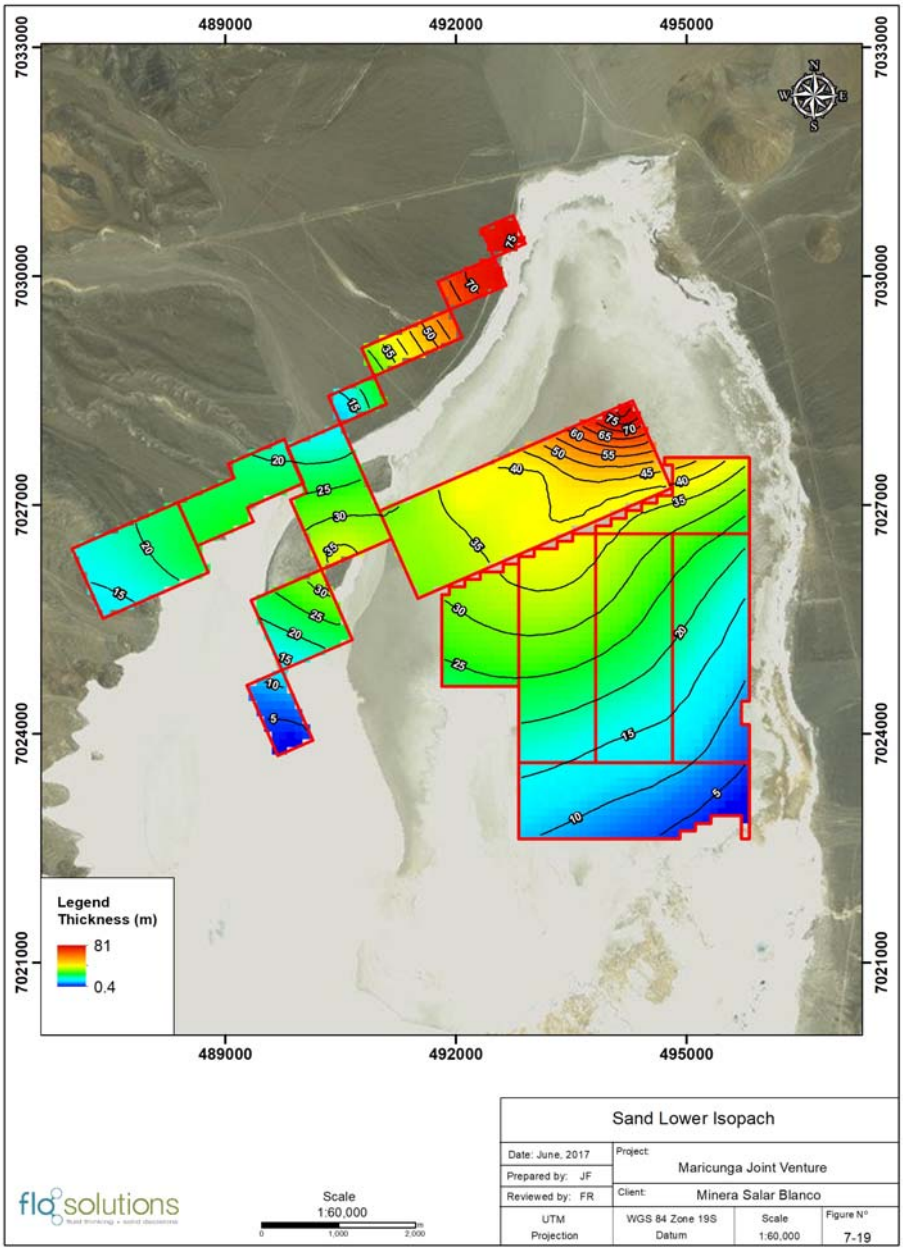

Figure 7.20 Drill cuttings of the Lower Sand (Borehole S-5)

Lower Volcaniclastic (LV)

The oldest and deepest unit in the Salar consists of volcaniclastics identified in boreholes S-5, S-6, S-11 and S-19. The unit has a thickness of 78 m in borehole S-19. No borehole has penetrated the full thickness of the LV and therefore its thickness is not known. This LV unit is characterized by a homogeneous sequence of friable volcaniclastics and is very similar in composition to the upper volcaniclastics unit.

7.3 Mineralization

The brines from Maricunga are solutions saturated in sodium chloride with an average concentration of total dissolved solids (TDS) of 311 g/L. The average density is 1.20 g/cm3. The other components present in the Maricunga brine are K, Li, Mg, Ca, SO_4, HCO_3 and B. Elevatedvalues of strontium (mean of 359 mg/L) also have been detected.

Table 7.1 shows a breakdown of the principal chemical constituents in the Maricunga brine including maximum, average, and minimum values, based on 487 brine samples used in the brine resource estimate herein that were collected from the 2011 and 2016 drilling programs and analyzed at the University of Antofagasta.

Table 7.1 Maximum, average and minimum elemental concentrations of the MJV brine

Analyte	HCO_3	B	Ca	Cl	Li	Mg	K	Na	SO4	Density
Units	mg/L as $CaCO_3$	mg/L	mg/L	mg/L	mg/L	mg/L	mg/L	mg/L	mg/L	g/cm^3
Maximum	2,730	1,193	36,950	230,902	3,375	21,800	20,640	104,800	2,960	1.31
Average	471	596	13,490	190,930	1,123	7,337	8,237	85,190	709	1.20
Minimum	76	234	4,000	89,441	460	2,763	2,940	37,750	259	1.10

Figures 14.3 and 14.4 show the kriged lithium and potassium concentration distribution in the Salar at approximate 30 m, 70 m and 130 m depth. Typically, high and low concentrations of lithium and potassium are correlated. The kriged three-dimensional distribution of lithium and potassium concentrations were used in the updated resource model as further described in Section 14.

Brine quality is evaluated through the relationship of the elements of commercial interest, such as lithium and potassium, with those components that in some respect constitute impurities, such as Mg, Ca and SO_4. The calculated ratios for the averaged chemical composition are presented in Table 7.2.

Table 7.2 Average values (g/L) of key components and ratios for the Maricunga brine

K	Li	Mg	Ca	SO_4	B	Mg/Li	K/Li	$(SO_4+2B)/(Ca+Mg)^*$
8.23	1.12	7,34	13.49	0.71	0.60	6.55	7.35	0.092

*SO_4+2B/ (Ca+Mg) is a molar ratio

As indicated in Table 7.2, the brines from Maricunga have an Mg/Li ratio (6.6) very similar to the Atacama brine (6.4). However, Maricunga has a low sulfate content, which is illustrated by the very low molar ratio (SO_4+2B)/(Mg+Ca) that is also influenced by a relatively high calcium content. This is an advantage as it will reduce lithium losses as lithium sulfate salts in the ponds when a conventional solar evaporation process is used to recover the lithium. Treatment of the brine to remove the calcium would make the process similar to that utilized by SQM and Albermarle at Salar de Atacama.

As in other natural brines in the region, such as those of the Salar de Atacama and Salar del Hombre Muerto, the higher content of ions Cl^-, $SO_4^=$, K^+, Mg^{++}, Na^+ at Maricunga, allows a simplification for the study of crystallization of salts during an evaporation process. The known phase diagram (Janecke projection) of the aqueous quinary system (Na^+, K^+, Mg^{++}, $SO_4^=$, Cl^-) at 25°C and saturated in sodium chloride (equilibrium data in the technical literature) can be used when adjusted for the presence of lithium in the brines. The Janecke projection of $MgLi_2$-SO_4-K_2 in mol % is used to make this adjustment. The Maricunga brine composition has been represented in this diagram (field of KCl), as shown in Figure 7.21 along with brine compositions from other salars. The Maricunga brine composition is compared with those of Silver Peak, Salar de Atacama, Salar del Hombre Muerto, Salar de Cauchari, Salar de Rincon and Salar de Uyuni in Table 7.3.

Figure 7.21 Comparison of brines from various salars in Janecke Projection

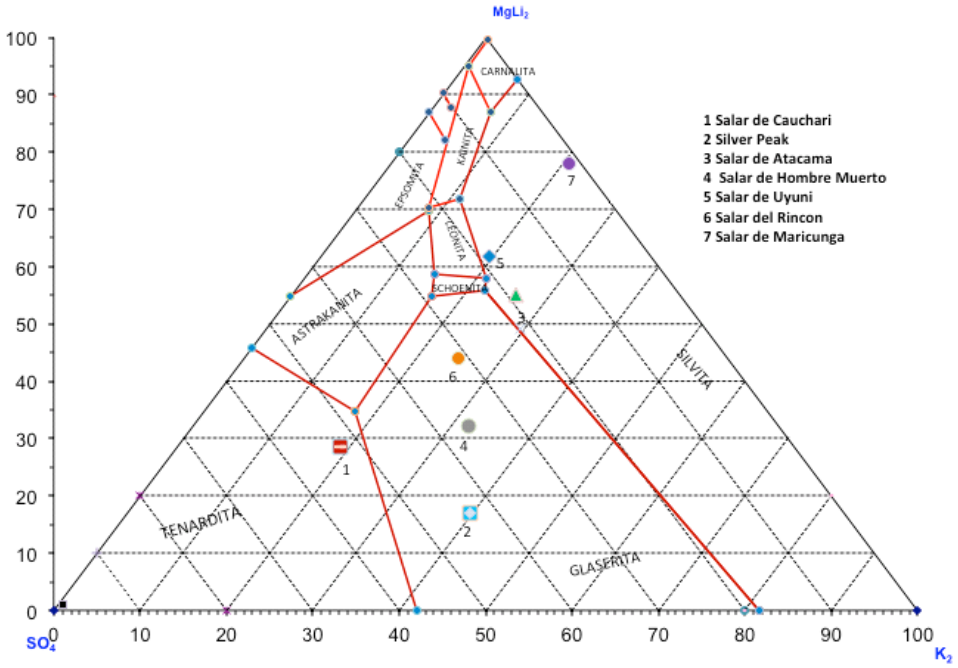

Table 7.3 Comparative chemical composition of various salars (weight %)

	Salar de Maricunga (Chile)	Silver Peak (USA)	Salar de Atacama (Chile)	Hombre Muerto (Argentina)	Salar de Cauchari (Argentina)	Salar del Rincon (Argentina)	Salar de Uyuni (Bolivia)
Na	7.10	6.20	7.60	9.79	9.55	9.46	8.75
K	0.686	0.53	1.85	0.617	0.47	0.656	0.72
Li	0.094	0.023	0.150	0.062	0.052	0.033	0.035
Mg	0.61	0.03	0.96	0.085	0.131	0.303	0.65
Ca	1.124	0.02	0.031	0.053	0.034	0.059	0.046
SO_4	0.06	0.71	1.65	0.853	1.62	1.015	0.85
Cl	15.91	10.06	16.04	15.80	14.86	16.06	15.69
HCO_3	0.039	n.a.	Traces	0.045	0.058	0.030	0.040
B	0.050	0.008	0.064	0.035	0.076	0.040	0.020
Density	1.200	n.a.	1.223	1.205	1.216	1.220	1.211
Mg/Li	6.55	1.43	6.40	1.37	2.52	9.29	18.6
K/Li	7.35	23.04	12.33	9.95	9.04	20.12	20.57
SO_4/Li	0.64	30.87	11.0	13.76	31.06	31.13	24.28
SO_4/Mg	0.097	23.67	1.72	10.04	12.33	3.35	1.308
Ca/Li	9.5	0.87	0.21	0.86	0.65	1.79	1.314

Source: Published data from various sources

8 DEPOSIT TYPE

8.1 General

Salars occur in closed (endorheic) basins without external drainage, in dry desert regions where evaporation rates exceed stream and groundwater recharge rates, preventing lakes from reaching the size necessary to form outlet streams or rivers. Evaporative concentration of surface water over time in these basins leads to residual concentration of disslved salts (Bradley et al., 2013) to develop saline brines enriched in one or more of the following constituents: sodium, potassium, chloride, sulfate, carbonate species, and, in some basins, metals such as boron and lithium.

Houston et al., 2011 identified two general categories of salars: 1) mature, halite dominant, and 2) immature, clastic dominant. Figure 8.1 shows the general conceptual model for each salar type.

Figure 8.1 Conceptual model for mature and immature salars showing the distribution of the facies and the main hydrogeological components. (Houston, *et al*., 2011.)

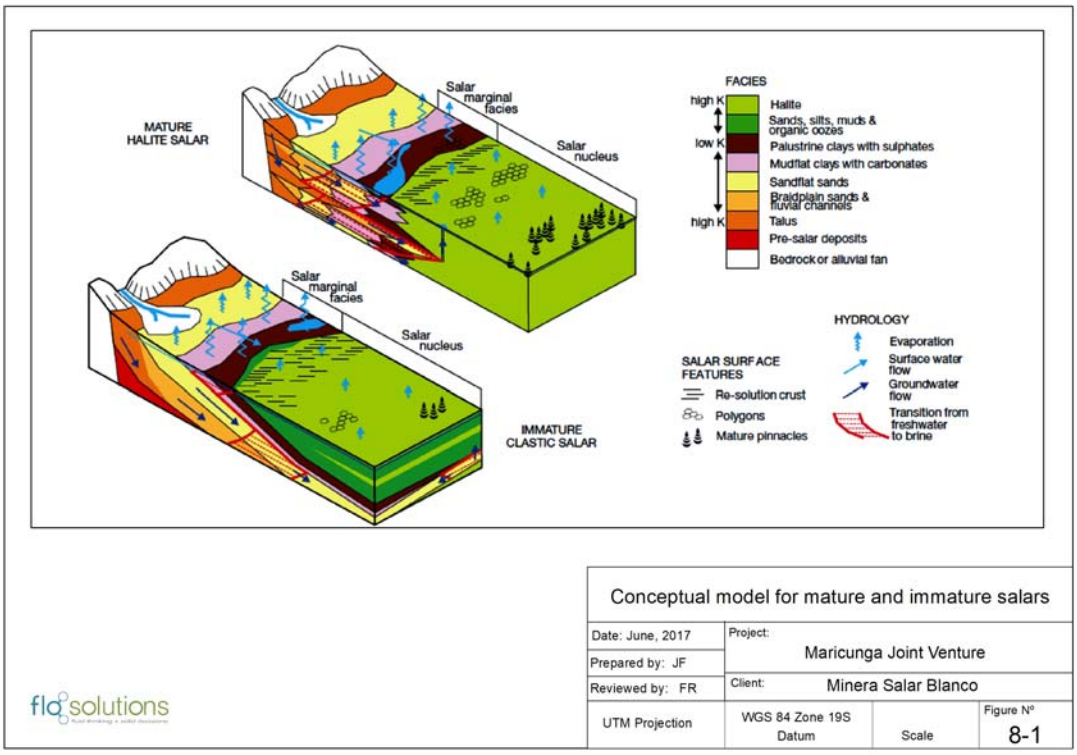

Immature salars are characterized by increased humidity (increased precipitation, less evaporation) and are more frequent at higher elevations and in the wetter northern and eastern parts of the region. They are characterized by alternate sequences of fine grained sediments and evaporitic beds of halite and/or ulexite, indicating the changes in sediment supply due to variable tectonic and climate history (Houston, et al., 2011). Immature salars include Olaroz, Cauchari, Diablillos and Centenario.

Mature salars are less humid and tend to be more common in lower and drier areas of the region. They are characterized by a relative thick and uniform sequence of halite deposits in variable sub-aquatic and

sub-aerial conditions. Nevertheless, ancient floods leading to widespread silty clay deposits and volcanic fallout have led to thin intercalated beds that can be recognized in drill core and geophysical surveys. The central portion of Salar de Atacama is a typical mature setting.

Salar de Maricunga, is a mixed type. The northern part of Salar de Maricunga has a well-developed halite crust with a thickness of up to 34 m. This halite unit is underlain by clastic sediments. Brine is saturated in respect to halite. Progressively to the south clastic facies become dominant (Tassara, 1997). As described in Section 7.2, drilling within the MJV properties has been able to identify the geometry of the clastic and halite dominant units. Pumping tests have been carried out to characterize the hydraulic behavior of both the clastic and halite units as further described in Sections 9 and 10 below.

8.2 Hydrogeology

The salar is the topographic low point within the Maricunga Basin. The Salar itself is surrounded by alluvial fans which drain into the salar. The floor of the Salar in the north and northeast is composed of chloride facies consisting of flat halite crust (more recently flooded) and coarse irregular- and pinnacle shaped halite blocks (absence of recent flooding). The floor of the Salar in the southeast is composed of boric and sulphate facies. In the nucleus of the Salar the water table can be within approximately 5 cm of the surface.

Interpretation of drilling and testing results in the salar and the surrounding alluvial fans by the MJV and other companies previously exploring for fresh water resources suggests the occurrence of several hydrogeological units of importance. Figure 8.2 is a hydrogeological section through the Salar showing the principal units and which are summarized as follows:

- Alluvial fans surrounding the salar. These are coarse grained and overall highly permeable units that drain towards the salar. Groundwater flow is unconfined to semi-confined; specific yield (drainable porosity) is high. Water quality in the fans on the east side of the salar is fresh to brackish.
- An unconfined to semi-confined Upper Halite aquifer can be identified in the northern part of the salar. This unit is limited in areal extent to the visible halite nucleus as observed in satellite images. This Upper Halite unit is highly permeable; has a medium drainable porosity; and contains high concentration lithium brine.
- The clay core. This clay unit underlies the upper halite aquifer in the center of the Salar and extends to the east below the alluvial fans. This clay unit has a very low permeability and forms a hydraulic barrier for flow between the Upper Halite aquifer and the underlying clastic units (deeper sand gravel and Volcaniclasticsaquifer). On the east side of the Salar fresh water in the alluvial fans sits on top of this clay core; while brine is encountered in the clastic sediments underlying the clay. In the nucleus of the Salar the clay unit contains high concentration lithium brine.
- A deeper brine aquifer occurs in the gravel, sand and Volcaniclasticsunits underlying the clay core. Below the nucleus of the Salar this deeper aquifer is overlain by the Clay Core and groundwater conditions are confined. On the west side of the Salar, in absence of the Clay Core, groundwater conditions become semi-confined to unconfined. The deeper brine aquifer is relatively permeable and has a relatively high drainable porosity.

A groundwater monitoring network has been installed across the Maricunga basin and is part of the baseline monitoring program for the EIA. An updated conceptual hydrogeological model, including a water balance, is being completed for the Maricunga basin. This conceptual model forms the basis for the development of a three-dimensional numerical groundwater / brine flow model to estimate brine reserves, optimize the configuration of the future brine wellfield and evaluate potential effects of the future proposed brine abstraction for the EIA.

Figure 8.2 W-E Hydrogeological cross section

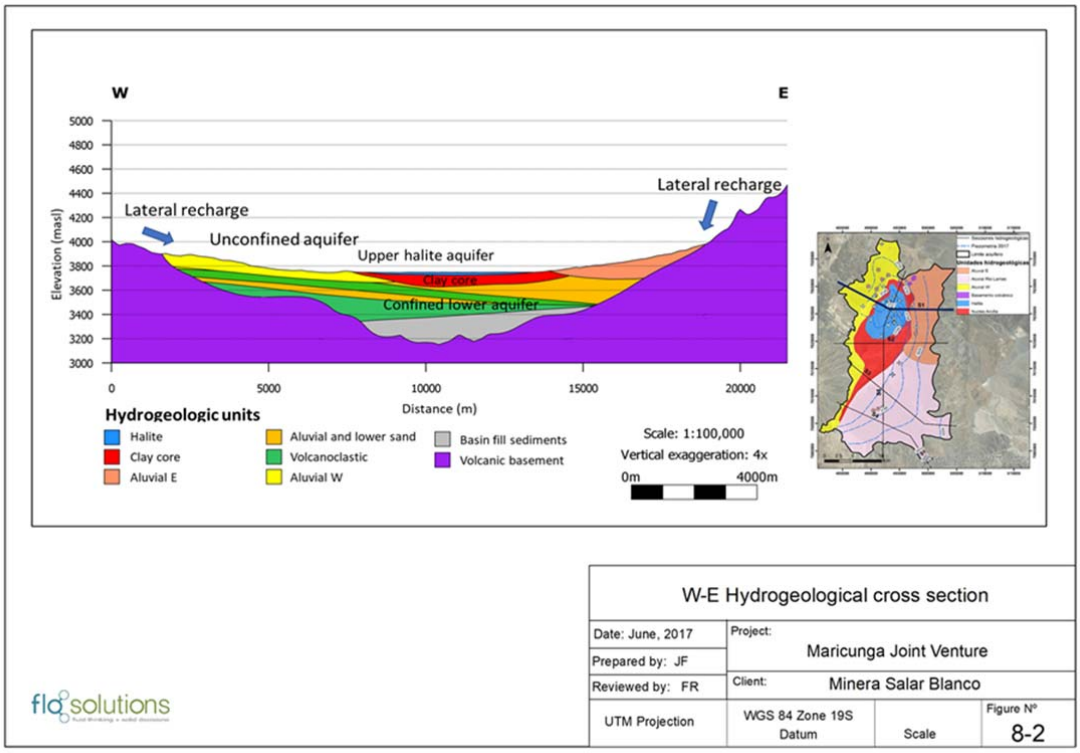

Figure 8.3 Salar de Maricunga hydrographic basin

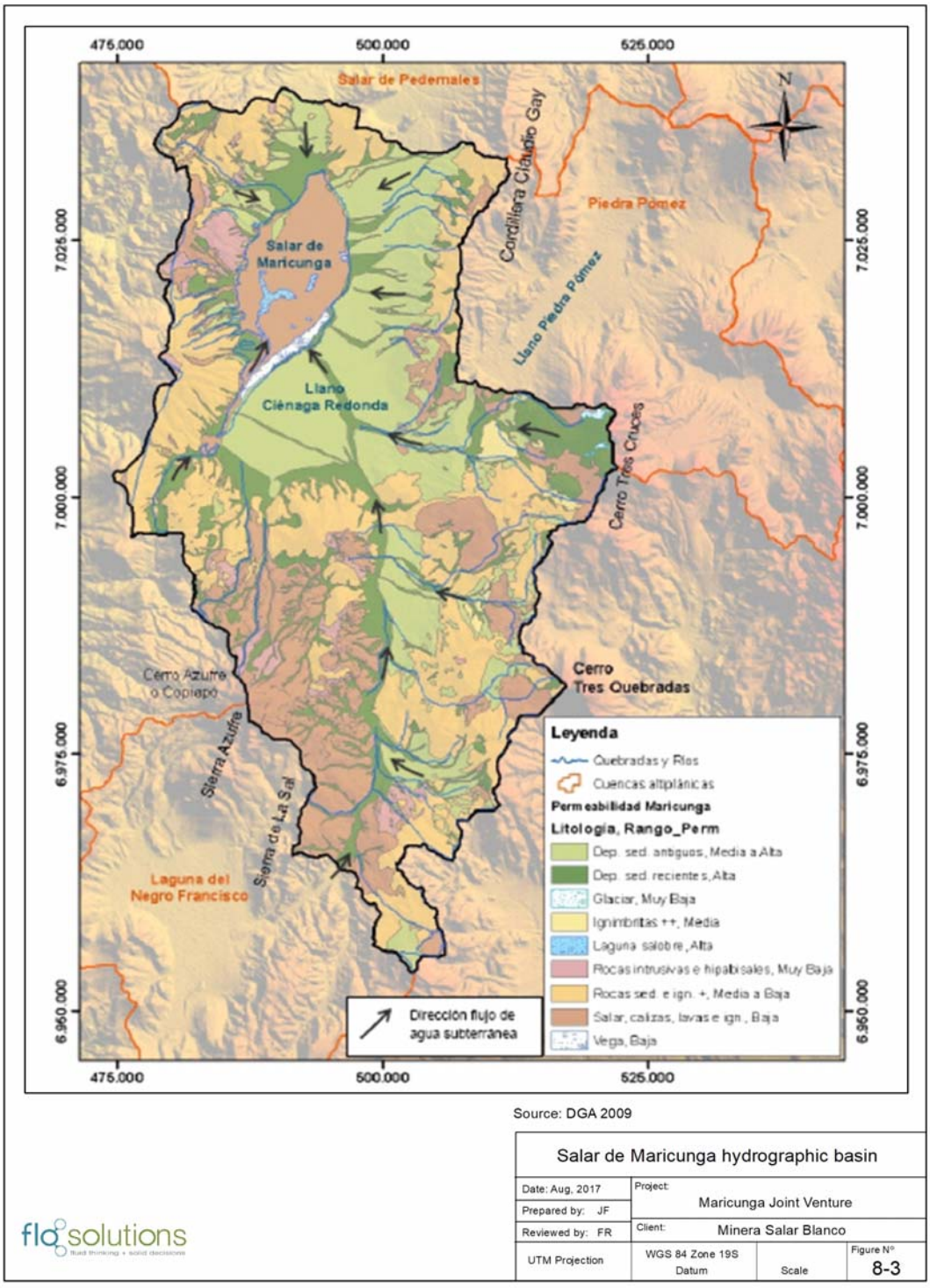

Source: DGA 2009

8.3 Water Balance (DGA 2009)

A water balance for Salar de Maricunga was prepared by the DGA in 2009. Figure 8.3 shows the general surface and groundwater flow patterns in the Salar de Maricunga watershed. Surface water flow generally only occurs at higher ground and infiltrates into the more permeable alluvial and fan sediments surrounding the Salar before reaching the Salar floor itself. The only surface water flow that occurs on the Salar floor is the natural discharge from Laguna Santa Rosa north towards the center of the Salar. There is no surface water outflow from the Maricunga watershed.

Groundwater flow patterns follow closely the surface water flow patterns. There are no known groundwater outflows from the Maricunga watershed. Inflow into the Maricunga watershed from the Laguna Negro Francisco has been demonstrated and is estimated at 80 l/s. It is speculated that potential groundwater inflow to the Maricunga watershed may take place from the Piedra Pomez Basin through the Claudio Gay mountain range. There exists uncertainty about potential groundwater interconnection between the Llano de Piedra Pomez and the Rio Lamas basin. Both potential groundwater inflow components need further investigation to refine the current water balance of the Salar de Maricunga hydrographic basin.

The majority of recharge to the Maricunga basin occurs through the direct infiltration of precipitation. The total average annual recharge to the Maricunga basin (including the inflow from Laguna Negro Francisco) is estimated at 1,450 l/s or 45.7 million cubic meters.

Discharge from the Maricunga basin is through evaporation, evapotranspiration and groundwater pumping. The total average annual discharge through evaporation has been estimated at 1,098 l/s or 34.6 million cubic meters.

According to DGA records, existing granted water rights in the Salar de Maricunga basin amount to 1,366 l/s, but actual authorized usage by the Environmental Evaluation System (SEA) is estimated at 153 l/s. Table 8.1 summarizes the water balance for the Salar de Maricunga watershed.

Table 8.1 Water Balance for the Salar de Maricunga Basin

Inflows	Average flow (l/s)
Recharge from precipitation	1,370
Inflow from Laguna del Negro Francisco	80
Other groundwater inflow	NA
Total inflows	1,450
Outflows	
Evaporation	1,098
Licensed abstraction (SEA authorised)	153
Total outflows	1,251
Balance (Inflows – Outflows)	199

Source: DGA 2009

Golder (2016) has prepared a modified water balance for the Salar de Maricunga basin as part of the EIA for the La Coipa Phase 7 Expansion. This modified water balance is currently being reviewed by the MJV as part of the development of an updated hydrogeological conceptual for the basin.

8.4 Drainable Porosity

Porosity is highly dependent on lithology. Total porosity is generally higher in finer grained sediments, whereas the reverse is true for drainable porosity or specific yield since finer grained sediments have a high specific retention. The lithology within the Salar is variable with halite and halite mixed units, clay and gravel-sand-silt-clay sized mixes spanning the full range of sediment types.

Based on the results of drainable porosity analyses carried out on 501 undisturbed samples from sonic core by GeoSystems Analysis, Daniel B Stephens and Associates, Corelabs, and the British Geological Survey it was possible to assign drainable porosity values to the specific lithological units encountered during the various drilling programs in the Salar. Table 8.2 summarizes the results of the porosity analysis. The analysis of drainable porosity is further discussed in Section 12.

Table 8.2 Results of drainable porosity analyses (2011-2017)

Lithology	Drainable Porosity		
	Average	Min	Max
Halite	0.09	0.01	0.15
Gypsum	0.01	-0.01	0.02
Clay	0.025	-0.01	0.03
Clay with Halite	0.04	-0.01	0.11
Silty Clay	0.06	0.01	0.25
Sand	0.09	0.037	0.16
Clayey sand	0.045	0.01	0.08
Silty sand	0.08	0.01	0.30
Clayey gravel	0.09	0.02	0.19
Sandy gravel	0.19	0.01	0.31
Volcaniclastics	0.15	0.06	0.31

8.5 Permeability

Permeability (or hydraulic conductivity) is also a parameter that is highly dependent of lithology. Generally finer grained and well-graded sediments have a lower permeability than coarser grained poorly graded sediments. The permeability of halite can be enhanced though fracturing and solutions features. MSB has carried out four pumping tests within the Salar and third parties have carried out numerous other pumping tests in the alluvial sediment surrounding the Salar. The results of the permeability calculations from these pumping tests are summarized in Table 8.3. The analysis of the pumping tests is further discussed in Section 10 below.

Table 8.3 Summary of permeability values

Unit	Description	K (m/d)
Halite	Confined and fractured	192-637
Clay core	Clay with sands and gravels - confined	0.9-11
East Alluvium	Semi-confied to confined	1-10
West Alluvium	Unconfined to semi-confined	4-40
Lower alluvium	Confined	0.4-0.9
Volcaniclastic	Confined	0.4-0.9

9 EXPLORATION

9.1 Overview

This section provides an description of the exploration work that has been carried out on the MJV properties between 2011 and 2017 by the various owners.

The following work was carried out on the *Litio 1-6* claims by MLE in 2011

- Seismic refraction tomography survey along 6 profiles for a total of 23 km to map lithological units and basin geometry.
- Construction of six test trenches to carry out 24 hour pumping trials to determine hydraulic parameters.

The following work was carried out by BBL in 2015:

- AMT / TEM survey along 6 profiles for a total of 75 km across the Salar to map basin geometry and the interface between freshwater and brine.
- Topographic survey between Laguna Rosa and the Project area to map hydraulic gradients.

The following work was carried out by MSB in 2016/7:

- Gravity survey along 6 profiles for a total of 75 km across the Salar to map basin geometry and bedrock topography.

9.2 Geophysical Surveys

9.2.1 Seismic refraction tomography (2011)

Li3 contracted Geophysical Exploration and Consulting S.A. (GEC) from Mendoza Argentina to carry out a Seismic Refraction Tomography Survey to map lithological units and structure in the northern part of the Salar. A total of 23 line km of seismic tomography data were collected along six lines as shown in Figure 9.1. Prior to the seismic data collection all lines were surveyed using a differential GPS system. All data collection work was completed in the field between September and December 2011.

A 24-bit, ultra-high resolution 20 kHz bandwidth (8 to 0.02 ms sampling), low distortion (0.0005%), low noise (0.2uV) GEODE Acquisition System was used for the collection of the seismic tomography data. Geophone (14Hz Geospace) spacing was 5 m; inline source spacing was 15 m and outline offsets were 30 m, 60 m, 90 m, 150 m, 250 m and 500 m. The spread data acquisition layout included 48 active channels. The seismic source for the surveys was a 150 kg trailer-mounted accelerated drop-weight. Recording length was 250/500 ms with a 1.0 ms sampling rate.

During the seismic data acquisition, data quality control and pre-processing of the geophysical data were carried out in the field with PC based processing and interpretation packages called "F*irstpix"* / G*remix 15"* and *"Rayfract32".* Final data processing with the "*Rayfract 32*" software included tomography inversion techniques *Delta TV* and WET or *Wave Eikonal Traveltime* as follows:

- Delta T-V method (after Gebrande and Mille, 1985): The Delta TV method is a pseudo 2D Inversion method that delivers a continuous 1D velocity versus depth model for all geophone stations. The method handles geological situations such as velocity gradients, linear increasing of velocity with depth, velocity inversions, pinching out layers and outcrops, faults and local velocity anomalies.

- WET or Wave Eikonal Traveltime Tomography processing. Wave propagation is modelled in a physically meaningful way with ray paths, using the output from the Delta-TV inversion as starting model. It handles geological situations, such as discontinuities velocity distributions and sharp vertical or horizontal velocity gradients. Quality control of geological models is performed by direct graphical comparison of the measured travel time data to those calculated from the model solution.

Figure 9.2 shows as an example of the result of the WET processing and inversion with the geological interpretation below along Profile 1 and is considered representative of the overall seismic survey results obtained. Data from the 2011 sonic and RC boreholes was included in the final interpretation. The seismic tomography survey provided valuable information on the vertical distinction and lateral continuity of lithological layers, however bedrock was not clearly detected along any of the profiles.

Figure 9.1 Location map of seismic refraction tomography, AMT and gravity profiles

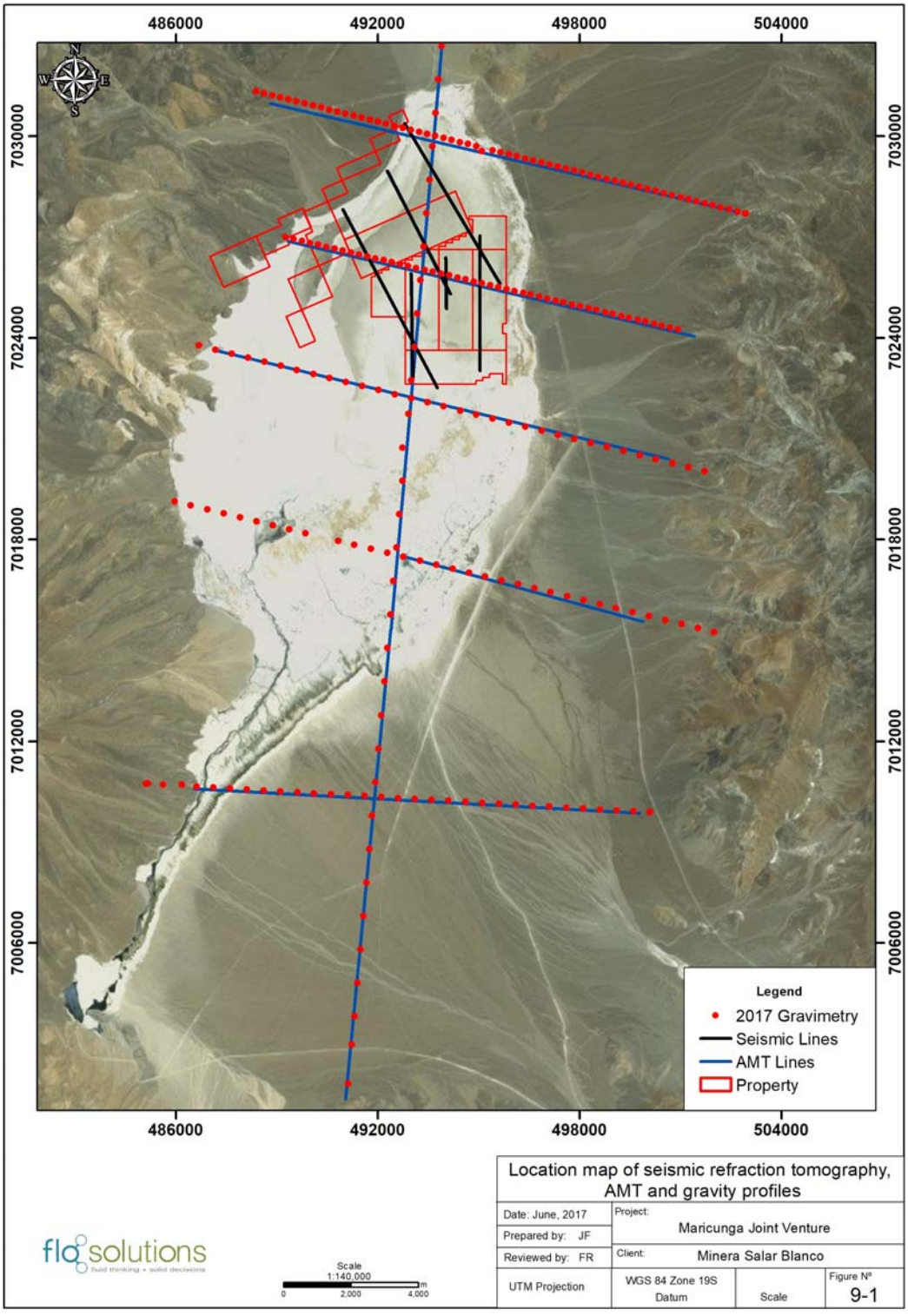

Figure 9.2 Seismic Tomography Line 1

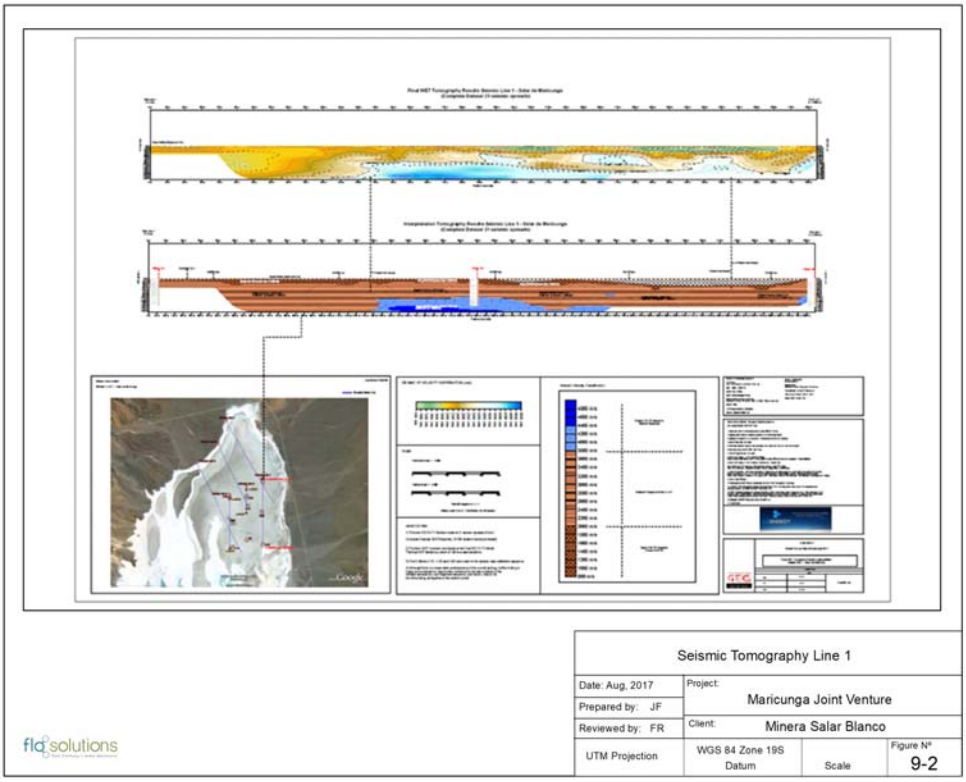

9.2.2 AMT / TEM (2015)

Six profiles of Audio Magnetotellurics were carried out across Salar de Maricunga to map the bedrock geometry and identify the interface between freshwater and brine along the perimeter of the Salar. The work was carried out by Wellfield Services Ltda. The survey consisted of 60.8 km of AMT profiles with a station spacing of 200 m and 14 km with a station spacing of 250 m. 360 stations were measured with scalar methodology and 23 stations were measured with the tensorial array. 15 TEM soundings were carried out at the ends of the AMT lines and at the intersection with Line 6. Figure 9.1 shows the location of the AMT profiles.

AMT data were collected in the range of 10,000 – 1 HZ and MT data in the range of 4 – 0,01 Hz to include the deeper portion of the frequency spectrum. Seven GPS synchronized systems were operated by two teams with data collection taking place overnight for a period of 15-18 hours at each station.

Due to logistical and climatic conditions (partial flooding of the Salar) the survey was carried out in 3 stages during March and April 2015. The AMT data were inverted into 2D resistivity models using the software WinGLink.

9.2.3 Gravimetry

A gravity survey was carried out in the Salar along Prolifes 1 - 6 (immediately over the AMT lines) as shown in Figure 9.1. Station spacing along Line 1 and 2 was 250 m, while station spacing along lines 3 to 6 was 500 m. Each station was surveyed in with a differential GPS with a precision of +/- 5 cm. The gravity data was collected with a Scintrex micro-gravimeter Model CG-5 with resolution of 0.001mgals and with an automatic drift correction.

Data processing included the Free Air, Simple Bouguer, and Total Terrain corrections; the final product included final Bouguer anomaly maps and 2D inversion models. An average density contract of 0.45 g/cc was used between the bedrock and the Salar basin fill sediments to prepare depth-to-bedrock models along each of the gravity profiles. The density contract was based on results of laboratory (Univerisdad de Chile) density measurements on 18 rock samples collected in outcrop at the end of Lines 1 – 6 and the density measurements carried out by GSA on the basin fill sediments. The geological model described in Section 7 was used to constrain the geometry of the lithological units within the gravity interpretation. The gravity profiles were also overlain by the AMT resistivity sections to aid in the final depth-to-bedock model. The final bedrock topography was kriged based on interpolation from the line profiles.

9.3 Test Trenching (2011)

Six test trenches (T1 through T6) were constructed in 2011 on *the Litio 1-6* tenements to test the feasibility of brine production from trenches as an alternative to brine production from production wells. One trench was installed adjacent to each sonic borehole C-1 through C-6. The trenches were dug at 3 m width to a depth of 2.5 m. Each trench was completed in generally massive (relatively competent) halite and the trench walls did not encounter stability problems as shown in Figure 9.3.

A 24-hour pumping test was carried out in each trench at a flow rate of 5 l/s using a sump pump. Water level responses during each pumping test were observed in a shallow monitoring well (36 m depth) adjacent to each trench that allowed for the calculation of aquifer parameters. Figures 9.4a through 9.4e show the water level response in each observation well and the associated pumping test analyses. Table 9.1 summarizes the results of the pumping test analyses. The relatively high S_y values obtained from the pumping tests are representative of the halite mix sediments and suggest enhanced porosity in the halite through dissolution and fracture features.

Figure 9.3 Test Trench T6 in the Upper Halite

Table 9.1 Results of Trench pumping tests

Trench	Hydraulic Conductivity (K) m/d	Specific Yield (S_y)
T1	208	0.24
T2	84	0.28
T3	145	0.24
T4	No water level response in piezometer	
T5	15	0.12
T6	45	0.04

The results of these tests indicate that the upper halite is highly permeable and that brine production from trenches is a feasible alternative to production wells from the upper metres of the upper halite.

Figure 9.4a – 9.4e Pumping test analyses for Trench pumping tests T1, T2, T3, T5 and T6

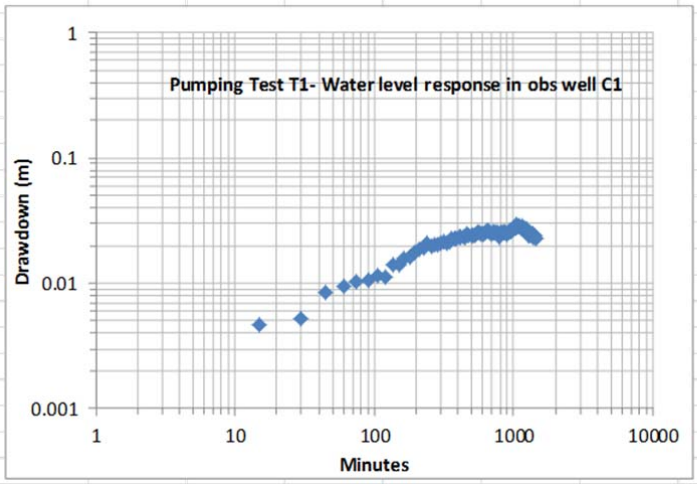

After Papadopulos 1967		
a	0.01	
1/u	100	
F(u)	1	
t	190	min
s	0.0055	m
r	12.9	m
Q	529	m3/d
KD	7513	m2/d
Sy	0.24	

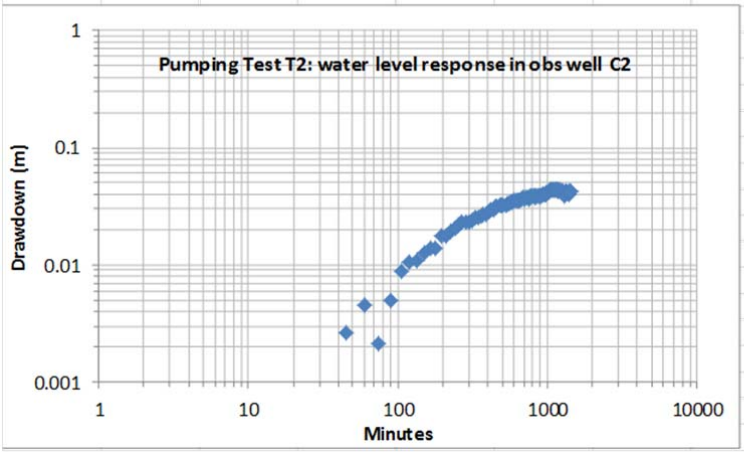

After Papadopulos 1967		
a	0.1	
1/u	10	
F(u)	1	
t	350	min
s	0.015	m
r	32.47	m
Q	573	m3/d
KD	3041	m2/d
Sy	0.28	

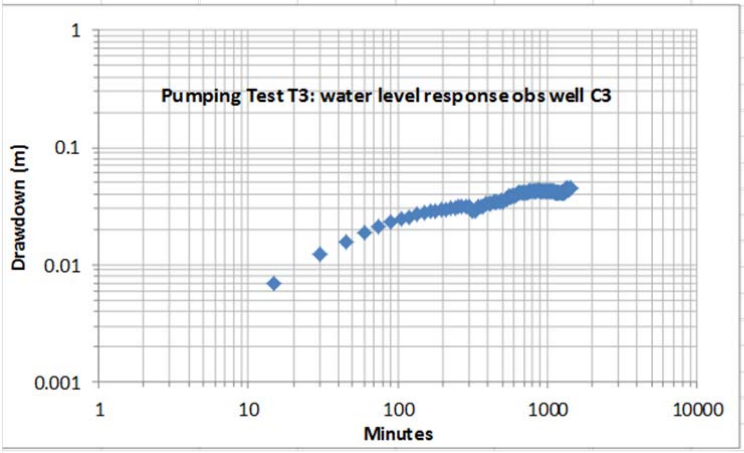

After Papadopulos 1967		
a	0.1	
1/u	10	
F(u)	1	
t	35	min
s	0.009	m
r	14.6	m
Q	593	m3/d
KD	5237	m2/d
Sy	0.24	

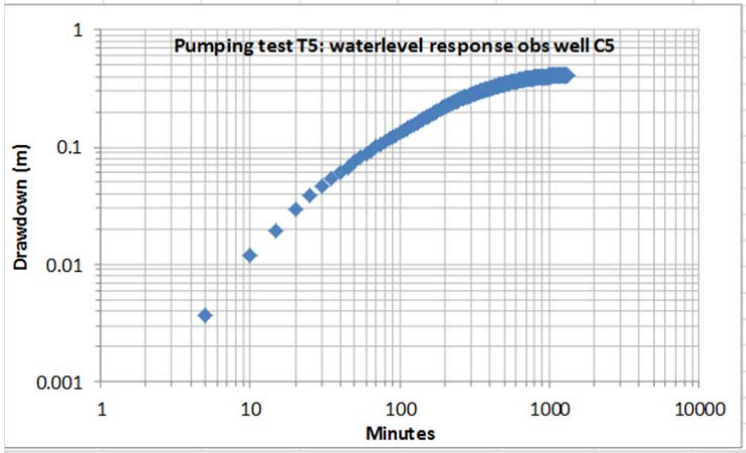

After Papadopulos 1967		
a	0.01	
1/u	100	
F(u)	1	
t	300	min
s	0.085	m
r	6	m
Q	562	m3/d
KD	526	m2/d
Sy	0.12	

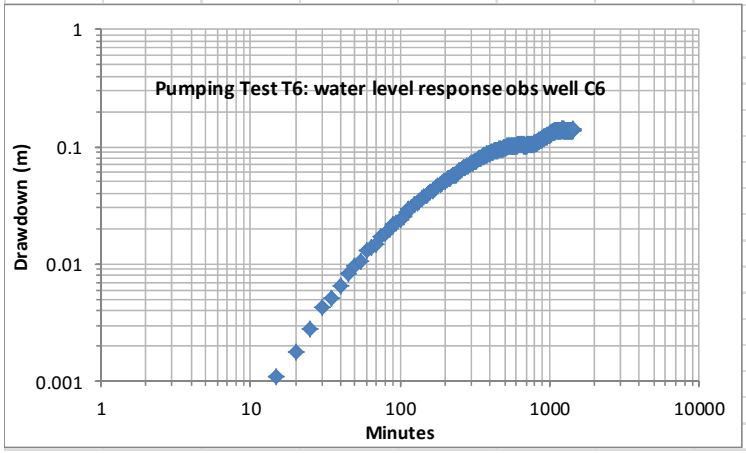

After Papadopulos 1967		
a	0.01	
1/u	100	
F(u)	1	
t	410	min
s	0.025	m
r	22.6	m
Q	518	m3/d
KD	1650	m2/d
Sy	0.04	

10 DRILLING

10.1 Overview

Two principal drilling campaigns were carried, the first in 2011 on the *Litio 1-6* claims by MLE and a second on the MJV properties by MSB in 2016/7.

The objectives of each drilling campaign can be broken down into three general categories:

1) Exploration drilling on a general grid basis to allow the estimation of "in-situ" brine resources. The drilling methods were selected to allow for 1) the collection of continuous core to prepare "undisturbed" samples at specified depth intervals for laboratory porosity analyses and 2) the collection of depth-representative brine samples at specified intervals without the possibility of contamination by drilling fluids. The 2011 campaign included six (6) sonic boreholes (C-1 through C-6) on the *Litio 1-6* claims. The 2016 campaign included four (4) sonic boreholes (S-1[M1], S-2, S-18 and S-20) and eight (8) tricone /HWT boreholes (S-3, S-3A, S-5, S-6, S-10 [M-10], S-11[M2], S-13, and S-19). Figure 10.1 shows the location of the exploration boreholes.

2) Production- and monitoring well drilling. Test production wells were installed to carry out pumping tests to determine the hydraulic parameters of the Salar sediments and investigate the behavior of the brine aquifer under pumping stress. Monitoring wells were installed adjacent to production wells to observe water levels changes during the pumping tests and in other locations to monitor baseline groundwater conditions around the Salar. Monitoring wells were drilled using the reverse circulation (air) drilling method (RC) to allow hydraulic test work. Production wells were installed using conventional rotary methods at large diameter. Production wells P-1 and P-2 along with piezometers P1-1, P1-2, P1-3, P1-4, P2-1, P2-2, P2-3, P2-5 and P-3 were installed in the 2011 campaign. Production well P-4 and monitoring wells S-7, S-8, S-12, S-15, S-16A, S-17, and S-21 were installed during the 2016/7 campaign. The analytical results of brine samples collected during the production and monitoring well drilling were not used in the resource model.

3) Pumping tests. Long-term pumping tests were carried out on wells P-1 and P-2 during 2015 and on wells P-4 and P-2 (shallow) in 2017.

10.2 Exploration drilling

10.2.1 Sonic Drilling

Boart Longyear (BLY) was contracted to carry out sonic drilling for the collection of continuous core and brine samples for both the 2011 and 2016 programs. Sonic boreholes C1 through C6 were drilled to a depth of 150 m in 2011 and S-1A, S-2, and S-18 to depths of up to 200 m in 2016. Sonic hole S-20 was drilled as a twin hole to S-11 to a depth of 40 m to correlate porosity information. Core recovery was consistently high and exceeded 90%.

Figure 10.1 Location map of the boreholes (2011 and 2016 programs)

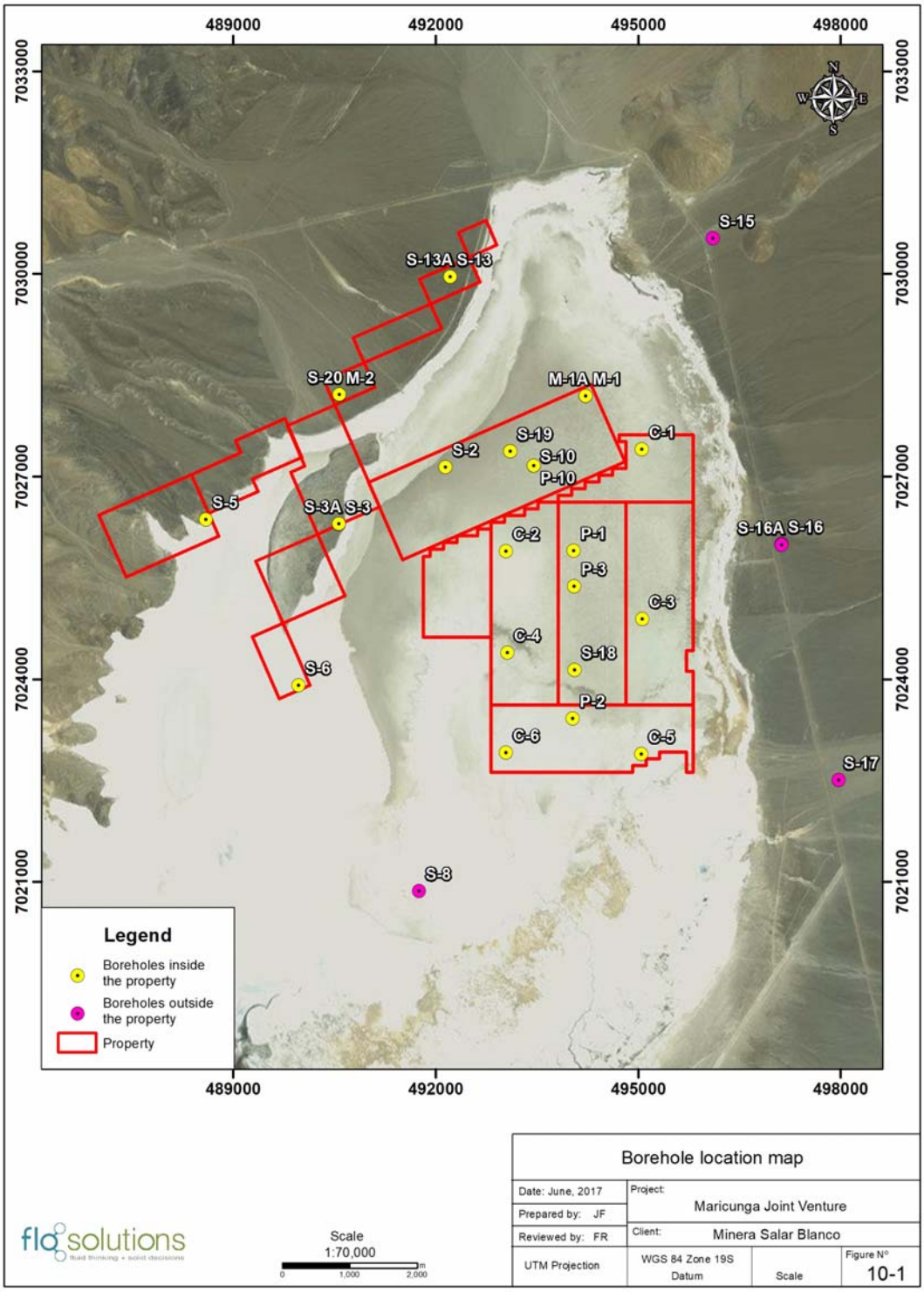

The drilling equipment consisted of a BLY (SR-162 SRF 600T) sonic rig and support equipment utilizing a 4-inch diameter coring by 6-inch casing system. No drilling additives/fluids were used thereby preventing possible brine sample contamination. All holes were drilled vertically. The drilling was carried out in 1.5 m runs and core was collected in alternating plastic bags (1.5 m) and lexan core barrel liners (1.5 m). The retrieved lexan core liners were capped and sealed with tape at each end. All retrieved core was labeled with its borehole number and the drilling depth interval and stored in wooden core boxes. The 6-inch diameter casing was advanced at the end of each core run.

Brine samples were collected at 3 m intervals during the 2011 program and at 6 m intervals during the 2016. Brine level measurements were made inside the drill casing to calculate the required volume of brine to be bailed from the hole prior to obtaining a brine sample. Up to three well volumes were bailed prior to collecting the final brine sample from the bottom of the hole. This procedure was repeated to total depth (TD).

On completion of drilling, each sonic borehole was completed as a monitoring well with 2-inch diameter PVC blank and slotted casing, gravel pack and cement seal.

Table 10.1 Summary of 2011 and 2016 boreholes

Borehole	North	East	Elevation	TD (m)	Method	Year	Objective	Screened interval	SWL
C1	7,027,408	495,052	3,747.51	150	Sonic	2011	Resource	abandoned	na
C2	7,025,899	493,041	3,747.35	150	Sonic	2011	Resource	jun-34	0.11
C3	7,024,895	495,056	3,746.86	150	Sonic	2011	Resource	mar-26	0.12
C4	7,024,400	493,058	3,747.35	150	Sonic	2011	Resource	jun-29	0.24
C5	7,022,900	495,045	3,746.58	150	Sonic	2011	Resource	06-nov	0.15
C6	7,022,918	493,039	3,746.78	150	Sonic	2011	Resource	06-nov	0.23
P1	7,025,904	494,043	3,747.25	150	Rotary	2011	Production	6-24;60-144	0.18
P1.1	7,025,891	494,032	3,747.59	150	DTRC	2011	Monitoring	60-149	0.72
P1.2	7,025,894	494,061	3,747.34	30	DTRC	2011	Monitoring	jun-24	0.18
P1.3	7,025,905	494,032	3,747.69	70	DTRC	2011	Monitoring	54-66	0.37
P1.4	7,025,915	494,032	3,747.74	30	DTRC	2011	Monitoring	jun-24	0.12
P2.1	7,023,393	494,035	3,746.44	113	DTRC	2011	Monitoring	102-108	0.26
P2.3	7,023,410	494,03	3,746.38	30	DTRC	2011	Monitoring	dic-30	0.2
P2.4	7,023,403	494,034	3,746.44	150	DTRC	2011	Monitoring	60-145	0.27
P2.5	7,023,397	494,061	3,746.60	150	DTRC	2011	Monitoring	60-145	0.77
P3	7,025,380	494,052	3,747.62	192	DTRC	2011	Monitoring	127-185	-0.37
P2	7,023,422	494,03	3,746.22	150	Rotary	2011	Production	6-24; 66-144	0.25
S 1A	7,028,201	494,22	3,748.95	200	Sonic	2016	Resource	29-119	0.23
S 2	7,027,141	492,143	3,748.84	200	Sonic	2016	Resource	184-190	1.43
S-3	7,026,300	490,56	3,751.54	40	Tricone/HWT	2016	Resource	Abondoned	na
S-3A	7,026,306	490,563	3,751.53	200	Tricone/HWT	2016	Resource	Abondoned	na
S-5	7,026,366	488,59	3,750.17	200	Tricone/HWT	2016	Resource	182-188	1.55
S-6	7,023,913	489,964	3,749.09	200	Tricone/HWT	2016	Resource	184-195	3.09
S-8	7,020,871	491,753	3,748.72	40	Rotary	2016	Monitoring	28-34	1.18
S-11	7,028,215	490,569	3,757.61	200	Tricone/HWT	2016	Resource	144-150	8.95
S-12	7,013,856	493,74	3,769.28	40	Rotary	2016	Monitoring	22-28	na
S-13	7,029,964	492,213	3,755.88	200	Tricone/HWT	2016	Resource	194-200	9.18
S-15	7,030,533	496,104	3,781.23	40	Rotary	2016	Monitoring	34-40	25.11
S-17	7,022,516	497,969	3,789.94	40	Rotary	2016	Monitoring	32-38	29.8
S-16A	7,026,005	497,122	3,769.89	150	Tricone/HWT	2016	Monitoring	50-62	11.3
S-16B	7,025,991	497,123	3,769.99	18	Tricone/HWT	2016	Monitoring	sept-15	14.72
S-18	7,024,141	494,054	3,748.64	173	Sonic	2016	Resource	1160-172	2.58
S-19	7,027,381	493,104	3,748.17	360	Tricone/HWT	2016	Resource	196-208	2.98
S-20	7,028,217	490,569	3,757.64	40	Sonic	2016	QA/QC	abandoned	na
S-21	7,037,751	491,855	3,863.06	85	Rotary	2016	Monitoring	72-84	dry
P-4.1	7,027,224	493,194	3,748.81	200	Tricone/HWT	2016	Monitoring	160-172	2.26
P-4.2	7,027,242	493,172	3,748.65	2	Auger	2016	Monitoring	0-2	0.1
P-4.3	7,027,250	493,16	3,748.70	2	Auger	2016	Monitoring	0-2	0.12
P-4.4	7,027,265	493,139	3,748.74	2	Auger	2016	Monitoring	0-2	0.11

10.2.2 Rotary tricone/HWT drilling

Eight (8) tricone /HWT boreholes (S-3, S-3A, S-5, S-6, S-10 or M-10, S-11, S-13, and S-19) were drilled as part of the 2016 program. Rotary drilling with HWT casing was substituted for conventional diamond drilling as core recovery of the coarse grained sediments on the western side of project area did not prove to be successful. The rotary drilling was carried out by AK drilling using a EDM rig. Rotary drilling was carried out using a 3-7/8 inch tricone bit, with sample recovery through the HWT casing to surface. Cuttings were collected at surface in cloth bags with representative sub-samples at 2 m intervals stored in labelled chip trays. Brine samples were collected at six meter intervals during the rotary drilling. The brine sampling methodology is further described in Section 11. Selected boreholes were completed as monitoring wells with blank and slotted PVC.

10.3 Monitoring - and Production Well Drilling

10.3.1 Reverse circulation (RC) drilling and piezometer installations (2011)

A total of 915 m of RC drilling (P1-1, P1-2, P1-3, P1-4, P2-1, P2-2, P2-3, P2-5 and P-3) was carried out for the collection of chip samples for geologic logging, brine samples for chemistry analyses and airlift data. Rock Drilling S.A. provided an Ingersoll Rand T3-W reverse circulation rig equipped with a 350 psi, 1000 cfm air compressor and support equipment. The exploration drilling was carried out at 5 ½-inch diameter using dual tube reverse circulation pipe and air; no additives/fluids were used during the drilling. Exploration drilling depths ranged from 30 m to 192 m. Chip samples were collected at 2 m intervals for geological logging, brine samples were collected at 3 m intervals (directly from the cyclone) and airlift tests were completed at 6 m intervals. The RC exploration boreholes were completed as monitoring wells for use during the future pumping tests. The distance between each monitoring well and the associated production well ranges from 10 m to 35 m. Table 10.2 shows the details of the RC exploration drilling completed.

10.3.2 Production well drilling (2011 and 2016)

Drilling of production wells P1 and P2 was carried out by Rock Drilling S.A. using the Ingersoll Rand T3-W rig in 2011. The wells were drilled in two passes at 11-inch and 17-inch diameter to a final total depth of 150 m using flooded reverse circulation (rotary) drilling. The wells were completed with a 10-inch diameter PVC production casing string in both the upper halite aquifer and the lower gravel and volcanoclastics aquifer. The annulus of each test well was completed with gravel pack. Well development was carried out over a 72 hour period in each well using a double swab/airlift system. Table 10.2 shows the construction details of P-1 and P-2.

Production well P-4 was drilled by Hellema Holland Engineering using a Prakla rig. The well was drilled using conventional rotary drilling at 17-1/2 inch diameter to a depth of 180 m. The well was completed with screened 12-inch diameter PVC production casing in the lower aquifer between 70 m and 180 m depth. A bentonite / cement seal was installed (on top of the gravel pack) from ground surface to a depth of 56 m. Well development was carried out over a 48 hour period using a double swab/airlift system. Table 10.2 shows the construction details of P-4.

10.3.3 Piezometer installations - 2016

Piezometers S-7, S-8, S-12, S-15, S-16A, S-17, and S-21 were installed as part of the 2016 campaign. These monitoring wells were drilled using conventional rotary methodology to depths of up to 150 m. Fuid samples were taken at selected intervals during the drilling of the monitoring wells. The wells were completed with 2-inch diameter schedule 80 blank and screened PVC casing. A geomembrane filter

was placed over the screened casing to prevent silting. No materials were installed in the annulus. Table 10.1 shows the completion details of each of these installations.

Figure 10.2 Collecting RC Airlift Flow Measurements (2011)

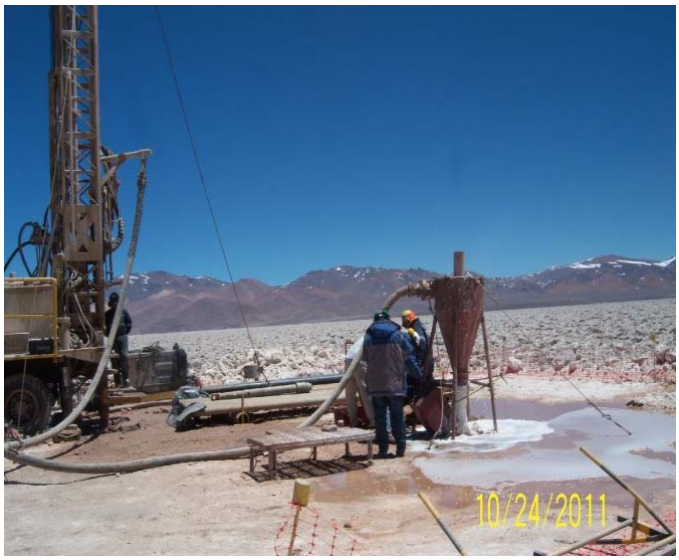

Figure 10.3 Installation of surface casing in well P-1 (2011)

10.4 Pumping Tests (2015 and 2017)

Pumping tests were carried out on wells P-1, P-2, and P-4 between 2015 and 2017. Table 10.2 summarizes the construction details of each pumping test.

Table 10.2 Wells P1, P2 and P4 pumping test layout

Well	Type	UTM E	UTM N	Screened interval (mbgs)	Unit
P-1 Test					
P-1	Pumping	494,043	7,025,903	0-12,18-24 ,60-144	Upper Halite and Lower Alluvium
P1-1	Observation	494,032	7,025,890	60-149	Clay Core and Lower Alluvium
P1-2	Observation	494,061	7,025,893	7-24	Upper Halite
P1-3	Observation	494,032	7,025,905	55-66	Clay Core
P1-4	Observation	494,031	7,025,915	7-24	Upper Halite
P-2 Test					
P-2	Pumping	494,030	7,023,422	0-16, 62-141	Upper Halite and Lower Alluvium
P2-1	Observation	494,034	7,023,392	102-108	Clay core
P2-3	Observation	494,030	7,023,409	11-28	Upper Halite
P2-4	Observation	494,033	7,023,402	58-140	Clay Core and Lower Alluvium
P2-5	Observation	494,060	7,023,397	55-144	Clay core and Lower Alluvium
P-4 Test					
P-4	Pumping	493,040	7,025,899	70-180	Lower alluvium
P4-1	Monitoring	495,055	7,024,994	170-182	Lower alluvium
P4-2	Monitoring	493,057	7,024,400	0-2	Upper halite
P4-3	Monitoring	495,045	7,022,900	0-2	Upper halite
P4-4	Monitoring	493,038	7,022,917	0-2	Upper halite

P-1 Pumping test (2015)

Production well P-1 has two completion intervals: the upper completion between 6 and 24 m depth in the Upper Halite aquifer and the lower completion between 60 m and 144 m depth in the lower part of the Clay Core and the under-laying Lower Alluvium. Four monitoring wells (P1-1, P1-2, P1-3 and P1-4) are installed adjacent to well P-1 at radial distances from 11 to 20 m as shown in Figures 10.4 and 10.5. Piezometers P1-2 and P1-4 are completed in the Upper Halite unit. Piezometer P1-3 is completed in a deeper halite layer within the Clay Core and Piezometer P1-1 is completed in the lower part of the Clay Core and the Lower Alluvium.

A 14-day constant rate test was conducted at 38 L/s between May 31 and June 13, 2015, followed by recovery. Pumped brine was piped through a 1,200 m plastic line to a V-notch tank where final discharge took place on to the Salar as shown Figure 10.6. The pumping rate was measured by an inline flow meter, manual measurements and in the V-notch tank. Pressure transducers were installed in all piezometers and the V-notch tank to record water level responses during the test in addition to manual measurements. Observed water level responses to the test are shown in Figure 10.7. The curve fitting and interpretation results of the P-1 constant rate test are shown in Figure 10.8 and Table 10.3

Figure 10.4 Layout of pumping test P-1 and P-2

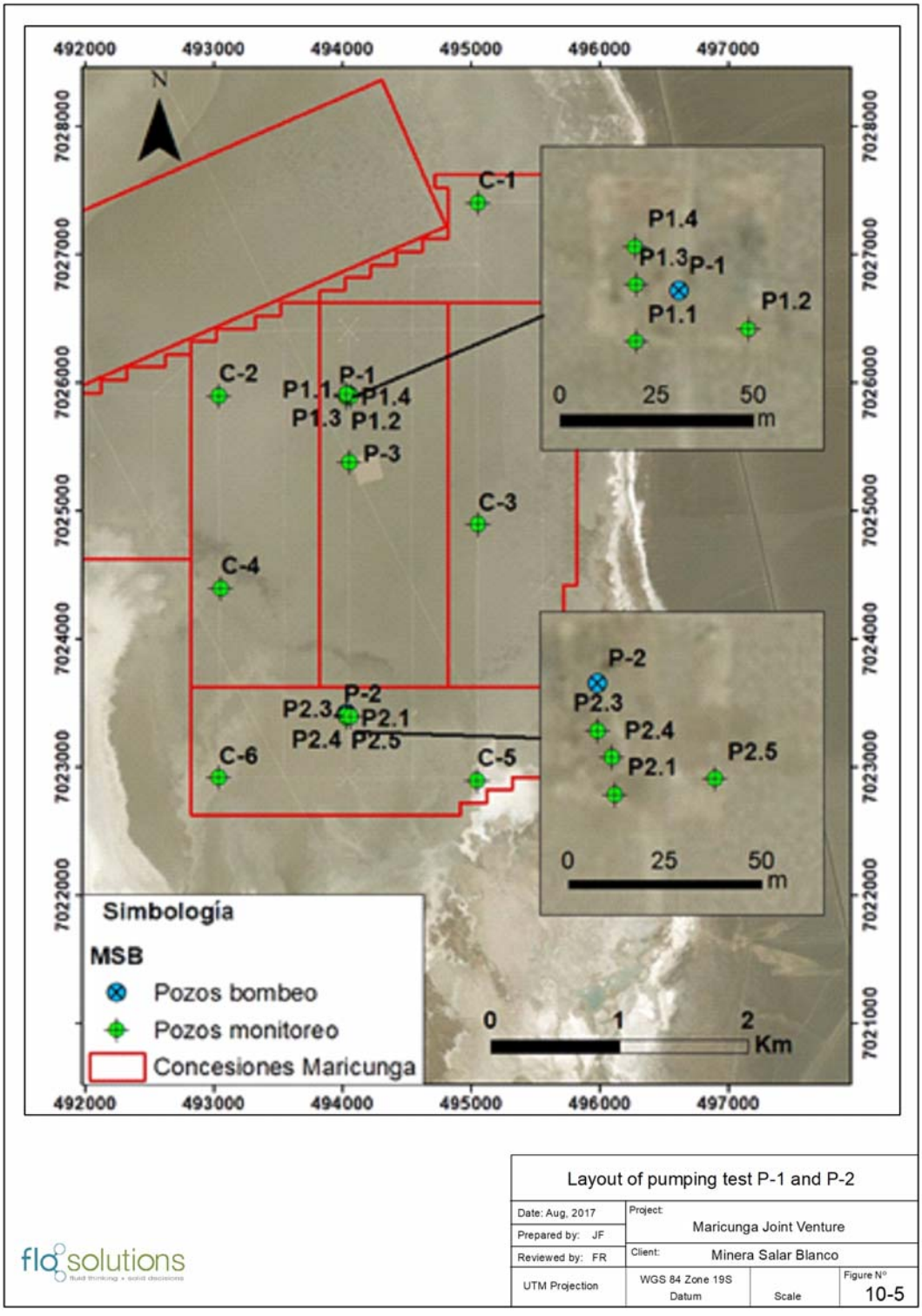

Figure 10.5 Pumping test P-1 layout

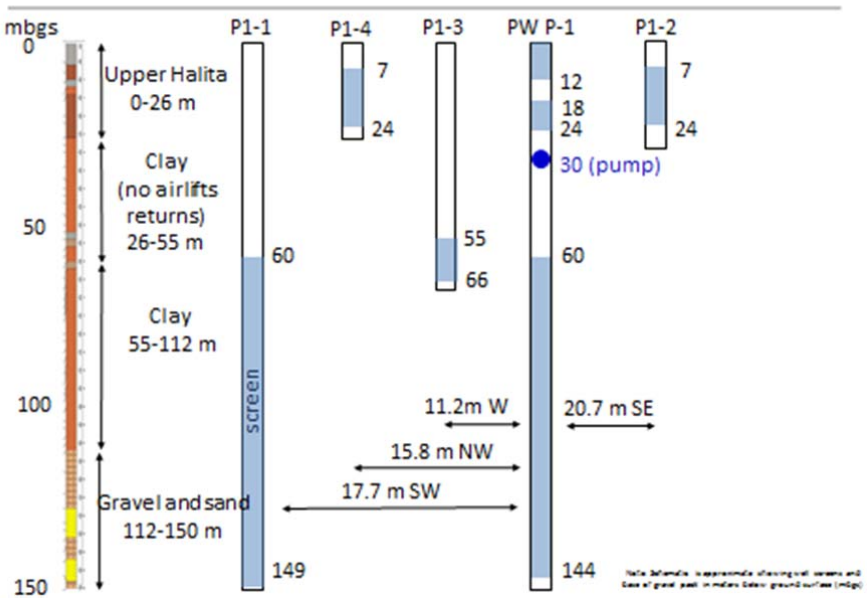

Figure 10.6 V-notch tank during P-1 constant rate test

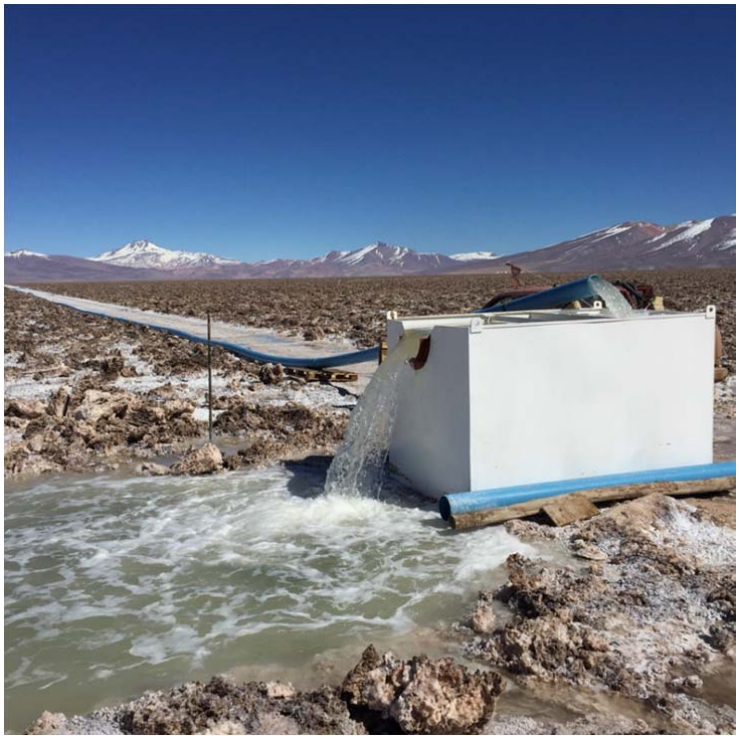

Figure 10.7 Water level responses P 1 constant rate test

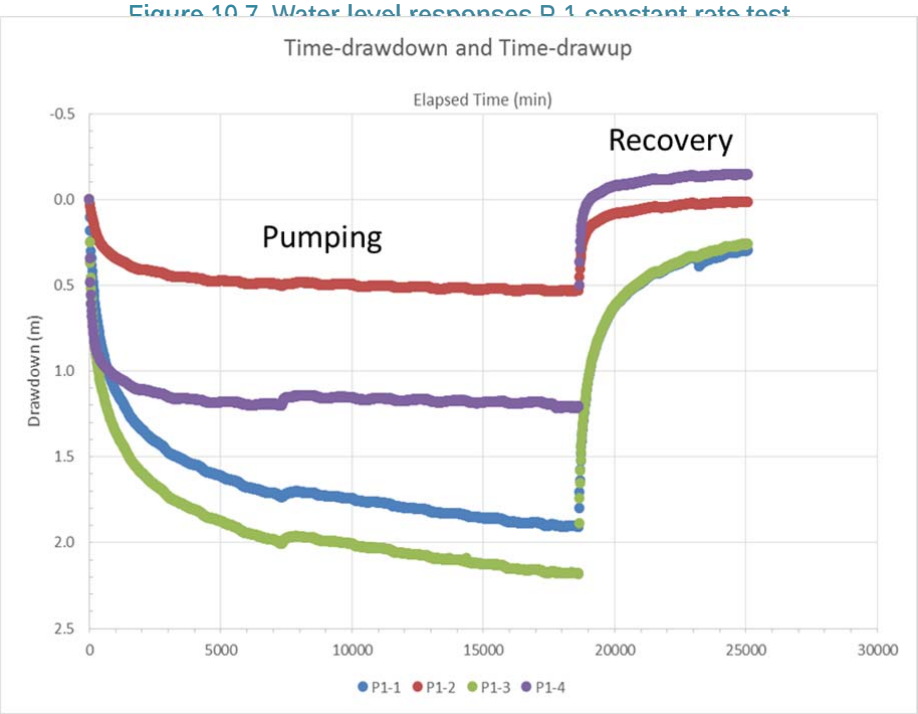

Source: FloSolutions 2015b

Figure 10.8 P-1 pumping test interpretation

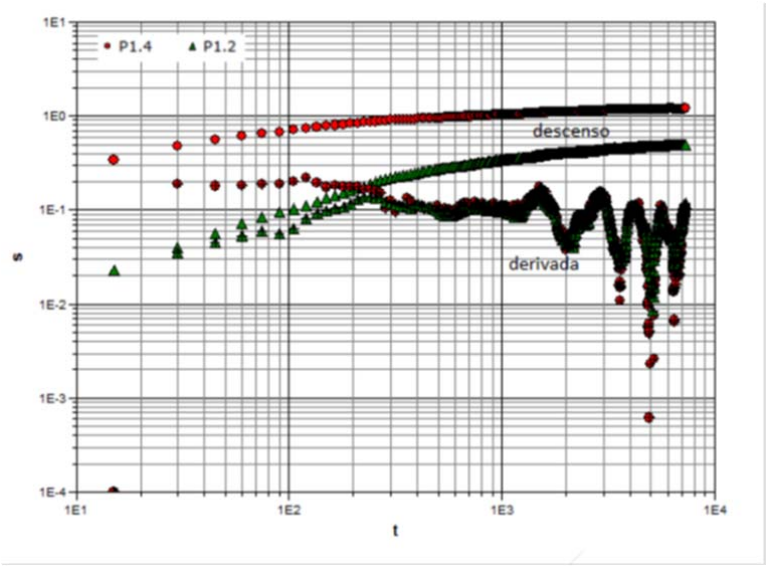

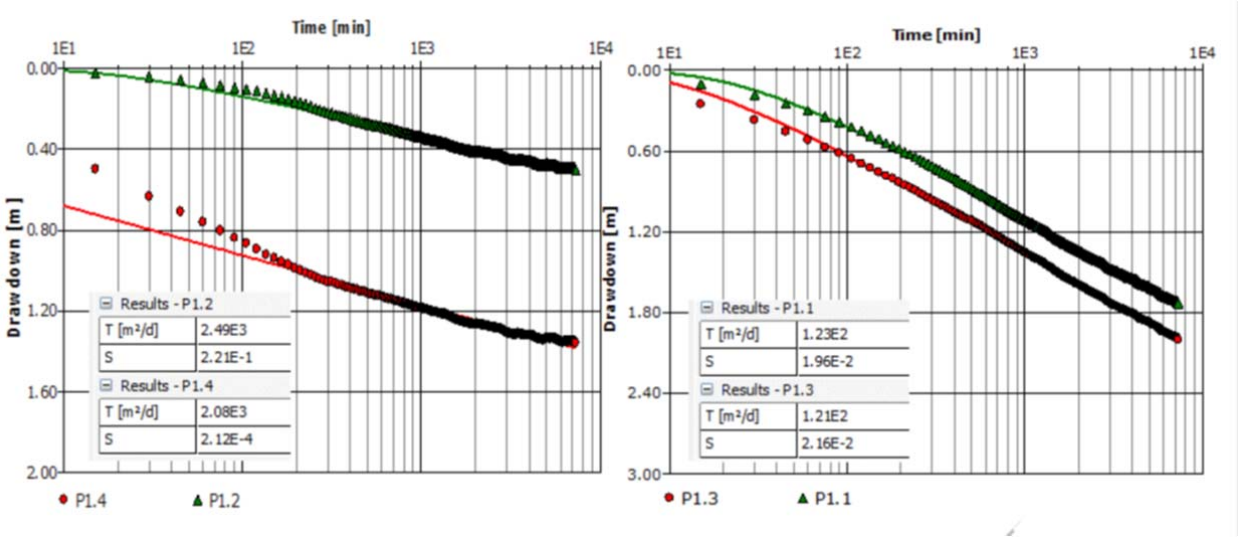

Table 10.3 P-1 pumping test results

Well	Unit	Max Drawdown (m)	Fit	T (m2/d)	S(-)	K (m/d)*	Ss (1/m)
P-1.2	Upper Halita	0.531	Theis	2,490	2.21E-01	146.5	1.3E-02
P-1.4	Upper Halite	1.362	Theis	2,080	2.12E-04	122.4	1.2E-05
P-1.1	Lower aquifer	1.906	Theis	123	1.96E-02	1.4	2.2E-04
P-1.3	Lower aquifer	2.181	Theis	121	2.16E-02	11.0	2.0E-03

P-2 Pumping test (2015)

Production well P-2 has two completion intervals: the upper completion between 0 and 16 m depth in the Upper Halite aquifer and the lower completion between 60 m and 144 m depth in the lower part of the Clay Core and the underlaying Lower Alluvium. Four monitoring wells (P2-1, P2-3, P2-4 and P2-5) are installed adjacent to well P-2 at radial distances from 12 to 40 m as shown in Figures 10.5 and 10.9. Piezometer P2-3 is completed in the Upper Halite unit. Piezometer P2-1, P2-4 and P2-5 are completed within the lower part of the Clay Core and the Lower Alluvium.

A 30-day constant rate test was conducted at 37 L/s during July/ August 2015, followed by recovery. Pumped brine was piped through a 1,200 m plastic line to a V-notch tank where final discharge took place on to the Salar. The pumping rate was measured by an inline flow meter, manual measurements and in the V-notch tank. Pressure transducers were installed in all piezometers and the V-notch tank to record water level responses during the test in addition to manual measurements. Observed water level responses to the test are shown in Figure 10.10 The curve fitting and interpretation results of the P-2 constant rate test are shown in Figure 10.11 and Table 10.4

Figure 10.12 shows the variation of lithium and potassium concentrations during the P-1 and P-2 pumping tests, which is within the range of laboratory analytical variability.

Figure 10.9 Pumping test P-2 layout

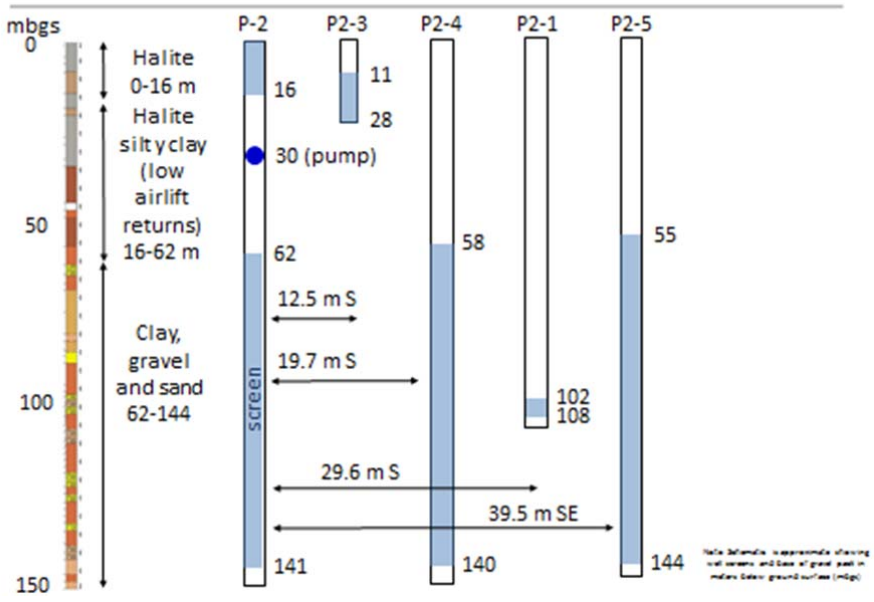

Figure 10.10 Water level responses P-2 constant rate test

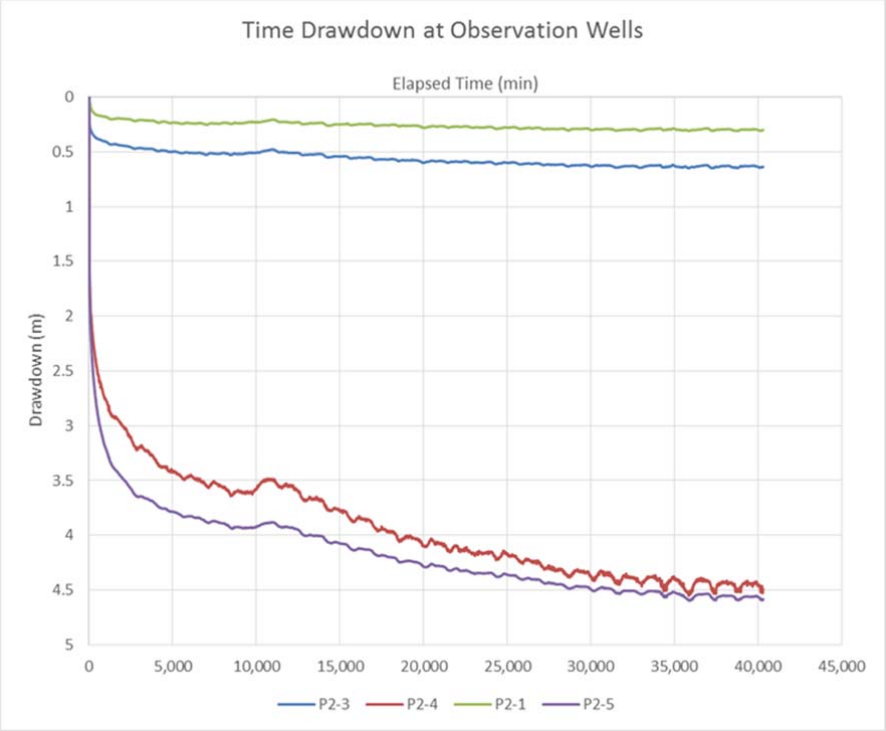

Figure 10.11 P-2 pumping test interpretation

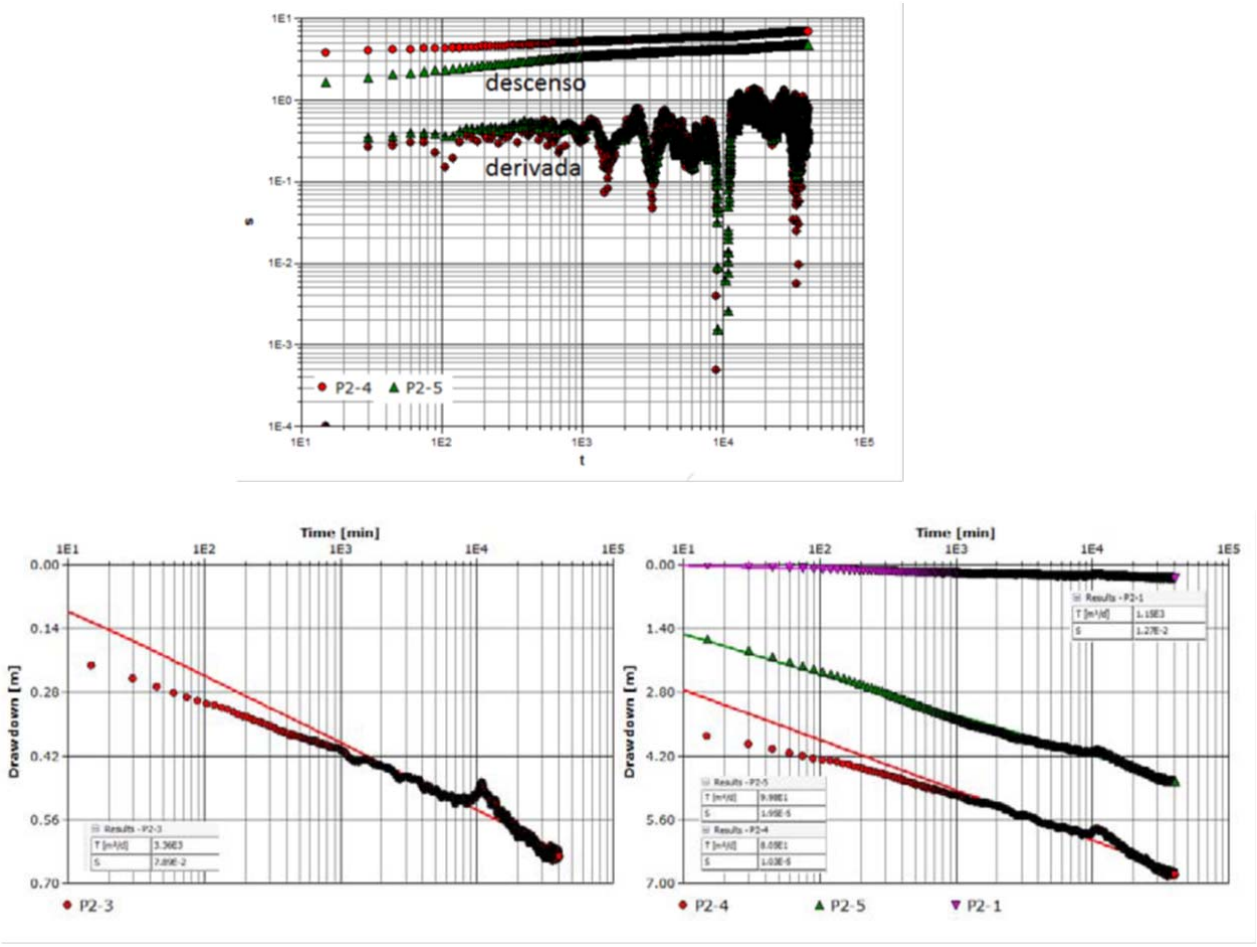

Table 10.4 P-2 pumping test results

Well	Unit	Max Drawdown (m)	Fit	T (m2/d)	S(-)	K (m/d)*	Ss (1/m)
P-2.3	Upper Halite	0.637	Theis	3,360	7.89E-02	197.6	4.64E-03
P-2.1	Upper Halita-clay	0.299	Theis	1,150	1.27E-02	191.7	2.12E-03
P-2.5	Clay core/ lower alluvium	4.723	Theis	99.8	1.95E-05	1.1	2.19E-07
P-2.4	Clay core/ lower alluvium	6.795	Theis	80.5	1.03E-05	0.9	1.17E-07

Figure 10.12 Li and K concentrations during the P-1 and P-2 pumping tests

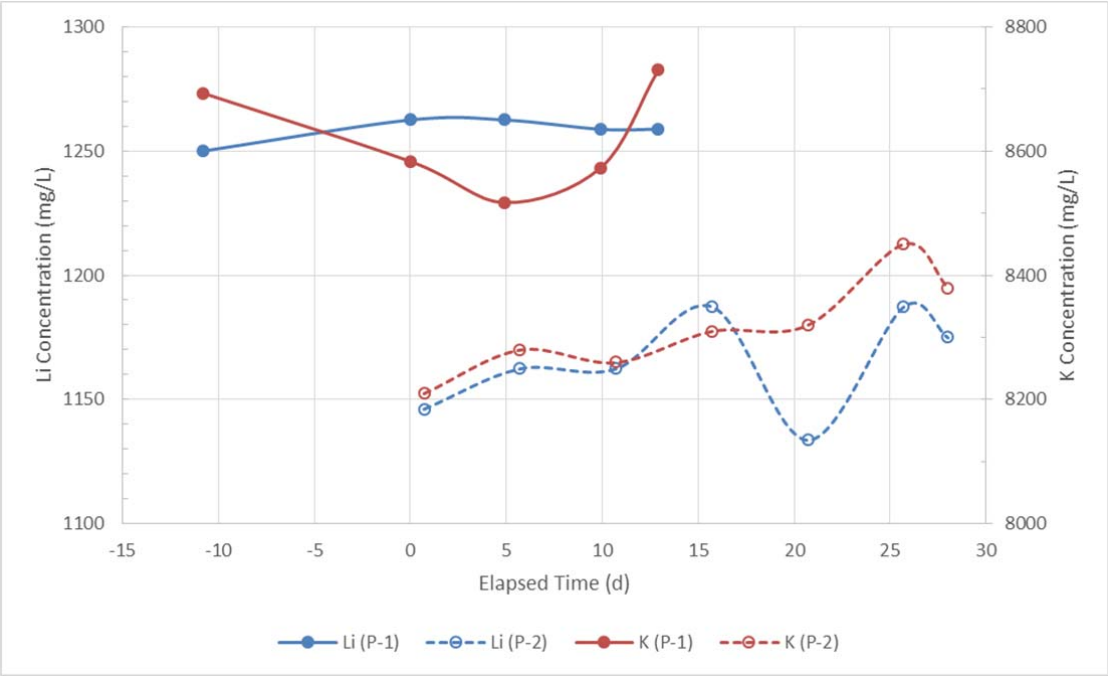

Source: FloSolutions 2015

P-2 Pumping test – shallow (2017)

A second pumping test was carried out on production well P-2 during 2017. During this test a packer was installed in the well at 40 m depth to isolate the deeper screened interval of the well and pump brine from just the Upper Halite unit. As expected some brine still entered the upper section of the well via upward vertical flow through the gravel pack. This second test was carried out at 45 L/s over a 7 day period during February 2017. Water level responses were measured in the adjacent monitoring wells (P2-1, P2-3, P2-4 and P2-5). The pumping rate was measured by an inline flow meter, manual measurements and in the V-notch tank. Pressure transducers were installed in all piezometers and the V-notch tank to record water level responses during the test in addition to manual measurements. Observed water level responses to the test are shown in Figure 10.13. The curve fitting and interpretation results of the second P-2 constant rate test are shown in Table 10.5

Sou

Figure 10.13 Water level responses P-2 constant rate test (2017)

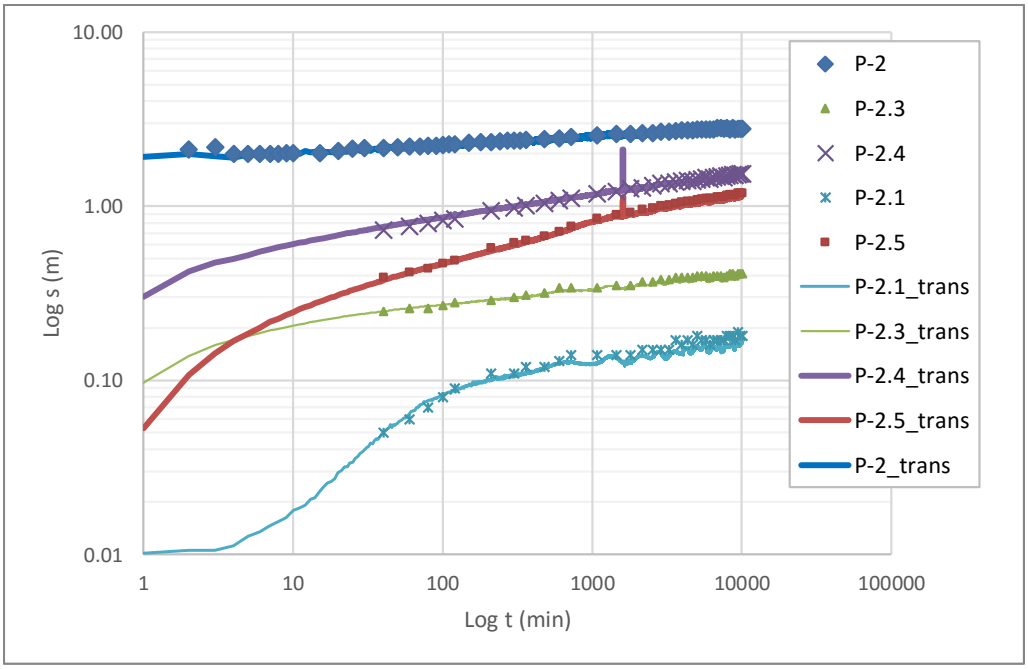

Table 10.5 P-2 pumping test results (2017)

Well	Unit	Max Drawdown (m)	Fit	T (m2/d)	S(-)	K (m/d)*	Ss (1/m)	Sy (%)
P-2.1	Upper Halite	0.17	Neuman	287	7.00E-03	47.8	1.17E-03	19
P-2.3	Upper Halite and clay	0.4	Theis	10,830	6.00E-04	637.1	3.53E-05	
P-2.4	Clay Core / Lower Alluvium	2.12	Theis	96	1.00E-04	1.1	1.14E-06	
P-2.5	Clay Core / Lower Alluvium	1.14	Theis	95	3.80E-04	1.1	4.27E-06	

P-4 Pumping test (2017)

Production well P-4 is completed with screened casing from 70 and 180 m depth in sands and gravels of the Lower Alluvium (lower aquifer). A bentonite and cement seal was installed in the annulus of the well between 57 m depth and ground surface so that no water from the upper aquifer (Upper Halite) could enter the well. Four monitoring wells (P4-1, P4-2, P4-3 and P4-4) are installed adjacent to well P-4 at radial distances from 10 to 40 m as shown in Figure 10.14. Piezometer P4-1 is completed in the Lower Alluvium, while piezometers P4-2, P4-3 and P4-4 are all shallow completions in the Upper Halite.

A 30-day constant rate test was conducted at 25 L/s during January / February 2017, followed by recovery. Pumped brine was piped through a 1,200 m plastic line to a V-notch tank where final discharge took place on to the Salar. The pumping rate was measured by an inline flow meter, manual measurements and in the V-notch tank. Pressure transducers were installed in all piezometers and the V-notch tank to record water level responses during the test in addition to manual measurements.

Observed water level responses to the test are shown in Figure 10.15. It should be noted that no water level responses were observed in shallow monitoring wells P4-2, P4-3 and P4-4. The curve fitting and interpretation results of the P-4 constant rate test are shown in Figure 10.16 and Table 10.6

Figure 10.14 Pumping test P-4 layout

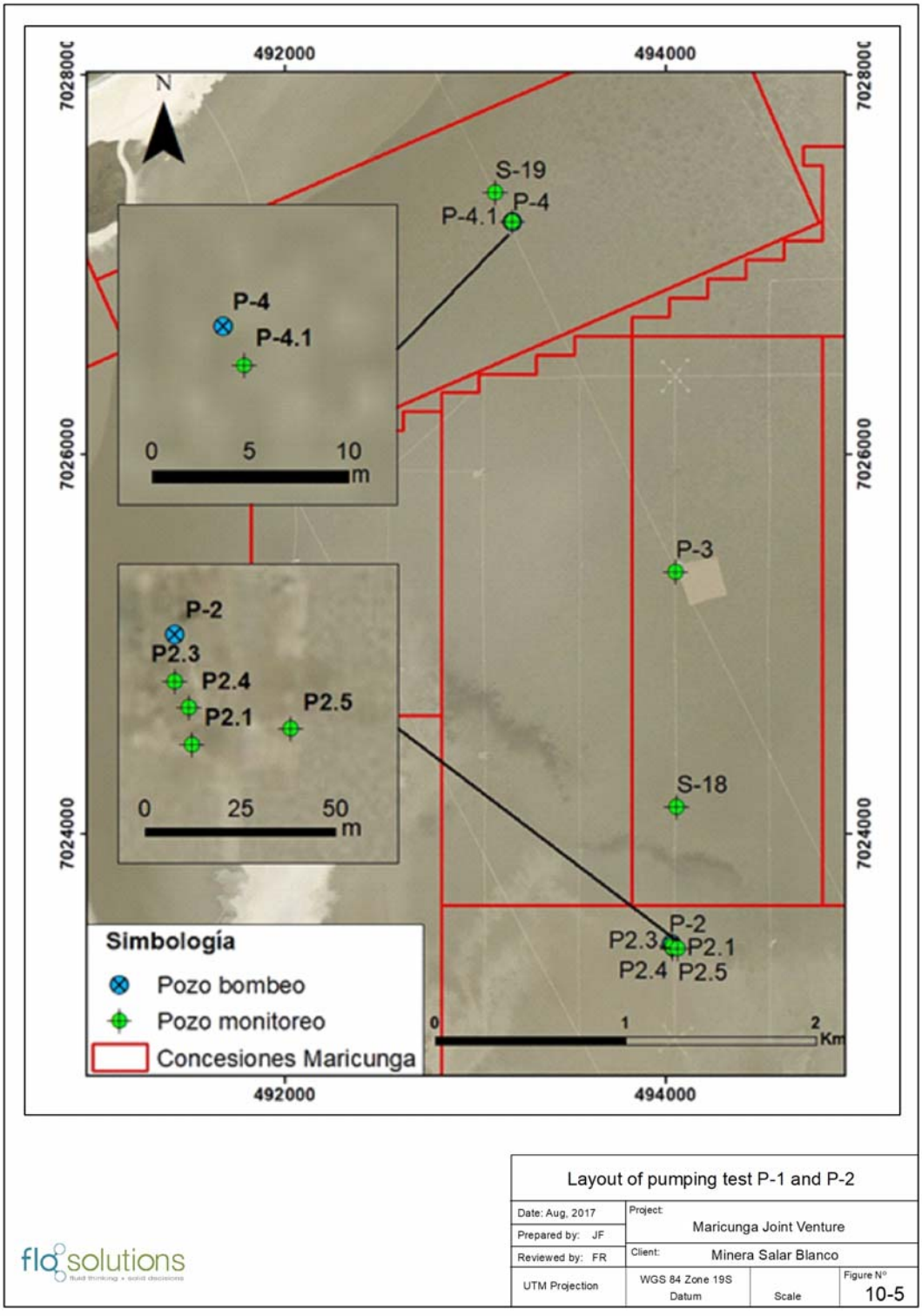

Figure 10.15 Water level responses P-4 constant rate test (2017)

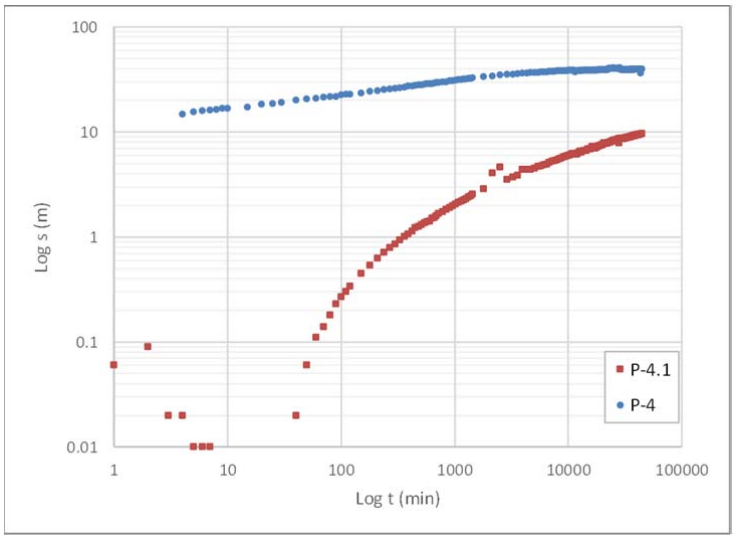

Figure 10.16 P-4 pumping test interpretation

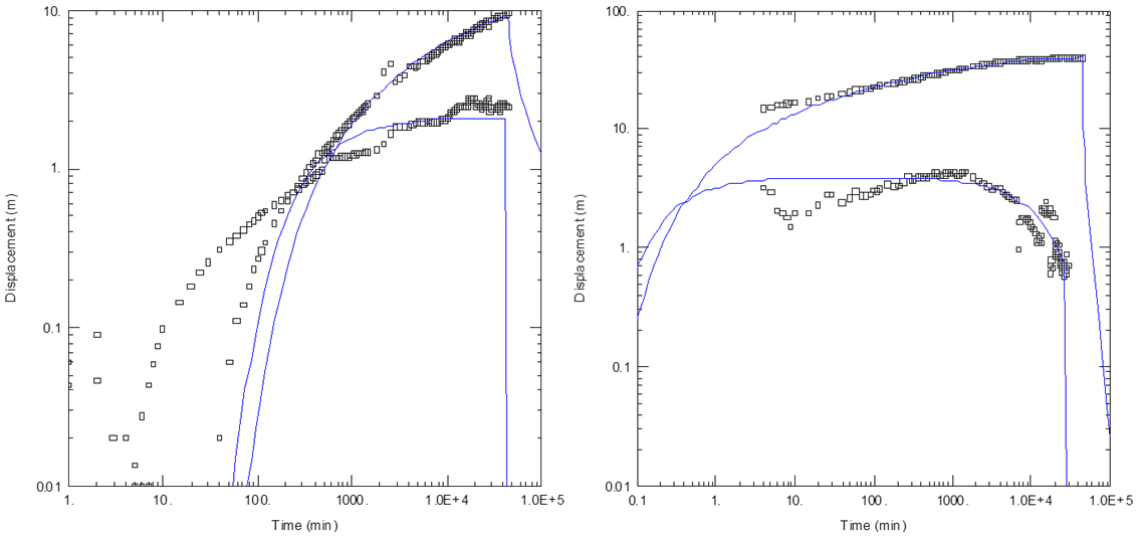

Table 10.6 P-4 pumping test results (2017)

Well	Unit	Max Drawdown (m)	Fit	T (m2/d)	S(-)	K (m/d)	Ss (1/m)
P-4	Lower aquifer	40.73	Hantush	44		0.4	
P-4.1	Lower aquifer	9.58	Theis	82	4.00E-01	0.9	4.44E-03

11 SAMPLE PREPARATION, ANALYSIS, AND SECURITY

11.1 Sampling Methods

Sampling and sample preparation protocols for the sonic drilling and RC drilling Programs in 2011 were developed by Frits Reidel, CPG, Don Hains, P.Geo, and Pedro Pavlovic, Chem Eng. All protocols were implemented at the start-up of the drilling programs in October 2011 under the supervision of Frits Reidel, CPG and included extensive day to day training and supervision of Li3 field staff and experienced MWH hydrogeologists and field technicians. Frits Reidel, CPG was present throughout the drilling program on regular intervals to review the day to day execution of these protocols.

Sampling and sample preparation protocols for the 2017 drilling programs were developed by Frits Reidel, CPG and Murray Brooker, RPGeo. All protocols were implemented at the start-up of the drilling programs in October 2017 under the supervision of Frits Reidel, CPG. Both authors were present throughout the drilling program on regular intervals to review the day to day execution of these protocols.

11.1.1 Sonic drilling sampling procedures

Porosity samples

Sonic core was collected in 1.5 m lexan core liners in alternating 1.5 m intervals as described in Section 10 above. A 10 cm sub-sample was cut from the lexan core liner; caps were placed on each end of the porosity sub-sample and taped to prevent any fluid loss. The samples were labelled with the borehole number and depth interval. Each day the porosity samples were transferred to the workshop in the on-site camp where the samples were labelled with a unique sample number. Prior to shipping each sample was wrapped in bubble plastic to prevent disturbance during shipping.

- 285 porosity samples were shipped to Daniel B Stephens and Associates (DBS&A) Laboratory in the USA in 2011
- 32 porosity check samples were shipped to the British Geological Survey (BGS) in the UK in 2011
- 198 core samples were shipped to Geosystems Anaylsis (GSA) in 2017 from which 28 samples were analysed by Corelabs as check samples.

Brine samples

Brine samples were collected at three-meter intervals during the 2011 sonic drilling where possible. Based on the experience from the 2011 program the brine sampling interval for the 2016/7 program during was 6 m. In some cases where the formation permeability was low, it was not possible to collect a brine sample after a one hour waiting period. The borehole was purged by bailing up to three well volumes of brine from the drill casing as calculated from the water level measurement prior to collecting the final brine sample from the bottom of the hole. The final brine sample was discharged from the bailer into a 20 liter clean bucket from which three one-liter sample bottles were rinsed and filled with brine. Each bottle was taped and marked with the borehole number and depth interval. A small sub-sample from the bucket was used to measure field parameters (density, electric conductivity, pH and temperature) at the wellhead (Figure 11.1).

Figure 11.1 Collection of field parameters of the brine samples at the wellhead

The samples were moved from the drill site to secure storage at the camp on a daily basis. All brine sample bottles are marked with a unique label. One sample bottle was stored as a permanent back-up sample in the on-site warehouse. One sample bottle was prepared for shipment and the third bottle was either used as a duplicate or discarded. No filtration was carried out on the brine samples prior to shipment to laboratories. Figure 11.2 illustrates the porosity samples and brine samples.

Figure 11.2 Porosity and brine samples

11.1.2 RC drilling sampling procedures

RC drill cuttings (2011)

During RC drilling, rock chip and brine were collected directly from the cyclone. Drill cuttings were collected over two meter intervals in plastic bags that were marked with the borehole number and depth interval. Sub-samples were collected from the plastic bag by the site geologist to fill chip trays (also at two meter interval). At the end of each borehole all chip trays were removed to storage in the on-site office (Figure 11.3). All plastic sample bags were stored in a secure on-site warehouse.

Figure 11.3 RC drill chip samples

RC brine sampling (2011)

Brine samples were collected at three-meter intervals during the RC drilling from the cyclone where possible. In some cases where the formation permeability was low, it was not possible to collect a brine sample. Brine samples were collected in three one-liter (rinsed) sample bottles. Each bottle was taped and marked with the borehole number and depth interval. A small sub-sample from the cyclone was used to measure field parameters (density, electric conductivity, pH and temperature) at the wellhead.

11.1.3 Rotary /HWT brine sampling procedures 2017

Rotary drill cuttings (2017)

During the rotary drilling, cuttings were collected directly at the head of the borehole in cloth, flow-through bags that minimize the loss of fines but allow fluid to drain at 2 m intervals. The cloth bags were marked with the borehole number and depth interval. Sub-samples were collected from the bags by the site geologist to fill chip trays (also at two meter interval). At the end of each borehole all chip trays were removed to storage in the on-site office. All sample bags were moved and stored in a secure warehouse in Copiapo.

- 196 rotary chip samples were shipped to Geosystems Anaylsis (GSA) in 2017 for GSA classification and consolidation tests.

Rotary brine sampling (2017)

A plug-type device connected to the wireline cable was used to purge the hole, rather than using a bailer. This consists of a very stiff rubber plug on a steel tool which is lowered down the hole. When this tool is pulled up from the base of the hole the rubber plug expands to flush with inside of the drill rods, drawing brine up the drill rods above the plug, with the brine flowing out of the rods at surface. This works in a similar fashion to the bailer, but in a continuous mode, rather than numerous repetitions of lowering and raising a bailer.

In the case of the rotary drilling it was not possible to lower the HWT casing to a meter above the base of the hole in many cases and consequently inflows from around the sides to the base of the hole could occur. The raising of the plug is likely to have had a suction effect around the base of the hole, stimulating inflows into the hole over a larger area than with the sonic drill holes.

Drilling fluids (in this case brine) are required during the rotary drilling to lift the cuttings out of the hole. The drilling fluid was mixed with a rhodamine / fluorescein tracer dye in portable tanks adjacent to the rig to distinguish the drilling fluid from the natural formation brine (Figure 11.4). Purging of the drill hole was continued until no tracer dye was observed in the purged brine. Any trace of dye observed in brine samples was noted to indicate the potential for contamination with drilling fluid. Brine samples were collected in duplicate at every sampling interval and in triplicate at every fifth sampling interval.

Figure 11.4 Fluorescein tracer dye in the rotary drilling fluid

11.2 Brine Analysis and Quality Control Results

11.2.1 Analytical methods

The University of Antofagasta in northern Chile was selected as the primary laboratory to conduct the assaying of the brine samples collected as part of the 2011 and 2017 drilling program. The laboratory of the University of Antofagasta is not ISO certified, but it is specialized in the chemical analysis of brines and inorganic salts, with extensive experience in this field since the 1980s, when the main development studies of the Salar de Atacama were begun. Other clients include SQM, FMC, LAC and Orocobre.

Alex Stewart Argentina in Mendoza, Argentina was used for the analysis of external check samples during the 2011 drilling campaign, while NOA Alex Steward Argentina in Jujuy was used for external

check samples during 2017 campaign. This laboratory is accredited to ISO 9001 and operates according to Alex Stewart Group standards consistent with ISO 17025 methods at other laboratories.

Table 11.1 lists the basic suite of analyses requested from both laboratories. Both of them used the same analytical methods based on the Standard Methods for the Examination of Water and Wastewater, published by American Public Health Association (APHA) and the American Water Works Association (AWWA), 21st edition, 2005, Washington DC. The University of Antofagasta used Atomic Absorption Spectrometry (AAS) was used for the determination of lithium, potassium, magnesium and calcium. Alex Stewart (Mendoza) employed Inductively Coupled Plasma (ICP), which is generally used for a large suite of elements (multi-elemental analysis), including the detection of trace metals. ASA included 10 elements in the determination with this analytical technique: B, Ba, Ca, Fe, K, Li, Mg, Mn, Na and Sr.

Table 11.1 List of analyses requested from the University of Antofagasta and Alex Stewart Argentina SA Laboratories

ANALYSIS	UNIVERSITY OF ANTOFAGASTA	ALEX STEWART	METHOD
Chemical-Physical Parameters			
Total Dissolved Solids	SM 2540-C	SM 2540-C	Total Dissolved Solids Dried at 180ºC
PH	SM 4500-H^+B	SM 4500-H^+B	Electrometric Method
Density	CAQ – 001DS	IMA-28	Pycnometer
Alkalinity	SM 2320-B	SM 2320-B	Acid-Base Titration
Inorganic Parameters			
Boron (B)	CAQ – 005 BS	ICP - OES	Acid-Base Titration
Chlorides (Cl)	SM 4500-Cl^-B	SM 4500-Cl^-B	Argentometric Method
Sulfates (SO4)	SM 4500^{2-}D (Drying of Residue)	SM 4500^{2-}C (Ignition of Residue)	Gravimetric Method
Dissolved metals			
Sodium (Na)	SM 3111 B	ICP-OES 10	Direct Aspiration-AA or ICP Finish
Potassium (K)	SM 3111 B	ICP-OES 10	Direct Aspiration-AA or ICP Finish
Lithium (Li)	SM 3111 B	ICP-OES 10	Direct Aspiration-AA or ICP Finish
Magnesium (Mg)	SM 3111 B	ICP-OES 10	Direct Aspiration-AA or ICP Finish
Calcium (Ca)	SM 3111 D	ICP-OES 10	Direct Aspiration-AA or ICP Finish

11.2.2 Analytical Quality Assurance and Quality Control ("QA/QC") 2011 Program

A full QA/QC program for monitoring accuracy, precision and potential contamination of the entire brine sampling and analytical process was implemented. Accuracy, the closeness of measurements to the "true" or accepted value, was monitored by the insertion of standards, or reference samples, and by check analysis at an independent secondary laboratory.

Precision of the sampling and analytical program, which is the ability to consistently reproduce a measurement in similar conditions, was monitored by submitting blind field duplicates to the primary laboratory. Contamination, the transference of material from one sample to another, was measured by inserting blank samples into the sample stream at site. Blanks were barren samples on which the presence of the main elements undergoing analysis has been confirmed to be below the detection limit.

Approximately 31% of the 623 samples submitted for chemical analysis during the 2011 campaign were quality control samples. The QA/QC procedures adopted for the Project are discussed below, and included the following:

- Three standards (A, B and C) were inserted at a frequency of 1 in 15 samples (1/3 of each type of standard, randomly inserted). The specially prepared samples were submitted to five laboratories as a Round Robin (each analyzing five 1-L sub-samples from each type of standard) to establish an accepted mean and standard deviations for the analytical variables. These three standards were prepared from Maricunga brine and each with a different dilution factor.
- The University of Antofagasta made an internal check on overall analytical accuracy for the primary constituents of the brine by using ion balance. This calculation was checked and also the ratio of measured to calculated TDS was added as another procedure for checking the correctness of analyses.
- Duplicate samples at a frequency of 1 in 10 samples in the analysis chain were submitted to the University of Antofagasta as unique samples (blind duplicates) to monitor precision.
- Stable blank samples (distilled water) were inserted at a frequency of 1 in 30 samples to measure cross contamination.
- Duplicates at a frequency of 1 in 10 samples, and including blind control samples (a total of 70 samples), were submitted to the secondary laboratory (Alex Stewart in Mendoza) as check samples (external duplicates).

11.2.3 Analytical accuracy 2011 Program

Anion-cation balance

The anion-cation balance was used as a measure of analytical accuracy. The anion and cation sums, when expressed as equivalents or milliequivalents per liter, must balance in an ideally perfect analysis, because mixtures of electrolytes are electrically neutral. The term meq/L is defined as:

$$\text{Meq/L} = (\text{mg/L} * \text{valence number} / \text{molecular weight of ion})$$

The charge balance is expressed as a percentage, as follows:

$$\% \text{ Difference} = ((\sum Cations - \sum Anions)/(\sum Cations + \sum Anions)*100,$$

Although this test does not monitor individual elements, it is recommended by APHA-AWWA-WPCF in their Standard Methods, 21st edition, 2005 (1030 E) as a procedure for checking correctness of water analyses. The typical criterion for acceptance is a maximum difference of 5%, which is used by the University of Antofagasta as well as by Alex Stewart.

The performance of the University of Antofagasta in the analyses of 431 primary samples and 61 duplicates show a balance within 2%, i.e. much less than the maximum acceptable difference of 5%. All the check samples analyzed by Alex Stewart had a balance within a value of 5%.

Measured versus calculated TDS

Measured versus calculated Total Dissolved Solids (TDS) was used as a second evaluation test of analytical accuracy. The recommended ratio according to the APHAA/AWWA/WPCF Standard Method should be between 1.0 and 1.2. Results for the submitted samples to the University of Antofagasta (431 primary samples plus 61 duplicates) ranged from 0.983 to 1.043, with 10% of the samples below the acceptable ratio (1.0) and most of these between 0.994 and 1.0. This is considered as a very good performance given the high dissolved solids content of the brine.

Based on the results detailed above, the authors are of the opinion that the sample analytical results are reliable and accurate.

Certified analytical standards

Three standard reference samples, prepared at site with original brine (Standard A, 100% natural brine; Standard B, 80%; Standard C, 60%, dilution with distilled water) were used in the sampling program. Sets of randomized replicates were sent in a Round Robin analysis program to five laboratories (15 sub-samples to each lab) to determine the certified values used to monitor the accuracy of analyses. Statistics were done on the Round Robin assay results and the standard reference samples certified for the elements that met the criteria of having a global Relative Standard Deviation (RSD) of near 5% or less.

The results of the standards analyses for Li, K and Mg are summarized in Table 11.2. This table lists the statistics, number of samples exceeding the acceptable failure criteria of the mean ± 2 standard deviations, and the relative standard deviation (RSD) for each standard. Standard analyses at the University of Antofagasta indicate very acceptable accuracy. There are only two exceptions: one failure for potassium analysis of the Standard A and one failure for Mg analysis of the Standard B. Each of these failures is not significant. From Table 11.2 the relative standard deviation values (measure of precision) for the University of Antofagasta analyses range from 1.36 to 2.67, indicating very good analytical reproducibility for the standard analyses conducted at the primary laboratory. Based on the analysis detailed above, the authors are of the opinion that the lithium, potassium and magnesium analyses are accurate. There is also a good reproducibility or precision in the assay values reported by the University of Antofagasta for these three elements.

Table 11.2 Standards analysis results from U. Antofagasta (2011)

Statistics	Li (mg/L)		
Standard	A	B	C
Count	14	14	14
Min	1095	855	675
Max	1150	950	725
Mean	1128	914	699
Standard Deviation	15.3	21.9	14.2
Mean ± 2 Standard Deviation			
Mean + 2SD	1159	958	728
Mean - 2SD	1098	870	671
No of Failures >2SD	0	0	0
Relative Standard Deviation			
RSD	1.36	2.40	2.04
Statistics	K (mg/L)		
Standard	A	B	C
Count	14	14	14
Min	7896	6291	4883
Max	8510	6830	5215
Mean	8090	6533	5033
Standard Deviation	157.8	142.7	87.3
Mean ± 2 Standard Deviation			
Mean + 2SD	8405	6818	5207
Mean - 2SD	7774	6247	4858
No of Failures >2SD	1	0	0
Relative Standard Deviation			
RSD	1.95	2.18	1.74
Statistics	Mg (mg/L)		
Standard	A	B	C
Count	14	14	14
Min	6875	5588	4275
Max	7450	6225	4600
Mean	7169	5915	4487
Standard Deviation	148.4	157.7	101.8
Mean ± 2 Standard Deviation			
Mean + 2SD	7466	6231	4691
Mean - 2SD	6872	5600	4284
No of Failures >2SD	0	1	0
Relative Standard Deviation			
RSD	2.07	2.67	2.27

Check Analyses

Checks analyses were conducted at Alex Stewart located in Mendoza, Argentina. About 15% of external duplicates (61 samples) were submitted. In addition, some blanks and standard control samples were inserted to monitor accuracy and potential laboratory bias. The total number of samples in the batch was 70. The standards indicated acceptable accuracy and precision for Li and K.

Statistical analysis of the 61 pairs of check sample assay values was conducted using Reduction-to-Major-Axis ("RMA") multiple linear regressions for Li, K and Mg. StatGraphics software was used for this analysis. The results are summarized in Table 11.3.

Table 11.3 Check assays (U. Antofagasta vs. Alex Stewart): RMA regression statistics

Maricunga Project - RMA Parameters							
Element	R^2	Pairs	m	Error (m)	B	Error (b)	Bias
Li (mg/L)	0.98223	61	0.8598	0.01511	83.2787	19.2822	14.02%
K (mg/L)	0.98675	61	1.0207	0.01539	521.422	141.618	-2.07%
Mg (mg/L)	0.97183	61	1.0978	0.02433	-217.714	206.109	-9.78%

The R-squared statistic is the indicator of the quality of the fit. High values of this coefficient reflect a good fit and low values a poor fit.

The bias, which is a measure of accuracy (the higher the bias, the lower the accuracy), is calculated as Bias (%) = 1 – RMAS where RMAS is the slope (m) of the Reduction-to-Major-Axis regression line of the secondary laboratory ICP values (ASA) versus the primary laboratory AAS values (University of Antofagasta) for each element. Because of different analytical finish, in general the UoA obtained a little higher assay values for lithium and a little lower for potassium and magnesium, as shown in Table 11.4.

Table 11.4 Check assays between the University of Antofagasta and Alex Stewart

Statistics	UA Li (mg/L)	ASA Li (mg/L)	UA K (mg/L)	ASA K (mg/L)	UA Mg (mg/L)	ASA Mg (mg/L)
Count	61	61	61	61	61	61
Min	470	447	3,828	4,123	2,838	3,030
Max	1,850	1,697	13,750	14,396	13,200	14,574
Mean	1,240	1,149	8,946	9,654	8,199	8,783
Std Dev	304	264	2,152	2,209	2,146	2,390
Precision		7.5		7.8		7.6
% Bias		14.02		-2.07		-9.78
Correlation		0.98		0.99		0.97
%<10%		88		85		87
%<15%		98		100		98

Precision in Table 11.4 was assessed through the Relative Percent Difference or Relative Error, defined as the absolute value of the difference between two similar analyses, and divided by the average between these two assays. Precision of the external duplicate analyses is acceptable for Li, K and Mg.

Eighty-eight per cent of the Li assays are within ± 10% of one another (ASA considers acceptable 10% RPD for check samples analyzed in the same lab).

Based on the analysis detailed above, the authors are of the opinion that the check assays indicate that the lithium and potassium concentrations determined for the primary sample assays are suitable for use in a resource calculation.

Sample Duplicate Analyses

Sixty-one duplicate samples were collected in the field to confirm the overall sampling precision, and shipped also to the University of Antofagasta laboratory. Table 11.5 lists the statistics, as well as the calculated precision, bias, correlation and percent of duplicate analyses with results within 5% of one another. The bias and correlation were calculated through RMA plots, constructed with StatGraphics software. The duplicate analysis repeated exceedingly well, as was shown in these RMA plots.

Table 11.5 Duplicate analyses from the University of Antofagasta

Statistics	Li (mg/L)	Duplicate Li (mg/L)	K (mg/L)	Duplicate (mg/L)	Mg (mg/L)	Duplicate Mg (mg/L)
Count	61	61	61	61	61	61
Min	470	470	3,853	3,918	3,031	3,006
Max	1,938	1,950	13,506	13,519	14,425	14,250
Mean	1,261	1,265	9,098	9,090	8,444	8,445
Std Dev	298	299	2159	2,134	2,107	2,090
Precision		1.17		1.25		1.31
% Bias		0.03		1.42		1.07
Correlation		0.99		0.99		0.99
%<5%		100		100		95

Assay results for duplicate samples at the U. Antofagasta indicate excellent precision (within 5% or less) for Li, K and Mg. Bias between duplicates and main samples are within 2% and correlation is high (R^2=0.9938 to 0.9950) for the three elements.

Sample Contamination

Potential sources of sample contamination are related to sample mis-ordering errors or insufficient washing of analytical equipment between samples. A field blank consisting of distilled water was inserted into the sample stream 20 times. New plastic bottles were used in all the cases to avoid eventual contamination with brine samples.

Results reported by the University of Antofagasta indicate <0.05 mg/L (detection limit for lithium) in the majority of blank samples. However, there are four results, corresponding to the last two sample batches with 0.07 (2), 0.08 and 0.09 mg/L for lithium. This reveals that some small contamination with brine was produced in the manipulation of the plastic bottles, either at the project site, or in the lab. This issue is not considered to detract from the validity of the overall sampling and assay results and the use of the assay results in resource estimates.

11.2.4 Analytical Quality Assurance and Quality Control ("QA/QC") 2017 Program

A total of 343 primary brine samples were analyzed from the 2016-17 drilling campaign. An additional 133 brine samples from pumping tests and baseline monitoring were analyzed. These primary analyses were supported by a total 159 QA/QC analyses consisting of:

- 47 standard samples (7%),
- 85 duplicates (13%) and
- 27 blank samples (4%).

In addition to evaluation of standards, field duplicates and blanks the ionic balance (the difference between the sum of the cations and the anions) was evaluated for data quality. Balances are generally considered to be acceptable if the difference is <5% and were generally <1%. No samples were rejected as having > 5% balances. The results of standard, duplicate and blank samples analyses are considered to be adequate and appropriate for use in the resource estimation described herein.

11.2.5 Analytical accuracy 2017 Program

Anion-cation balance

The performance of the University of Antofagasta in the analyses of 308 main samples and 30 duplicates show a balance within 3%, i.e. less than the maximum acceptable difference of 5%. All the check samples analyzed by Alex Stewart had a balance within a value of 2%.

Measured versus calculated TDS

Measured versus calculated Total Dissolved Solids (TDS) was used as a second evaluation test of analytical accuracy. The recommended ratio according to the APHAA/AWWA/WPCF Standard Method should be between 1.0 and 1.2. Results for the submitted samples to the University of Antofagasta (308 main samples plus 30 duplicates) ranged from 0.97 to 1.02, with 9% of the samples below the acceptable ratio of 1.0, and most of these between 0.99 and 1.0. This is considered as a very good performance given the high dissolved solids content of the brine.

Results for the submitted samples to the external laboratory (28 duplicate samples) ranged from 0.98 to 1.14, with only one sample below the acceptable ratio of 1.0, and most of these between 1.02 and 1.14. This is considered as a good performance given the high dissolved solids content of the brine.

Based on the results detailed above, the authors are of the opinion that the sample analytical results are reliable and accurate.

Certified analytical standards

Two standard reference samples, SRM-1 and SRM-2 were used in the sampling program. Sets of randomized replicates were sent in a Round Robin analysis program to five laboratories to determine the certified values used to monitor the accuracy of analyses. Statistics were done on the Round Robin assay results and the standard reference samples certified for the elements that met the criteria of having a global Relative Standard Deviation (RSD) of near 5% or less. Overall the performance of University of Antofagasta laboratory and the external laboratory were satisfactory.

The results of the standards analyses for Li, K and Mg, are summarized in Table 11.6. This table lists the statistics, number of samples exceeding the acceptable failure criteria of the mean ± 2 standard deviations, and the relative standard deviation (RSD) for each standard. Standard analyses at the University of Antofagasta indicate an acceptable accuracy. There is one failure for Li and K analysis, and 2 failures for Mg analysis of the Standard SRM-1, and there is no failure for Li analysis and one failure for K and Mg analysis of Standard SRM-2. Overall these failures are not significant. From Table 11.6 the relative standard deviation values (measure of precision) for the University of Antofagasta analyses range from 1.3 to 2.4, indicating very good analytical reproducibility for the standard analyses conducted at the primary laboratory. Based on the analysis detailed above, the authors are of the opinion that the lithium, potassium and magnesium analyses are accurate. There is also a good reproducibility or precision in the assay values reported by the University of Antofagasta for these three elements.

Table 11.6: Standards analysis results from U. Antofagasta (2017)

Statistics	Li (mg/L)	
Standard	SRM-1	SRM-2
Count	15	14
Min	476	1,040
Max	500	1,087
Mean	**486**	**1,059**
Standard Deviation	7	15
Mean ± 2 Standard Deviation		
Mean + 2SD	499	1,090
Mean - 2SD	473	1,029
No of Failures >2SD	1	0
Relative Standard Deviation		
RSD	1.4	1.4
Statistics	**K (mg/L)**	
Standard	SRM-1	SRM-2
Count	15	14
Min	6,150	7,760
Max	6,630	8,540
Mean	**6,341**	**7,986**
Standard Deviation	123	195
Mean ± 2 Standard Deviation		
Mean + 2SD	6,588	8,377
Mean - 2SD	6,094	7,596
No of Failures >2SD	1	1
Relative Standard Deviation		
RSD	1.9	2.4
Statistics	**Mg (mg/L)**	
Standard	SRM-1	SRM-2
Count	15	14
Min	4,415	5,915
Max	4,730	6,250
Mean	**4,557**	**6,052**
Standard Deviation	69	81
Mean ± 2 Standard Deviation		
Mean + 2SD	4694	6214
Mean - 2SD	4420	5890
No of Failures >2SD	2	1
Relative Standard Deviation		
RSD	1.5	1.3

Check Analyses

Checks analyses were conducted at Alex Stewart located in Mendoza, Argentina. A total of 28 samples were submitted. In addition, some blanks and standard control samples were inserted to monitor accuracy and potential laboratory bias. The total number of samples in the batch was 35. The standards indicated acceptable accuracy and precision for Li and K.

Statistical analysis of the 28 pairs of check sample assay values was conducted using Reduction-to-Major-Axis ("RMA") multiple linear regressions for Li, K and Mg. StatGraphics software was used for this analysis. The results are summarized in Table 11.7.

In general, there is an acceptable correlation between the main samples and the external duplicates, with R2 ranging from 0.919 to 0.955.

The bias is below 5% with the highest bias (0.55%) for lithium, lower bias (-3.79 and -3.23) for potassium and magnesium, indicating that the UoA obtained a little higher assay values for lithium and a little lower for potassium and magnesium, as shown in Table 11.7.

Precision of the external duplicate analyses is acceptable for Li, K and Mg. Eighty-three per cent of the Li assays are within ± 15% of one another.

Table 11.7: Check assays between the University of Antofagasta and Alex Stewart

Statistics	UA Li (mg/L)	ASA Li (mg/L)	UA K (mg/L)	ASA K (mg/L)	UA Mg (mg/L)	ASA Mg (mg/L)
Count	28	28	28	28	28	28
Min	660	566	4,520	4,446	3,880	3,456
Max	1,626	1,517	12,620	12,833	11,000	10,675
Mean	1,015	931	7,744	7,642	6,308	6,064
Std Dev	248	246	1,982	2,053	1,702	1,755
Precision		9.43		5.83		5.94
% Bias		0.55		-3.79		-3.23
Correlation		0.955		0.919		0.955
%<10%		63		77		80
%<15%		83		83		90

Based on the analysis detailed above, the authors are of the opinion that the check assays indicate that the lithium and potassium concentrations determined for the primary sample assays are suitable for use in a resource calculation.

Sample Duplicate Analyses

Thirty duplicate samples were collected in the field to confirm the overall sampling precision, and shipped also to the University of Antofagasta laboratory. Table 11.8 lists the statistics, as well as the calculated precision, bias, correlation and percent of duplicate analyses with results within 5% of one another. The bias and correlation were calculated through RMA plots, constructed with StatGraphics software. The duplicate analysis repeated exceedingly well.

Table 11.8 Duplicate analyses from the University of Antofagasta

Statistics	Li (mg/L)	Duplicate Li (mg/L)	K (mg/L)	Duplicate K (mg/L)	Mg (mg/L)	Duplicate Mg (mg/L)
Count	30	30	30	30	30	30
Min	523	516	2,940	2,940	3,215	3,300
Max	3,375	3,342	20,640	20,020	21,800	21,760
Mean	1,123	1,121	8,079	8,101	7,074	7,101
Std Dev	511	511	3,220	3,120	3,370	3,351
Precision		1.79		1.96		1.47
% Bias		0.15		-3.21		-0.58
Correlation		0.997		0.995		0.998
%<5%		93		93		97

Assay results for duplicate samples at the U of Antofagasta indicate excellent precision (within 5% or less) for Li, K and Mg. Bias between duplicates and main samples are within 3% and correlation is high (R^2=0.995 to 0.998) for the three elements.

Sample Contamination

A field blank consisting of distilled water was inserted into the sample stream 20 times. New plastic bottles were used in all the cases to avoid eventual contamination with brine samples. Results reported by the University of Antofagasta indicate <0.05 mg/L (detection limit for lithium) in all of the blank samples. This indicates no lithium contamination during all the sampling and analysis stages.

11.2.6 Additional QA/QC analysis 2017 Program

A comparison was carried out between centrifuged brine samples from sonic core and bailed brine samples collected during sonic drilling. Eight sonic cores were centrifuged at 1/3 bar by Corelabs and the released brine was collected and shipped to University of Antofagasta in small sealed glass containers for Li concentration analysis. Table 11.9 shows the selected core samples (borehole and depth interval) with the analysis of the Li concentration of the centrifuged brine and the Li concentration of the bailed brine sample during the sonic drilling at the same depth interval. Figure 11.5 shows the comparison between the bailed and the centrifuged brine samples. The two methodologies show a good correlation.

Table 11.9 Comparison of lithium concentrations in centrifuge and bailed brine samples

Borehole	Depth (m)	Centrifuge Li (mg/L)	Bailed Li (mg/L)
S-1	5	1,834	1,854
S-1	11	990	913
S-1	19	1,980	2,006
S-2	11	1,180	1,460
S-2	89	664	660
S-2	110	725	770
S-2	134	639	670
S-2	152	681	716

Figure 11.5 Comparison of lithium concentrations in centrifuge and bailed brine samples

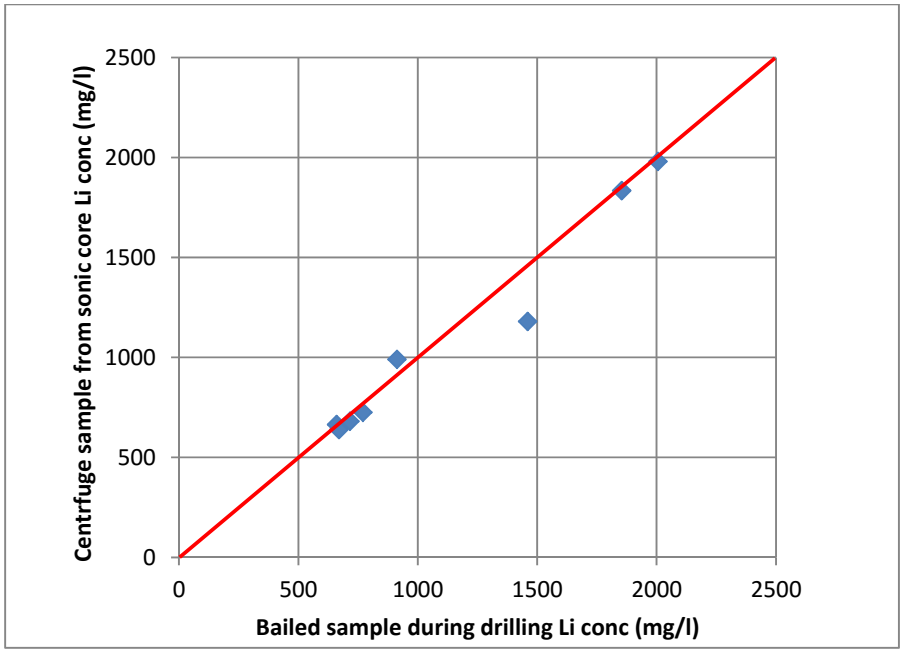

11.3 Drainable Porosity Analysis and Quality Control Results

11.3.1 DBSA 2011

Daniel B. Stevens & Associates Inc. in Albuquerque, New Mexico (DBSA) was selected as the prime laboratory for determination of drainable porosity (or specific yield) on the 2011 sonic core samples from boreholes C-1 though C-6. DBSA also undertook analysis of particle size, density and other physical properties of the core samples. DBSA received a total of 285 core samples which had been initially prepared by Li3 staff at the field camp on the salar. All samples were prepared and shipped to DBSA as detailed in section 11.1 of this report. On receipt of samples at DBSA, the samples were treated in one of three ways in preparation for determination of Relative Brine Release Capacity. These were:

1) the entire intact sample was used,
2) an intact sub-sample was obtained by cutting the original sample acetate sleeve with a chop saw,
3) an intact sub-sample was obtained by pushing a smaller diameter testing ring into the original sample.

All but six samples received were subject to RBRC testing. The six samples not used for RBRC testing were considered to be too brittle or crumbly to obtain an appropriate sub-sample. Thirty-four (34) verification tests (duplicates) were also performed, for a total of 313 RBRC tests. After completion of RBRC tests, 30 samples were selected for particle size analysis.

Relative Brine Release Capacity Test

The Relative Brine Release Capacity test predicts the volume of solution that can be extracted from an unstressed geologic sample which is equivalent to drainable porosity. The test method is briefly described below:

Undisturbed samples from the site are saturated in the laboratory using site specific brine solution. The bottom of the samples are then attached to a vacuum pump using tubing and permeable end caps, and are subjected to a suction of 0.2 to 0.3 bars for 18 to 24 hours. The top end cap is fitted with a one-gallon air bladder which allows sufficient drainage while inhibiting continuous atmospheric air flow. The vacuum system permits testing multiple samples simultaneously in parallel. The samples are then oven dried at 60°C.

Based on the density of the brine, the sample mass at saturation, and the sample mass at 'vacuum dry', the volumetric moisture (brine) contents of the samples are calculated. The difference between the volumetric moisture (brine) content of the saturated sample and the volumetric moisture (brine) content of the 'vacuum dry' sample is the "relative brine release capacity".

This methodology has been widely accepted by companies involved in the lithium brine exploration activities and is regarded as being a suitable method for determination of Specific Yield (Houston, 2011).

DBSA also undertook several verification tests related to RBRC testing. These included the following:

- "Remolded" samples in cases where there was insufficient intact original material for secondary testing. Samples were prepared for testing by remolding the material to target the initial density after the initial testing was performed.

- Samples designated as 'Sub-sample #2' were prepared for testing by obtaining a separate intact sub-sample from the original core.
- Samples designated as 'Day 1' and 'Day 2' are the same sub-sample, only the time the sample was subjected to vacuum suction was varied (18-24 hours and 36-28 hours, respectively).

Particle Size Analysis

After RBRC testing, thirty (30) of the samples were chosen to be used for particle size analysis (PSA). The samples were chosen with the intent to represent each of the material types present in the sample batch. Several of the sample results indicate discontinuity between the physical particle size analysis and the hydrometer analysis due to high clay and/or salt content.

DBSA employed the following standard test methods for determination of other physical properties of the samples:

- Dry Bulk Density: ASTM D7263
- Moisture Content: ASTM D7263
- Calculated Porosity: ASTM D7263
- Particle Size Analysis: ASTM D422
- USDA Classification: ASTM D422, USDA Soil Textural Triangle

DBSA relied upon the brine solution density (1.20) provided by Li3 in calculating the volumetric moisture (brine) content. Particle densities of the samples were calculated based on the assumption that the samples were 100% saturated after the saturation stage of the test procedure. The calculated particle density was then used to calculate the total porosity of each of the samples. Volume measurements for each sample were obtained at the “as received”, “saturated”, and “vacuum dry” conditions. It is noted that due to irregularities on the sample surfaces, volume measurements should be considered as estimates.

A total of 20 samples tested were noted to have questionable integrity (QI) relative to the in-situ conditions described by Li3. For sands, silts, and clays a ‘questionable integrity’ designation indicates that the sample may, or may not, accurately represent in-situ conditions (material appeared loose initially) relative to presumed in-situ conditions. For halite cores a ‘questionable integrity’ designation indicates that the sample core had grooves, pits, or other void spaces that may, or may not, be a result of the sampling technique employed. For halite cores a 'questionable integrity’ may indicate that some dissolution has occurred during testing.

RBRC test results

Drainable porosity is largely dependent on lithology which is highly variable as observed from the drilling results. Figure 11.6 shows a plot of total porosity vs drainable porosity based on the results of the DBSA analyses. Therefore, based on visual inspection and particle size analyses the samples were grouped in three types as follows: 1) a halite mix, 2) a silt-clay mix and 3) a sand mix. Table 11.10 shows the results of the laboratory drainable porosity analyses.

Figure 11.6: DBSA laboratory specific yield (S_y) analyses against total porosity

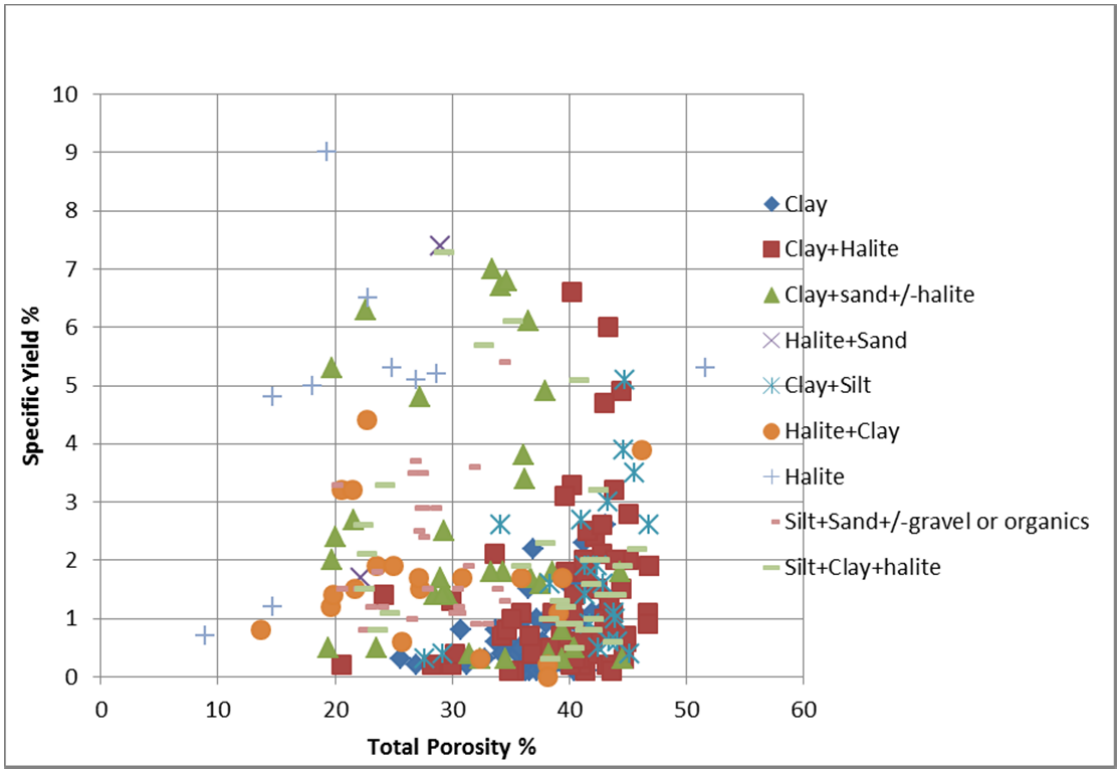

Table 11.10: Results of laboratory specific yield (S_y) analyses

	S_y - Halite mix	S_y - Silt-clay mix	S_y - Sand mix
Number of samples	56	195	29
Max	0.203	0.066	0.310
Min	0.002	0.001	0.015
Mean	0.034	0.012	0.061
Standard Deviation	0.038	0.011	0.058

British Geological Survey QA/QC tests 2011

Thirty (30) sonic core samples were shipped to the British Geological Survey (BGS) for determination of porosity and specific yield as a check against the DBSA results. The samples were duplicates of samples shipped to DBSA for RBRC testing. Samples were initially centrifuged to release pore fluid to determine Sy in "as received conditions". The chemistry of released pore fluid was analyzed as a double check against UoA and ASA results and found to be similar. The samples were then re-saturated and allowed to drain (similar to the RBRC test) and then oven dried to obtain total porosity values

Results of the BGS test work showed significantly higher and drainable porosity values than reported by DBSA, as shown in Figure 11.7, however DBSA shows significantly higher total porosity values (Figure 11.8). It is possible that the DBSA testing methodology systematically under-estimates drainable porosity for finer grained sediments (clay and silt).

Figure 11.7 Comparison of BGS and DBSA specific yield (S_y) analyses

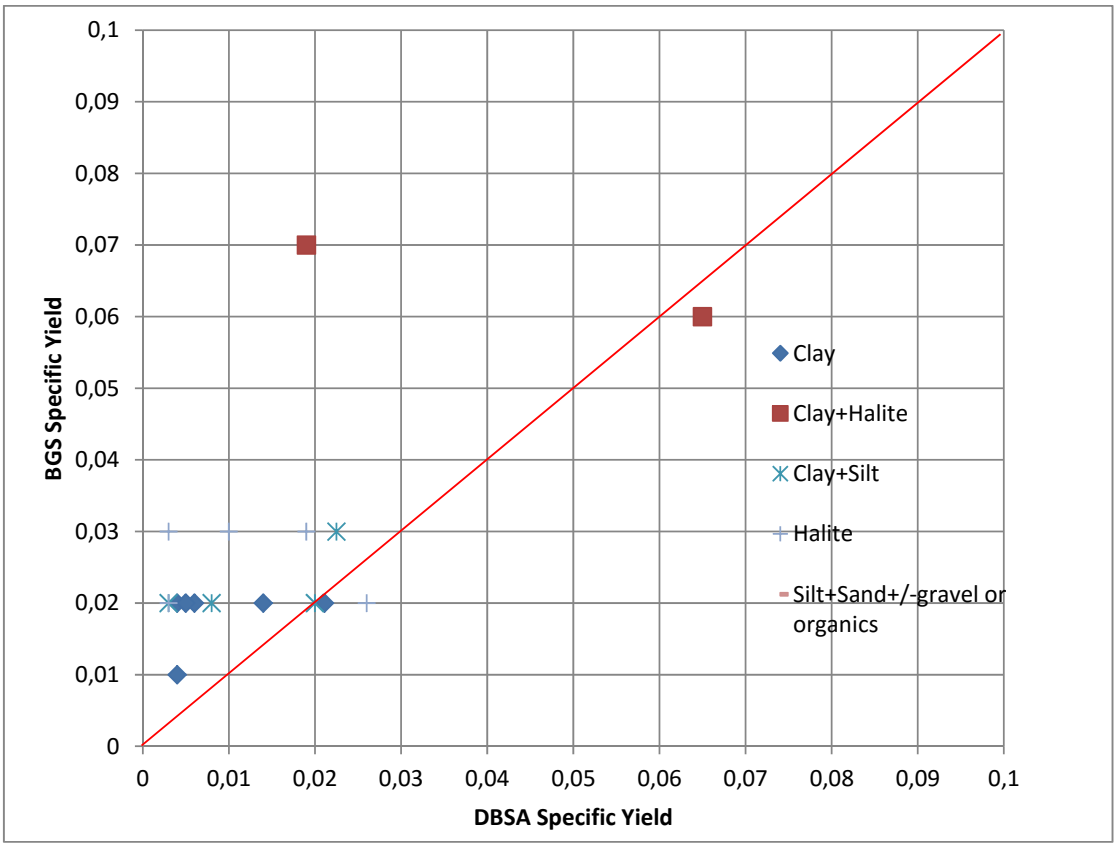

Figure 11.8 Comparison of BGS and DBSA total porosity (P_t) analyses

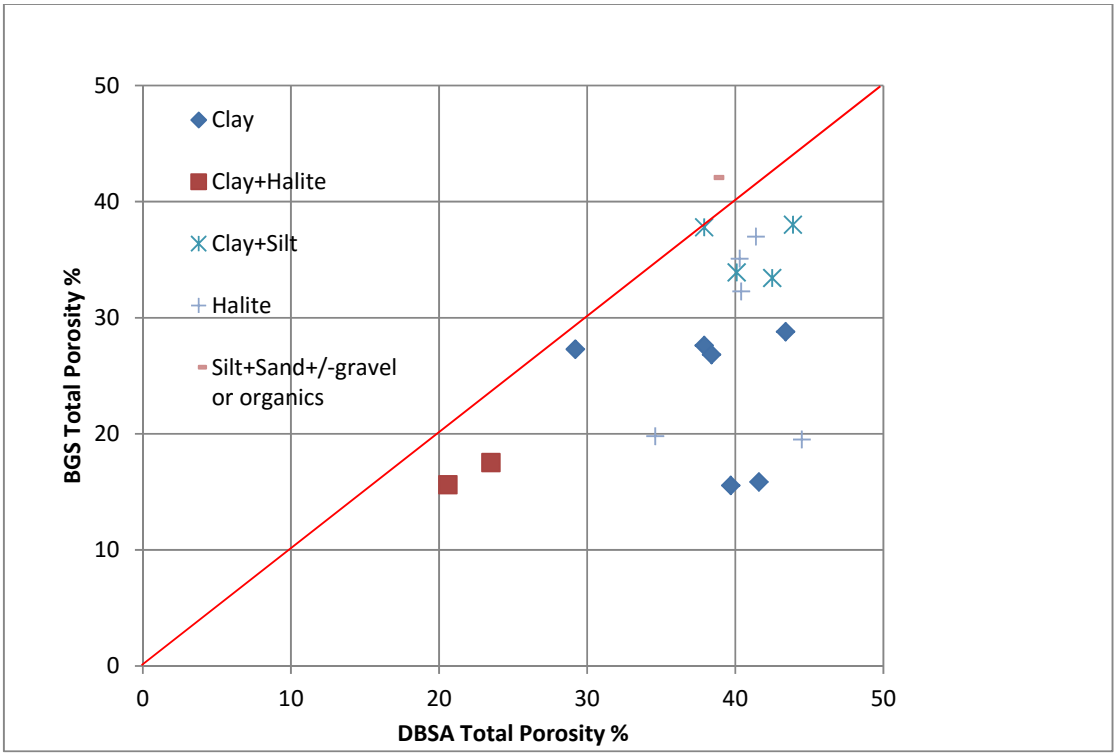

11.3.2 GSA 2017

The Relative Solution Release Curve (RSRC) method was used by the GSA Laboratory (Tucson, AZ) to determine *Sy* and *Pt.* A subset of paired samples was tested using the Centrifuge Moisture Equivalent of Soils (Centrifuge) method by Core Laboratories (Houston, TX). The goals of the test work were to provide *Sy* and *Pt* values for each sample and summary statistics of *Sy* and *Pt* values by lithological group; to compare the results from the core and tri-cone samples; and to compare the *Sy* and *Pt* values for paired sonic core samples derived from the RSRC and Centrifuge methods. Table 11.11 shows an overview of the laboratory test work performed by GSA.

170 10-cm diameter sonic drill intact core samples (core) from boreholes S-1A, S-2, S-18, and S-20 and 196 unconsolidated tri-cone samples from boreholes S-3A, S-5, S-6, S-11, S-13, and S-19 were received by GSA. The core samples which ranged in length from 10 to 20 cm, were received wrapped in cellophane and bubble-wrap in a re-sealable bag or in a clear, lexan sleeve with end caps duct-taped; the tri-cone rotary samples were in plastic bags. Table 11.12 lists the lithology of the samples received. For interpretation of RSRC and Centrifuge method results, samples were classified into the following categories: clay-dominated, sand-dominated, gravel-dominated, halite, ulexite, and volcaniclastic material.

Table 11.11 GSA laboratory tests performed

Test Type	Sample Type and Number	Test Method	Testing Laboratory	Standard
Physical	164 Core samples 49 Tri-cone samples	Bulk Density	GSA Laboratory, (Tucson, AZ)	ASTM D2937-10
	29 Tri-cone samples	1-D Consolidation	Pattison Engineering and Geo-Logic Associates, (Tucson, AZ)	ASTM D2435
Hydraulic	28 Core samples	Centrifuge Moisture Equivalent of Soils	Core Laboratories (Houston, TX)	Modified ASTM D425-17
	164 Core samples 49 Tri-cone samples	Estimated Total Porosity	GSA Laboratory (Tucson, AZ)	MOSA Part 4 Ch. 2, 2.3.2.1
		Estimated Field Water Capacity		MOSA Part 4 Ch. 3, 3.3.3.2
		Relative Solution Release Capacity (RSRC)		Modified ASTM D6836-02 MOSA Part 4 Ch. 3, 3.3.3.5

Table 11.12 Sample lithology and GSA clasification

Lithology Code	Lithology	Number of Sonic Core Samples	Number of Tri-cone Samples	GSA Material Classification
C	Clay	51	1	Clay dominated
C+H	Clay and halite	4		Clay dominated
SC	Sandy clay	5		Clay dominated
S	Sand	4	92	Sand dominated
SS	Silty sand	10	9	Sand dominated
CS	Clayey sand	7	4	Sand dominated
CG	Clayey gravel	7		Gravel dominated
SG	Sandy gravel	15	7	Gravel dominated
H	Halite	8	3	Halite
H+C	Halite and clay	12		Halite
U	Ulexite	5		Ulexite
V	Volcaniclastic	42	80	Volcaniclastic

Sample Preparation

Undisturbed 10-cm diameter by 10 to 20-cm length sonic core samples were prepared to fit into HQ (6.35 cm diameter by 2.5 cm length) stainless steel liners by driving the liners into the in-tact sonic cores using a hydraulic press in order to maintain the core sample bulk density. The soil cores were carefully trimmed to the same height and width as the liners. Care was taken to reduce core handling that could modify the physical structure of the core and effect porosity and drainage measurements. The core samples were prepared using identical procedures for the RSRC and Centrifuge methods, except the samples for the Centrifuge method were prepared in 3.8-cm diameter and 5-cm length stainless steel sleeves. Seventeen core samples appeared to contain a significant amount of material greater than 0.63 cm in diameter. The bulk density of these in-tact cores were measured (ASTM D2937-10) and then the material was re-packed into a 15-cm diameter Tempe cell for RSRC testing.

It was not possible to test six of the S-18 borehole core samples: 2 H, 1 V, and 1 H+C cores from 120 m to 127 m depth and 1 U and 1 C core from 152 m to 155 m depth, because these cores were dominated by solid salt crystals and could not be prepared for testing. Figure 11.9 shows the rejected samples.

Figure 11.9 Rejected core samples

To seal the stainless steel liner of the HQ samples, a pre-wetted micro-pore membrane (rated 760 mbar air entry) was placed into a bottom PVC cap and top cap was added and the sample was sealed air-tight with gaskets and connectors between both PVC caps as shown in Figure 11.10.

The HQ core assembly was then saturated with a brine solution prepared to mimic the Maricunga brine solution (specific gravity = 1.2 g/cm3). Saturation was achieved by repetitively applying solution from the bottom of the assembly and then applying vacuum (30 to 50 mbar) from the top of the core to assist the saturation. The core samples for the Centrifuge method were prepared by immersing the core samples into brine solution for 24 hours and allowing the solution to saturate from the bottom. The 15-cm cells and HQ core assemblies packed with tri-cone samples were slowly injected withthe brine solution from the bottom of the assembly until the material was saturated. The 15-cm cells and HQ core assemblies packed with tri-cone samples saturated quickly, so no vacuum was needed. Any standing brine solution was carefully removed prior to starting the test.

Relative Solution Release Capacity (RSRC) Sample Testing

HQ core samples and the 15-cm diameter repacked core samples were tested in the GSA laboratory using the RSRC method to measure the amount of brine that may be released under gravity drainage conditions from saturated porous media (i.e. the specific yield, S_y). The RSRC is based on the moisture retention characteristic method using the Tempe cell design (Modified ASTM D6836-02). Total porosity (P_t) is also measured in the RSRC method.

Each core assembly was transferred to a test rack for the pressure extraction procedure as shown in Figure 11.x. Three pressure steps were applied to each core assembly: the first step was applied without pressure for a day and any free water due to over saturation was removed from this step. Two sequential pressure steps, 120 mbar and 333 mbar (estimated field water capacity, MOSA Part 4 Ch. 3, 3.3.3.2), were used to approximate brine solution release at 120 mbar and 333 mbar of the brine solution. The 120 mbar pressure step was maintained for two days and the 333 mbar was continued for another two to four days. Core assemblies were weighed prior to saturation, after saturation, and then

two to three times daily to determine loss of brine solution content over time. Samples were oven dried after the final step to determine P_t (MOSA Part 4 Ch. 2, 2.3.2.1). P_t was calculated as:

$$1 - (Bulk\ density / Particle\ density)$$

Brine solution release volumes at the 120 mbar and at 333 mbar pressure steps were estimated as the difference of the brine weight divided by the brine specific gravity (1.2 g/cm3) between the initial cell assembly mass and the mass after each pressure plate step (MOSA Part 4 Ch3, 3.3.3.5). The solution release volume (specific yield) from saturation to 333 mbar can be considered to approximate the maximum solution drainage under gravity/pumping conditions and was calculated as follows:

$$Sy = (ws - w333\ mbar)/(A * L * Bsg)$$

Where: w_s is the saturated weight, $w_{2\ mbar}$ is the weight at 333 mbar, A is sample area, L is sample length, and B_{sg} is the specific gravity of the brine solution.

One hundred and sixty-four (164) core samples were measured for *Pt* and *Sy* using the RSRC method

Figure 11.6 Relative Solution Release Capacity (RSRC) HQ core sample testing

Centrifuge Moisture Equivalent of Soils Sample Testing

The repeatability of *Sy* and *Pt* measurements was assessed by testing 28 paired samples using the RSRC method by GSA and the Centrifuge Moisture Equivalent of Soils (Centrifuge) method by Core Laboratories (Houston, TX). GSA packed all of the samples in stainless steel sleeves, saturated them with a brine solution prepared to mimic the Maricunga brine solution, and shipped to Core Laboratories.

The sample pairs were of adjacent sections of the same core section and thus reflect similar lithologies as closely as possible, although there is no way of repeating the analysis on exactly the same sample.

Saturated samples were weighed, placed in a low-speed centrifuge for four hours, and then removed from the centrifuge and weighed for a second time. The centrifuge speed was selected to produce suction on the samples equivalent to 330 mbar. Specific yield was calculated as described in Section 11.3.3. Cores were oven dried at a low temperature for five days to determine the residue brine content and bulk density. Particle density was measured using Boyle's Law on oven-dried samples. *Pt* was calculated as above.

GSA Drainable Porosity Results

In order to assess the relationship between the porosity parameters (*Pt* and *Sy*) and lithology, samples were classified into the following categories: clay-dominated, sand-dominated, gravel-dominated, halite, ulexite, and volcaniclastic material as shown in Table 11.12 and Figure 11.11. Histograms and normal distributions for the GSA core data are shown in Figure 11.12 by category and a summary of all of the data is given in Table 11.13. Figures 11.13 and 11.14 compare all of the *Pt* and *Sy* data, respectively, by borehole as measured by GSA and Core Laboratories.

Pt generally increases from gravel-dominated material (lowest porosity) to sand and then clay-dominated material (highest porosity). Volcaniclastic material also had high *Pt* values, similar to the gravel-dominated material. The halite material had low *Pt* values, similar to gravel-dominated material, but three halite samples could not be tested because they contained cemented salt crystals. Only five ulexite samples were tested; these also had low porosity (mean= 0.35). Mean values were in good agreement with literature values for these types of sediments (Morris and Johnson, 1967).

In contrast, *Sy* increased with increasing particle size; therefore, the gravel-dominated material showed the highest *Sy* values, followed by sand and then clay-dominated material with the lowest *Sy* values. The volcaniclastic material showed similar *Sy*, values to the gravel-dominated material. The halite samples had intermediate *Sy* values similar to the sand-dominated material, but not all of the halite samples could be tested because some were cemented and solid, and therefore would have little to no *Sy*. Ulexite material had lower *Sy* values than the sand-dominated material.

Mean values for *Sy* were in good agreement with literature values for these types of sediments (Johnson, 1967). The halite samples showed a relatively wide range of *Pt* values. There was a relatively wide range of *Sy* values for the gravel-dominated, volcaniclastic, and halite material. The gravel-dominated material included clayey-gravels, which had lower *Sy* values than the sandy gravels.

Figure 11.7 GSA specific yield vs GSA total porosity

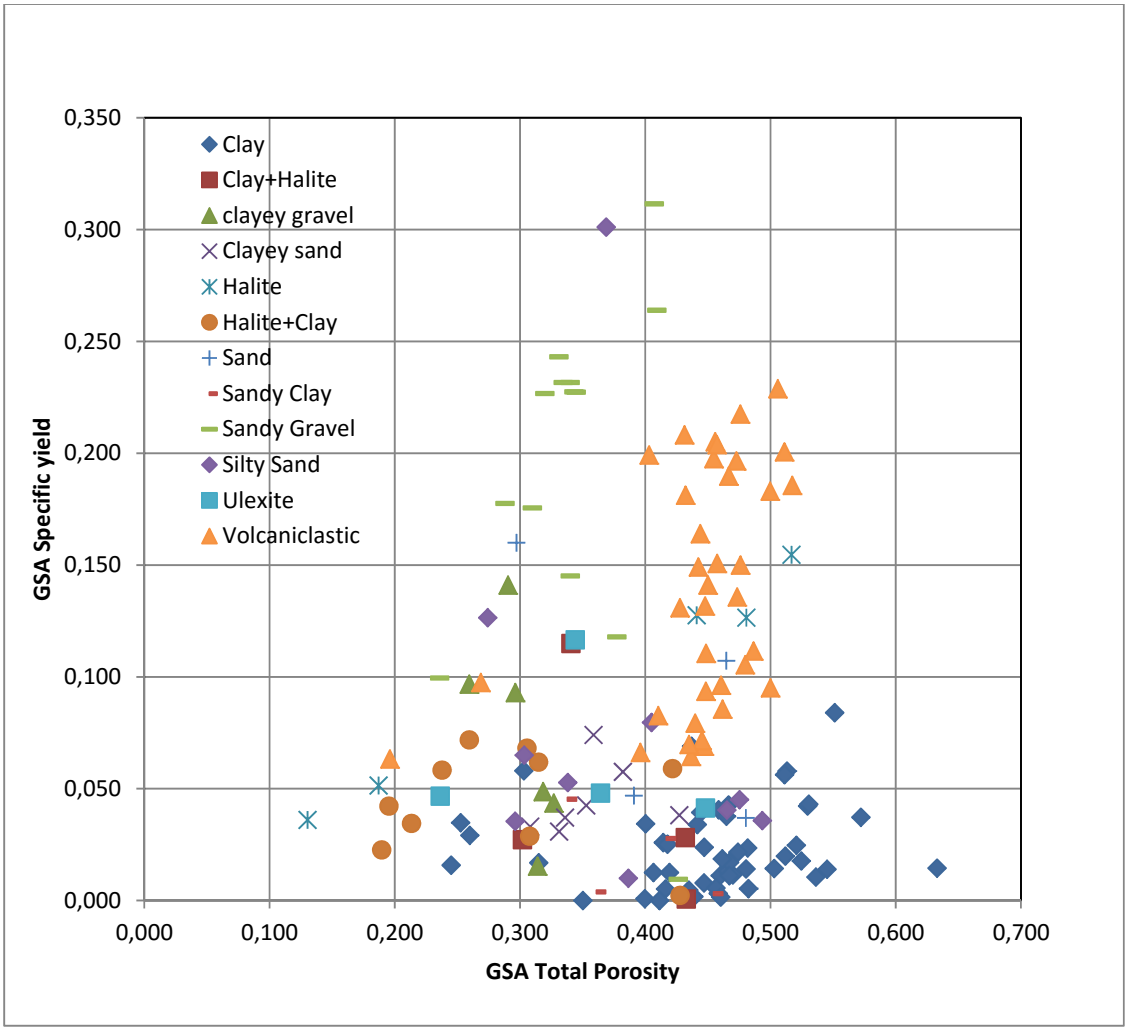

Figure 11.8 Lithologically classified *Pt* and *Sy* distributions and statistics.

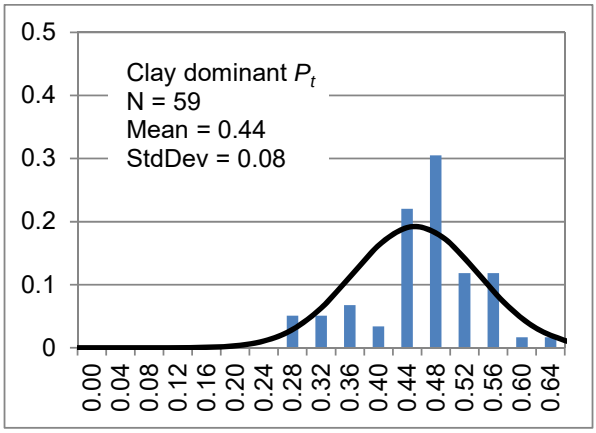

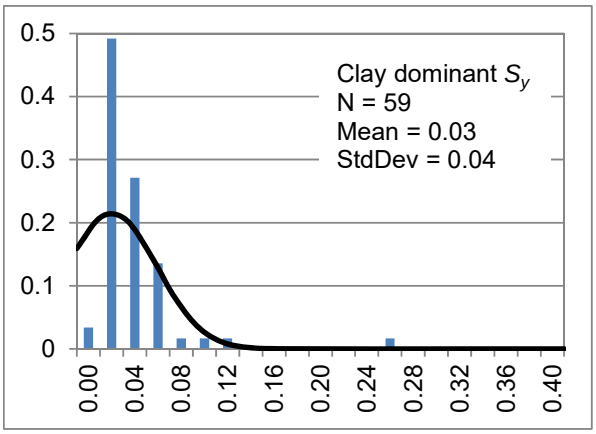

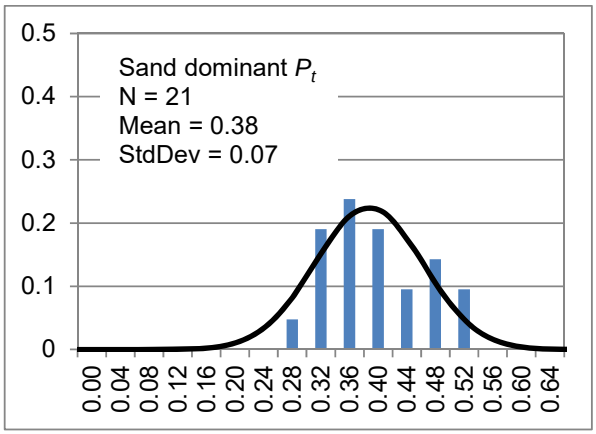

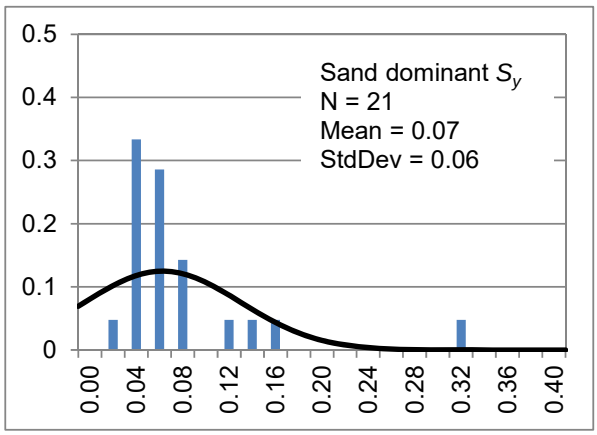

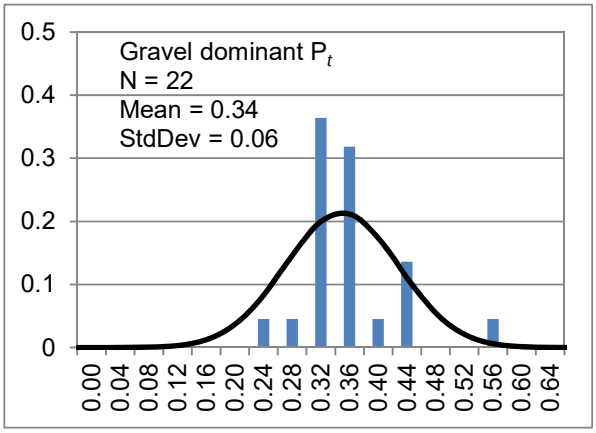

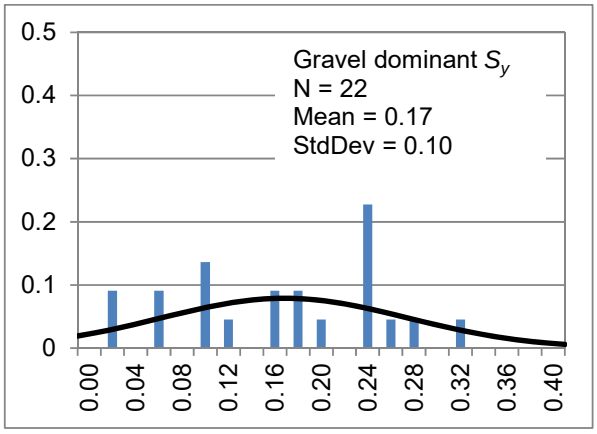

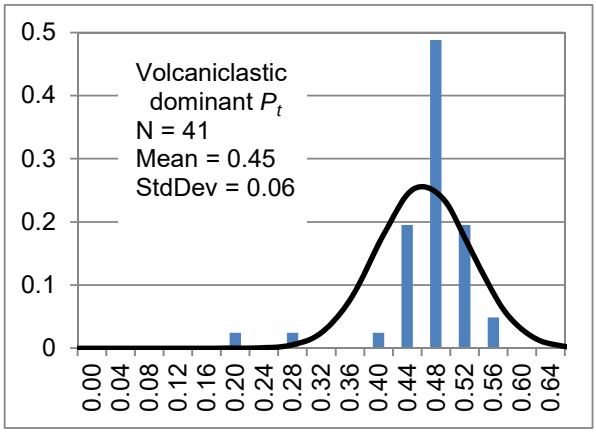
Volcaniclastic
dominant P_t
N = 41
Mean = 0.45
StdDev = 0.06
0.5
0.4
0.3
0.2
0.1
0
0.00 0.04 0.08 0.12 0.16 0.20 0.24 0.28 0.32 0.36 0.40 0.44 0.48 0.52 0.56 0.60 0.64

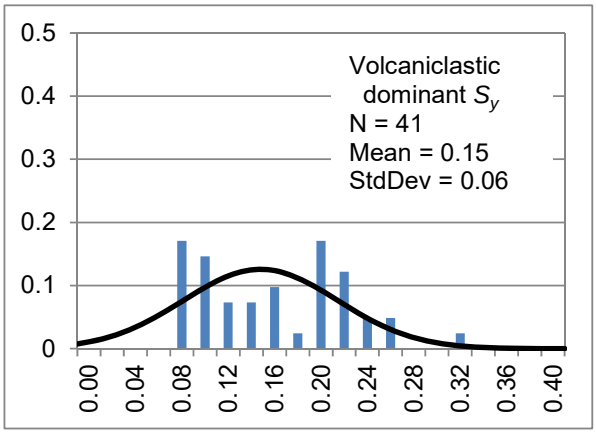
Volcaniclastic
dominant S_y
N = 41
Mean = 0.15
StdDev = 0.06
0.5
0.4
0.3
0.2
0.1
0
0.00 0.04 0.08 0.12 0.16 0.20 0.24 0.28 0.32 0.36 0.40

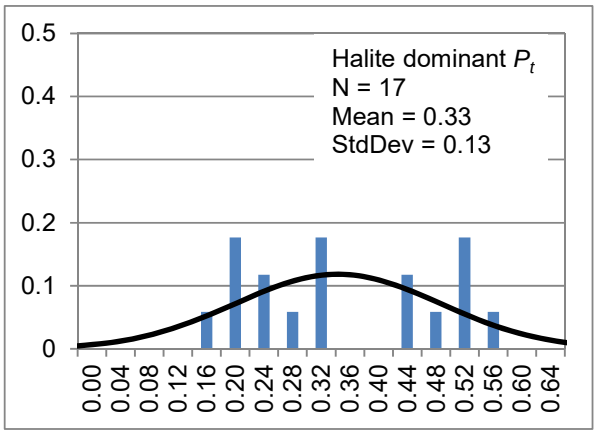
Halite dominant P_t
N = 17
Mean = 0.33
StdDev = 0.13
0.5
0.4
0.3
0.2
0.1
0
0.00 0.04 0.08 0.12 0.16 0.20 0.24 0.28 0.32 0.36 0.40 0.44 0.48 0.52 0.56 0.60 0.64

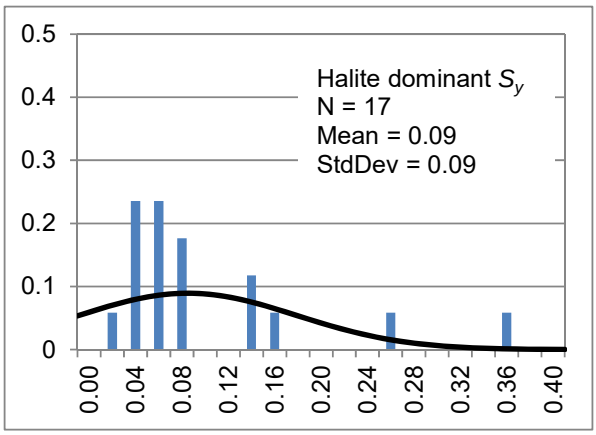
Halite dominant S_y
N = 17
Mean = 0.09
StdDev = 0.09
0.5
0.4
0.3
0.2
0.1
0
0.00 0.04 0.08 0.12 0.16 0.20 0.24 0.28 0.32 0.36 0.40

Table 11.13 Summary of total porosity and specific yield by lithological group and laboratory

Lithological Group	Core Lab Total Porosity (P_t)			GSA Total Porosity (P_t)			Core Lab Specific Yield (S_y)		GSA Specific Yield (S_y)	
	N	Mean	StdDev	N	Mean	StdDev	Mean	StdDev	Mean	StdDev
Clay dominated	6	0.53	0.05	59	0.44	0.08	0.02	0.03	0.03	0.04
Sand dominated	3	0.45	0.08	21	0.38	0.07	0.05	0.04	0.07	0.06
Gravel dominated	3	0.32	0.02	22	0.34	0.06	0.10	0.07	0.17	0.10
Volcaniclastic	13	0.46	0.05	41	0.45	0.06	0.13	0.05	0.15	0.06
Halite	2	0.35	0.08	17	0.33	0.13	0.07	0.05	0.09	0.09
Ulexite	1	0.49	N/A	5	0.35	0.09	0.04	N/A	0.05	0.04

Figure 11.9 Comparison of total porosity estimated by GSA using RSRC method and Core laboratory using the Centrifuge method

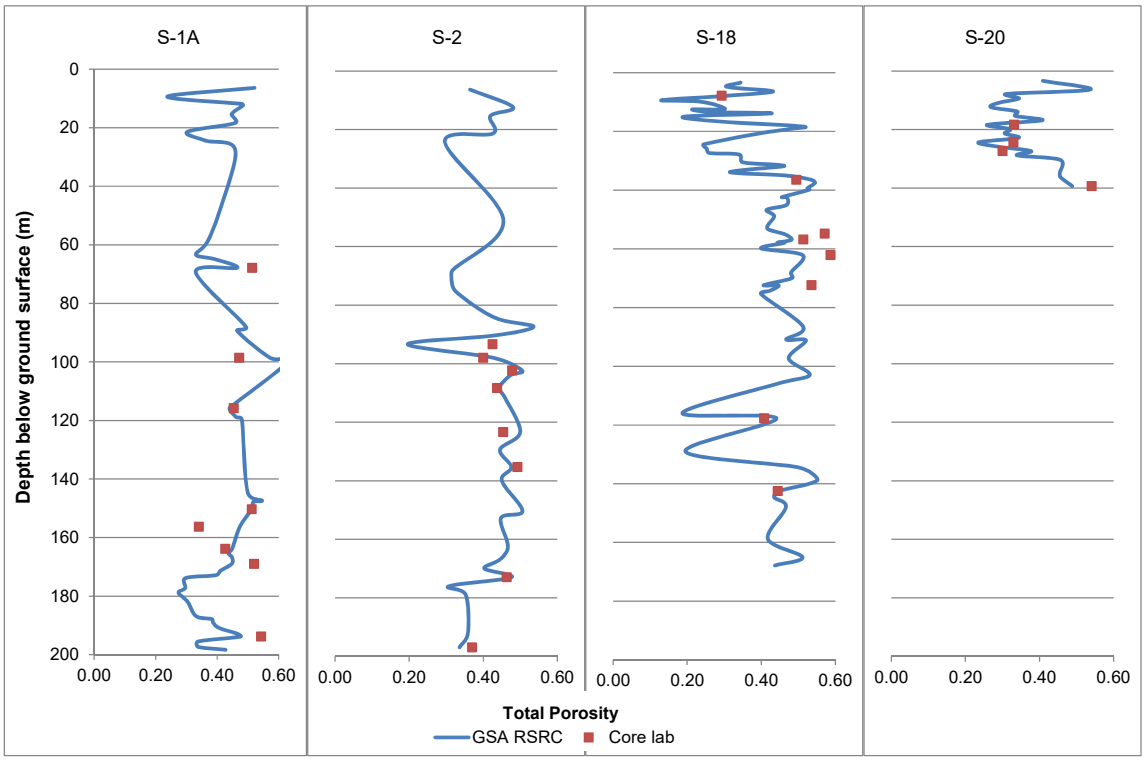

Figure 11.10 Comparison of specific yield estimated by GSA using RSRC method and Core laboratory using the Centrifuge method

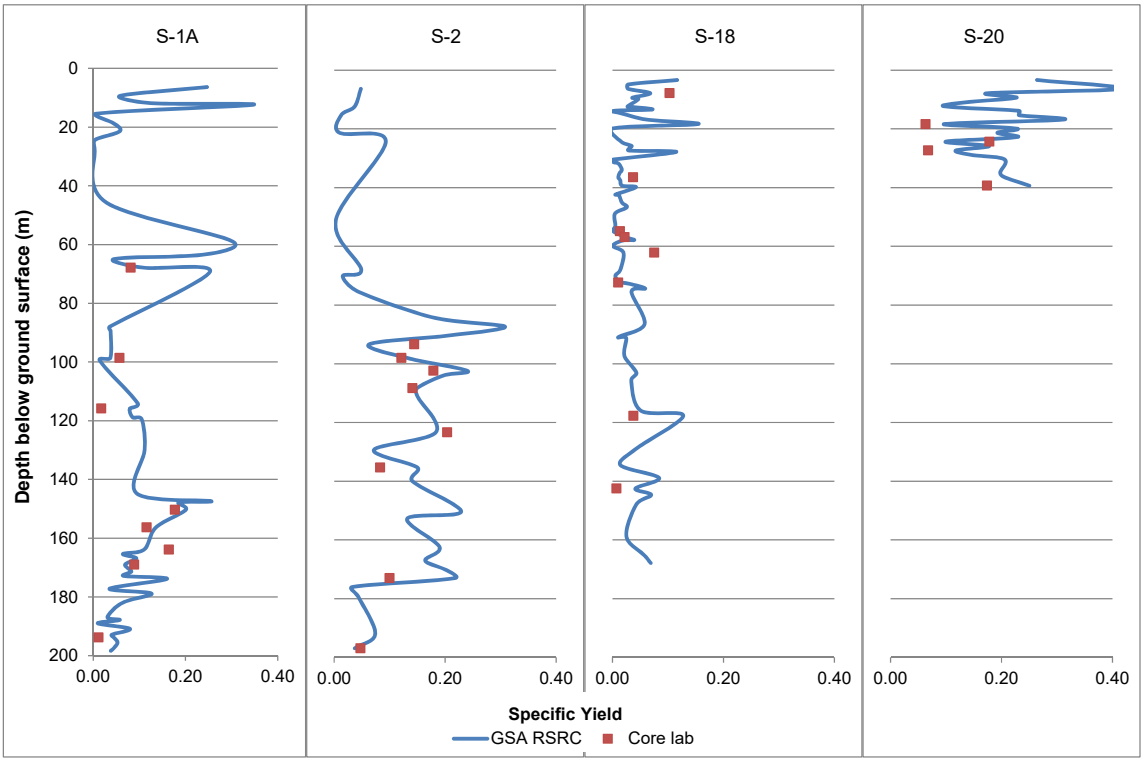

11.3.5 Quality Control – GSA and Core Laboratory Determinations of *Sy* and *Pt*

Table 11.14 provides summary statistics and Figure 11.15 compares the measured *Sy* (drainable porosity) values by lithological category between the laboratories. There is good agreement between the specific yield data (R2 = 0.62); correlation is lower between the total porosity data (R2 = 0.39). The *Sy* values measured by GSA are in general similar or slightly higher than the *Sy* measured by Core Laboratories, except for the clay samples, where the results from GSA were slightly lower than the Core Laboratories results. The largest difference in the paired results was for volcaniclastic material.

Table 11.15 provides summary statistics and Figure 11.16 compares the measured total porosity *Pt* values by lithology between the laboratories. The *Pt* was frequently higher measured by Core Laboratories compared to GSA.

Table 11.14 Comparison of S_y values between GSA and Corelabs

	Clay dominated		Sand dominated		Gravel dominated		Halite		Ulexite		Volcani-clastic	
	Core	GSA	Core	GSA	Core	GSA	Core	GSA	Core	GSA	Core	GSA
N	7	7	3	3	3	3	1	1	1	1	13	13
Mean	0.03	0.02	0.05	0.06	0.10	0.10	0.10	0.13	0.04	0.04	0.13	0.15
Standard Deviation	0.02	0.02	0.04	0.04	0.07	0.01	N/A	N/A	N/A	N/A	0.05	0.06
Average Relative Percent Difference	3%		21%		1%		21%		11%		13%	

Figure 11.11 Comparison of S_y values between GSA and Corelabs

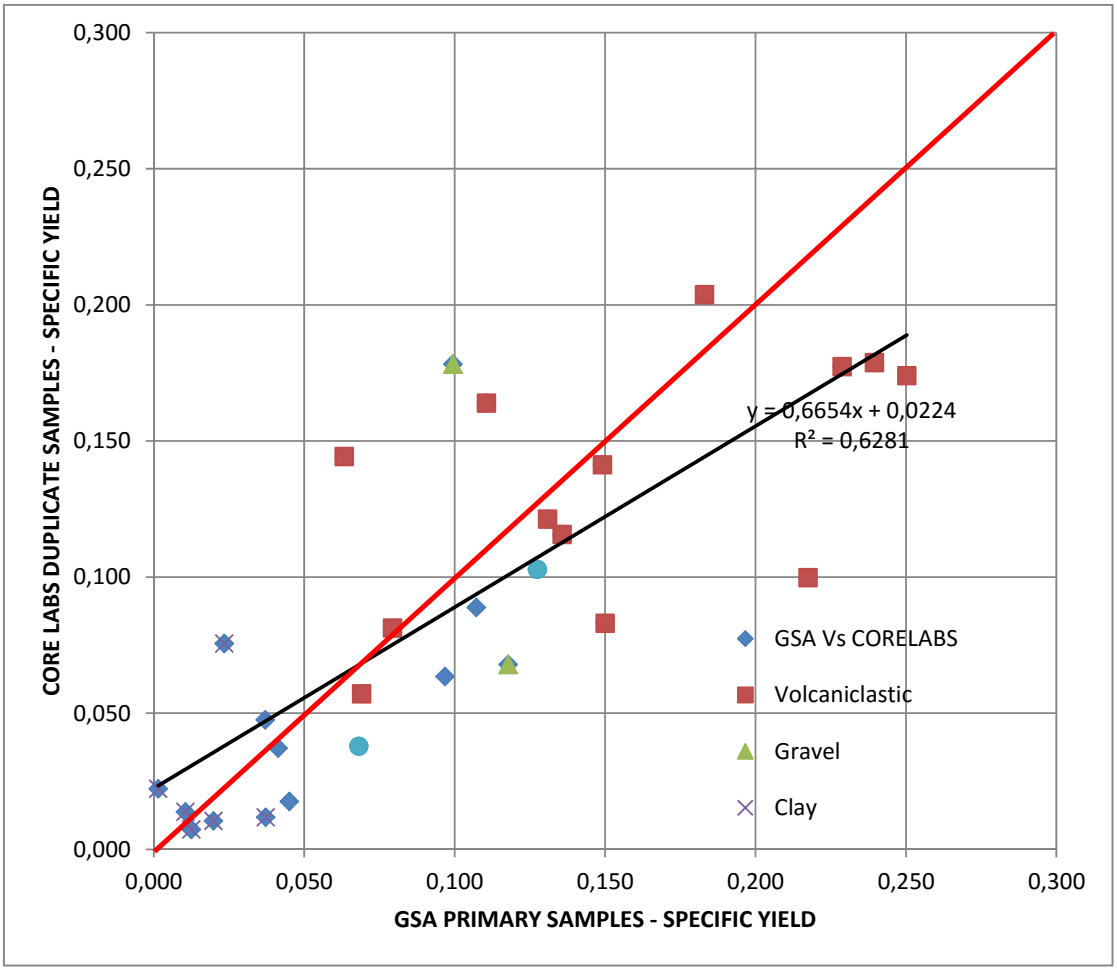

Table 11.15 Comparison of Total Porosity between GSA and Corelabs

	Clay dominated		Sand dominated		Gravel dominated		Halite		Ulexite		Volcani-clastic	
	Core	GSA	Core	GSA	Core	GSA	Core	GSA	Core	GSA	Core	GSA
N	7	7	3	3	3	3	1	1	1	1	13	13
Mean	0.51	0.47	0.45	0.43	0.32	0.29	0.29	0.44	0.49	0.45	0.46	0.45
Standard Deviation	0.07	0.09	0.08	0.08	0.02	0.08	N/A	N/A	N/A	N/A	0.05	0.08
Average Relative Percent Difference	10%		5%		10%		40%		10%		2%	

Figure 11.12 Comparison of Total Porosity between GSA and Corelabs

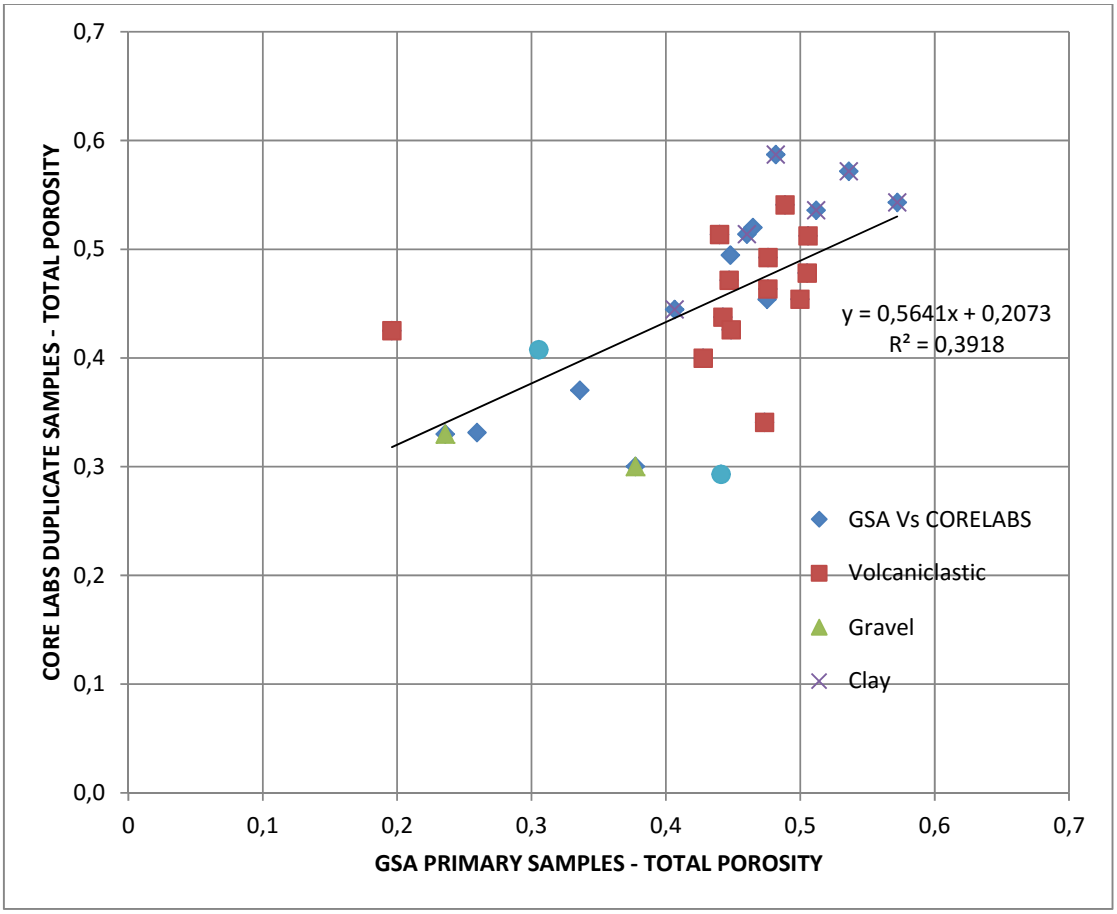

12 DATA VERIFICATION

The author, Frits Reidel was involved with the planning, execution and oversight of the 2011, 2015, and 2016/7 drilling and testing programs in Salar de Maricunga. The author was responsible for developing drilling and sampling methodologies and the implementation of field sampling protocols. The author spend a significant amount of time in the field during each of 2011, 2015 and 2016/7 field campaigns overlooking the implementation and execution of drilling, testing, and sampling protocols. The second author; Murray Brooker also spent time on site during the 2016 drilling and testing program. QP Mr Peter Ehren has visited the site periodically since 2011.

The authors were responsible for the oversight and analysis of the QA/QC programs related to brine sampling and laboratory brine chemistry analysis as well as the laboratory porosity analysis. A significant amount of QA/QC protocols were implemented for the brine chemistry and drainable porosity analysis programs that allowed continuous verification of the accuracy and reliability of the results obtained. As described in Section 11 no issues were found with the results of the brine and porosity laboratory analysis. It is the opinion of the authors that the information developed and used for the brine resource estimate herein is adequate, accurate and reliable.

13 MINERAL PROCESSING AND METALLURGICAL TESTING

13.1 Background - Li3 / LME 2011 Exploration Program

In order to study the phase chemistry of the Maricunga brine, the initial step for designing a lithium recovery process, a simulated lab solar evaporation test work was conducted at the University of Antofagasta, northern Chile. Two batch wise evaporation tests at laboratory scale were carried out at a relatively constant temperature of 20ºC. The natural brine was used in the first test and in the second one a treated brine with sodium sulfate, to remove most of the high calcium content that characterizes the Maricunga brine. Both tests provided information on the nature of the crystallized salts along the different stages of an evaporation process, which has been useful for process simulations.

A summary of the experimental procedure and the main results of both tests are presented below:

13.2 Experimental Procedure

A total brine feed of 192.04 kg was used in the first test (natural brine), distributed in four fiberglass glass reinforced plastic pans, each of 75.5 cm diameter and 12.3 cm height. The brine evaporation takes place at a temperature of 20 deg. C into a thermally insulated chamber (3.5-m long by 1-m wide by 0.8-m high), where a fan with variable speed propels air. Temperature, air speed and relative humidity, are measured through a data acquisition system to monitor the evaporation. This evaporation chamber operates continuously (24 hours) with air having relative humidity of 60% to 75%.

The amount of salt deposited in the pans, weighed by a digital scale, was used to define each stage (harvest) of evaporation, as well as determining the cumulative percentage of evaporated water. Samples of the solution and the salts after filtration were collected from every stage for chemical analysis and X-ray diffraction.

When the Maricunga brine is getting more concentrated and the brine volume has diminished significantly, the evaporation is continued in another insulated chamber (1.18-m long by 0.70-m wide by 0.46-m high). The concentrated brine has a much lower brine activity (vapor pressure of the brine divided by the vapor pressure of the water), which results in lower evaporation rates.

The second chamber operates continuously with dehumidified air, which circulates through three PVC columns containing silica gel as drying agent. Under these conditions, the air can reach a relative humidity of the order of 40%. When the silica gel gets saturated, heating in a dryer at 120ºC activates it for re-use.

As per the brine treated previously with anhydrous sodium sulfate (10% excess was used to precipitate 88.7% of Ca^{++}), a total of 156.04 kg, distributed in three pans, was fed to the evaporation system. Table 13.1 shows the composition of the natural brine and treated brine used in the evaporation test work.

Table 13.1 Chemical composition (% weight) of brines used in the test work

Brine	Na	K	Li	Ca	Mg	Cl	SO4	H3BO3	HCO3	Density
Natural	7.81	0.676	0.0933	0.743	0.616	16.44	0.059	0.216	0.044	1.20761
Treated	8.59	0.547	0.0927	0.102	0.578	16.10	0.440	0.234	0.040	1.20787

A general view of the two evaporation chambers is shown in Figure 13.1.

Figure 13.1 General view of evaporation chambers

13.3 Results of the Evaporation Tests

The natural brine was concentrated up to 0.925% lithium and 3.95% magnesium in twelve stages of evaporation, being 69.1% the cumulative evaporation. The treated brine was concentrated up to 1.98% lithium and 6.08% magnesium in nine stages of evaporation, with a cumulative evaporation of 68%. Due to the low activity of the concentrated brine, it was necessary to increase the evaporation temperature to 30°C during the last stages of both tests. Tables 13.2 and 13.3 show the changes in the chemical composition of the untreated brine as well as the wet salt composition after every harvest (12) of the pans. Table 13.3 also shows a mass balance (crystallized salts, solution and evaporated water) referred to the initial weight of brine for each evaporating stage at 20°C. The brine has been concentrated until the end of the carnallite field.

Table 13.2 Brine compositions during evaporation of the untreated brine

Brine									Density 20ºC	Activity, 20ºC
Mg	Ca	Na	K	Li	Cl	SO4	B	H_2O	kg/l	(Vpbrine /Vpwater)
%	%	%	%	%	%	%	%	%		
0.616	0.743	7.810	0.676	0.093	16.440	0.059	0.038	73.525	1.20761	0.775
1.080	1.300	6.150	1.220	0.167	16.560	0.062	0.069	73.392	1.21768	*
1.280	1.710	5.370	1.490	0.204	17.600	0.040	0.090	72.216	1.22526	*
1.790	2.340	4.030	1.990	0.280	18.220	0.040	0.114	71.196	1.23663	*
2.500	3.160	1.900	2.620	0.394	20.260	0.010	0.158	68.998	1.26965	*
2.650	3.520	1.480	2.430	0.423	20.390	0.010	0.169	68.928	1.26902	0.606
2.690	3.580	1.480	2.380	0.431	20.500	0.020	0.171	68.748	1.27017	0.618
3.130	4.110	0.868	1.910	0.508	22.220	0.020	0.204	67.030	1.28485	0.570
3.389	4.540	0.506	1.500	0.561	22.940	0.037	0.216	66.311	*	*
3.417	5.165	0.366	0.907	0.655	24.040	0.022	0.245	65.183	1.32527	0.398
3.263	5.550	0.347	0.873	0.685	24.660	0.005	0.247	64.370	1.31376	0.518
3.570	5.670	0.299	0.679	0.709	25.120	0.018	0.257	63.678	1.32864	0.404
3.950	7.630	0.086	0.088	0.925	30.670	0.000	0.268	56.383	1.37405	0.292

* No measurements

The density and activity of the brine along the concentration process is also indicated. Additionally, the moisture of the crystallized salts after harvesting and filtration of the solution is included in Table 13.3.

Table 13.3 Salts compositions during evaporation of the untreated brine

	Salts	Brine	Evapor	Mg	Ca	Na	K	Li	Cl	SO_4	B	H_2O	Mois
	kg	kg	kg	%	%	%	%	%	%	%	%	%	%
Brine feed		192.04											
Harvest 1	19.91	117.91	54.22	0.069	0.122	36.210	0.082	0.009	57.890	0.136	0.008	5.47	4
Harvest 2	8.85	84.09	26.10	0.135	0.296	35.430	0.282	0.016	56.520	0.360	0.014	6.95	4
Harvest 3	6.04	61.23	16.76	0.182	0.248	35.670	0.312	0.021	56.600	0.170	0.018	6.78	5
Harvest 4	5.05	41.43	14.74	0.220	0.351	34.970	1.815	0.033	57.690	0.250	0.013	4.66	4
Harvest 5	0.74	39.00	1.58	0.080	0.109	37.230	0.128	0.013	58.920	0.380	0.016	3.12	3
Harvest 6	0.12	37.46	1.35	0.378	0.528	20.560	16.940	0.060	50.790	0.110	0.026	10.61	9
Harvest 7	1.29	31.92	4.98	0.426	0.536	17.940	21.440	0.066	50.960	0.150	0.035	8.45	8
Harvest 8	0.78	17.78	2.70	5.556	0.709	6.890	11.830	0.042	40.100	0.092	0.041	34.74	5
Harvest 9	2.68	21.22	4.30	6.410	0.665	6.480	10.590	0.037	40.730	0.058	0.069	34.96	4
Harvest 10	0.24	6.21	1.39	7.425	0.779	2.370	10.670	0.089	37.770	0.034	0.054	40.81	8
Harvest 11	0.97	16.64	3.16	5.660	3.090	2.580	7.010	0.263	33.040	0.129	0.919	47.31	3
Harvest 12	1.64	12.27	2.72	6.670	3.920	1.730	5.060	0.362	36.420	0.001	0.173	45.66	14

Table 13.4 shows the main estimated crystallized salts in each harvest according to mineralization calculated by chemical assay and X-ray diffraction analysis.

Table 13.4 Crystalized Salts in the harvest

	NaCl	KCl	CaSO4.2H20 and/or Na2Ca(SO4)2	KCl*MgCl2*H2O	$CaCl_2$ *2$MgCl_2$ *12H_2O	CaB6O10*6H2O
Harvest 1	1		1			
Harvest 2	1		1			
Harvest 3	1		1			
Harvest 4	1		1			
Harvest 5	1	1	1			
Harvest 6	1		1			
Harvest 7	1	1	1			
Harvest 8	1		1			
Harvest 9	1	1	1			
Harvest 10	1		1	1		
Harvest 11	1		1	1	1	
Harvest 12	1		1	1	1	1

According to the salt composition, harvests 11 and 12 should have tachhydrite; however analyzing the brine evaporation curves of the ions presented by K/Li and Ca/Mg pairs, it is expected that this salt has not yet been crystallized, and the author suspects that the calcium and lithium are still entrained in the brine in the harvested salts.

Figure 13.2 illustrates the complete evaporation curve for the untreated brine while Figure 13.3 is a representation for the concentrated brine when the levels of sodium and potassium are very low.

However, since the brine is saturated in sodium chloride, the known phase diagram (Janecke projection) of the aqueous system Na^+, K^+, Mg^{++}, $SO_4^=$, Cl^- at 25°C (Figure 13.4) is more appropriate for representation of the evaporation path, as shown by Figure 13.5, where lithium has been associated to magnesium.

Figure 13.2 Evaporation curves plotted versus % Li in the brine

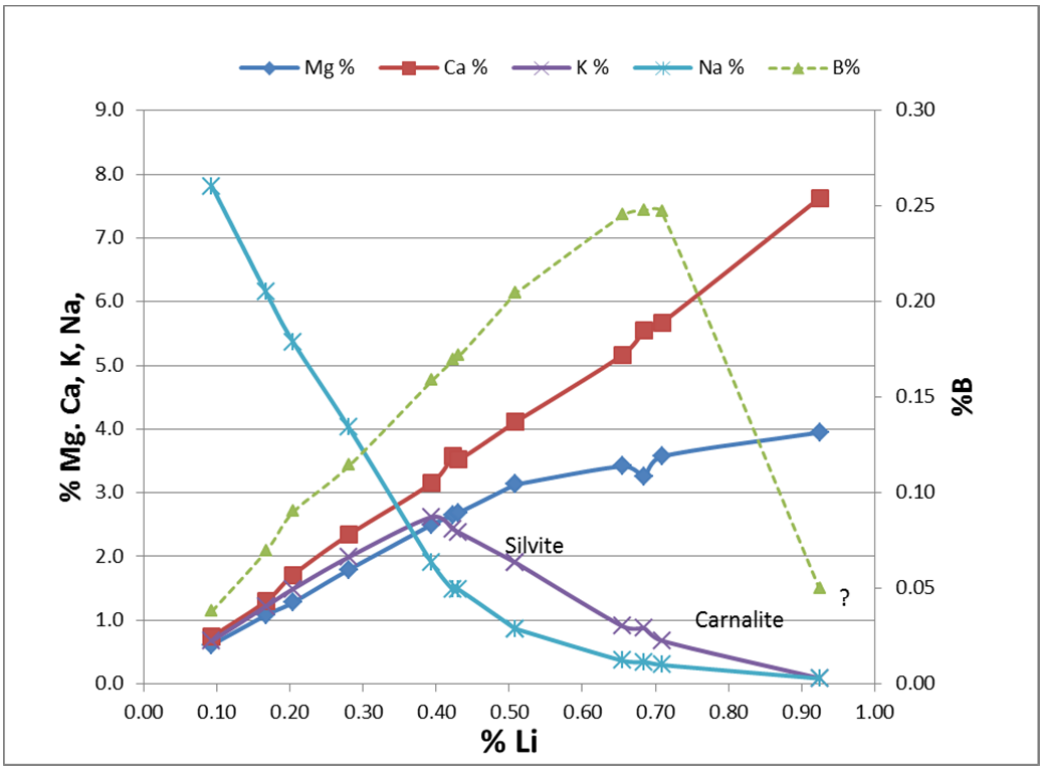

The results of the brine evaporation, after treatment with sodium sulfate to remove most of the calcium, are presented in Tables 13.5 and 13.6.

Table 13.5 Brine composition during evaporation of the treated brine

Brine									Density 20 º C	Activity, 20 º C
Mg	Ca	Na	K	Li	Cl	SO_4	B	H_2O	Kg/l	(Vpbr/Vpwater)
%	%	%	%	%	%	%	%	%	%	
0.578	0.102	8.590	0.547	0.093	16.100	0.440	0.041	73.509	1.20787	*
0.984	0.108	7.910	1.110	0.154	16.590	0.510	0.062	72.572	1.21019	*
1.240	0.127	7.160	1.404	0.199	16.910	0.600	0.079	72.281	1.2273	0.664
1.540	0.077	6.270	1.800	0.261	16.980	0.650	0.101	72.321	1.21899	0.706
1.920	0.088	5.140	2.250	0.325	17.230	0.730	0.129	72.188	1.22507	0.693
2.600	0.141	3.910	3.000	0.428	18.130	0.860	0.168	70.763	1.23517	0.535
3.130	0.030	2.730	3.007	0.514	18.510	1.000	0.178	70.901	1.23518	0.443
4.705	0.013	1.050	2.007	0.764	20.620	1.380	0.305	69.156	*	*
6.771	0.016	0.160	0.133	1.130	25.960	0.466	0.571	64.793	1.31812	0.248
6.080	0.012	0.093	0.062	1.980	28.080	0.084	0.721	62.888	1.32492	*

Table 13.6 Wet salt compositions during evaporation of the treated brine

	Salts	Brine	Evap	Mg	Ca	Na	K	Li	Cl	SO_4	B	H_2O	Moist
	Kg	kg	kg	%	%	%	%	%	%	%	%	%	%
Brine feed		156.24											
Harvest 1	16.87	95.42	43.90	0.070	0.592	36.410	0.088	0.010	57.630	0.740	0.006	4.454	3
Harvest 2	6.27	70.38	18.60	0.139	0.290	35.020	0.171	0.021	55.670	0.770	0.012	7.907	8
Harvest 3	3.92	47.28	19.10	0.128	0.241	36.510	0.160	0.020	56.730	0.730	0.016	5.465	5
Harvest 4	2.94	30.84	6.40	0.791	1.052	20.540	13.51	0.127	49.740	0.620	0.066	13.55	2
Harvest 5	1.43	23.39	6.00	0.141	0.318	37.120	11.55	0.022	59.230	0.990	0.019	1.943	1
Harvest 6	2.34	15.24	5.80	0.259	0.338	30.180	7.820	0.020	56.000	0.950	0.027	4.406	2
Harvest 7	2.10	4.15	1.80	5.556	0.709	6.890	11.83	0.042	40.100	0.092	0.041	34.74	3
Harvest 8	0.56	6.36	4.00	6.004	0.088	2.830	8.430	1.840	31.670	0.217	0.085	37.50	3
Harvest 9	2.51	2.56	1.29	9.910	0.009	0.247	0.230	0.599	32.380	0.836	0.605	55.18	12

13.4 POSCO Process Tests – 2012/13

Pilot plant evaluation of the POSCO direct extraction process was undertaken in late 2012 – early 2013. The POSCO process is a proprietary process for direct extraction and recovery of lithium from brine. Details of the process were not made available to LI3. The test work used brine recovered from trenches on the *Litio 1-6* claims, with the brine being processed in a pilot plant established at Copiapo. POSCO reported the process test work was successful but did not provide details of the results to Li3. Subsequent to 2013, POSCO decided not to pursue further evaluation of the use of the process at Maricunga.. The reasons for the POSCO decision are unknown.

13.5 2016 and 2017 Evaporation Pond Tests

A series of evaporation pond tests were initiated in late 2016 using brine from Well P1. During the Q4/16 a total of ten trial evaporation ponds were constructed in series in order to measure the precipitation of salts, the evolution of brine, and evaporation rates over a minimum one-year period to determine the optimal processing methodology and process flow sheet for the extraction of lithium, potassium, and other by-products. The evaporation pond test site is illustrated in Figure 13-6.

The average grade of the brine from the pump well fed to the first of the evaporation test ponds was 1,260 mg/L lithium and over an initial 9-month period, the brine concentration increased seven-fold to 8,600 mg/L lithium on a continuous way and up sixteen-fold to 20,460 mg/l. In addition, sodium chloride (NaCl), potassium chloride (KCl) and carnalite ($KCl*MgCl2*6H_20$) is precipitating in the pilot ponds as the concentration of the brine increases.

Sampling and assay procedures for the pond evaporation tests incorporated the following:

- Collection of brine samples on a periodic basis to measure brine properties such as chemical analysis, density, brine activity, etc. Samples were assayed at the University of Antofagasta using the same methods and QA/QC procedures as for brine samples collected from drill holes and from pumping tests;
- Collection of precipitated salts from the ponds for chemical analysis to evaluate the evaporation pathways, brine evolution and physical and chemical properties of the salts.
- The concentrated lithium brines and the potassium salts are sent to equipment providers for further testing and process optimization. The test work is undergoing.

Figure 13.3 MSB evaporation ponds

14 BRINE RESOURCE ESTIMATES

14.1 Overview

The essential elements of a brine resource determination for a salar are:

- Definition of the aquifer geometry,
- Determination of the drainable porosity or specific yield (Sy) of the hydrogeological units in the salar, and
- Determination of the concentration of the elements of interest.

Resources may be defined as the product of the first three parameters. The use of specific yield allows the direct comparison of brine resources from the widest range of environments.

Aquifer geometry is a function of both the shape of the aquifer, the internal structure and the boundary conditions (brine / fresh water interface). Aquifer geometry and boundary conditions can be established by drilling and geophysical methods. Hydrogeological analyses are required to establish catchment characteristics such as ground and surface water inflows, evaporation rates, water chemistry and other factors potentially affecting the brine reservoir volume and composition in-situ. Drilling is required to obtain samples to estimate the salar lithology, specific yield and grade variations both laterally and vertically.

14.2 Resource Model Domain and Aquifer Geometry

The model resource estimate is limited to the MSB mining concessions in Salar de Maricunga that cover an area of 2,563 ha as shown in Figure 4.2.

The resource model domain is constrained by the following factors:

- The top of the model coincides with the brine level in the Salar that was measured in the monitoring wells shown in Table 10.1.
- The lateral boundaries of the model domain are limited to the area of the MSB mining claims in the Salar.
- The bottom of the model domain coincides with a total depth of 200 m.

14.3 Specific Yield

Specific yield is defined as the volume of water released from storage by an unconfined aquifer per unit surface area of aquifer per unit decline of the water table.

The specific yield values used to develop the resources are based on results of the logging and hydrogeological interpretation 10 sonic boreholes, results of drainable porosity analyses carried out on 501 undisturbed samples from sonic core by GeoSystems Analysis, Daniel B Stephens and Associates, Corelabs, BGC, and four pumping tests. The boreholes within the measured and indicatedresource areas are appropriately spaced at a borehole density of one bore per 1.5 km^2. Table 14.1 shows the drainable porosity values assigned to the different geological units for the resource model.

Table 14.1 Drainable porosity values applied in the resource model

Unit	Sy
Upper Halite	0.07
Clay Core	0.02
Deep Halite	0.05
NW Aluvium	0.15
Lower Alluvium	0.06
Volcaniclastics	0.10
Lower Sand	0.06
Lower Volcaniclastics	0.10

14.4 Brine Concentrations

The distributions of lithium and potassium concentrations in the model domain are based on a total of 487 brine analyses (not including QA/QC analyses). Table 14.2 shows a summary of the brine chemical composition.

Table 14.2 Summary of brine chemistry composition

	B	Ca	Cl	Li	Mg	K	Na	SO4	Density
Units	mg/L	mg/L	mg/L	mg/L	mg/L	mg/L	mg/L	mg/L	g/cm^3
Maximum	1,193	36,950	230,902	3,375	21,800	20,640	104,800	2,960	1.31
Average	596	13,490	190,930	1,123	7,337	8,237	85,190	709	1.20
Minimum	234	4,000	89,441	460	2,763	2,940	37,750	259	1.10

14.5 Resource Category

The CIM Council (May 10, 2014) adopted the following definition standards for minerals resources:

Inferred Mineral Resource

An Inferred Mineral Resource is that part of a Mineral Resource for which quantity and grade or quality are estimated on the basis of limited geological evidence and sampling. Geological evidence is sufficient to imply but not verify geological and grade or quality continuity.

An Inferred Mineral Resource has a lower level of confidence than that applying to an Indicated Mineral Resource and must not be converted to a Mineral Reserve. It is reasonably expected that the majority of Inferred Mineral Resources could be upgraded to Indicated Mineral Resources with continued exploration.

An Inferred Mineral Resource is based on limited information and sampling gathered through appropriate sampling techniques from locations such as outcrops, trenches, pits, workings and drill holes. Inferred Mineral Resources must not be included in the economic analysis, production schedules,

or estimated mine life in publicly disclosed Pre- Feasibility or Feasibility Studies, or in the Life of Mine plans and cash flow models of developed mines. Inferred Mineral Resources can only be used in economic studies as provided under NI 43-101.

There may be circumstances, where appropriate sampling, testing, and other measurements are sufficient to demonstrate data integrity, geological and grade/quality continuity of a Measured or Indicated Mineral Resource, however, quality assurance and quality control, or other information may not meet all industry norms for the disclosure of an Indicated or Measured Mineral Resource. Under these circumstances, it may be reasonable for the Qualified Person to report an Inferred Mineral Resource if the Qualified Person has taken steps to verify the information meets the requirements of an Inferred Mineral Resource.

Indicated Mineral Resource

An Indicated Mineral Resource is that part of a Mineral Resource for which quantity, grade or quality, densities, shape and physical characteristics are estimated with sufficient confidence to allow the application of Modifying Factors in sufficient detail to support mine planning and evaluation of the economic viability of the deposit.

Geological evidence is derived from adequately detailed and reliable exploration, sampling and testing and is sufficient to assume geological and grade or quality continuity between points of observation.

An Indicated Mineral Resource has a lower level of confidence than that applying to a Measured Mineral Resource and may only be converted to a Probable Mineral Reserve.

Mineralization may be classified as an Indicated Mineral Resource by the Qualified Person when the nature, quality, quantity and distribution of data are such as to allow confident interpretation of the geological framework and to reasonably assume the continuity of mineralization. The Qualified Person must recognize the importance of the Indicated Mineral Resource category to the advancement of the feasibility of the project. An Indicated Mineral Resource estimate is of sufficient quality to support a Pre-Feasibility Study which can serve as the basis for major development decisions.

Measured Mineral Resource

A Measured Mineral Resource is that part of a Mineral Resource for which quantity, grade or quality, densities, shape, and physical characteristics are estimated with confidence sufficient to allow the application of Modifying Factors to support detailed mine planning and final evaluation of the economic viability of the deposit.

Geological evidence is derived from detailed and reliable exploration, sampling and testing and is sufficient to confirm geological and grade or quality continuity between points of observation.

A Measured Mineral Resource has a higher level of confidence than that applying to either an Indicated Mineral Resource or an Inferred Mineral Resource. It may be converted to a Proven Mineral Reserve or to a Probable Mineral Reserve.

Mineralization or other natural material of economic interest may be classified as a Measured Mineral Resource by the Qualified Person when the nature, quality, quantity and distribution of data are such that the tonnage and grade or quality of the mineralization can be estimated to within close limits and that variation from the estimate would not significantly affect potential economic viability of the deposit. This category requires a high level of confidence in, and understanding of, the geology and controls of the mineral deposit.

14.6 Resource Model Methodology and Construction

The resource estimation for the Project was developed using the Stanford Geostatistical Modeling Software (SGeMS) and the geological model as a reliable representation of the local lithology. The following steps were carried out to calculate the lithium and potassium resources.

- Generation of histograms, probability plots and box plots for the Exploratory Data Analysis (EDA) for lithium and potassium. No outlier restrictions were applied, as distributions of the different elements do not show anomalously high values. Calculation of the experimental variograms with their respective variogram models for lithium and potassium in three orthogonal directions.
- Definition of the block model (34,560,000 blocks) and block size (x=50 m, y=50 m, z=1 m) The block size has been chosen for being representative of the fine units inside the geological model.
- Interpolation of lithium and potassium concentrations for each block in mg/L using ordinary kriging with the variogram models shown in Figure 14.1 to Figure 14.2. The presence of brine is not necessary followed by the lithologies. Therefore, we are not considering any hard boundaries inside the geological units for the estimation.
- Validation using a series of checks including comparison of univariate statistics for global estimation bias, visual inspection against samples on plans and sections, swath plots in the north, south and vertical directions to detect any spatial bias.
- Calculation of total resources using the average porosity value for each geological unit, based on the boreholes data. Each geological unit will represent a particular porosity value as shown in Table 14.1. The total resources are shown in Table 14.5.

14.6.1 Variography

The spatial correlation for the lithium and potassium concentrations were reviewed using experimental variograms with the parameters shown in Table 14.3. The spatial variability was modelled using three experimental directions adjusted to a three-dimensional ellipsoidal model using one spherical structure.

The spatial models were calculated for lithium and potassium. The experimental variograms for lithium and potassium with their respective variogram models are shown in Figures 14.5 and 14.6.

Table 14.3 Parameters for the calculation of the experimental variograms

Variogram Parameters				Tolerance	
Lag (m)	Max. No. Of Lags	Azimuth (°)	Dip (°)	Bandwidth (m)	Angular (°)
500	50	-45	0	500	45
500	50	-135	0	500	45
5	40	0	90	25	89

The interpolation methodology for estimating lithium and potassium was Ordinary Kriging (OK). The estimation was carried out separately for each parameter using their respective variogram models as appropriate

Figure 14.1 Experimental variogram and variogram model for lithium

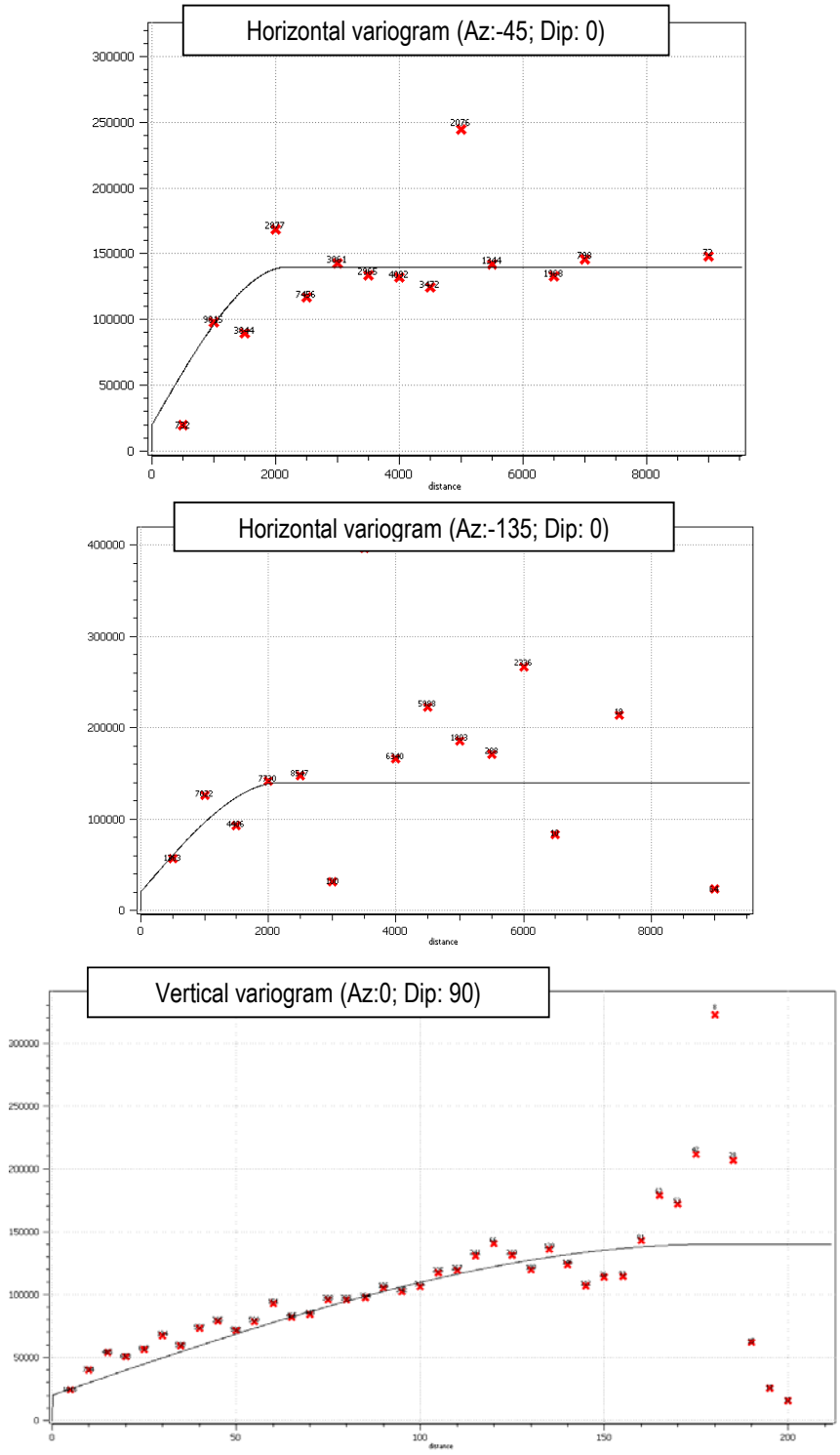

Figure 14.2 Experimental variogram and variogram model for potassium

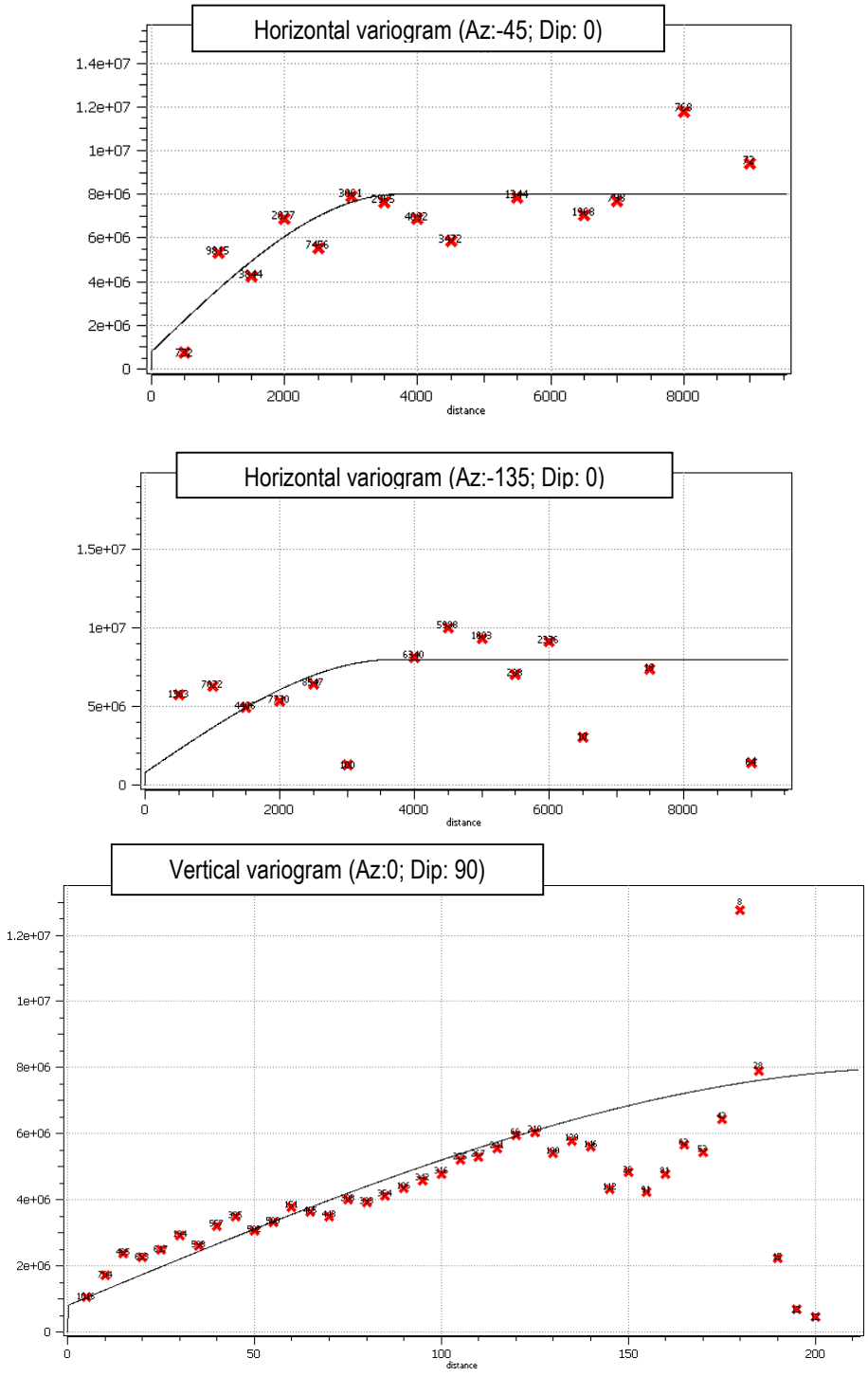

14.6.2 Model validation

The block model was validated using a series of checks including comparison of univariate statistics for global estimation bias, visual inspection against samples on plans and sections, swath plots in the north, south and vertical directions to detect any spatial bias.

An independent nearest-neighbor (NN) model was generated for each parameter in order to verify that the estimates honor the borehole data. The NN model also provides a de-clustered distribution of borehole data that can be used for validation.

Visual validation shows a good agreement between the samples and the OK estimates (Figure 14.3 and Figure 14.4). A global statistics comparison shows relative differences between the ordinary kriging results and the nearest-neighbor is below 0.3% for measured resources and below 3% for indicated resources (Table 14.4), which is considered acceptable.

Table 14.4 Comparison between the Ordinary Kriging results and the Nearest-Neighbor

Category	Element	Ordinary Kriging	Nearest-Neighbor	Difference	% Difference
Measured Resources	Li	1,189	1,188	0.64	0.05%
	K	8,747	8,721	25.43	0.29%
Indicated Resources	Li	1,073	1,045	26.92	2.57%
	K	7,581	7,496	84.88	1.13%
Inferred Resources	Li	1,256	1,290	-34.52	-2.67%
	K	9,559	9,817	-257.91	-2.63%

Figure 14.3 Lithium concentration distribution

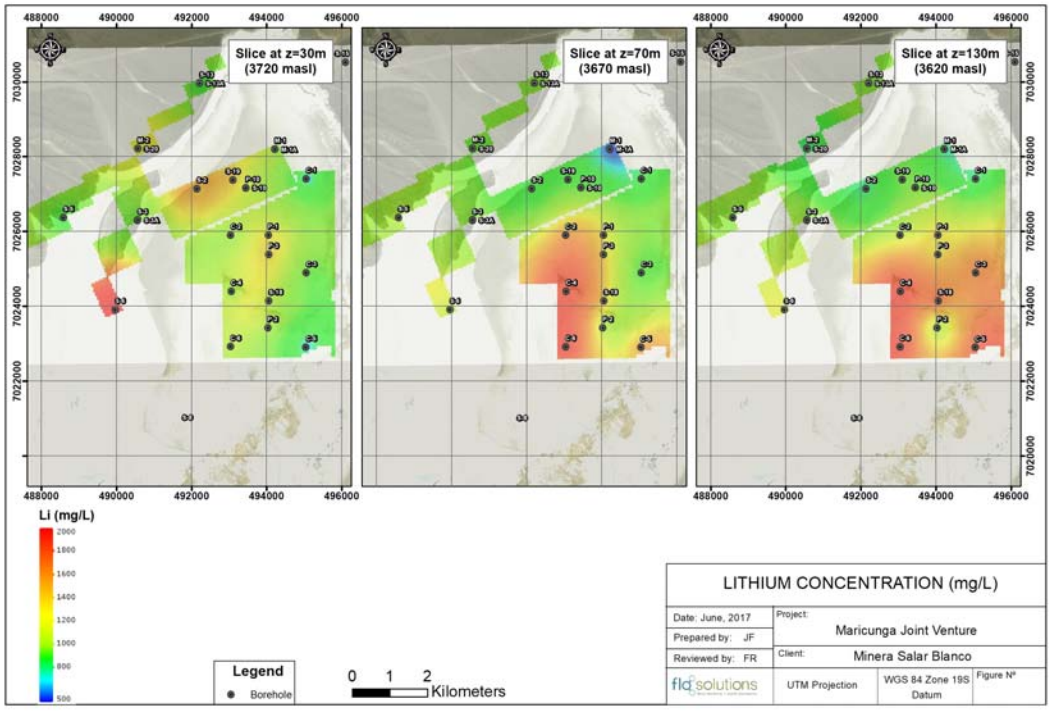

Figure 14.4 Potassium concentration distribution

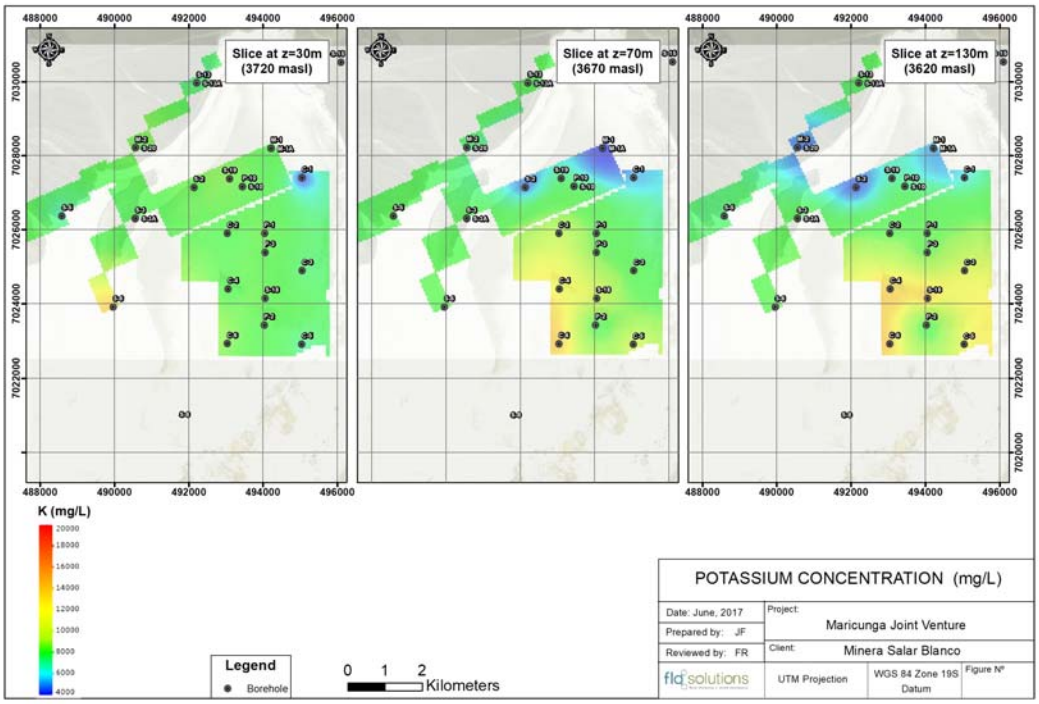

14.7 Resource Estimate

The grade estimates of lithium and potassium in each block inside the model were calculated applying the following operation:

$$R_i = C_i . Sy_i$$

Where: i is the indice of the block, going from 1 to 34,560,000

R_i: Grade value to be assigned (g/m3)

C_i: Concentration value assigned from the estimation (mg/L)

Sy_i: Porosity value assigned from the estimation (%)

Figure 14.5 through Figure 14.7 shows N-S, W-E, and NW-SE sections through the resource model showing lithium grade distributions in g/m^3. All the resource classification was made in the limits of the block model. The measured, indicated and inferred resource areas are shown in Figure 14.8.

Figure 14.5 N-S section through the resource model showing the lithium grade distribution

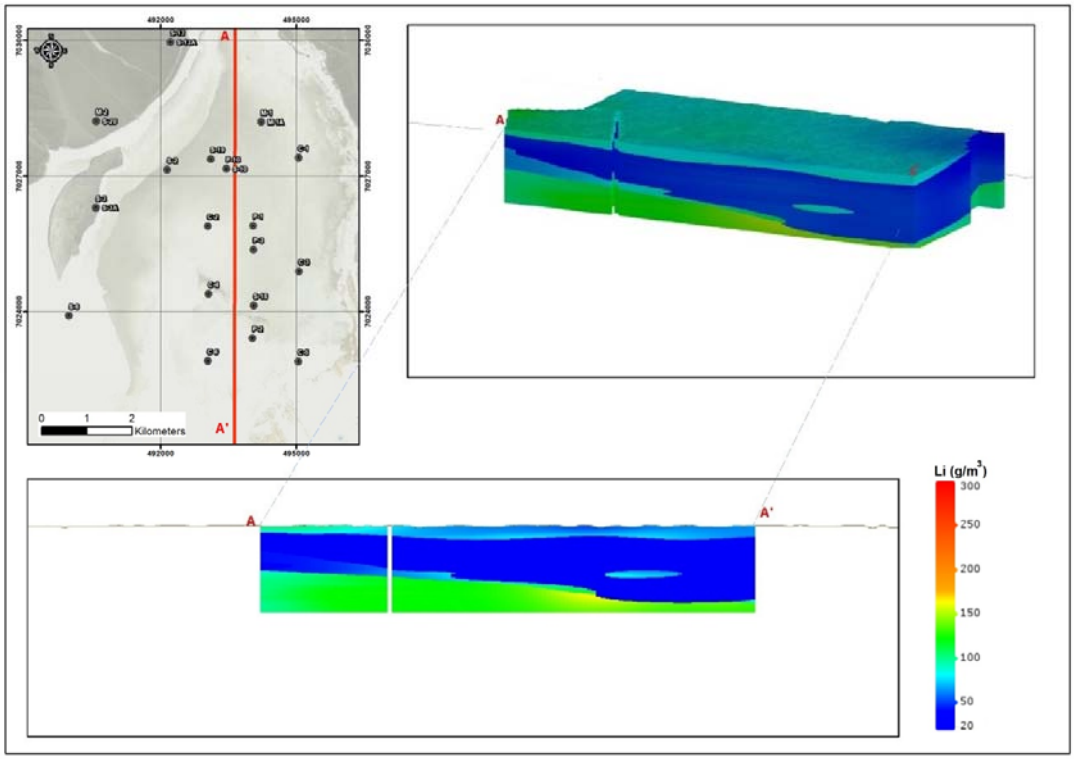

Figure 14.6 W-E section through the resource model showing the lithium grade distribution

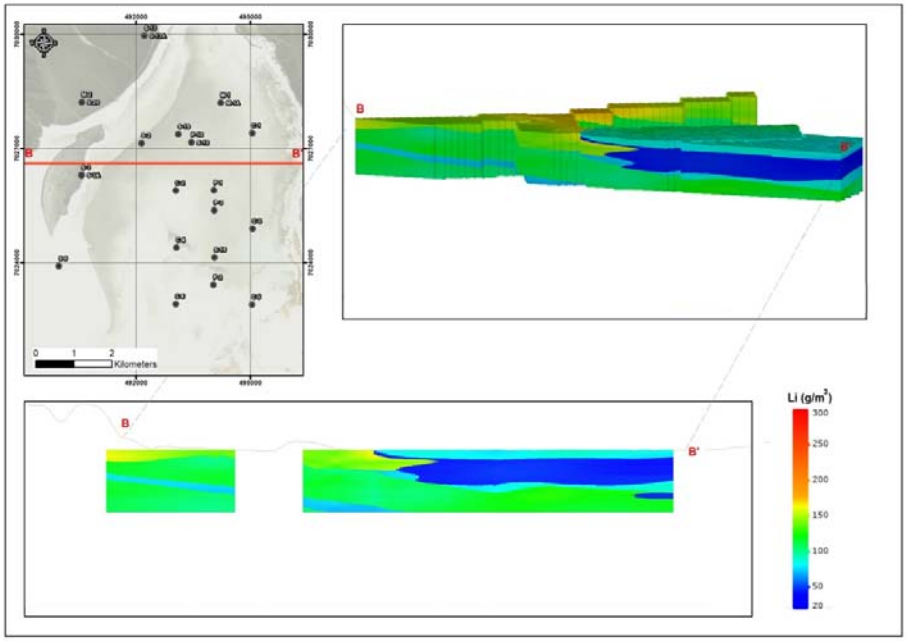

Figure 14.7 NW-SE section through the resource model showing the lithium grade distribution

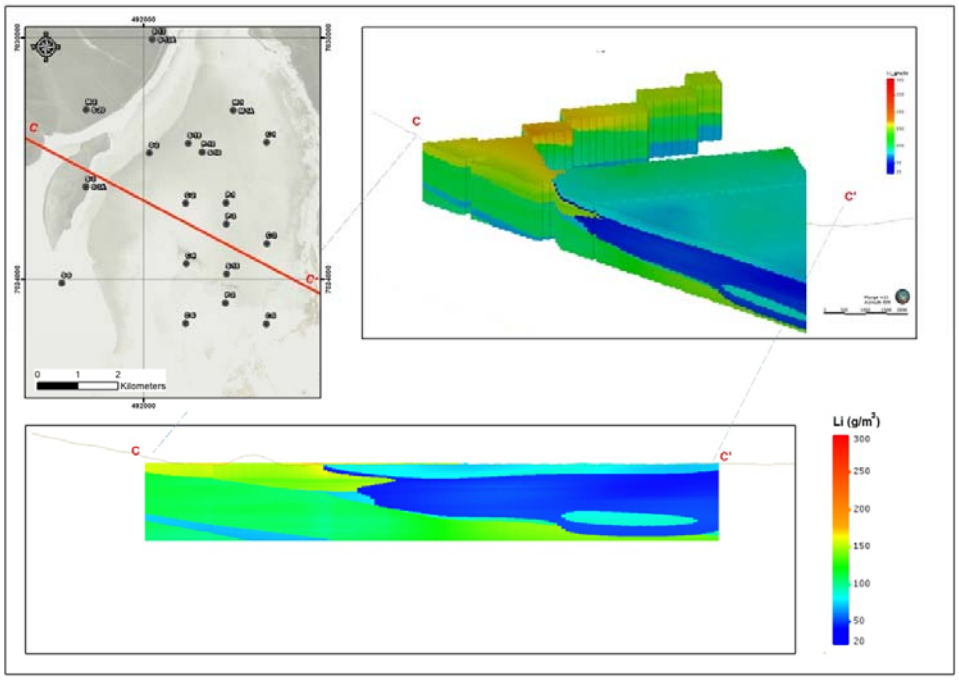

Figure 14.8 Distribution of resource classification areas

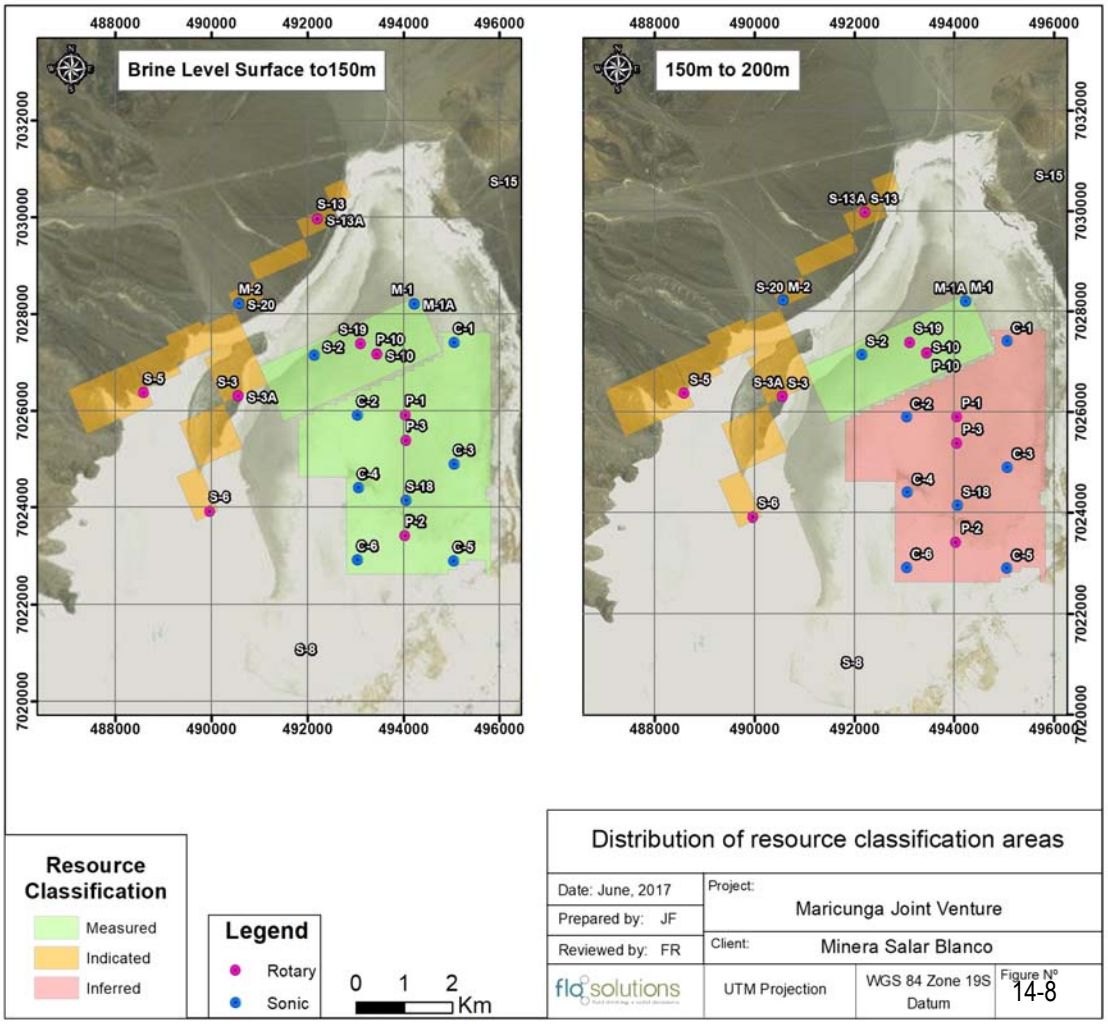

The lithium and potassium resources are summarized in Table 14.5.

Table 14.5 Measured, Indicated and Inferred Lithium and Potassium Resources of the MJV Project – Dated July 12, 2017

	Measured		Indicated		Inferred		M+I	
	Li	K	Li	K	Li	K	Li	K
Area (Km2)	18.88		6.76		14.38		25.64	
Aquifer volume (km3)	3.06		1.35		0.72		4.41	
Mean specific yield (Sy)	0.05		0.11		0.09		0.07	
Brine volume (km3)	0.15		0.14		0.06		0.30	
Mean grade (g/m3)	56	409	114	801	114	869	74	529
Concentration (mg/L)	1,174	8,646	1,071	7,491	1,289	9,859	1,143	8,292
Resource (tonnes)	170,000	1,250,000	155,000	1,100,000	80,000	630,000	325,000	2,350,000

Notes to the resource estimate:

1. CIM definitions were followed for Mineral Resources.
2. The Qualified Persons for this Mineral Resource estimate are Frits Reidel, CPG and Murray Brooker, PGeo
3. No cut-off values have been applied to the resource estimate.
4. Numbers may not add due to rounding
5. The effective date is July 12, 2017.

Table 14.6 shows the mineral resources of the MJV Project expressed as lithium carbonate equivalent (LCE) and potash (KCl). The lithium grade-tonnage curve for the resources (Figure 14.9) shows the tonnage is not very sensitive to lithium concentration cut-off below 700 mg/ L (the resource is calculated with no cut-off for lithium or potassium concentrations)

Table 14.6 MJV resources expressed LCE and potash

	Measured and Indicated		Inferred	
	LCE	KCL	LCE	KCL
Tonnes	1,725,000	4,500,000	425,000	1,200,000

1. Lithium is converted to lithium carbonate (Li2CO3) with a conversion factor of 5.32.
2. Potassium is converted to potash with a conversion factor of 1.91
3. Numbers may not add due to rounding

It is the opinion of the authors that the Salar geometry, brine chemistry composition and the specific yield of the Salar sediments have been adequately characterized to support the Measured, Indicated and Inferred Resource estimate for the Project herein.

It is the opinion of the authors the resource estimated and described in the current report meet the requirements of reasonable prospects for eventual economic extraction, as defined in Form 43-101F1. The resource described herein has similar lithium concentrations, chemical composition and hydraulic

parameter values (drainable porosity values between 0.05 and 0.11 and hydraulic conductivities values between 0,5 m/d and 300 m/d) to resources currently in commercial production such as those in Salar de Atacama or Salar de Olaroz located in the Puna region of Northen Argentina. The hydraulic parameters of the resource area determined from the results of the pumping tests suggests that it is reasonable to expect brine extraction by a conventional production wellfield at a commercially viable rate, while the geochemical characteristics of the brine suggest that conventional processing techniques may be employed to produce saleable lithium products in an economically profitable manner.

These conventional processing techniques are employed in most lithium brine operations, including the two operations at Salar de Atacama (Chile), one at Salar de Olaroz (Argentina), and one at Clayton Valley (USA)

Figure 14.9: Lithium grade tonnage curve

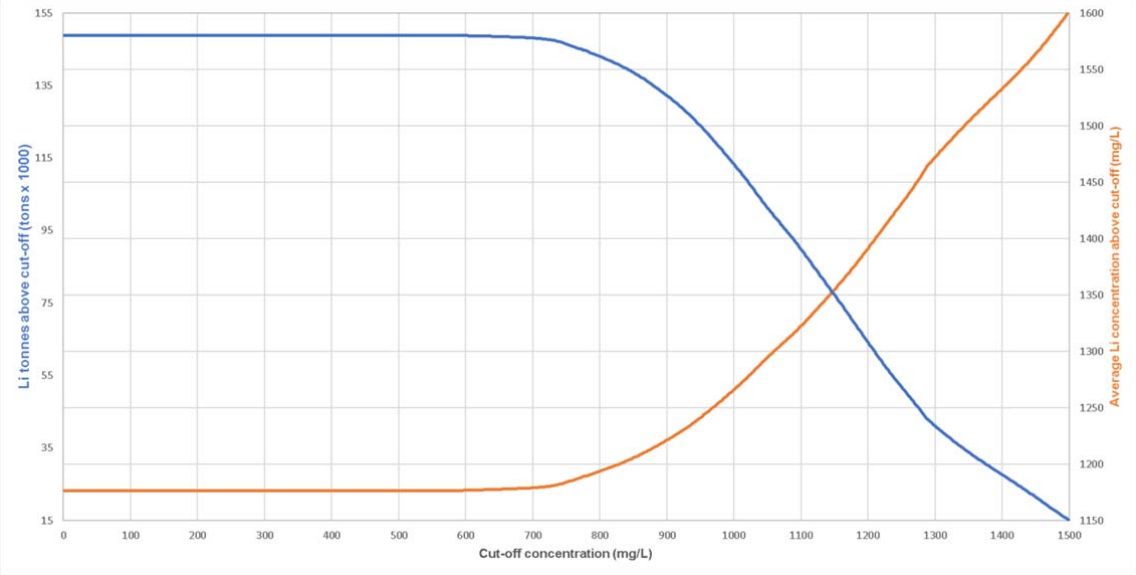

15 MINERAL RESERVE ESTIMATES

No reserve estimate have been prepared for the MJV.

16 MINING METHODS

Based on the results of the pumping tests carried out on the MJV (as described in Section 10 above) it is most likely that brine abstraction from the Salar could take place by installing and operating a conventional production wellfield. Pumping rates of individual wells could range between 20 l/s and 45 l/s. Well completion depths will vary between 40 m (upper brine aquifer) and to 200 m or more (lower brine aquifer).

17 RECOVERY METHODS

The Salar de Maricunga brine is suitable for conventional processing, which principally consists in solar evaporation of the brine to a suitable concentration where the brine can be treated in a lithium carbonate production plant. The concentrated Maricunga brine will require boron, calcium and magnesium removal stages. The ongoing test work is optimizing these stages in order to have the lowest operational costs and most environmentally friendly process. Finally, a soda ash solution will be added to the concentrated and purified lithium brine to precipitate lithium carbonate.

Potassium chloride can be produced by conventional processes. The process principally consists of silvinite salt harvesting from the ponds and subsequently milling, and flotation of the silvite (KCl) salts. The carnalite salts will be decomposed in brine or water in order to produce potassium chloride. Other potential by-products are magnesium chloride and calcium chloride salts. The lithium recovery for this process was simulated to be around 55% and the potassium recovery around 70%, which is common in the industry.

Details of the final process technology to be used by the MJV to process brine from the Salar de Maricunga is not known as of the effective date of this technical report.

18 PROJECT INFRASTRUCTURE

MSB is currently preparing a PFS for the MJV. Infrastructure requirements will include a brine production wellfield and pipeline, evaporation ponds, power plant, water supply, accommodation facilities, sewage system, laboratory, office facilities, equipment storage and maintenance facilities, roads, waste salt storage facility, chemical raw material storage facility, etc.

19 MARKET STUDIES AND CONTRACTS

Lithium finds application in a diverse range of uses from glass and ceramics to chemicals to batteries to aluminum alloys. In recent years, the focus on lithium supply and demand has been on use of lithium in various battery applications, especially portable electronics, electric vehicles and power storage.

19.1 Lithium Supply

Lithium is commercially extracted from two primary deposit types: as a hard rock mineral and in natural evaporative saline brines. Lithium minerals, in the form of spodumene or petalite concentrate, find primary application in glass and ceramics products. Lithium recovered from brine deposits is primarily produced as lithium carbonate (Li_2CO_3) or lithium hydroxide ($LiOH{\cdot}H_2O$) and is used in a wide variety of chemical and (especially) battery applications. Lithium brine deposits are estimated to account for 90% of global lithium reserves and approximately 50% of global production. Lithium brine operations are confined to Chile, Argentina, the USA and China, with South America hosting the largest producers. Lithium mineral concentrates can be converted to lithium chemicals such as lithium carbonate and used in similar applications as lithium recovered from brines, but at higher production cost than brine-derived lithium chemicals. The major producers of lithium minerals are located in Australia, China and Zimbabwe, with emerging producers in Canada (Roskill 2016).

Global supply of lithium minerals has been historically dominated by hard rock mineral sources. Development of large-scale lithium brine operations in South America commenced in the early 1980's and brine sources now account for approximately 50% of supply. Global lithium supply has increased at a 7% compound annual growth rate ("CAGR") from 1995 to 2015 to meet increased demand from mobile phones and other electronics. As of 2016, global lithium supply was around 171 kt lithium carbonate equivalent ("LCE"), split roughly 50:50 between hard-rock and brines (Deutsche Bank, 2016). Figure 19.1 illustrates recent changes in global lithium supply by country and projected changes in supply through 2025. Key aspects of lithium supply from brine and hard rock deposits are summarized in Table 19.1

Table 19.1: Key attributes of brine and hard rock lithium deposits

Characteristic or Property	Salt Lake Brines	Hard Rock Deposits
Resource approachable	Abundant but low recoveries	Very few high-grade deposits
High-technology required	Yes	No
Scalable	Yes	Yes
Processing time	Long[1]	Short
Weather dependent	Yes[2]	No
Capital intensity	High	Moderate
Operating costs	Low	High
As % of global lithium supply	50%	50%

Source: Deutsche Bank, 2016

1. New non-solar evaporation technology can substantially reduce time frame
2. Not for new, non-solar evaporation technology

Brine deposits are anticipated to account for an increasing share of production due to the relative availability of brines, their lower operating costs, and changes in brine processing technology resulting in significant capital cost reduction on a per tonne of final product produced.

Lithium is sold and consumed as a number of different mineral and chemical compounds, depending upon the desired end product. Given the numerous types of lithium products, to standardize supply and demand, lithium statistics are typically expressed either on a contained lithium basis or, more commonly as lithium carbonate equivalent or LCE, as lithium carbonate currently holds the largest share of the overall lithium market. For conversion purposes, lithium comprises approximately 18.8% of total mass in lithium carbonate (conversion ratio of 5.323 kg LCE to 1.0 kg Li).

The type of lithium compound produced and sold by a mining operation is partially dependent upon the type of deposit. For example, a lithium brine project cannot produce lithium mineral compounds but its direct product can be lithium carbonate whereas a hard rock lithium project requires an additional conversion step to take its lithium mineral concentrate to lithium carbonate. Therefore, lithium brines cannot supply certain lithium mineral demand and lithium brines can have a cost advantage for lithium carbonate markets (e.g. batteries).

Generally accepted industry specifications for lithium carbonate and lithium hydroxide products are as follows:

- Lithium carbonate – battery grade is minimum 99.5% Li2CO3
- Lithium carbonate – technical grade is minimum 99% Li2CO3; and
- Lithium hydroxide – minimum 56% LiOH.

Figure 19.1: Lithium supply by country and forecast supply to 2025

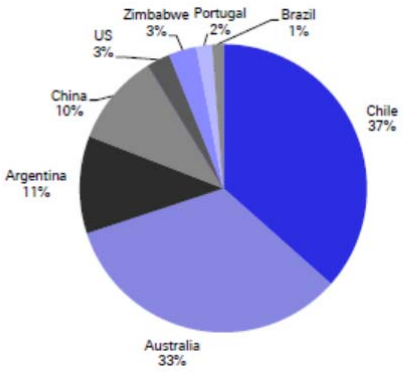

Lithium Supply by Country – 2015

LCE Basis

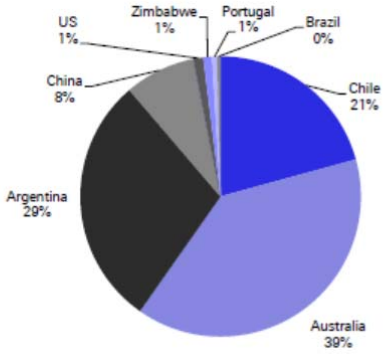

Lithium Supply by Country – 2025

LCE Basis

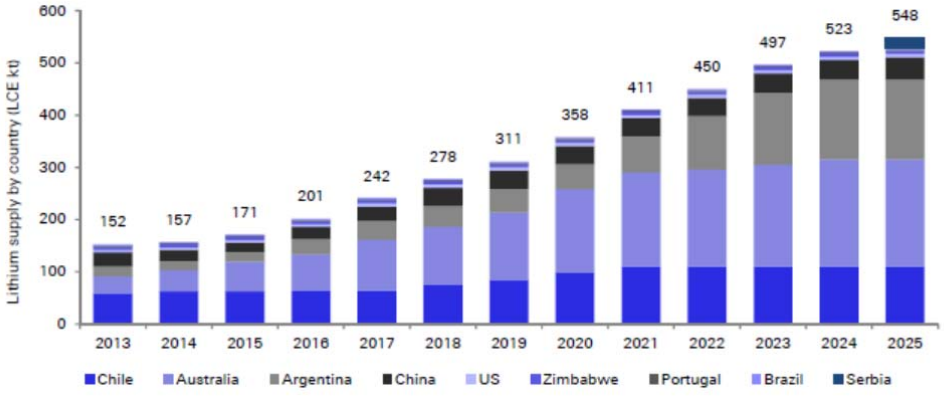

Source: Deutsche Bank, 2016

19.2 Lithium Demand

Global lithium demand has been estimated to be approximately 184 kt LCE in 2015 (Deutsche Bank, 2016), with the difference between supply (171 kt LCE) and demand being made up by inventory drawdown. Demand has been growing at a compound annual rate of approximately 7% since 1995, driven primarily by increases in battery applications. Battery applications accounted for an estimated 40% of total lithium demand in 2015 and are forecast to account for 70% of total demand in 2025. By 2025, total lithium demand is forecast by Deutsche Bank to be approximately 525 kt of lithium carbonate equivalent (Figure 19.2).

Figure 19.2: Global lithium demand – 2013 – 2025

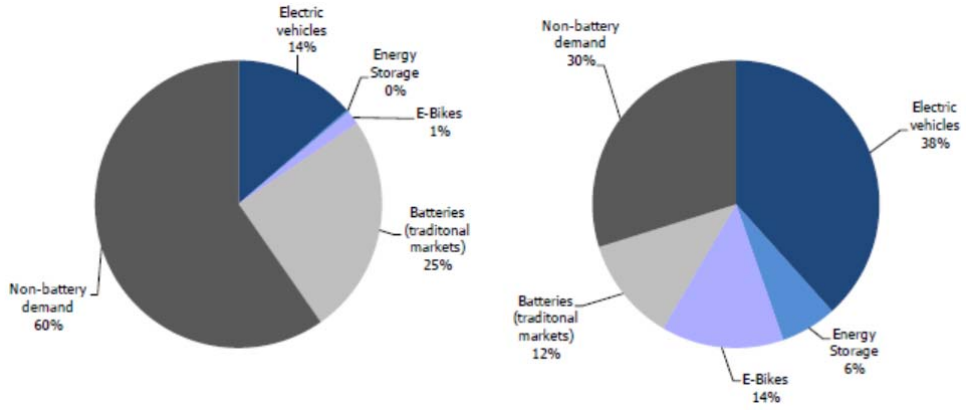

Lithium Demand by Application – 2015 Lithium Demand by Application – 2025

LCE Basis

LCE Basis

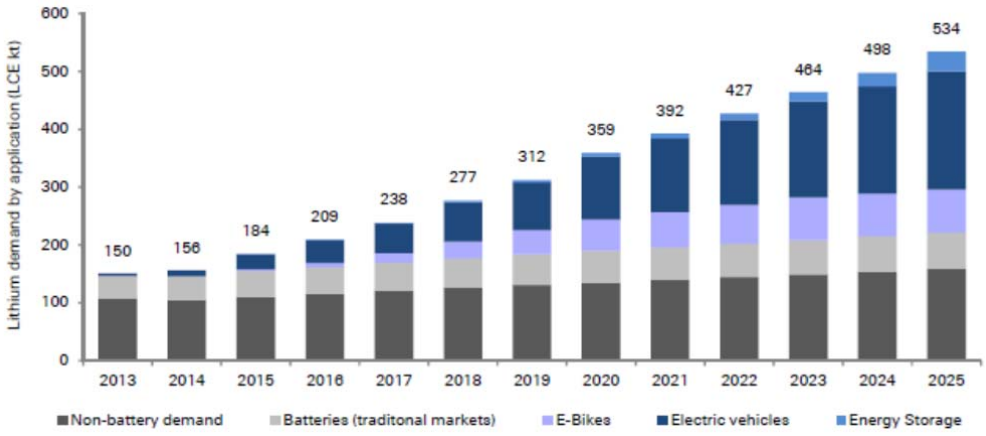

Source: Deutsche Bank, 2016

Forecast lithium consumption rates are heavily influenced by assumptions around rechargeable battery demand. Rechargeable lithium batteries have in the past been used primarily in the portable consumable electronics sector but in recent years this has been overtaken by use in electric vehicles and grid/off-grid energy storage systems. South Korea and China are the dominant rechargeable battery and battery material producers, but production centres have recently been commissioned also in the USA and elsewhere. Roskill notes that growth rates for non-battery sectors have slowed significantly since 2012.

Forecasts for electric vehicle uptake, either as hybrids, plug in hybrids or full electric vehicles have recently been revised significantly upward by several industry observers (Deutsche Bank, 2016; Exane BNP Paribas, 2016; Roskill, 2017) based on rapidly decreasing battery production costs, regulatory requirements in Europe and China, and most importantly, significantly improved battery technology permitting greater range and higher power. Many industry observers expect full electric battery vehicle production costs to equal internal combustion engine (ICE) vehicle production costs between 2020 to 2025 (Exane BNP Paribas, 2016). At that point, demand for full electric vehicles will increase significantly as there will no longer be a major price premium between EVs and standard vehicles and the operating costs savings for EVs compared to standard vehicles will drive demand. Deutsche Bank's forecast of electric vehicle demand is shown in Figure 19.3. BNP Paribas has a more robust forecast, as illustrated in Table 19.2.

Figure 19.3: Electric vehicle demand to 2025

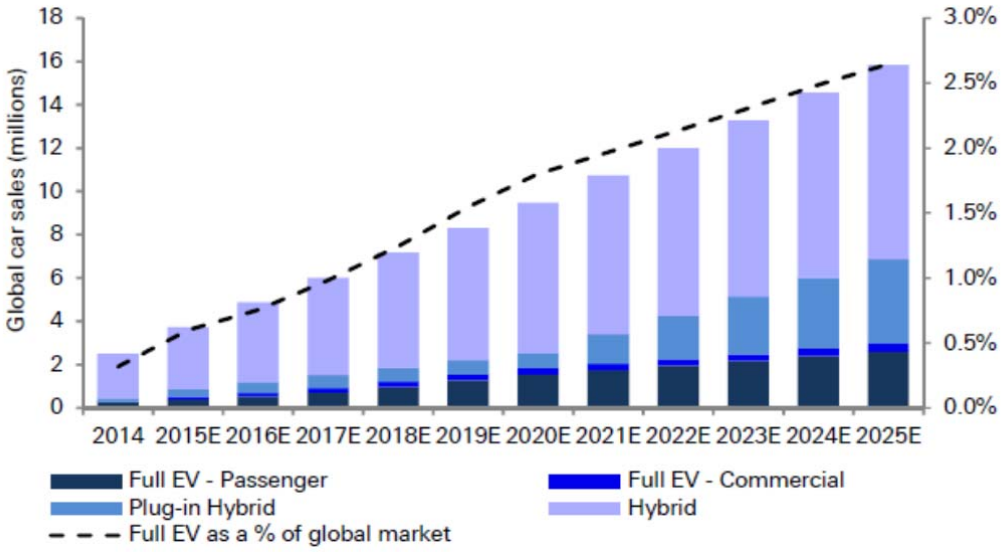

Source: Deutsche Bank, 2016

Table 19.2: New vehicle build by engine type

Engine Type	2015	2020e	2025e	2030e
Internal Combustion Engine	94%	84%	57%	29%
Mild Hybrid	0%	4%	14%	23%
Full Hybrid (HEV & PHEV)	3%	7%	15%	20%
Full EV	0%	2%	11%	26%
Diesel	18%	16%	11%	9%

Source: Exane BNP Paribas, 2016

Alternative forecasts by industry research group Roskill project much more robust demand growth scenarios through 2025. Their forecast is based on both robust vehicle demand growth, especially in rapidly developing economies; and a significant shift to electric vehicles. Projected changes are illustrated in Figures 19.4 and 19.5.

Figure 19.4: Vehicle demand to 2030

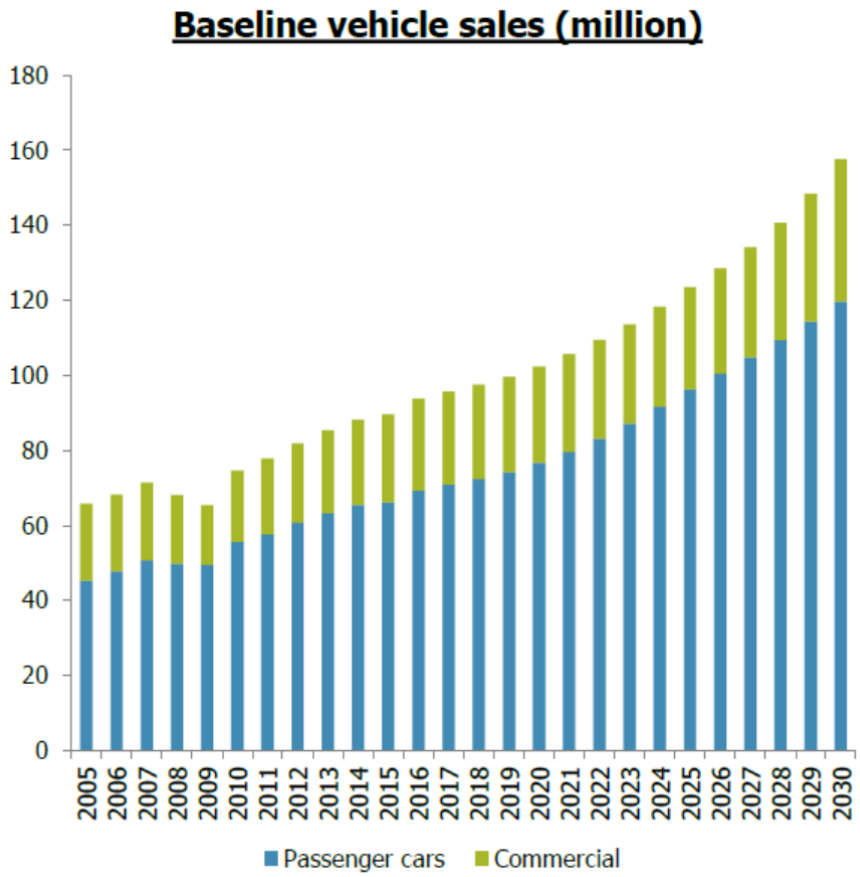

Source: Roskill, 2017

Figure 19.5: Electric vehicle demand to 2030

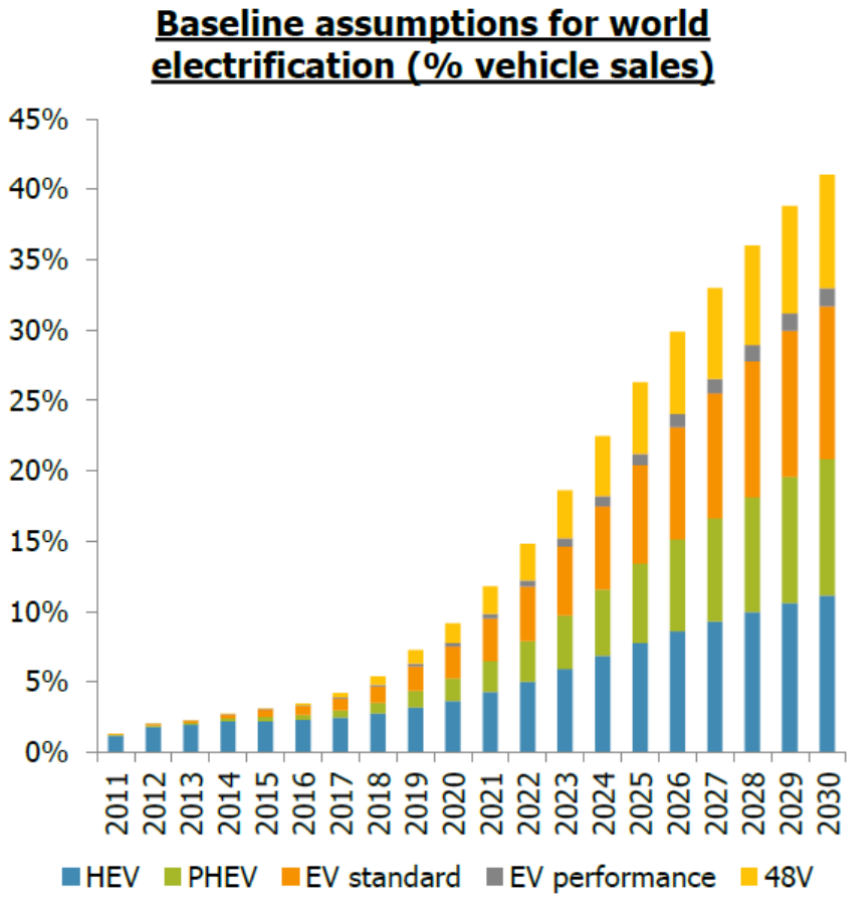

Source: Roskill, 2017

Based on the projected growth in electric vehicles and expanded use of lithium-ion batteries in energy storage applications, as well as continued use of lithium ion batteries in consumer electronics and use of lithium in non-electric applications, Roskill projects lithium demand could exceed 1.0 million tonnes of LCE by 2026 (Figure 19.6):

Figure 19.6: Lithium demand forecast to 2026

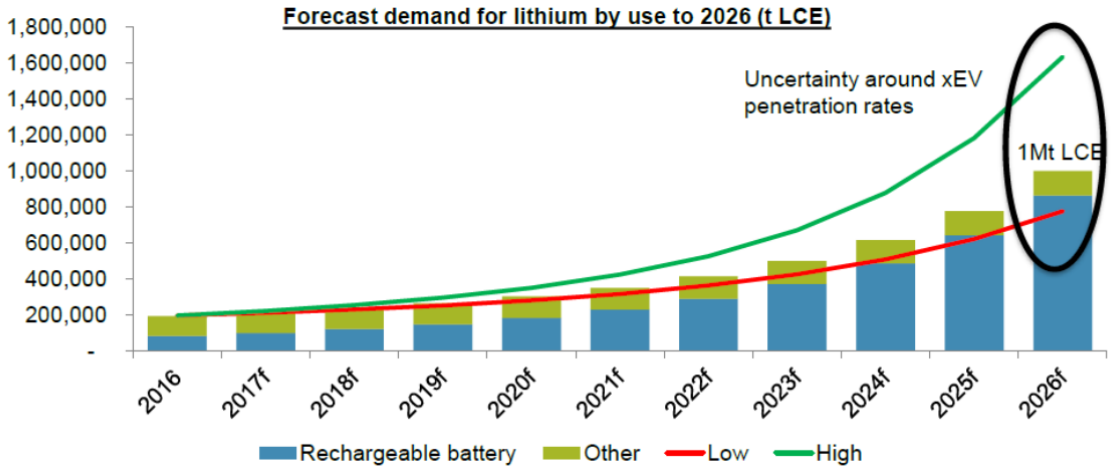

Source: Roskill, 2017

Under Roskill's revised forecast lithium demand is anticipated to grow at a rate of 17.7% [per annum] from 2016 through 2026 versus the previous projection of 6.4% per annum. The primary reason for the increase is the larger than expected sales of electric vehicles in the past two years, as well as government and automaker plans for the near and long term as reflected in recent announcements from France, the UK, Renault, Volvo, BMW and Volkswagen. Rechargeable batteries are anticipated to account for an increasing share of lithium demand, increasing from 50% of lithium demand in 2016 to as much as 85% in 2026.

New large-scale lithium battery factories currently under development are attempting to reduce the cost of lithium batteries based on economies of scale in production to encourage more rapid uptake of electric vehicles as well as open new market sectors to lithium batteries. It is important to recognize that lithium represents a very small component of electric vehicle battery production costs, typically less than 3% of total battery cost, depending on the battery chemistry. The majority of battery production costs are represented by pack assembly, cell manufacturing and processed materials. Raw materials account for about 21% of total manufacturing costs, but lithium represents only about 4% of the raw material costs based on NMC (Nickle-Manganese-Cobalt) battery chemistry, which uses lithium carbonate (Figure 19.7).

Figure 19.7: Battery pack production costs

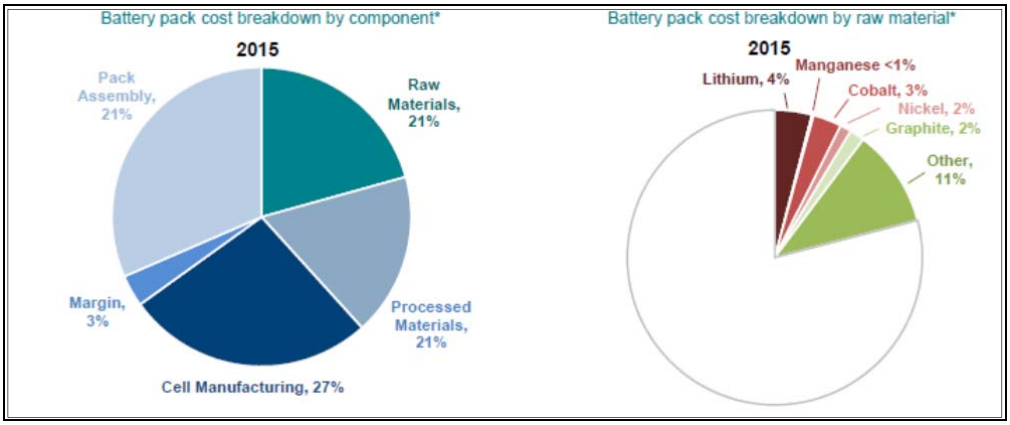

source: exane bnp paribas (2016), * assumes nmc battery chemistry

As a consequence, lithium prices do not have a significant impact on total battery production costs and the total vehicle selling prices and thus lithium demand in battery applications will not be significantly impacted by increased prices for the raw material. This is illustrated in Table 19.3 which shows the impact of lithium carbonate pricing on selected electric vehicle manufacturers. It is seen that even a doubling of the lithium carbonate price will have only a very modest impact on the average vehicle selling price.

Table 19.3: Lithium carbonate price impact on electric vehicle selling price

OEM & Model	Battery	List Price ($US)	Lithium Cost*	Lithium Carbonate Price ($US/t)						
				7,500	10,000	12,500	15,000	17,500	20,000	22,500
Tesla Model S	90 kWh	90,000	Lithium Cost	$987	$1,317	$1,646	$1,975	$2,304	$2,633	$2,962
			% of Cathode	33%	39%	45%	49%	53%	56%	59%
			% ASP	1.1%	1.5%	1.8%	2.2%	2.6%	2.9%	3.3%
Nissan Leaf	30 kWh	34,000	Lithium Cost	$329	$439	$549	$658	$768	$878	$987
			% of Cathode	33%	39%	45%	49%	53%	56%	59%
			% ASP	1.0%	1.3%	1.6%	1.9%	2.3%	2.6%	2.9%
BMW i3	33 kWh	39,900	Lithium Cost	$362	$483	$603	$724	$845	$965	$1.086
			% of Cathode	33%	39%	45%	49%	53%	56%	59%
			% ASP	0.9%	1.2%	1.5%	1.8%	2.1%	2.4%	2.7%

Source: Exane BNP Paribas (2016); *Assumes NMC cathode technology

Global lithium production is dominated by four companies: Talison Lithium in Australia (a joint venture between Tianqi Lithium and Albermarle, SQM in Chile, Albemarle in Chile and the USA and FMC Lithium in Argentina. Together, the “Big 4” produced about 87% of the lithium supply in 2015 (Table 19.4).

Table 19.4: Global mine production of lithium by company - 2015

(t LCE)

Company	Location	2009	2010	2011	2012	2013	2014	2015p
Talison	Greenbushes, WA, Australia	33,300	47,100	51,800	62,000	54,500	65,600	70,000
SQM	Atacama, Chile	21,300	32,400	40,700	45,700	36,100	39,500	37,000
Albemarle	Atacama, Chile & Silver Peak, NV, USA	13,305	21,229	22,950	24,000	28,400	26,915	28,500
FMC	Hombre Muerto, Argentina	12,634	17,537	13,398	13,200	13,015	18,020	15,000
China Mineral	See table below	3,900	4,100	6,250	6,200	6,700	6,050	6,550
China Brine	See table below	5,500	4,510	5,025	3,830	5,530	6,030	6,100
Other Mineral	See table below	9,521	8,188	8,136	8,230	8,220	8,200	8,200
Orocobre	Olaroz, Argentina	-	-	-	-	-	-	1,700
Galaxy Resources	Mt. Cattlin, WA, Australia	-	244	9,471	8,914	-[1]	-	-
RB Energy	Val d'Or, QC, Canada	-	-	-	-	5,000	-[1]	-
Total		**99,461**	**135,308**	**157,730**	**172,074**	**156,465**	**168,315**	**171,050**

Note 1: placed on care and maintenance

Source: Roskill, 2015

To date, lithium production has kept up with rapid increases in demand, largely through production increases at higher cost swing producers such as Talison's Greenbushes hard rock mineral operation and production increases at Chinese brines. Future production increases to meet continued increases in consumption are still possible from these producers, especially Talison, but new, lower cost producers will be needed in the medium-term and could displace these high cost swing producers in the short term.

19.3 Prices

Prices for lithium carbonate and lithium hydroxide, the primary lithium ion battery materials, are set by negotiation between buyer and seller. Prices have increased rapidly in the recent past from indicative pricing of $US 5,000 - $6,000/t in 2013 and 2014 for 99.0% - 99.5% lithium carbonate to a current range of $US 9,500 to $US 12,500/t for lithium carbonate and approximately $US 15,500/tonne for lithium hydroxide. Spot prices in China for lithium carbonate and lithium hydroxide are considerably higher, most recently in the range of $US 25,000/tonne to $US 30,000.

19.4 Contracts

The MSB has not entered into any contracts for production or sale of lithium or potassium salts as of the date of this technical report.

19.5 Chilean Regulations Respecting Lithium Production

Lithium is considered a non-concessionable mineral in Chile. As such, production is controlled under regulations promulgated under various acts and regulations, the key one being D.L. No 2886/1979, which established lithium as a strategic resource based on Article 19, No. 24, paragraphs 6-10 of the Constitution; Constitutional Organic Law No. 18,097 (21 January, 1982) on Mining Concessions; the Mining Code Law 18,248 of Oct. 3, 1983 and the Regulations of the Mining Code of 27 Feb. 1987.

Under the above laws and regulations, lithium production can only be undertaken by state companies or under Special Operating Contracts (CEOL) or Administrative Concessions by private companies. It is to be noted that mineral tenements, including lithium tenements, registered under the 1938 Mining Law are "grandfathered" from the provisions of the 1982 Mining Law and D.L. No 2886/1979 which means that they don´t need a CEOL to be exploited. Of the total 2,563 hectares for which the resource has been defined at the Maricunga JV project, 1,125 hectares are grandfathered tenements. Lithium production in Chile is regulated also by the Chilean Nuclear Commission (CChEN) which gives the permit to sell lithium based products.

In 2014, Chile undertook to modernize the laws and regulations respecting lithium production. The Chilean National Lithium Commission completed a process of consultations and the Government of Chile announced in early 2016 a number of short and medium-term objectives and programs for development of the Chilean lithium industry. Key amongst the recommendations were the following:

- Renegotiation of the existing concession agreements between CORFO and SQM and Albermarle with respect to lithium production on Salar de Atacama;
- Mandate the state-owned companies CORFO, ENAMI and CODELCO as the government vehicles to develop lithium projects through private-public joint ventures (over mining concessions where the state has ownership).
- Creation of the CORFO Non-metallic Mining and Governance Committee
- Promoting local and indigenous community involvement in lithium development projects;
- Enhancing technological capabilities in Chile for sustainable production in the salars;
- Developing policies and programs for value added lithium production in Chile;
- Reinforcing public institutions; and,
- Promoting research, innovation and technological development.

Since the adoption of the recommendations of the Lithium Commission, CORFO has renegotiated the production contracts with SQM and Albermarle with respect lithium extraction on salar de Atacama. Albermarle has increased its production quota to 262,132 tonnes lithium (1,395,328 tonnes LCE) through to 2044. Albermarle agreed to a change in royalty payments and obtained an option to construct a lithium hydroxide plant. In addition, Albermarle agreed to provide a specified percentage of lithium carbonate production at preferential prices to Chilean processors for value added production in Chile and to commit to a specified annual R&D program.

20 ENVIRONMENTAL STUDIES, PERMITTING AND SOCIAL OR COMMUNITY IMPACT

20.1 Environmental Studies

MLE completed various environmental studies required to support its exploration programs between 2011 and 2017. The MJV has initiated baseline environmental, hydrogeological and biological studies in support of the MJV EIA. MWH-Stantec has been contracted to prepare the EIA .

The EIA is required prior to approval for construction of any lithium brine extraction and processing plant. It is expected that the EIA for the future brine operation will be completed during early Q1 of 2018. The review and approval process period of an EIA by the Servicio de Evaluación Ambiental (SEA) is generally 12 to 18 months.

20.2 Project Permitting

Sectorial permits (PS) need to be obtained from the local authorities in the III Region (as a matter of formality) once EIA approval is obtained and before construction is initiated.

20.3 Social or Community Requirements

The III Region of Chile has a well-established mining industry and culture. The MJV is remote from any communities and population centers and therefore will not create any direct impacts. The EIA permitting process will address community and socio-economic issues; it is expected the project will have a positive impact through the creation of new employment opportunities and investment in the region.

21 CAPITAL AND OPERATING COSTS

No capital and operating costs have been prepared as part of this mineral resource estimate. MSB is currently undertaking a PFS to be completed during Q4 2017.

22 ECONOMIC ANALYSIS

No economic analysis has been carried out as part of this mineral resource estimate. MSB is currently preparing a PFS that will be completed during Q4 2017.

23 ADJACENT PROPERTIES

The MJV mining concessions (*Litio 1-6, Cocina 19-27, San Francisco, Despreciada and Salamina)* are located in the northern part of Salar de Maricunga. Other adjacent mining concessions in the Salar are held by SQM, Cominor and Codelco. SQM is a major lithium carbonate producer with operations at Salar de Atacama. Codelco is a Chilean government-owned copper producer. Codelco, Cominor and SQM have not undertaken any significant exploration work on their properties in the Salar. To date no lithium production is taking place from the Salar and the MJV is at the most advanced stage of project evaluation.

.

24 EXPLORATION POTENTIAL

The Measured and Indicated categories comprise 80% of the updated resource of the MJV reported herein, with the Inferred category the remaining 20% of the total 2.15 mt LCE resource defined to a depth of 200 m. One deep borehole (S19) was drilled to 360 m depth on the MJV in 2016. Borehole S-19 encountered a continuation of the lower brine aquifer in the Lower Alluvium and volcanoclastics units below 200 m depth with lithium concentrations above 900 mg/l. An exploration target is therefore defined below the base of the current resource to a depth up to 400 m as shown in Figure 24.1. Results of AMT and gravity surveys suggest that the Salar sediments may extend to over 500 m depth.

Figure 24.1 Schematic of the deep lithium exploration target (200-400 m) below the MJV

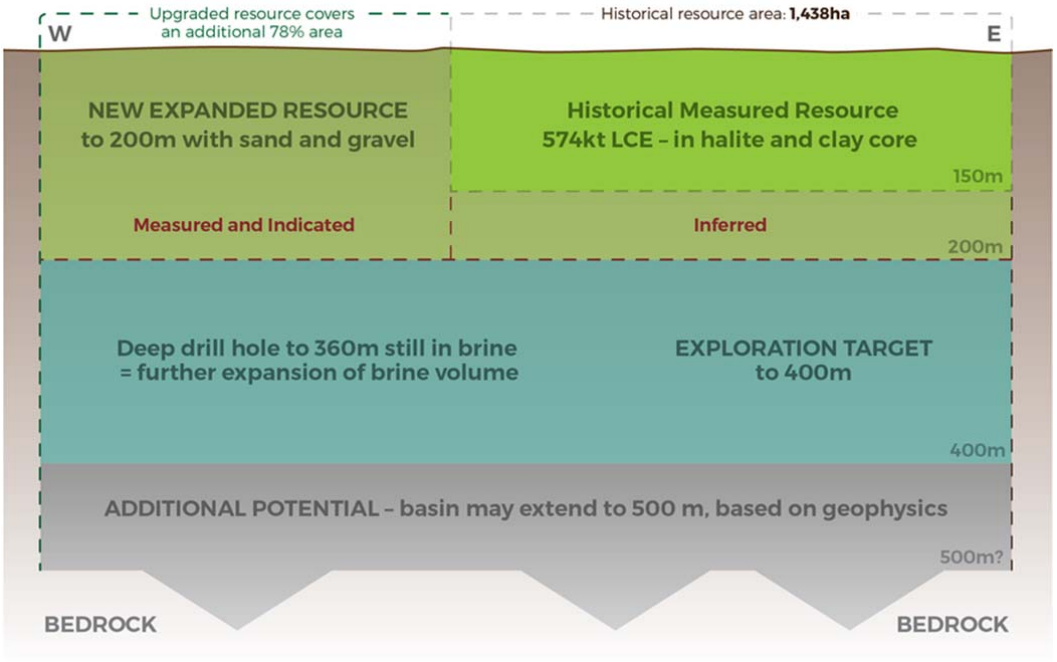

Source: LPI 2017

The exploration target is where, based on the available geological evidence, there is the possibility of defining a mineral resource. The timing of any drilling with the objective of defining resources in the exploration target area has not been decided at this stage. In keeping with Clause 18 of the JORC Code and CIM requirements the exploration target defined at Maricunga is:

- Not to be considered a resource or reserve; and
- Based on information summarized below.

It is a requirement of stating an exploration target that it is based on a range of values, which represent the potential geological conditions. Values have been selected to present an upper and a lower exploration target size. It is likely that the lithium and potassium contained in the exploration target lies

somewhere between the Upper and Lower Cases. The following parameters have been used to estimate an Upper Assumption and Lower Assumption case for lithium and potassium

Area

The exploration target covers 25.63 km^2 (2,563 hectares) beneath the area of all the exploration properties (effectively the area of the properties extending downward beneath the resource).

Figure 24.2 Outline of the exploration target

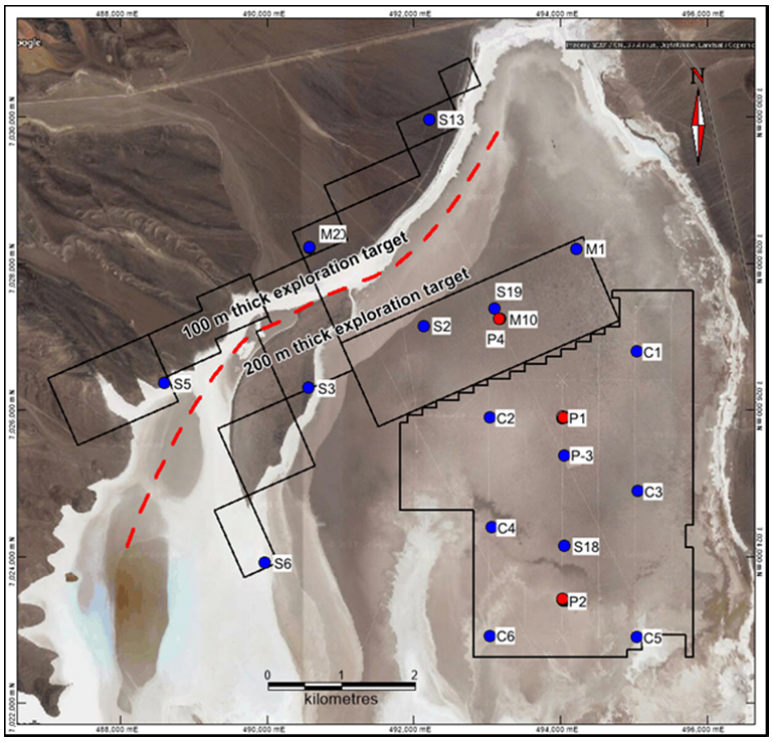

Thickness

- The western area of the exploration target is assigned a thickness of 100 m; and
- The central area of the exploration target is assigned a thickness of 200 m.

The difference in thickness is treated simplistically as a change from 200 to 100 m across the line shown in Figure 24.2.

Porosity

- For the Upper Assumption 10% is used as the specific yield for the volcaniclastic unit in the western and eastern properties; and
- For the Lower Assumption 6% is used as the specific yield, allowing for the presence of a much finer matrix, reducing the specific yield.

Lithium and Potassium Concentrations

- A value of 1,000 mg/l for lithium and 6,000 and 7,500 mg/l potassium (in the Western and Central parts) is used in the upside case for the central and western properties; and
- A value of 700 mg/l lithium and 5,500 mg/l potassium is used in the Lower Assumption case in the central area with 600 mg/l lithium and 5,000 mg/l potassium in the western properties.

Table 24.1 MJV exploration target estimate

EXPLORATION TARGET ESTIMATE MARICUNGA										
Subarea	Area km²	Thickness m	Mean drainable porosity %	Brine volume million m³	Lithium Concentration mg/L	Contained Lithium tonnes	Lithium Carbonate LCE tonnes	Potassium Concentration mg/L	Contained Potassium tonnes	Potassium Chloride KCl tonnes
UPPER RANGE SCENARIO										
Western	4.23	100	10%	42.3	1,000	40,000	200,000	6,500	270,000	500,000
Central	21.41	200	10%	428.0	1,000	430,000	2,300,000	7,500	3,200,000	6,100,000
	Continues from directly below the resource					**470,000**	**2,500,000**		**3,470,000**	**6,600,000**
LOWER RANGE SCENARIO										
Western	4.23	100	6%	25.4	600	15,000	80,000	5,000	130,000	240,000
Central	21.41	200	6%	257.0	700	180,000	950,000	5,500	1,400,000	2,700,000
	Continues from directly below the resource					**195,000**	**1,030,000**		**1,530,000**	**2,940,000**

Lithium is converted to lithium carbonate (Li_2CO_3) with a conversion factor of 5.32. Numbers may not add due to rounding.
Potassium is converted to potassium chloride (KCl) with a conversion factor of 1.91

Source: LPI 2017

Figure 24.3 shows growth of the Maricunga resource and exploration target and how Maricunga, with high grades, compares to other lithium brine projects. It must be stressed that an exploration target is not a mineral resource. The potential quantity and grade of the exploration target is conceptual in nature, and there has been insufficient exploration to define a Mineral Resource in the volume where the Exploration Target is outlined. It is uncertain if further exploration drilling will result in the determination of a Mineral Resource in this volume.

Figure 24.3 Comparison of the MJV with other lithium projects

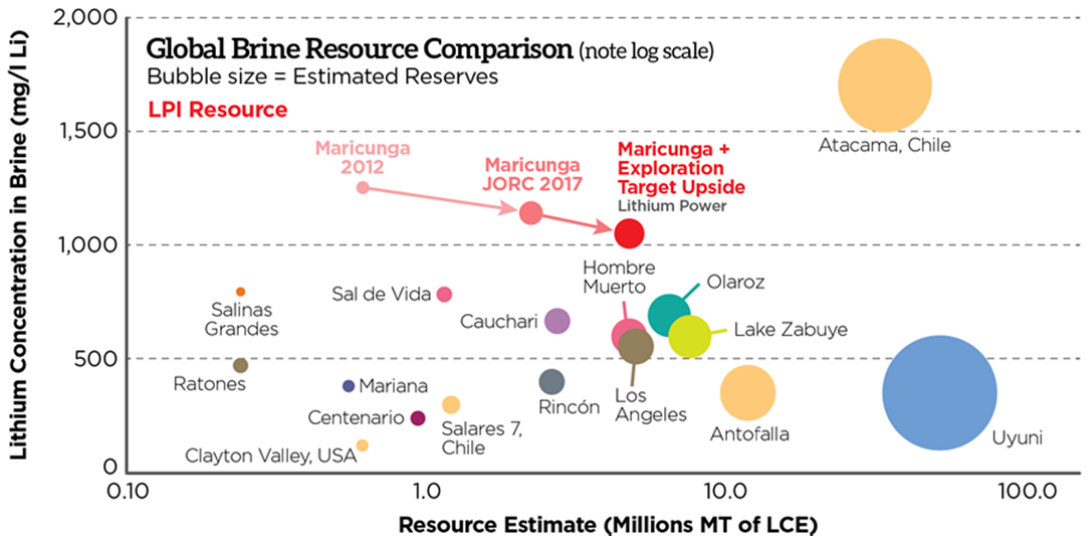

Source: LPI 2017

25 INTERPRETATION AND CONCLUSIONS

Based on the analyses and interpretation of the results of the exploration work carried out on the MJV in Salar de Maricunga between 2011 and 2017, the following concluding statements are prepared:

- The entire MJV project area has been covered by exploratory drilling between 2011 and 2017 at an approximate borehole density of one exploration borehole per 1.5 km2; it is the opinion of the authors that such borehole density is appropriate for the mineral resource estimate described herein.
- The results of the drilling (10 sonic boreholes and 8 rotary/HWT boreholes) and the analysis of 487 primary brine samples identify distinct brine composition and grade at specific depth intervals, showing a relatively uniform distribution of lithium bearing brines throughout the MJV project area to a depth of 200 m. (Table 25.1);

Table 25.1 Summary of the avarage MJV brine composition (g/L)

K	Li	Mg	Ca	SO_4	B	Mg/Li	K/Li	$(SO_4+2B)/(Ca+Mg)^*$
8.23	1.12	7,34	13.49	0.71	0.60	6.55	7.35	0.092

- The lithium bearing brine contain sufficient levels of lithium and potassium to be potentially economic for development;
- The geology the MJV consists of a permeable upper halite brine aquifer with a thickness of up to 34 m in the central part of the Project area. This upper aquifer is underlain for most parts by a low permeable clay core. Below the Clay Core occurs a lower brine aquifer hosted in relatively permeable sediments belonging to the Lower Alluvium and volcaniclastics units. Permeable alluvial fans extend into the Salar on the western side of the MJV. The fan material at depth grades into the Lower Alluvial and is underlain by the volcaniclastics.
- The results of four (4) pumping tests and 501 drainable porosity analyses suggest that the specific yield (or drainable porosity) for the Upper Halite unit averages 0.07; sediments of the lower brine aquifer have a drainable porosity between 0.06 to 0.1; and the Clay Core 0.02.
- It is the opinion of the authors that the Salar geometry, brine chemistry composition and the specific yield of the Salar sediments have been adequately defined to a depth of 200 m to support the Measured, Indicated and Inferred Resource estimate described in Table 25.2.

Table 25.2 Measured, Indicated and Inferred Lithium and Potassium Resources of the MJV Project – Dated July 12, 2017

	Measured		Indicated		Inferred		M+I	
	Li	K	Li	K	Li	K	Li	K
Area (Km2)	18.88		6.76		14.38		25.64	
Aquifer volume (km3)	3.06		1.35		0.72		4.41	
Mean specific yield (Sy)	0.05		0.11		0.09		0.07	
Brine volume (km3)	0.15		0.14		0.06		0.30	
Mean grade (g/m3)	56	409	114	801	114	869	74	529
Concentration (mg/L)	1,174	8,646	1,071	7,491	1,289	9,859	1,143	8,292
Resource (tonnes)	170,000	1,250,000	155,000	1,100,000	80,000	630,000	325,000	2,350,000

Notes to the resource estimate:

1. CIM definitions were followed for Mineral Resources.
2. The Qualified Persons for this Mineral Resource estimate are Frits Reidel, CPG and Murray Brooker, PGeo.
3. No cut-off values have been applied to the resource estimate.
4. Numbers may not add due to rounding.
5. The effective date is July 12, 2017.

Table 25.3 MJV resources expressed LCE and potash

	Measured and Indicated		Inferred	
	LCE	KCL	LCE	KCL
Tonnes	1,725,000	4,500,000	425,000	1,200,000

1. Lithium is converted to lithium carbonate (Li2CO3) with a conversion factor of 5.32.
2. Potassium is converted to potash with a conversion factor of 1.9
3. Numbers may not add due to rounding

- Based on results of exploration borehole S-19 to a depth of 360 m, it is the opinion of the authors that a significant exploration target exists below the current resource defined to 200 m depth as described in Section 24.

26 RECOMMENDATIONS

It is recommended by the authors that the PFS and FS for the MJV are completed as is planned during 2017 and 2018 respectively. Studies in support of the EIA should be completed as is currently planned by early 2018.

There are several opportunities to increase the current MJV resource base through 1) acquisition of adjacent mining claims and 2) further exploration at depth on the existing claims.

A work program should be initiated to continue expanding the MJV resource estimate through the exploring of the deep exploration target as described in Section 24. It is recommended that the proposed work program includes the following components:

- Obtain the necessary permits from the regulatory agencies to carry out a deep drilling program on the MJV mining concessions.
- Deep drilling (7-10 holes) using a suitable drilling method to a depth of 400 m across the MJV properties. The drilling target will be the coarser grained sediments in the Lower Alluvium and Volcaniclastics.
- Sampling protocols need to be developed to properly characterize the hydraulic parameters and the brine chemistry of these deeper units.

The estimated cost for the above exploration program is approximately USD 6 million and is summarized in Table 26.1.

Table 26.1 Estimated costs for the deep exploration program

	Deep Exploration	K-USD
1	Exploration drilling (7 holes)	3,500
2	Downhole geophysics	400
3	Laboratory analyses (porosity / brine)	300
4	Monitoring / pumping tests	700
5	Brine and process evaluation	500
6	Analyses, resource and reserve modeling, reporting	600
	Estimated Total Costs (K USD)	6,000

27 REFERENCES

Brüggen, J. 1950. Fundamentos de la Geología de Chile. Instituto Geográfico Militar (Chile), 378 p.

CORFO (1982): Informe Prospecion Preliminar salar de Maricunga; Comite de Salas Mixtas CORFO, Santiago, Chile.

Cornejo, P., Mpodozis, C., Ramírez, C., y Tomlinson, A., 1993a. Estudio geológico de la región de Potrerillos y El Salvador (26°–27° lat. S): Santiago, Reporte registrado, IR-93–01, 2 volúmenes, 12 mapas escala 1:50000,Servicio Nacional de Geología y Minería.

Cornejo, P., y Mpodozis, C., 1996. Geología de la región de Sierra Exploradora (25°–26° Lat. S): Santiago, Chile, Reporte registrado, IR-96–09, 2 volúmenes, 8 Mapas, escala 1:50000, Servicio Nacional de Geología y Minería.

Cornejo, P., Mpodozis, C., y Tomlinson, A., 1998. Hoja Salar de Maricunga: Santiago, Servicio Nacional de Geología Minería, Mapa Geológico N°7, escala 1:100000.

Dirección General de Aguas, (DGA) 1987. Balance Hídrico de Chile.

DGA, 2006, Análisis de la Situación Hidrológica e Hidrogeológica de la Cuenca del Salar de Maricunga, III Región. DGA, Departamento de Estudios y Planificación (2006). S.D.T. Nº 255.

DGA, 2009, Levantamiento Hidrogeologico para el Desarrollo de Nuevas Fuentas de Agua en Areas Prioritarias de la Zone Norte de Chile, Regiones XV, I, II, y III. Etapa 2 Sistema Piloto III Region Salares de Maricunga y Pedernales. Realizado por Departamento de Ingeniera Hidraulica y Ambiental Pontifica Universidad Catolica de Chile (PUC). SIT No. 195, Noviembre 2009.

EDRA, 1999, Hidrogeología Sector Quebrada Piedra Pómez- Placer Dome

Ehren-Gonzalez Limitada, 2015: Salar de Maricunga Desktop Study, Update of May, 2014 report, prepared for Minera Salar Blanco SPA, October, 2015

Flosolutions, 2015a: Proyecto Blanco, Programma 2015, Presentación de resultados, September 16, 2015

Flosolutions, 2015b: Proyecto Blanco, Informe Técnico: Programma de Pruebas de Bombeo 2015, Análisis y Resultados

Gabalda G., Nalpas T. y Bonvalot S., 2005. Base of the Atacama Gravels Formation (26°S, Northern Chile): first results from gravity data. ISAG YI, Barcelona.

García, F. 1967. Geología del Norte Grde de Chile. In Symposium sobre el Geosinclinal Yino No. 3, Sociedad Geológica de Chile: 138 p.

Gardeweg, M., Mpodozis, C., Clavero, J., y Cuitiño, L., 1997. Mapa Geológico de la Hoja Nevado Ojos de Salado, Región de Atacama, escala 1:100000: Santiago, Servicio Nacional de Geología y Minería.

Golder Associates, 2011, Linea Base Hidrogeologica y Hidrologica Marte Lobo y Modelo Hidrogeologico Cienaga Redonda – Kinross Gold Corporation.

González-Ferrán, O., Baker, P.E., y Rex, D.C., 1985. Tectonic-volcanic discontinuity at latitude 27° south, Yean Range, associated with Nazca plate subduction: Tectonophysics, v. 112, p. 423–441.

Hartley, A.J., May, G., 1998. Miocene Gypcretes from the Calama Basin, northern Chile. Sedimentology 45, 351–364.

Houston, J, 2006. Evaporation in the Atacama desert: An empirical study of spatio-temporal variations and their causes. Journal of Hydrology, 330:402-412.

Houston, J., Butcher, A., Ehren, P., Evans, K., Godfrey, L. 2011. The Evaluation of Brine Prospects y the Requirement for Modifications to Filing Styards. Economic Geology, v. 106, pp. 1225–1239.

Isacks, B.L. 1988. Uplift of the Central Yean plateau y bending of the Bolivian orocline. Journal Geophysical Research, Vol. 93: 3211-3231.

Iriarte D., Sergio.,1999, Mapa hidrogeológico de la cuenca Salar de Maricunga: sector Salar de Maricunga, Escala 1:100.000, Región de Atacama. Nº Mapa: M62. SERNAGEOMIN, 1999.

Iriarte, S, Santibáñez, I y Aravena, 2001. Evaluation of the Hydrogeological Interconnection between the Salar de Maricunga and the Piedra Pomez Basins, Atacama Region, Chile; An Isotope and Geochemical Approach

Kay, S.M., Coira, B., y Viramonte, J., 1994. Young mafic back-arc volcanic rocks as indicators of continental lithospheric delamination beneath the Argentine Puna plateau, central Andes: Journal of Geophysical Research, v. 99, p. 24,323–24,339.

Kay, S.M., y Mpodozis, C., 2002. Magmatism as a probe to the Neogene shallowing of the Nazca plate beneath the modern Chilean fl at-slab: Journal of South American Earth Sciences, v. 15, p. 39–59.

Kay, S.M., y Copely, P., 2006. Early to middle Miocene back-arc magmas of the Neuquén Basin of the southern Andes: Geochemical consequences of slab shallowing y the westward drift of South America, en Kay, S.M. y Ramos, V.A., eds., Evolution of an Yean margin: A tectonic y magmatic perspective from the Andes to the Neuquén Basin (35°–39°S lat.): Geological Society of America Special Paper 407, p. 185–213.

Lara L, Godoy E, 1998. Hoja Chañaral-Diego de Almagro, III Región de Atacama: Santiago, Chile. Servicio Nacional de Geología y Minería, Mapas Geológicos, escala 1:100000.

Mercado, M., 1982. Hoja Laguna del Negro Francisco, Región de Atacama: Servicio Nacional de Geología y Minería, Carta Geológica de Chile, N° 56, p. 73.

Mortimer, c., 1980. Drainage evolution of the Atacama Desert of northernmost Chile. Revista Geológica de Chile, no. II, p. 3-28

Moscoso, R., Maksaev, V., Cuitiño, L., y Díaz, F., Koeppen, R., Tosdal, R., Cunningham, C., McKee, E., y Rytuba, J., 1993. El complejo volcánico Cerro Bravos, región de Maricunga, Chile: Geología, alteración hidrotermal y mineralización, in Investigaciones de Metales Preciosos en el complejo volcánico neógeno-cuaternario de los Andes Centrales:Bolivia, Servicio Geológico, Banco Interamericano de Desarrollo, p. 131–165.

Mpodozis, C., Cornejo, P., Kay, S.M., y Tittler, A., 1995. La Franja de Maricunga: Síntesis de la evolución del frente volcánico oligoceno-mioceno de la zona sur de los Andes Centrales: Revista Geológica de Chile, v. 22, p. 273–314.

Mpodozis, C., y Clavero, J., 2002. Tertiary tectonic evolution of the southwestern edge of the Puna Plateau: Cordillera Claudio Gay (26°–27°S): Toulouse, Proceedings of Fifth International Symposium on Yean Geodynamics, p. 445–448.

Muntean, J.L., y Einaudi, M.T., 2001. Porphyry-epithermal transition: Maricunga belt, northern Chile: Economic Geology y the Bulletin of the Society of Economic Geologists, v. 96, p. 743–772.

Nalpas, T.; Dabard, M-P.; Ruffet, G.; Vernon, A.; Mpodo-zis, C.; Loi, A.; Hérail, G. 2008. Sedimentation y preservation of the Miocene Atacama Gravels in the Pedernales-Chañaral Area, Northern Chile: Climatic or tectonic control? Tectonophysics 459: 161-173.

Risacher, Alonso y Salazar, Geoquímica de Aguas en Cuencas Cerradas: I, II y III Regiones de Chile, Volumen I, Síntesis. S.I.T Nº 51, Convenio de Cooperación DGA – UCN – IRD, 1999.

Risacher, F., Alonso, H. and Salazar, C. 2003. The origin of brines and salts in Chilean Salars: a hydrochemical review. Earth Science Reviews, 63: 249-293.

Riquelme, R., 2003. Evolution geomorphologique neogene de Andes Centrales du Desert d'Atacama (Chili): interaction tectonique-climat, Ph.D. Thesis, Université Paul Sabatier (Toulouse, France) y Universidad de Chile (Santiago, Chile), 258 p.

SRK Consulting, 2011, Hidrogeologia Campo de Pozos Piedra - Compania Minera Casale.

Sillitoe, R.H., Mortimer, C; y Clark, A.H., 1968. A chronology of lyform evolution y supergene mineral alteration, southern Atacama Desert, Chile. Institute of Mining y Metallurgy Transactions, v. 77, p.

Sillitoe, R.H., McKee, E.H., y Vila, T., 1991. Reconnaissance K-Ar geochronology of the Maricunga gold-silver belt, northern Chile: Economic Geology y the Bulletin of the Society of Economic Geologists, v. 86,p. 1261–1270.

Tassara, A. 1997. Geología del Salar de Maricunga, Región de Atacama. Servicio Nacional de Geología y Minería (SERNAGEOMIN). Informe Registrado IR-97-10.

Tomlinson, A., Mpodozis, C., Cornejo, P., Ramirez, C.F., y Dimitru, T.,1994, El sistema de Fallas Sierra Castilllo-Agua Amarga: Transpresión sinistral Eocena en la Precordillera de Potrerillos-El Salvador: Congreso Geológico Chileno VII, Actas, v. 2, p. 1459–1463.

Tomlinson, A., Cornejo, P., y Mpodozis, C., 1999, Hoja Potrerillos, Región de Atacama: Santiago, Servicio Nacional de Geología y Minería, Mapa Geológico no. 14, escala 1:100000.

Venegas, M.; Iriarte, S. y Aguirre, I., 2000, Mapa hidrogeológico de la Cuenca Salar de Maricunga: sector Ciénaga Redonda, escala 1:100.000, Región de Atacama. N° Mapa: M65. SERNAGEOMIN, 2000.

Vila, T., y Sillitoe, R.H., 1991, Gold-rich porphyry systems in the Maricunga belt, northern Chile: Economic Geology y the Bulletin of the Society of Economic Geologists, v. 86, p. 1238–1260.

Zentilli, M., 1974, Geological evolution y metallogenetic relationships in the andes of northern Chile between 26° y 29° south. Kingston, Ontario, Queen's University.

Qualified person Frederik Reidel

I, Frederik Reidel, CPG, as author of this report entitled “NI 43-101 Technical Report: Lithium and Potassium Resource Estimate, Maricunga Joint Venture, III Region Chile, prepared for Minera Salar Blanco S.A., dated August 25, 2017 do hereby certify that:

1. I am employed as Principal Hydrogeologist and General Manager by FloSolutions-Chile, residing at: Roger de Flor 2950, Piso 5, Las Condes, Santiago, Chile.
2. I am a graduate of New Mexico Institute of Mining and Technology with a Bachelors of Science Degree in Geophysics, 1986
3. I am registered a Certified Professional Geologist (#11454) with the American Institute of Professional Geologists
4. I have worked as hydrogeologist for a total of 29 years since my graduation. My relevant experience for the purpose of the Technical Report is:
    - Qualified Person for the Sal de los Angeles Project, Salta Argentina for LiX Energy Corp 2016 – to date).
    - Qualified Person and Member of the technical commitees of Li3 Energy Ltd and Minera Salar Blanco for the development of the Maricunga Lithium Project in Chile (2011 – to date).
    - Co-author of the NI 43-101 Technical Report on the lithium and potash resources in Salar de Maricunga for Li3 Energy Ltd (2012).
    - Evaluation of lithium and potash resources in Salar de Olaroz for Orocobre Ltd. in support of the project’s DFS and NI 43-101 Technical Report (2010-2011).
    - Evaluation of lithium and potash resources in Salar de Cauchari for Lithium Americas Corporation; NI 43-101 Technical Report preparation; member of the company’s Technical Advisory Panel (2009-2010).
    - Evaluation of brine resources in Salar de Hombre Muerto for FMC (1992-1993)
    - Consulting hydrogeologist in the evaluation and development of groundwater resources for international mining companies in North- and South America (1989-2012).
5. I have read the definition of "qualified person" set out in National Instrument 43-101 (NI 43-101) and certify that by reason of my education, affiliation with a professional association (as defined in NI 43-101) and past relevant work experience, I fulfill the requirements to be a "qualified person" for the purposes of NI 43-101.
6. I have visited the Salar de Maricunga and the MJV project area numerous times between August 2011 and to date. I was present on site on a regular basis during the 2011, 2015 and 2016 drilling and testing programs.
7. I have been involved as a QP with the property since 2011, but have no previous involvement with Minera Salar Blanco.
8. I am responsible for the overall preparation of this report.
9. I am independent of the Issuer applying the test set out in Section 1.4 of NI 43-101.
10. I have read NI 43-101, and the Technical Report has been prepared in compliance with NI 43-101 and Form 43-101F1.
11. To the best of my knowledge, information, and belief, the Technical Report contains all scientific and technical information that is required to be disclosed to make the technical report not misleading.

Dated this 25th day of August, 2017

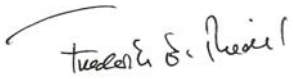

Frederik Reidel, CP

Qualified Person Murray Brooker

I, Murray Brooker, M.Sc., Geol., M.Sc. Hydro, do hereby certify that:

1. I am an indep8endent consultant of:

   63 Carlotta St,

   Greenwich, NSW 2065, Australia.

2. I have the following academic and professional qualifications:

Academic:

I. B.Sc.(Honours) in Geology from Victoria University of Wellington, New Zealand in 1988

II. M.Sc. in Geology from James Cook University of North Queensland, Australia, in 1992

III. M.Sc. in Hydrogeology from the University of Technology, Sydney, Australia, in 2002.

Professional:

I. Australian Registered Professional Geoscientist (RPGeo) in the fields of mineral exploration and hydrogeology

II. Member of the Australian Institute of Geoscientists (MAIG)

III. Member of the International Association of Hydrogeologists (MIAH).

3. I have practiced my profession for twenty six years.
4. I have read the definition of "qualified person" set out in National Instrument 43-101 ("NI 43-101") and certify that by reason of my education, past relevant work experience, and affiliation with a professional association (as defined in NI 43-101) I fulfill the requirements to be a "qualified person" for the purposes of NI 43-101. This report is based on my personal review of information provided by the Issuer and on discussions with the Issuer's representatives. My relevant experience for the purpose of this report is:
   - 2010-Present Principal Hydrominex Geoscience Consultants
   - 2006-2010 Principal Geoscientist – Global Ore Discovery – Mining Industry Consultants
   - 2004-2006 Acting Manager Hydrogeology – Parsons Brinckerhoff.
   - 2003-2004 Hydrogeologist, Otek Environmental
   - 2002-2003 Hydrogeologist, Parsons Brinckerhoff
   - 1991-2000 Exploration Geologist and Exploration Manager, North Limited, Argentina, Chile, Mexico, Australia

   I have previously been involved in the following brine resource projects:

   - Salar de Olaroz for Orocobre, Argentina (2010-2017)
   - Salar de Cauchari for Orocobre and Advantage Lithium, Argentina (2010-2017)

- Salar Salinas Grandes for Orocobre, Argentina (2010)
- Salar de Centenario (2011, 2016) for Lacus Minerals and Lithium Power
- Salar de Pocitos (2011, 2016) for Lacus Minerals
- Lake Mackay, Western Australia for Agrimin (2015-2016)

5. I am jointly responsible for sections 7, and 10 of the technical report entitled "Lithium & Potassium Resource Estimate Maricunga Joint Venture, III Region, Chile" (the "Technical Report"") prepared for The Maricunga JV and dated effective August 25, 2017. I am independent of the Maricunga JV. I visited the Salar de Maricunga and the project area numerous times between August 2016 and to date.
6. I have not had prior involvement with the properties that are the subject of the Technical Report.
7. As of the date of this certificate, to the best of my knowledge, information and belief, the Technical Report contains all scientific and technical information that is required to be disclosed to make the Technical Report not misleading.
8. I have read NI 43-101 and Form 43-101F1 (the "Form"), and the Technical Report has been prepared in compliance with NI 43-101 and the Form.

Effective date: 25th Day of August 2017

Signature of Murray Brooker M.Sc, RPGeo

Murray Brooker M.Sc, RPGeo.

Qualified Person Peter Ehren

I, Peter Ehren, MSc., AusIMM (CP = Chartered Professional), do hereby certify that:

1. I am an independent consultant and owner of Ehren-González Limitada at Alberto Arenas 4005 112, La Serena, Chile
2. I graduated with a Master of Science Degree in Mining and Petroleum Engineering, with a specialization in Raw Materials Technology and Processing Variant at the Technical University of Delft, The Netherlands in the year 1997
3. I am an independent consultant, a Member of the Australasian Institute of Mining (AusIMM) and metallurgy and a Chartered Professional of the AusIMM.
4. I have practiced my profession for 19 years.
5. I have read the definition of "qualified person" set out in National Instrument 43-101 ("NI 43-101") and certify that by reason of my education and past relevant work experience, I fulfill the requirements to be a "qualified person" for the purposes of NI 43-101. This report is based on my personal review of information provided by the Issuer and on discussions with the Issuer's representatives. My relevant experience for the purpose of this report is:
   - 1997 Final Thesis of MSc.degree: "Recovery of Lithium from Geothermal
   - Brine, Salton Sea", BHP Minerals, Reno Nevada.
   - 1998-2001 Process Engineer, Salar de Atacama, SQM
   - 2001-2006 R&D Manager, Lithium and Brine Technology, SQM.
   - 2006 Process Project Manager, SQM
   - 2007 till data Independent Lithium and Salt Processing Consultant,
   - Ehren-González Limitada

   I have previously been involved in the several brine resource projects, where under:

   - Salar de Olaroz for Orocobre, Argentina (2009-2016)
   - Salar de Cauchari for Orocobre, Argentina (2010)
   - Salar Salinas Grandes for Orocobre, Argentina (2010-2013)
   - Salar de Maricunga for Li3 Energy and Minera Salar Blanco, Chile (2011-2016)
   - Salar de Atacama and Silver Peak for Albermarle, Chile (2014 - 2016)
   - Rann of Kutch, Archean Group, India (2015)
   - Lake Mackay, Agrimin, Australia (2014-2016)
6. I am responsible for sections 12 and 16 of the technical report entitled "Lithium & Potassium Resource Estimate Maricunga Joint Venture, III Region, Chile" (the "Technical Report") prepared for the Maricunga JV. and dated effective August 25th, 2017. The latest site visit was for the duration of one day in May, 2017. I am independent of the Maricunga JV.
7. I have not had prior involvement with the properties that are the subject of the Technical Report.
8. As of the date of this certificate, to the best of my knowledge, information and belief, the technical report contains all scientific and technical information that is required to be disclosed to make the technical report not misleading.

9. I am independent of the issuer applying all of the tests in section 1.5 of National Instrument 43-101.
10. I have read National Instrument 43-101 and Form 43-101F1, and the Technical Report has been prepared in compliance with that instrument and form.
11. I consent to the filing of the Technical Report with any stock exchange and other regulatory authority and any publication by them for regulatory purposes, including electronic publication in the public company files on their websites accessible by the public, of the Technical Report.

Effective date:- 25th Day of August, 2017

Date of signing:- 25th Day of August, 2017

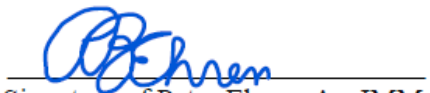

Signature of Peter Ehren, AusIMM.

Peter Ehren
Printed name of Peter Ehren, AusIMM (CP)